Multi-Scale Analysis of Liquid-Based Pretreatment in Lignocellulosic Biorefineries

Multiskalen-Analyse von flüssigkeitsbasierter Vorbehandlung in Lignocellulose-Bioraffinerien

Von der Fakultät für Maschinenwesen der
Rheinisch-Westfälischen Technischen Hochschule Aachen
zur Erlangung des akademischen Grades einer

Doktorin der Ingenieurwissenschaften

genehmigte Dissertation

vorgelegt von

Caroline Marks

Berichter: Universitätsprofessor Alexander Mitsos, Ph.D.
Professor Jason P. Hallett, Ph.D.

Tag der mündlichen Prüfung: 10. Dezember 2021

Titel: Multi-Scale Analysis of Liquid-Based Pretreatment in Lignocellulosic Biorefineries

Autorin: Caroline Marks

Reihe: Aachener Verfahrenstechnik Series
AVT.SVT - Process Systems Engineering
Band 21 (2022)

Herausgeber: Aachener Verfahrenstechnik
Forckenbeckstraße 51
52074 Aachen
Tel.: +49 (0)241 80 97717
Fax.: +49 (0)241 80 92326
E-Mail: secretary.svt@avt.rwth-aachen.de
https://www.avt.rwth-aachen.de

Vorwort

Die vorliegende Arbeit entstand während meiner Zeit als wissenschaftliche Mitarbeiterin am Lehrstuhl für Systemverfahrenstechnik (AVT.SVT) der RWTH Aachen.

Herzlicher Dank gilt meinem Doktorvater Prof. Alexander Mitsos, Ph.D. für seine kontinuierliche Unterstützung und seine Ratschläge während der Promotion. Ebenso danke ich Prof. Jason P. Hallet, Ph.D. für seine Tätigkeit als Zweitprüfer und Prof. Marek Behr, Ph.D. für die Übernahme des Prüfungsvorsitzes.

Besonderer Dank geht an meinen Gruppenleiter Dr.-Ing. Jörn Viell für unzählige Diskussionen und Feedback zu diversen Fragestellungen meiner Dissertation. Ich danke Prof. Dr.-Ing. Wolfgang Marquardt, der mir die Möglichkeit gegeben hat mein Promotionsvorhaben an der AVT.PT zu starten, und Prof. Alexander Mitsos, Ph.D., der mir die Möglichkeit gegeben hat meine Promotion an der AVT.SVT fortzuführen.

Ich bedanke mich bei allen SVTlern und AVTlern für die tolle Atmosphäre, fachliche und nichtfachliche Diskussionen und für eine gute Gemeinschaft sowohl innerhalb des Lehrstuhls als auch in der gesamten AVT. Weiterhin möchte ich mich bei meinen Bürokollegen und -kolleginnen für die viele unterhaltsame und produktive miteinander verbrachte Zeit bedanken, insbesondere bei Kirsten Skiborowski, Andrea König und Alexander Echtermeyer. Darüber hinaus bedanke ich mich bei allen Studierenden, die durch ihre studentischen Arbeiten oder durch Tätigkeiten als wissenschaftliche Hilfskräfte zum Gelingen dieser Arbeit beigetragen haben. Ein großes Dankeschön geht an alle Mitarbeitenden aus Sekretariat, Buchhaltung und IT, die mit ihrer täglichen Unterstützung einen essentiellen Beitrag zum reibungslosen Ablauf an der SVT leisten.

Ohne Ausgleich in der Freizeit wäre diese Promotion nicht gelungen. Darum bedanke ich mich für die Freundschaften, die im Laufe meiner Zeit an der SVT entstanden sind, besonders bei Johannes Faust, Tobias Ploch, Olga Walz, Luisa Brée und Moll Glass.

Nicht zuletzt möchte ich mich bei meiner Familie bedanken. Ich danke meinen Eltern von Herzen, dass sie mich auf meinem Weg immer unterstützt haben. Meinen beiden Töchtern Carlotta und Leni danke ich für die nötige Abwechslung neben der Promotion und die Geduld, insbesondere in der Schlussphase. Mein größter Dank gilt meinem Partner Jan: Danke, dass du durch deine Zuversicht und deinen Rückhalt mein Durchhaltevermögen gestärkt hast und mich auf dem langen Weg durch die Promotion begleitet hast!

Zürich, im Juli 2022 *Caroline Marks*

Contents

Notation

Abbreviations

Ac	acetate
bio	biomass
BMIM	1-butyl-3-methylimidazolium
c	cellulose
CL	carbon loss
CML	compound middle lamella
CrI	crystallinity index
CSF	combined severity factor
DA	dilute acid
DES	deep eutectic solvent
DoD	degree of disintegration
EMIM	1-ethyl-3-methylimidazolium
hc	hemicellulose
HSP	Hansen solubility parameter
IC	investment costs
IL	ionic liquid
KT	Kamlet–Taft
l	lignin
LHW	liquid hot water
ML	middle lamella
NMR	nuclear magnetic resonance
NFU	number of functional units
OC	organocat
OS	organosolv
P	primary wall
R	reaction
RNFA	reaction network flux analysis

S1	secondary wall 1
S2	secondary wall 2
SF	severity factor
SSF	simultaneous saccharification and fermentation
T	tertiary wall
TIC	total investment costs
TT	tulip tree

Latin Symbols

A	peak area	(-)
b	product stream	($\mathrm{kmol\,year^{-1}}$)
c	concentration	($\mathrm{g\,L^{-1}}$)
c	constant	(-)
C	cost	(USD)
E	energy of vaporization	($\mathrm{J\,mol^{-1}}$)
f	conversion factor	($\mathrm{mol^{-1}}$)
f	input stream	($\mathrm{kmol\,year^{-1}}$)
H	enthalpy	($\mathrm{J\,mol^{-1}}$)
H	heating value	($\mathrm{J\,mol^{-1}}$)
H_0	Hammett acidity	(-)
ir	interest rate	($\mathrm{year^{-1}}$)
k	reaction rate constant	($\mathrm{s^{-1}}$)
k	parameter of logistic function	($\mathrm{L\,mol^{-1}}$)
K	equilibrium constant	($\mathrm{mol\,L^{-1}}$)
m	mass	(g)
M	molar mass	($\mathrm{g\,mol^{-1}}$)
n	number	(-)
n	amount of substance	(mol)
P	specific price	($\mathrm{USD\,kg^{-1}}$)
pH	logarithmic hydronium ion activity	(-)
$\mathrm{p}K_\mathrm{a}$	logarithmic acid dissociation constant	(-)
r	reaction rate	($\mathrm{mol\,L^{-1}\,s^{-1}}$)
R	ideal gas constant	($\mathrm{J\,mol^{-1}\,K^{-1}}$)
R_0	reaction ordinate	(h)
t	time	(s)/(year)

T	temperature	(°C)/(K)
V	volume	(m^3)
w	side-product stream	($kmol\,year^{-1}$)
w	weight fraction	($g\,g^{-1}$)
x	mole fraction	($mol\,mol^{-1}$)
XYZ	physicochemical property	(-)
Y	yield	($mol\,mol^{-1}$)

Greek Symbols

α	Kamlet–Taft acidity	(-)
β	Kamlet–Taft basicity	(-)
δ	Hansen solubility parameter	($MPa^{1/2}$)
δ	Hildebrand solubility parameter	($MPa^{1/2}$)
η	efficiency	(-)
λ	wavelength	(m)
π^*	Kamlet–Taft polarity/polarizability	(-)
ρ	density	($kg\,m^{-3}$)
τ	residence time of pretreatment	(h)

Subscripts and Superscripts

AA	acetic acid
B	base
BH^+	protonated base
bio	biomass
c	cellulose
C	carbon
cat	catalyst
comb	combustion
D	deuterated
D	dispersive/nonpolar
dw	deuterated water
f	forward
fuel	fuel

g	glass transition
glu	glucose
h	hydrolysis
H	hydrogen
H	hydrogen bond
H	protonated
hc	hemicellulose
i	control variable
int	integration
j	control variable
l	lignin
m	moisture
m	molar
man	mannose
max	maximum
norm	normalized
nr	non-recovered
obs	observed
p	pretreatment
P	polar
p-liq	pretreatment liquid
r	recovered
r	reverse
R	reference
raw	raw material
rel	relative
rem	removed
s	solubilized
spec	specific
t	time
tot	total
v	vaporization
w	water
waste	waste
wood	wood
xyl	xylose

Kurzfassung

Zur Reduktion von CO_2-Emissionen können erdölbasierte Produkte alternativ aus erneuerbaren Kohlenstoffquellen wie lignocellulosehaltiger Biomasse hergestellt werden. Die stoffliche Umwandlung der kompositartig vernetzten Biomasse erfordert eine Vorbehandlung, oft gefolgt von enzymatischer Hydrolyse zur Abspaltung von Zuckern für weitere Prozessschritte. Die Vorbehandlungsmechanismen sind jedoch unvollständig verstanden, vor allem die Rolle der unterschiedlichen zur Vorbehandlung eingesetzten Mischungen aus Lösemitteln und Ionen. In dieser Arbeit wird die Biomassevorbehandlung auf mehreren Skalen untersucht: von der molekularen Ebene in Form von Interaktionen zwischen Komponenten in Vorbehandlungslösungen bis zur Prozessebene mit dem Einfluss der Zuckerausbeute auf die Biokraftstoffproduktion.

Kombiniert mit enzymatischer Hydrolyse erzielt die ionische Flüssigkeit 1-Ethyl-3-methylimidazolium Acetat (EMIMAc) eine effektive Vorbehandlung und Desintegration von Buchenholz. Allerdings sinkt die Zuckerausbeute mit steigendem Wassergehalt in EMIMAc. Molekulare Interaktionen zwischen EMIMAc und Wasser werden in dieser Arbeit mit Niederfeld-NMR-Spektroskopie und deuterierten Lösemitteln charakterisiert. Der beobachtete Wasserstoff-Deuterium-Austausch wird modellgestützt ausgewertet um die zugrundeliegenden Kinetiken zu bestimmen. Änderungen der Austauschkinetiken deuten darauf hin, dass Ionennetzwerke bis zu einem EMIMAc-Stoffmengenanteil von 0,3 stark assoziiert bleiben. Damit leistet diese Untersuchung einen ersten Beitrag, um den Effekt von Wasser in EMIMAc-Gemischen zu verstehen.

Wie EMIMAc kann die essigsäurebasierte Acetosolv-Vorbehandlung Buchenholz effektiv desintegrieren, allerdings mit geringeren Zuckerausbeuten. Die Experimente dieser Arbeit zeigen, dass Phänomene wie der neu definierte Desintegrationsgrad und die durch Vorbehandlung aus dem Holz entfernte Fraktion sowohl untereinander abhängig sind, als auch durch Art und Konzentration des Katalysators in der Vorbehandlungslösung bestimmt werden. Weiterhin korrelieren Desintegration und entfernte Fraktion mit der Zusammensetzung der vorbehandelten Biomasse. Anders als in EMIMAc ermöglicht Wasser in Acetosolvlösungen Desintegration und Delignifikation.

Um den Einfluss von Vorbehandlung und Hydrolyse auf den Vergleich von Prozesspfaden zur Produktion von zwei Biokraftstoffen zu bewerten, werden Kohlenstoffverlust und Kraftstoffkosten mithilfe der Reaktionsnetzwerkflussanalyse geschätzt. Die Analyse von variierenden Biomassezusammensetzungen gemeinsam mit vorbehandlungsspezifischer Fraktionierung der Biomasse und Zuckerausbeuten zeigt, dass Kraftstoffkosten reziprok mit Kohlenstoffverlust korrelieren und, dass unter einem Massenanteil Zucker aus Holz von 0,4 die Kraftstoffkosten stark ansteigen. Somit bezeichnet dieser Wert die Mindestzuckerausbeute für machbare Biomassevorbehandlung.

Summary

To reduce CO_2 emissions, fossil-carbon-based fuels and chemicals can alternatively be produced from renewable carbon sources such as lignocellulosic biomass. The material conversion of biomass requires a pretreatment to cleave the composite-like structure of biomass, often followed by enzymatic hydrolysis to make sugars available for further processing. However, the mechanisms of liquid-based pretreatment concepts are not yet completely understood. Especially the role of the various mixtures of solvents and ions that are applied as pretreatment liquids remains unclear in many cases. In this thesis, pretreatment of biomass is investigated on multiple scales: from the molecular scale with interactions between components of pretreatment liquids to the process level with the influence of sugar yield on the production pathway performance of biofuels.

In combination with enzymatic hydrolysis, the ionic liquid 1-ethyl-3-methylimidazolium acetate (EMIMAc) effectively pretreats and disintegrates beech wood, but sugar yields decrease with increasing water content in EMIMAc. In this work, molecular interactions between EMIMAc and water are characterized using low-field NMR spectroscopy and deuterated solvents. Model-based evaluation of the observed hydrogen–deuterium exchange allows for the determination of the underlying kinetics. Composition-dependent changes of exchange kinetics imply that strongly associated ion networks remain active down to 30 mol % EMIMAc. Hence, this investigation presents a first step towards the understanding of the effect of water in mixtures of EMIMAc.

Analogously to EMIMAc pretreatment, acetic acid-based acetosolv pretreatment can effectively disintegrate beech wood, albeit with lower sugar yields. The experiments conducted for this thesis reveal that pretreatment phenomena such as the newly defined degree of disintegration and the non-recovered fraction of wood after pretreatment are not only interdependent but also relate to the type and concentration of catalyst acid in the pretreatment liquid. Furthermore, disintegration and non-recovered fraction correlate with the composition of pretreated biomass. Unlike with EMIMAc pretreatment, the presence of water in acetosolv pretreatment liquids facilitates both disintegration and delignification.

To evaluate the influence of the effectiveness of both pretreatment and hydrolysis on the production pathway performance of two biofuels, carbon loss and fuel cost are estimated with reaction network flux analysis. The analysis of changing biomass composition in combination with pretreatment-specific fractionation effectiveness and sugar yield after hydrolysis shows that fuel cost and carbon loss correlate reciprocally. Below a threshold of 40 wt % sugars from wood, fuel costs increase strongly. Hence, this value describes the minimal viable sugar yield of biomass pretreatment.

Publications and Copyrights

This thesis originates from the research performed by the author during her time at the Chair of Process Systems Engineering at Aachener Verfahrenstechnik (AVT.SVT) between November 2013 and June 2021. Most parts of this thesis have already been published. The publications are integrated into this thesis as described in the following. Alexander Mitsos and Jörn Viell provided ideas, guidance and edits to these publications as well as the dissertation.

- Parts of the introduction in Chapter 1 as well as the overview of biomass pretreatment in lignocellulosic biorefineries in Chapter 2 are reproduced from Marks and Viell (2022) [1].

  Author contributions Caroline Marks performed the majority of the literature research and wrote the original draft of the manuscript.

- The experimental details and results on hydrogen–deuterium exchange in an ionic liquid in Section 3.2, Section 4.1 and Appendix A are reproduced from Marks et al. (2019) [2].

  Author contributions Caroline Marks performed the majority of the research (experiments and modeling) and wrote the original draft of the manuscript.

- The experimental details and results on acetosolv pretreatment of wood in Section 3.1, Section 4.2 and Appendix B are based on Marks and Viell (2021) [3].

  Author contributions Caroline Marks performed the majority of the research (experiments and evaluation) and wrote the original draft of the manuscript.

- The analysis of the impact of biomass pretreatment on process performance of biofuel production in Section 3.3, Section 4.3 and Appendix C is based on Marks et al. (2020) [4].

  Author contributions Caroline Marks had the idea for the study, performed the literature research, adapted the mathematical problem formulation, analyzed the results and wrote the original draft. Andrea König provided the background of reaction network flux analysis, adapted the mathematical problem formulation and implemented it in GAMS, reviewed and edited the manuscript.

While at the AVT.SVT, the author supervised or co-supervised the student theses of Andreas Kochs [5], Alexander Schwabauer [6], Mara Offermann [7], Frederik Bergs [8], Denise Hambsch [9], Christian Tomala [10], Marcel Galowy [11], Björn Hensel [12], Frederik Temme and David Böning [13], Jai Mathias [14], Hannah Ingendae [15], Marvin Huang and Dennis Pflug [16], Alexander Jachertz and Joel Kappes [17], and Tim Kitzing [18]. The theses were developed as a cooperation between the author and the students. The work of all students is acknowledged. Some of the work described in this thesis is partially based on the following student theses:

- Andreas Kochs. Screening ionischer Flüssigkeiten als Lösungsmittel für lignocelluläre Biomasse. *Internship report*, Process Systems Engineering, RWTH Aachen University, 2015 [5].

  Andreas Kochs first used the degree of disintegration to evaluate the macroscopic effectiveness of pretreatment of beech wood in ionic liquids. The degree of disintegration was also used to classify acetosolv-pretreated beech wood in Section 4.2.

- Denise Hambsch. Vorbehandlung von Holz in essigsäurebasierten Medien. *Bachelor's thesis*, Process Systems Engineering, RWTH Aachen University, 2015 [9].

  Denise Hambsch evaluated the disintegration of beech wood after pretreatment in acetosolv liquids with regard to the composition of the pretreatment liquid. Parts of these experiments are further analyzed in Section 3.1, Section 4.2 and Appendix B.

- Christian Tomala. Analyse von Biomasse und Biomasseaufschlusslösungen mittels NMR. *Master's thesis*, Process Systems Engineering, RWTH Aachen University, 2015 [10].

  Christian Tomala established a first protocol for the analysis of biomass components solubilized in pretreatment liquids after pretreatment that was further modified and used for the evaluation of acetosolv pretreatment experiments in Section 3.1, Section 4.2 and Appendix B.

- Hannah Ingendae. Reaktionsnetzwerke zur Vorbehandlung von Biomasse. *Project thesis*, Process Systems Engineering, RWTH Aachen University, 2017 [15].

  Hannah Ingendae carried out a first analysis of the impact of biomass pretreatment in reaction networks for the production of biofuels. This was the basis for a following detailed analysis of several types of pretreatment in Section 3.3, Section 4.3 and Appendix C.

During her time at AVT.SVT, the author additionally contributed to the following publications, which are not part of this thesis:

- J. Viell, H. Inouye, N. K. Szekely, H. Frielinghaus, C. Marks, Y. Wang, N. Anders, A. C. Spiess and L. Makowski. Multi-scale processes of beech wood disintegration and pretreatment with 1-ethyl-3-methylimidazolium acetate/water mixtures. *Biotechnology for Biofuels* 9:7, 2016 [19].
- S. Stiefel, C. Marks, T. Schmidt, S. Hanisch, G. Spalding and M. Wessling. Overcoming lignin heterogeneity: reliably characterizing the cleavage of technical lignin. *Green Chemistry* 18(2):531–540, 2016 [20].
- O. Walz, C. Marks, J. Viell, A. Mitsos. Systematic approach for modeling reaction networks involving equilibrium and kinetically-limited reaction steps. *Computers & Chemical Engineering* 98:143–153, 2017 [21].
- D. Di Marino, T. Jestel, C. Marks, J. Viell, M. Blindert, S. M. A. Kriescher, A. C. Spiess and M. Wessling. Carboxylic acids production via electrochemical depolymerization of lignin. *ChemElectroChem* 6(5):1434–1442, 2019 [22].
- J. Viell, N. K. Szekely, G. Mangiapia, C. Hövelmann, C. Marks, H. Frielinghaus. In operando monitoring of wood transformation during pretreatment with ionic liquids. *Cellulose* 27(9):4889–4907, 2020 [23].
- A. Echtermeyer, C. Marks, A. Mitsos, J. Viell. Inline Raman spectroscopy and indirect hard modeling for concentration monitoring of dissociated acid species. *Applied Spectroscopy* 75(5):506–519, 2021 [24].

Copyrights

Parts of the following publications, especially figures, are included in this thesis and are reprinted with permission:

- Reprinted by permission from Springer Nature Customer Service Centre GmbH: Springer *Journal of Solution Chemistry*, 48:1188–1205, Change of C(2)-hydrogen–deuterium exchange in mixtures of EMIMAc, C. Marks, A. Mitsos and J. Viell, [2] Copyright © (2019).
- Reprinted from C. Marks, A. König, A. Mitsos, J. Viell. Minimal viable sugar yield of biomass pretreatment. *Biofuels, Bioproducts & Biorefining*, 14(2):301–314, 2020. [4] Copyright © (2020), The authors. John Wiley & Sons, Ltd. Published under the creative commons attribution 4.0 international (CC BY 4.0).
- Reprinted from C. Marks and J. Viell. Acetosolv pretreatment of wood for biorefinery applications. *Biomass Conversion and Biorefinery*, 2021. [3] Copyright © (2021), The authors. Springer Nature. Published under the creative commons attribution 4.0 international (CC BY 4.0).
- Reprinted by permission from Elsevier Ltd.: Elsevier *Process Biochemistry*, 113: 241–257, Solvents and ions for pretreatment in lignocellulosic biorefineries, C. Marks and J. Viell, [1] Copyright © (2022).

Chapter 1

Introduction

The transition from a fossil-carbon-based economy to a decarbonized economy requires replacing finite fossil resources with alternative resources from sustainable carbon sources such as lignocellulosic biomass or CO_2 in combination with renewable H_2 [25–27]. Lignocellulosic biomass (i.e., terrestrial plant biomass including wood and grass) is an abundantly available, rather cheap raw material [28, 29]. Hence, it serves as a starting point to partially replace fossil resources.

The material conversion of lignocellulosic biomass is achieved in a lignocellulosic biorefinery [30, 31], which has to be very efficient for the economic production of biofuels and biochemicals [25, 32]. One major strategy for biorefineries is the catalytic [33, 34] or fermentative conversion of sugars from the lignocellulosic polysaccharides cellulose and hemicellulose. Together with lignin, cellulose and hemicellulose form a composite-like structure that is naturally resistant against degradation. To release sugars, lignocellulosic biomass can be hydrolyzed either chemically or enzymatically. Although chemical hydrolysis is faster than enzymatic hydrolysis, the advantage of enzymatic hydrolysis is the selective degradation of cellulose and hemicellulose into the desired sugar molecules. Nevertheless, enzymatic hydrolysis of native, untreated lignocellulosic biomass results in scarce sugar yields [35]. However, only high sugar yields enable carbon-efficient and economic processing. Increasing the enzyme load for higher sugar yields is not an option because enzymes are one of the major cost contributors in biorefineries [36–38]. To allow for a lower enzyme load during hydrolysis and thus reduce overall production costs, a pretreatment is required. Therefore, the development of more effective pretreatment strategies to facilitate subsequent enzymatic hydrolysis by reducing the natural biomass recalcitrance is one of the key challenges in lignocellulosic biorefineries [39, 40].

Enzymatic hydrolysis in biorefineries usually relies on cellulose-degrading cellulases or fungal enzymes for the degradation of polysaccharides [41, 42]. To increase hydrol-

ysis effectiveness, enzyme mixtures can be tailored for the conversion of lignocellulosic biomass [43]. This includes the exploitation of synergies between different types of enzymes that are required for the complete conversion of individual components of lignocellulosic biomass [44]. In addition, laccases that play a major role during natural lignin degradation might bear potential for application in several process steps of a biorefinery [45]. The above cited reviews give a comprehensive overview of the application of different types of enzymes in biorefineries and potentials for improving hydrolysis effectiveness. In this thesis, sugar yields after enzymatic hydrolysis serve as an evaluation criterion for pretreatment effectiveness. Notably, the sugar yield after pretreatment and subsequent enzymatic hydrolysis of one source of biomass can vary extensively depending on the applied pretreatment concept [46, 47]. This highlights that the final sugar yield is determined not only by the type of biomass but also by the mechanisms of the specific pretreatment concept.

Pretreatment concepts are often categorized into biological, physical, chemical and physicochemical concepts or combinations thereof that are to a different extent preserving structural elements of lignocellulosic biomass [38, 48–53]. This typical categorization is to some extent arbitrary [52] and the classification into different (sub-)categories depends on the individual concept. Another categorization approach is to compare the effects of pretreatment according to the applied pretreatment liquid, for example aqueous pretreatment concepts, such as liquid hot water (LHW), steam explosion, and acid and alkaline pretreatment [35, 54], or nonaqueous pretreatment concepts with organic solvents, the so-called organosolv (OS) pretreatment [55, 56], or ionic liquids (ILs) [57]. This leads to a detailed but limited description of phenomena that occur during pretreatment with one specific pretreatment concept only.

The development of novel, tailored pretreatment concepts requires knowledge of molecular kinetics of biomass pretreatment based on first principles. Since the application of various combinations of solvents and catalysts (i.e., the applied pretreatment liquid) leads to many reactions during fractionation and solubilization, empiric functions serve as a workaround so far. Furthermore, it is not yet completely understood how pretreatment phenomena such as removal of lignin and hemicellulose or reduction of cellulose crystallinity facilitate subsequent enzymatic hydrolysis. As a result, there is a lack of simple protocols to evaluate pretreatment effectiveness with regard to enzymatic hydrolysis although tools to evaluate pretreatment strategies for enzymatic hydrolysis would help to reduce the experimental effort for hydrolysis experiments. Overall, determining mechanistic correlations between pretreatment phenomena and parameters for the description of pretreatment liquids allows for the design of optimized pretreatment strategies with regard to the type of biomass and efficiency. To

this end, phenomena that occur during pretreatment should be described first and then used as a basis to derive mechanistic, kinetic relationships. The challenge that is addressed in this thesis is therefore to push forward the mechanistic knowledge and at the same time draft tools to evaluate pretreatment effectiveness with regard to enzymatic hydrolysis.

Figure 1.1 sketches the main process steps for the conversion of lignocellulosic biomass into biofuels relying on liquid-based pretreatment and enzymatic hydrolysis. Furthermore, the main aspects that are discussed in this thesis from molecular interactions in a pretreatment liquid to the impact of sugar output on the production of biofuels are indicated. Since in many cases the pretreatment liquid contains electrolytes, we refer to solvents and ions as a general term for components of a pretreatment liquid, while the specific components of pretreatment liquids that are investigated in this thesis are additionally highlighted in the sketch.

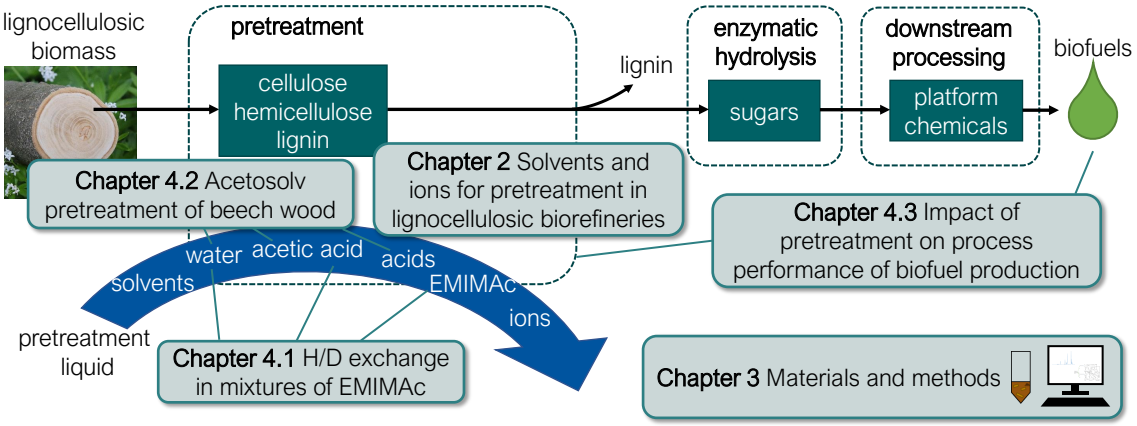

Figure 1.1: Main process steps for the conversion of lignocellulosic biomass to biofuels relying on liquid-based pretreatment in combination with enzymatic hydrolysis. The contribution of this thesis is highlighted by the light-turquoise boxes.

Chapter 2 comprises an analysis of pretreatment phenomena across the typical categorization of pretreatment: Research results are clustered according to relevant modifications of biomass during pretreatment from a phenomenological point of view, covering the macroscopic scale down to the molecular structure of biomass. With regard to the role of the pretreatment liquid, there are many cases in which a solvent additionally acts as catalyst, thus complicating the classification of components of the pretreatment liquid into solvent or catalyst. Therefore, we do not aim at differ-

entiating between the influence of solvent and catalyst but generally try to identify (re)active species in an electrolyte solution that is used for biomass pretreatment. To this end, we review parameters that have been applied to describe pretreatment severity as well as solvent and solubility parameters for the characterization of electrolyte solutions. We also discuss the potential of these parameters to be correlated with the identified pretreatment phenomena.

Since parameters such as pH and pK_a only enable a classification of aqueous pretreatment liquids, a more detailed investigation of nonaqueous concentrated electrolyte solutions (e.g., ILs or OS pretreatment liquids) is required. This topic is addressed in the following chapters of this thesis. Chapter 3 describes methods and details of the experiments conducted and models used for the investigations of this thesis. In Chapter 4, we present the results of our research on liquid-based pretreatment of biomass.

Section 4.1 discusses how pretreatment of beech wood in mixtures of EMIMAc is influenced by the addition of two protic solvents: water and acetic acid. These solvents are chosen to determine the influence of varying acid strengths added to EMIMAc. EMIMAc-based mixtures are investigated for the composition range from pure IL to pure solvent. To analyze potential molecular causes that lead to changes in pretreatment efficacy upon the dilution of EMIMAc, we monitor hydrogen–deuterium (H/D) exchange between EMIMAc and solvents with low-field nuclear magnetic resonance (NMR) spectroscopy. From spectral information, the amount of deuterated EMIM cations is estimated for the discussion of reaction order. We model the proton exchange kinetics considering pseudo-first-order and second-order reaction mechanisms as well as the influence of solvent content and dissociation of the solvent in the case of water.

In Section 4.2, we examine correlations between pretreatment phenomena with regard to the properties of pretreatment liquids aiming at the identification of simple criteria for the evaluation of pretreatment effectiveness. To this end, beech wood pretreated with a number of acetosolv liquids (i.e., acetic acid with different catalyst acids and varying water contents) serves as an exemplary pretreatment concept. To classify the macroscopic separation of wood fibers during pretreatment, we define five degrees of disintegration and we determine overall mass balances with classical component analysis as well as a newly developed method relying on low-field NMR spectroscopy. Evaluation of the compositional changes after pretreatment identifies removed components in relation to the observed disintegration. Lastly, we assess the performed pretreatment experiments based on sugar yields of enzymatic hydrolysis in view of a potential application of acetosolv pretreatment in biorefineries.

The impact of sugar yields resulting from pretreatment and hydrolysis effectiveness as well as biomass composition on different conversion pathways for the production of biofuels is evaluated with reaction network flux analysis (RNFA) in Section 4.3. To this end, we compile various pathways for liquid-based pretreatment and enzymatic hydrolysis from the literature in an existing reaction network for the production of ethanol and ethyl levulinate from lignocellulosic biomass. Biofuel production is optimized minimizing carbon loss and specific fuel cost. On the one hand, we determine the influence of pretreatment and hydrolysis efficiency on the production of a biofuel for beech wood as one specific species of biomass. On the other hand, we investigate published data on OS pretreatment as a well-known pretreatment concept to determine the range of carbon loss and fuel cost for one representative pretreatment concept with different species of lignocellulosic biomass. Naturally, numerous combinations of biomass species with different pretreatment technologies are conceivable but data from the literature is limited. Therefore, we conduct a generic analysis of pretreatment and hydrolysis yields in combination with changing compositions of biomass to describe the overall relation between carbon loss and fuel cost and to define the boundaries of economic fuel production. Lastly, we compare the conducted acetosolv pretreatment experiments with other pretreatment strategies for beech wood with regard to biofuel production.

Chapter 2

Solvents and Ions for Pretreatment in Lignocellulosic Biorefineries

This chapter introduces fundamentals of pretreatment of lignocellulosic biomass focusing on liquid-based pretreatment concepts that employ aqueous or organic electrolyte solutions containing salts and ions in varying concentrations. First, in Section 2.1, we discuss the relevance of the pretreatment step in combination with enzymatic hydrolysis for the production of sugars in the framework of a lignocellulosic biorefinery. Well-known liquid-based pretreatment concepts that could potentially be applied in a biorefinery are summarized in Tab. 2.1. The overview specifies the main components of pretreatment liquids, process conditions and main phenomena for each concept. As outlined in the last column, from a phenomenological point of view, pretreatment of lignocellulosic biomass is associated with a number of changes in morphology and composition of the biomass. Hence, in Section 2.2, major phenomena of liquid-based pretreatment are analyzed in order to identify relevant mechanisms that influence the overall sugar yield. To this end, morphology and composition of lignocellulosic biomass is explained (Subsection 2.2.1) followed by a detailed description of pretreatment phenomena from the macroscopic to the molecular scale (Subsection 2.2.2). Last but not least, we critically analyze the role of solvents and ions in pretreatment liquids (Subsection 2.2.3). In this context, we review parameters for the description of pretreatment processes and characterization of pretreatment liquids and we discuss the potential of these parameters to be correlated with the identified pretreatment phenomena.

Table 2.1: Liquid-based pretreatment concepts [35, 38, 54, 56–61].

Pretreatment concept	**Pretreatment liquid**	**Process conditions**	**Main phenomena**
liquid hot water	liquid hot water	160...240 °C minutes high pressure pH between 4 and 7	• solubilization of hemicelluloses • reduced formation of degradation products and inhibitors due to low release of monosaccharides • partial depolymerization and removal of lignin (complete delignification impossible with only water)
steam explosion	steam optional acid catalyst	up to 240 °C seconds to minutes quick depressurization	• solubilization of hemicelluloses • formation of degradation products • autohydrolysis of acetyl groups • fiber separation due to explosive decompression
acid pretreatment	dilute or concentrated acids	120...220 °C seconds to hours atmospheric/increased pressure	• hydrolysis of hemicelluloses • formation of degradation products and inhibitors • condensation and precipitation of solubilized lignin
alkaline pretreatment	NaOH, KOH, $Ca(OH)_2$, NH_4OH	−20...210 °C seconds to days atmospheric/increased pressure	• swelling of biomass • consumption of alkali by biomass • effective removal of lignin • deacetylation • dissolution of cellulose below 0 °C
organosolv	(aqueous) organic solvents optional acid/alkaline catalyst	60...250 °C minutes to hours atmospheric/increased pressure	• recovery of relatively pure lignin possible • solubilization of hemicelluloses
ionic liquids	typically large organic cations with small anions	up to 200 °C hours to days usually atmospheric pressure	• effective disruption of hydrogen bond network in biomass • lignin and carbohydrates solubilized • low formation of degradation products

2.1 Pretreatment in Biorefinery Processes

Pretreatment is the first process step in a lignocellulosic biorefinery as depicted in a simplified process scheme of lignocellulosic biorefineries in Fig. 2.1. After pretreatment, parts of the lignocellulosic biomass are dispersed and solubilized in the pretreatment liquid, whereas the remaining part is recovered as a solid fraction (changes in composition and structure of the recovered fraction are discussed in Subsubsections 2.2.2.2 and 2.2.2.3). Depending on the type of pretreatment, the three main components (cellulose, hemicellulose and lignin) can be separated into two or three fractions.

During pretreatment, compounds that inhibit hydrolyzing enzymes and fermenting microorganisms can be formed (inhibiting effects of specific compounds are discussed in Section 2.2.2.4). Inhibition of enzymes and microorganisms can be avoided either by adjusting process conditions to reduce formation of inhibiting components or by removing these components from process streams to keep concentrations low (not shown in Fig. 2.1) [62]. For further processing, the dispersed and solubilized biomass components are usually removed from the pretreatment liquid (e.g., using extraction or precipitation) to allow for recycling of the pretreatment liquid. This is necessary from an economic and sustainability perspective as the ratio between liquid streams and solid mass is often as high as 10/1 or even exceeds this value. In the next step, the cellulose-rich fraction is (enzymatically) hydrolyzed into sugars. Hemicellulose-based sugars are either obtained analogously from hydrolysis or recovered from the pretreatment liquid in case the majority of hemicellulose remains attached to the cellulose-rich fraction or is degraded during pretreatment, respectively. The sugars are converted to the final products—biofuels or bio-based (bulk) chemicals—using a variety of production pathways in the downstream processing [34, 63].

The lignin fraction is mostly chemo-catalytically (rarely enzymatically) degraded to produce lignin-based chemicals [45, 64] or combusted to generate energy. The production of liquid fuels from lignin is economically not feasible [63]. In contrast, the coproduction of value-added products from lignin enhances economic feasibility of lignocellulosic biorefineries especially in the case of biofuel production due to the low market price of fuels [30, 65]. Hence, the production and effective removal of high quality lignin is required for example in the context of costly OS pretreatment [66].

In a lignocellulosic biorefinery, pretreatment and hydrolysis are among the main cost drivers and bottlenecks. Costs associated with pretreatment and hydrolysis on average account for one third of installed capital costs and especially the costs for enzymes can contribute as much as 15%, 30% or even more to the overall production

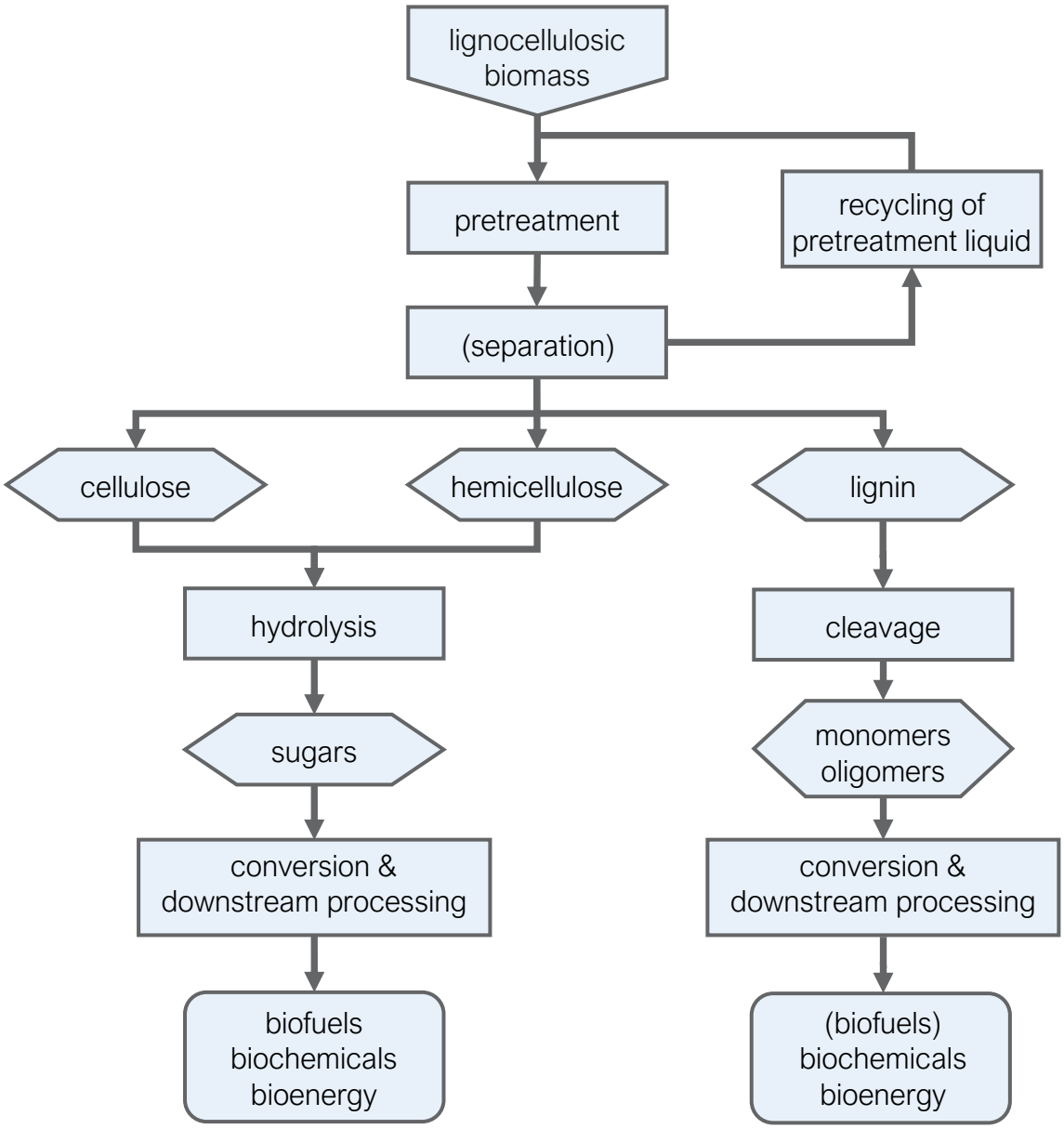

Figure 2.1: Process scheme of a lignocellulosic biorefinery focusing on process steps related to pretreatment, adapted from [30]. For simplicity, the three main components of lignocellulosic biomass—cellulose, hemicellulose and lignin—are shown as individual components. Truly, pretreatment does not achieve complete fractionation: Depending on the catalytic activity of the pretreatment liquid, biomass can be separated into a phenol-rich and/or a sugar-rich process stream. In some cases, the latter is further separated into a C5- and a C6-sugar stream (not shown for clarity). However, digestibility is also not exclusively correlated to fractionation. Recycling of liquids, in particular from pretreatment, is important for economic reasons and sustainability.

costs of biofuels or bioproducts and hence reduce economic feasibility [37, 67–70]. To improve economic feasibility of biorefinery processes, the process related costs need to be reduced, in particular costs associated with utilization and recovery of pretreatment liquids.

With regard to process related costs, OS pretreatment can be unprofitable in comparison to other chemical and hydrothermal pretreatment concepts [67] due to high costs for the solvent. In this context, high costs arise due to solvent losses that are associated with product and by-product streams as well as with recycling steps rather than with degradation of the solvent due to severe pretreatment conditions [71]. Further losses occur due to consumption of effective components of the pretreatment liquid during pretreatment such as the consumption of alkali during kraft pulping [72]. In contrast to losses associated with the size of the plant (i.e., depending on the total liquid volume), these consumptive losses depend on the amount of biomass that is processed. To improve economic viability of the pretreatment step, almost complete recycling of liquid streams is required especially in the case of expensive pretreatment liquids (i.e., nonaqueous liquids or liquids containing a high amount of acids and salts) [30, 65, 66]. Besides recycling of pretreatment liquids, recycling of yeast streams from fermentation can reduce production costs [73]. Another approach to reduce the total liquid volume and hence to reduce costs is to increase solid loading during pretreatment, hydrolysis and fermentation [66, 73].

Additionally, a higher yield of pretreatment and hydrolysis represents a large lever for an improvement of economic and environmental performance of biorefineries [74]. In this context, yield relates to the total carbohydrate content of the biomass that is used as feedstock [75, 76] as well as the sugar concentration after combined pretreatment and enzymatic hydrolysis [77, 78]. With regard to the development of pretreatment strategies for biorefineries, it should be noted that the lowest sugar costs are not necessarily expected at the highest yields because increased yields also lead to higher capital and operating costs and/or increased costs for enzymes [79]. Furthermore, a high glucose concentration causes end-product inhibition of cellulases during hydrolysis and thus leads to lower sugar yields [42] (see Section 2.2.2.4).

In conclusion, biorefineries require cost-effective pretreatment and hydrolysis strategies that allow for high biomass loadings, almost complete recycling of pretreatment liquids and valorization of lignin. In any case, the amount of sugars available after pretreatment and hydrolysis is a key factor to determine economically and environmentally viable ranges for biorefinery processes. All these factors are influenced by the choice of the pretreatment liquid. Therefore, a first step towards a more general understanding of sugar output is the determination of underlying mechanisms that in-

fluence pretreatment and subsequent hydrolysis as well as their connection to solvents and ions of the pretreatment liquid.

2.2 Mechanisms of Biomass Pretreatment

To understand the importance and influence of electrolyte solutions that are applied as pretreatment liquids, it is relevant to describe phenomenological changes of biomass morphology and structure that occur during pretreatment before parameters for the description of electrolyte solutions can be reviewed. In this section, we therefore first give an overview of the main morphological characteristics and structural elements of lignocellulosic biomass (Subsection 2.2.1). Second, we identify common pretreatment phenomena and analyze how they affect biomass morphology and structure (Subsection 2.2.2). Third, we discuss the role of the pretreatment liquid and examine how its composition as well as the presence of reactive species relate to the analyzed pretreatment phenomena (Subsection 2.2.3).

2.2.1 Morphology and Structural Components of Lignocellulosic Biomass

Lignocellulosic biomass is a natural composite mainly consisting of cellulose, hemicellulose and lignin but with a hierarchical structure on several scales. These include the macroscopic scale with the overall dimensions, the microscopic scale with cell structures, the macromolecular scale with cell walls and the molecular structure of them as sketched in Fig. 2.2.

2.2.1.1 Macroscopic and Microscopic Morphology of Wood

Macroscopically, wood from regions with seasonal climate changes has annual rings, which are composed of wide-lumened earlywood (i.e., large cavities within conducting cells) and narrow-lumened latewood.

Furthermore, wood is differentiated into softwood (e.g., spruce and fir) and hardwood (e.g., beech and poplar). While softwood has a relatively simple, regular structure composed of mainly one cell type, hardwood has a more complex structure with a variety of specialized cell types. Microscopically, the dimensions of hardwood fibers are smaller than those of softwood fibers: The cell walls are thicker with smaller lumina and the differences in wall thickness and lumen diameters between early- and

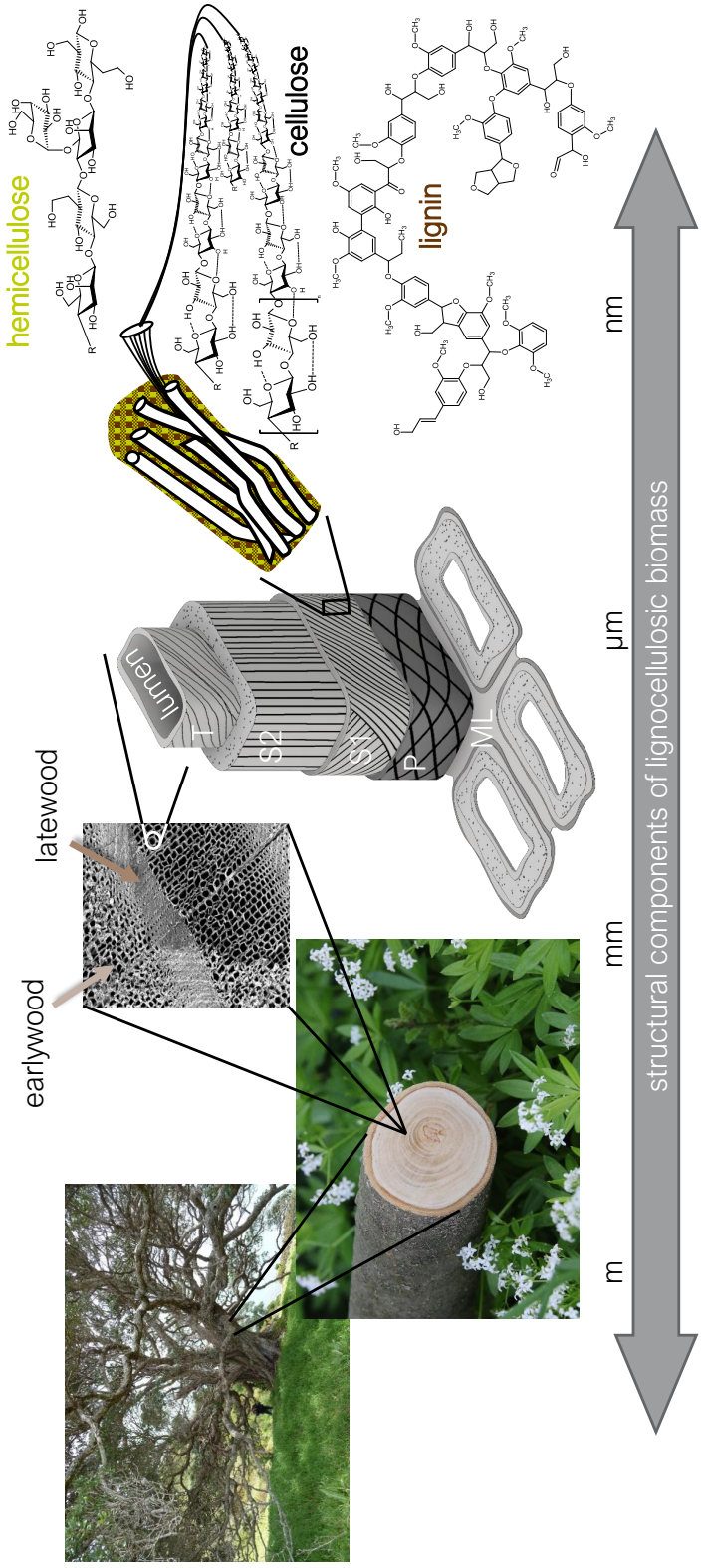

Figure 2.2: Scheme of wood structure with length scales of biomass that are affected during pretreatment (based on Marquardt et al. [27]).

latewood are not as distinct as in softwoods. For the transport of water and minerals within the tree, pits connect cells in both soft- and hardwood, whereas hardwood additionally relies on a macroporous network of vessels. [80, 81]

2.2.1.2 Cell Wall Structure

On an ultrastructural level (i.e., fine structure of cells that is not visible with an ordinary light microscope), the cell walls are composed of concentrically arranged cell wall layers (see Fig. 2.2), which differ in composition and orientation of the structure-giving component cellulose and the substructural components hemicellulose and lignin. The middle lamella (ML) connects the cells. It consists of a lignin-pectin complex and is virtually free of cellulose. Cellulose fibrils crossing each other in thin layers that allow for expansion of the cell during growth form the primary wall (P). Besides cellulose, hemicellulose and pectins are major constituents of P. Because the transition from ML to P is not always clear, ML including P and cell corners of two adjacent cells is referred to as compound middle lamella (CML). CML has the highest lignin density of all cell wall layers [82]. In the secondary wall 1 (S1), cellulose fibrils are arranged with a slightly helical slope, whereas in the secondary wall 2 (S2) fibrils are arranged in a steep angle to provide axial strength. The secondary wall mainly consists of cellulose with only little lignin. In all types of wood, S2 has the highest portion of the cell wall. The tertiary wall (T), sometimes also referred to as secondary wall 3, is the last fibrillar layer towards the cell lumen where fibrils are arranged rather loosely with a minor slope. Here, a higher concentration of nonstructural components results in a more or less smooth appearance of the surface. In general, the content of cellulose, hemicellulose and lignin in the individual cell wall layers differs from the overall average composition [81]. Besides the variation in composition, the distribution of micropores varies with cell wall layers. The number of pores increases from ML towards the lumen whereas the pore width decreases [83]. Thus, the highly lignified cell wall layers ML and T appear less porous than the S2 layer [84]. As a result, the reduced porosity in ML and T in combination with the hydrophobic nature of lignin act as a barrier to water movement in both soft- and hardwood [81, 84].

The main macromolecular cell wall components—cellulose, hemicelluloses (also referred to as polyoses) and lignin—are present in all wood species and account for 90 wt % or more of the wood material. Other macromolecular components such as pectins and starch occur in small quantities only. Low molecular weight components such as extractives (i.e., organic matter) and mineral substances (i.e., inorganic matter, ash) usually depend on the type of wood (see Tab. 2.2).[81]

Table 2.2: Composition of lignocellulosic biomass [81].

Biomass component (wt %)	**Softwood**	**Hardwood**
cellulose	40 – 61	37 – 56
hemicellulose	21 – 34	27 – 41
lignin	25 – 39	17 – 31
extractives	2 – 24	1 – 12
ash	0.1 – 1.4	0.1 – 1

2.2.1.3 Molecular Composition of Wood Components

On a molecular level, cellulose is a homopolymer composed of β-D-glucose with a high degree of polymerization, which makes cellulose insoluble in water. The linear glucan chains have an affinity to form strong intra- and intermolecular hydrogen bonds. The latter lead to the association of several chains into microfibrils (see Fig. 2.2). Furthermore, the hydrogen bonds cause the formation of crystalline structures in cellulose, which make cellulose and thus lignocellulosic biomass resistant against degradation. Cellulose is the major wood component in both soft- and hardwood with a share of sometimes more than 50 wt %.[81]

Hemicellulose is a heteropolymer consisting of pentoses (e.g., xylose and arabinose), hexoses (e.g., glucose, mannose, and galactose) and sometimes additionally uronic acids. The molecular chains are much shorter than in cellulose and they are usually branched with side groups (see Fig. 2.2). Generally, in hardwoods the portion of hemicelluloses is higher than in softwoods and composition is different. Softwood hemicellulose has a high fraction of mannose and contains more galactose than hardwood, whereas hardwood hemicellulose has a high fraction of xylose and contains more acetyl groups. The latter can account for up to 4 wt % of wood.[81]

Lignin, the characteristic component of wooden biomass, is an aromatic polymer mainly composed of the phenylpropane derivatives coniferyl alcohol, sinapyl alcohol and p-coumaryl alcohol. During the formation of a cell, these precursors are linked with ether and carbon–carbon bonds, forming a heterogeneous, amorphous network (see Fig. 2.2). Besides giving mechanical strength, lignin acts as an immune defense by inhibiting biomass-degrading pathogens thus making lignocellulosic biomass highly recalcitrant [85]. Generally, softwoods contain more lignin than hardwoods and moreover structural variations between soft- and hardwood lignin exist. Softwood lignin is mainly composed of coniferyl alcohol-derived units with a guaiacyl residue and hence

it is also referred to as guaiacyl lignin. In contrast, hardwood lignin (also referred to as guaiacyl–syringyl lignin) contains mainly coniferyl alcohol- and sinapyl alcohol-derived units with syringyl and guaiacyl residues in varying amounts [81, 86]. After extraction of lignin from wood, several types of bonds connecting lignin and carbohydrates have been observed, forming so-called lignin–carbohydrate complexes (LCC) [87]. However, their existence in native wood together with their possible contribution to recalcitrance are still under debate [88]. Upon heating, lignin undergoes chemical changes and as for all amorphous polymers, a glass transition temperature T_g can be observed in thermogravimetric analysis. T_g depends on the isolation technique as well as on the molecular size and water content of the sample [81, 86].

2.2.2 Modification of Lignocellulosic Biomass During Pretreatment

Biomass pretreatment includes macroscopic modifications of the biomass as well as changes in terms of composition and structural components. These are reviewed in the following to identify the main phenomena of effective pretreatment strategies. Furthermore, we discuss how compounds that are solubilized during pretreatment influence hydrolysis and fermentation yields.

2.2.2.1 Accessible Surface Area

For the hydrolysis of hemicellulose and cellulose to sugars, enzymes bind to those polysaccharides that are accessible at the biomass surface. Thus, an effective pretreatment of biomass increases the surface area that is accessible to enzymes in comparison to untreated biomass.

Without pretreatment, smaller particles of different types of biomass are hydrolyzed more easily (i.e., higher sugar yields) than larger particles (in µm, mm and cm range), whereas hydrolysis rates and yields of differently sized particles are comparable after pretreatment [89, 90]. Similarly, an extensive mechanical size reduction by milling of spruce wood prior to acid pretreatment does not increase sugar yields in comparison to wood chips [91]. Moreover, the energy required for size reduction of biomass prior to pretreatment increases with decreasing particle size (i.e., milling is an energy-intensive process step) [92, 93], which causes additional costs. Therefore, it seems sufficient to use wood chips (of a few cm length) directly for pretreatment without further comminution.

As a first step of pretreatment, the pretreatment liquid has to impregnate the lignocellulosic biomass. This refers to a penetration of the liquid through the lumina of cells due to external hydrostatic pressure as well as internal capillary forces together with a rather slow diffusion through cell wall layers due to concentration gradients. Ideally, a uniform distribution of the pretreatment liquid into the wood matrix is achieved to reach equally distributed pretreatment effects [72]. However, penetration varies with the size of the wood chip, the structure of wood and the type of pretreatment liquid [72, 94]. In case of OS pretreatment, penetration of soft- and hardwood structures is fast and uniform [95] whereas penetration is rather slow for pretreatment with more viscous ILs [96]. In comparison, acidic media penetrate faster than alkaline media at similar viscosity [72].

Like impregnation, swelling of wood varies with the type of wood and pretreatment liquid. In comparison, hardwoods swell to a greater extent than softwoods, which probably relates to the higher density of hardwoods [94]. Alkaline media induce a swelling of cell walls higher than water [72] that decreases further transport whereas in organic solvents, wood swells more or less than in water. More specifically, the larger the molecular size of the solvent, the higher the maximum swelling but the lower the rate of initial swelling or impregnation for several types of soft- and hardwood [94]. Furthermore, not only the type of organic solvent but also the water content influences swelling as observed for pinewood [97]. Overall, swelling of wood in ILs and organic solvents reaches an apparent maximum of 20% swelling in tangential direction [94, 98]. Hence, the increase in surface area by pure swelling is limited. However, a partial deconstruction of CML and outer cell wall layers is observable during swelling of pinewood in mixtures of organic solvents and water [97]. Similarly, after a certain extent of swelling in IL has been reached, parts of carbohydrates are removed from all cell wall layers and lignin preferentially from S1, S2 and S3 [96]. These observations show that swelling is closely related to the removal of wood components and thus acts as a prerequisite for the separation of wood fibers [96, 97, 99].

In the literature, several terms are used to describe the phenomenon of fiber separation during pretreatment: disintegration [19, 95], defibrillation [100], dissociation [99], deconstruction [57, 101] or fiber liberation [102, 103]. In this thesis, we refer to disintegration of lignocellulosic biomass. Disintegration of rice straw pretreated with cholinium-based ILs comes along with an up to 6-fold increase in surface area, while disintegration of pine wood pretreated with 1-ethyl-3-methylimidazolium (EMIM)-based ILs increases the accessible surface area up to 9-fold. In both studies, glucose yields increase correspondingly in a more or less linear manner reaching almost complete conversion [101, 104]. This shows that disintegration is closely linked to an

increase in accessible surface area, which is beneficial for high sugar yields. Nevertheless, extensive disintegration beyond the point of fiber separation could negatively influence sugar yields [105]. Furthermore, wood does not necessarily disintegrate uniformly during pretreatment. Macroscopically visible disintegration depends on the type of pretreatment, impregnation and ultrastructure [19]. Varying extents of disintegration of beech wood are illustrated in Fig. 2.3. However, the varying extent of disintegration has rarely been analyzed and there is no common protocol available. On an ultrastructural level, latewood cells of softwood pretreated with an EMIM-based IL disintegrate during pretreatment, whereas earlywood structures stay intact due to different recalcitrance and swelling characteristics [99, 106]. In contrast to softwood spruce, hardwood beech disintegrates faster and both early- and latewood cells are separated in EMIM Acetate (Ac) [106] with beech wood also showing higher sugar yields than spruce [107]. Disintegration of both soft- and hardwood in ethanol OS pretreatment is likely related to the removal of lignin and hemicellulose, loosening of ML and swelling of secondary cell walls [95]. Furthermore, chemical changes of lignin and cellulose can occur during disintegration [96, 99]. In comparison, the molecular causes leading to macroscopic disintegration seemingly differ, while the complete mechanism is unknown.

An increase in accessible surface area after pretreatment also relates to the accessible pore volume in biomass [101]. In untreated wood, less than 20% of the pore volume is accessible to cellulases (i.e., accessible to a solute of 5.1 nm as an indicator for the size of cellulases). Dilute acid pretreatment of mixed hardwood, poplar and pine increases the pore volume up to 10 times and the thus resulting accessible surface area correlates linearly to initial hydrolysis rates [108]. LHW pretreatment of corn stover leads to formation of pores in the µm-range as well as cell wall alterations that increase the accessibility of the inner cell parts towards the lumen after pretreatment [89]. Kraft pulping of spruce wood leads to a uniform distribution of pores throughout the fiber wall and a doubling of pore size in comparison to untreated wood. Furthermore, cellulose fibrils swell [83]. Similarly, after penetration of beech wood with EMIMAc, voids are formed along the longitudinal fibrils in wood and lastly cellulose fibrils swell and coalesce, corresponding to the macroscopic disintegration of wood [23].

Furthermore, increasing biomass–water interactions after pretreatment (i.e., increasing water retention value) correlate to a reduced recalcitrance, for example for acid pretreated spruce. In this context, physical characteristics such as particle size and pores are as important as the chemical composition of the pretreated biomass [109]. More specifically, the potential of cell wall components to inhibit enzymatic hydrolysis increases the more water these polymers constrain [110]. After LHW and

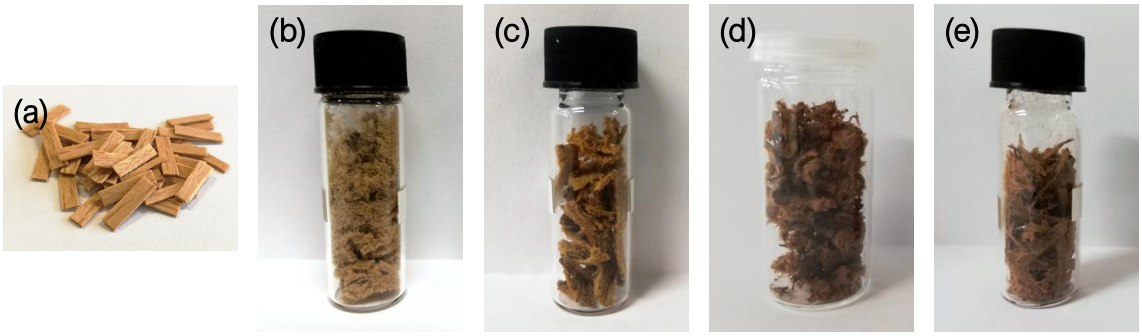

Figure 2.3: Examples of disintegration of beech wood after pretreatment: **(a)** untreated chips of beech wood veneer (2 mm×10 mm) **(b)** spongelike disintegration after pretreatment with EMIMAc (a small water content of $x_{H_2O} = 0.047$ is due to the hygroscopic nature of EMIMAc) **(c)** incomplete disintegration after pretreatment with EMIMAc–water mixture ($x_{EMIMAc} = 0.4403$, $x_{H_2O} = 0.5597$) **(d)** cotton-wool-like disintegration after pretreatment with acetic acid (AA) and H_3PO_4 catalyst ($x_{AA} = 0.7716$, $x_{H_3PO_4} = 0.1165$, $x_{H_2O} = 0.1119$) **(e)** incomplete disintegration after pretreatment with acetic acid and HCl catalyst ($x_{AA} = 0.9894$, $x_{HCl} = 0.0024$, $_{H_2O} = 0.0082$). Note also the varying change in color of the pretreated wood. All experiments carried out with 5 wt% biomass loading for 2 h at 115 °C.

alkaline pretreatment of switchgrass and corn stover, a linear correlation between an increased water retention value and increased glucose yields can be observed [111]. Furthermore, water retention linearly correlates with the accessibility of hydroxyl groups in wood [112]. Upon drying, hydrogen bonds between hydroxyl groups of adjacent cellulose fibrils form, which leads to a collapse of pores and hence, reduced accessibility [112, 113]. This mostly irreversible pore collapse is also referred to as hornification [113]. Hornification comes along with covalent bonds between carboxylic acid groups in neighbouring hemicellulose chains and it is more pronounced with increasing temperature [113, 114]. Thus, sugar yields could be negatively affected due to a reduced accessibility if pretreated biomass is dried before enzymatic hydrolysis (cf. Selig et al. [115]). For a realistic evaluation of new pretreatment strategies for biorefineries, biomass samples should therefore not be dried between harvest, pretreatment and enzymatic hydrolysis.

In conclusion, mechanical comminution does not seem sufficient to increase the accessible surface area for enhanced sugar yields, whereas various liquid-based pre-

treatment concepts successfully increase the accessible surface area. Macroscopically, this relates to a disintegration of biomass after pretreatment. However, disintegration is not uniform but changes with pretreatment liquid and type of wood, which makes it difficult to classify the extent of disintegration. On an ultrastructural level, effective pretreatment strategies increase the number of pores that are accessible to enzymes. Furthermore, a reduced recalcitrance of pretreated biomass is reflected in an increased water retention value due to more accessible hydroxyl groups. All aspects of an increased accessible surface area after pretreatment are connected to changes in biomass composition.

2.2.2.2 Changes in Biomass Composition

Changes of wood ultrastructure during pretreatment are accompanied by changes in biomass composition due to the partial removal of components. This removal of components in combination with disintegration of biomass is sometimes discussed as dissolution of biomass especially with neoteric solvents like ILs [116–118]. However, it is questionable whether biomass as a composite material really is dissolved, that is, whether biomass (the solute) is stabilized in the pretreatment liquid (the solvent) due to intermolecular interactions between both. For example, several types of wood solubilize only partially in the IL 1-butyl-3-methylimidazolium chloride (BMIMCl) and a complete dissolution of lignocellulosic biomass during pretreatment is assumed to be unlikely [57, 119]. There is a general misunderstanding that solvents which dissolve cellulose also dissolve wood and moreover extraction can be misunderstood as dissolution as pointed out by Kyllönen et al. [120]. In this section, we therefore discuss the removal of lignin and hemicellulose from the cellulose pulp during pretreatment as well as the relocation of lignin within the cell compound.

In untreated cell walls, the lignin content negatively correlates with enzyme accessibility and even an increased enzyme concentration as well as longer hydrolysis times cannot balance this lignin-related inaccessibility [121]. Conversely, selective removal of lignin from poplar with peracetic acid pretreatment significantly improves enzymatic digestibility albeit after long hydrolysis times [122, 123]. Similarly, enzymatic hydrolysis yields increase with removal of lignin after pretreatment of aspen wood with alkali metal hydroxide solutions [124]. More specifically, removal of lignin during pretreatment facilitates enzymatic digestibility of the pretreated biomass because lignin acts both as a physical barrier preventing access of cellulases to cellulose fibrils and as a direct inhibitor of cellulases [121, 125]. Enzyme activity decreases due to reversible and irreversible binding of cellulases to lignin for example in OS-type pre-

treated beech wood. Considering that the relative lignin content of the cellulose-rich pulp fraction increases in the progress of hydrolysis due to the release of sugars, this effect becomes more pronounced in time [126]. This increase in irreversible binding not only complicates recycling of the enzymes but also limits sugar yields. However, the highest glucose yield is not necessarily connected to samples with the lowest lignin content as in the case of OS-pretreated eucalyptus and bagasse [127]. Even with less than 50 wt % delignification and no delignification after EMIMAc pretreatment of beech and pine wood, respectively, sugar yields exceed 80 wt % but the IL pretreatment induced changes in functional groups of the beech wood lignin [19, 104]. Therefore, structural features of lignin influence enzymatic digestibility as well as the lignin content[128, 129].

Most commonly, the lignin content of (untreated and pretreated) biomass is determined by treating the biomass sample in concentrated sulfuric acid to hydrolyze the polysaccharides into soluble monosaccharides [130, 131]. The acid-insoluble residue (often termed Klason lignin) makes up for the majority of lignin. However, the acid-insoluble residue as a share of total lignin is not necessarily the same for samples from different types of biomass because the composition and structure of lignin vary with the type of biomass and are also influenced during pretreatment [64, 81]. As a result, the true fraction of lignin can only be approximated when determining the content of acid-insoluble lignin and it remains unclear to what extent the structure of lignin influences hydrolyzability.

Depending on the location of lignin within the wood structure, composition and bonds of lignin can vary and thus influence the hydrolysis outcome. In alkaline pretreatment of spruce, delignification starts around the pit canals and proceeds evenly across S2 and CML so that after pretreatment, the remaining lignin is mostly concentrated in cell corners [132]. Generally, pretreatments above the glass transition temperature of lignin (e.g., aqueous pretreatments above 120 °C) solubilize lignin from the cell compound. However, a further increase in pretreatment temperature and/or residence time can result in too strong pretreatment conditions (see Section 2.2.3.1) that lead to coalescence and redeposition of removed lignin on the pretreated biomass, primarily in pits, cell corners and delamination layers [133]. This redeposition of removed lignin on the pretreated biomass (i.e., an increased surface lignin content) reduces glucose yields for example after acid pretreatment of poplar wood [134, 135]. In some cases, the lignin droplets cannot be removed by a simple washing step prior to enzymatic hydrolysis because they are bound on the surface [136].

Lignin yields above 30 wt % correlate with high molecular weights of the extracted lignin of OS-pretreated pine sawdust. This means that first a fraction of lignin compo-

nents of small molecular weight is removed before larger lignin molecules are separated or recondensed [137]. Recondensation reactions during acidic pretreatment of lignocellulosic biomass can additionally lead to the formation of psuedo-lignin. Pseudo-lignin is an aromatic material that gives a positive value for the Klason lignin fraction but originates from degradation and condensation reactions of the cellulose and hemicellulose fraction with only partial incorporation of lignin. Similar to the redepostion of lignin droplets mentioned above, pseudo-lignin can hinder enzymatic hydrolysis due to unproductive binding to enzymes. One strategy to overcome this problem is to apply less severe pretreatment conditions such as reduced acid concentrations [138, 139]. Moreover, removal of extractives or partial delignficiation before pretreatment can reduce formation of pseudo-lignin (see [140] for an example with sugarcane).

For acetosolv-pretreated (OS with acetic acid) *Miscanthus sinensis* with less than 15 wt % lignin in pulp, the residual lignin content linearly correlates with pulp yield. In this study, the removal of lignin is accompanied by the removal of almost equal amounts of non-lignin components from wood [141] and it is hypothesized that lignin controls xylan accessibility which in turn controls cellulose accessibility [142]. Apparently, lignin and hemicellulose content are closely linked when evaluating their influence on digestibility after pretreatment [129, 143, 144]. At comparable lignin contents, a further removal of hemicelluloses during pretreatment is beneficial for hydrolysis yields [129, 144]. Thus, the removal of both lignin and hemicellulose leads to the formation of pores that facilitate access of enzymes to cellulose. Nevertheless, digestibility cannot be correlated to hemicellulose removal alone [101, 143] and the removal of hemicellulose appears less important than the removal of lignin [129, 145].

With regard to the solvent, lignin needs to be soluble in the pretreatment liquid to allow for high lignin removal. However, good solubility of lignin does not necessarily imply a high pretreatment effectiveness as is the case for deep eutectic solvents (DES) and similar solvent systems that show good lignin solubility [146] but mostly bad pretreatment effectiveness [147]. For OS pretreatment, aqueous organic acids (acetic and formic acid) more effectively delignify biomass than aqueous organic solvents because the acids show higher lignin solubility.

In conclusion, a high lignin solubility of the pretreatment liquid is essential for an effective removal of lignin. This is important because a reduced lignin content after pretreatment correlates with increased sugar yields after enzymatic hydrolysis. Nevertheless, the same overall lignin content may lead to different sugar yields, depending on the location of lignin within the biomass complex. Mild pretreatment conditions should be chosen so that solubilized lignin is not redeposited on the biomass surface. However, only few techniques are available to measure lignin distribution within

cell walls (e.g., UV microspectrophotometry [82, 132]) and therefore it is currently not common to analyze the location of lignin within the plant cells before and after pretreatment as a means to describe pretreatment effectiveness. Considering that in some cases high sugar yields are obtained without considerable removal of lignin during pretreatment, other mechanisms in combination with disintegration and changes of biomass composition are important for an effective pretreatment.

2.2.2.3 Structural Changes

In addition to changes in biomass composition, structural changes of biomass during pretreatment such as modifications of crystallinity and variation of acetyl group content influence enzyme digestibility.

Microcrystalline cellulose pretreated with varying concentrations of phosphoric acid shows a linear correlation between initial hydrolysis rate and reduction in crystallinity, but during enzymatic hydrolysis of untreated microcrystalline cellulose, the crystallinity index (CrI, i.e., the relative amount of crystalline cellulose in the cellulose fraction) does not change [148]. It therefore seems that cellulose crystallinity mostly influences the initial rates of hydrolysis. High initial hydrolysis rates are important to achieve high glucose yields in rather short hydrolysis times and thus reduce costs for the enzymatic hydrolysis step in a biorefinery.

Similar to the observations with cellulose, a reduced crystallinity in poplar wood after ball milling leads to high initial enzymatic hydrolysis rates as well as high sugar yields [122, 123]. In one study, the positive effect of decrystallization could be leveled off after long hydrolysis times of 72 h if the lignin content of the pretreated biomass was below 15 wt % (corresponding to more than 50 wt % delignification) [122]. In another study, poplar wood with low crystallinity showed high digestibility regardless of lignin content [123]. Thus, the interplay between removal of lignin and biomass crystallinity remains ambiguous. In contrast to ball milling of poplar wood, cholinium-based IL pretreatment of rice straw facilitates enzymatic digestibility although biomass crystallinity increases (i.e., a positive correlation between crystallinity and hydrolysis yields). Presumably, removal of lignin during the IL pretreatment causes an overall increase in biomass crystallinity due to the increased cellulose content but at the same time facilitates digestibility [101]. Furthermore, changes in CrI possibly correlate with changes in other morphological characteristics of cellulose [149]. This means that besides crystallinity, for example the accessible surface area, the formation of pores or the amount of productive binding sites influence hydrolysis yields more than the measured crystallinity and thus accessible surface area and lignin content show

stronger correlations to biomass digestibility than crystallinity [101, 150–153]. When evaluating the influence of crystallinity, it has to be taken into consideration that the magnitude of CrI is influenced by the measurement technique and that standards for calibration have not yet been established [149]. Thus, standardized measurement techniques for cellulose and biomass crystallinity should be developed (analogously to the determination of Klason lignin).

Overall, a low crystallinity of cellulose enhances enzymatic hydrolysis rates especially at the beginning of hydrolysis, which is beneficial for effective pretreatment strategies. The crystallinity of biomass, however, is affected by morphological characteristics of cellulose as well as the presence of lignin and hemicellulose. To quantify the relation between biomass crystallinity and sugar yields, a standardization of crystallinity measurements is required.

The acetyl group content in pretreated biomass is another important feature that influences enzymatic hydrolysis yields. For several types of wood in combination with different pretreatment concepts, the acetyl content of the pretreated biomass negatively correlates with sugar yields after hydrolysis [19, 124, 154–156]. Removal of the remaining xylan backbone after deacetylation did not further increase sugar yields of aspen wood pretreated with alkali metal hydroxide solutions. Thus, the acetyl groups attached to hemicelluloses affect enzymatic hydrolysis more than the presence of hemicellulose itself [124]. However, the benefit of removing acetyl groups is limited as has been shown for wheat straw and aspen wood: above 75% deacetylation, other inhibiting factors such as a high lignin content dominate [155]. It has to be noted that pretreatment does not necessarily reduce acetyl groups. In spite of a low lignin content, acetosolv-pretreated Douglas fir shows moderate sugar yields due to an acetylation of cellulose during pretreatment. Nevertheless, this acetylation of cellulose is reversible and sugar yields increase significantly after an additional deacetylation step [157]. A positive side-effect of deacetylation is a reduced toxicity of the fermentation medium after hydrolysis resulting from a lower acetate concentration [156].

By and large, pretreatment mostly reduces the acetyl content of biomass due to removal of acetyl groups from hemicellulose but sometimes increases the acetyl content due to acetylation of cellulose. In this context, a low acetyl content has a positive but limited influence on sugar yields after enzymatic hydrolysis.

2.2.2.4 Soluble Components

While insoluble components are tolerable during hydrolysis and fermentation in high concentrations of up to 20 wt %, soluble components and products of carbohydrate

degradation sometimes act as inhibitors downstream even at low concentrations [158]. This has to be taken into consideration during process design of biorefinery processes: if compounds are released during pretreatment in inhibiting concentrations, they either have to be removed in situ or an extra washing step has to be included between pretreatment and hydrolysis or fermentation to keep concentrations low.

Xylo-oligomers and monomeric sugars especially at concentrations higher than $130\,\mathrm{g\,L^{-1}}$ significantly inhibit enzyme activity [158, 159] (see Tab. 2.3 for details). Acetic acid and furan derivatives have only slight to no effect on hydrolysis rate [158–160], whereas formic acid inactivates enzymes [160]. In contrast, both formic and acetic acid negatively influence ethanol production of microorganisms during fermentation [160]. The role of phenols is rather unclear because they have been observed to either strongly inhibit enzymatic hydrolysis and fermentation [159, 160] or only slightly impact enzyme activity [158, 160].

In conclusion, there seems to be a component-specific threshold value above which soluble sugars, furan derivatives, organic acids or phenolic compounds have a toxic effect on enzymes and microorganisms, while it remains unclear which components act most inhibitory.

2.2.3 Solvents and Ions in Pretreatment Liquids: (Non-)Reacting Species?

As discussed above, different pretreatment phenomena influence the hydrolyzability of pretreated biomass. With regard to the pretreatment liquid, it can be observed that acidic pretreatments preferably remove hemicelluloses and possibly depolymerize cellulose whereas alkaline pretreatments preferably delignify biomass due to hydrolysis of carbohydrates and solubilization of lignin, respectively. Both acidic and alkaline pretreatments reduce cellulose crystallinity and remove lignin from the biomass surface [46, 47]. Accordingly, a single source of biomass pretreated with a variety of well-developed (acidic and alkaline) aqueous pretreatment strategies does not result in one value for total sugar yield but the yield varies as much as 30 wt % for corn stover [46] and 40 wt % for poplar wood [47]. This shows that besides the type of biomass, which determines the maximum available amount of sugars, especially differences between the specific pretreatment liquids and process conditions influence the outcome of a pretreatment and hydrolysis strategy (i.e., sugar yield). Hence, one pretreatment strategy might be more suited for a specific type of biomass than another due to varying interactions with the pretreatment liquid. In this section, we therefore review the role of solvents and ions in the pretreatment liquid.

Table 2.3: Influence of different concentrations c of soluble biomass components (lignin derivatives, organic acids, sugars) and products of carbohydrate degradation (furan derivatives, organic acids) on enzymatic hydrolysis and simultaneous saccharification and fermentation (SSF).

Type	**Component**	c **(g L^{-1})**	**Effect**
lignin derivatives	syringaldehyde + 4-hydroxybenzaldehyde + vanillin	0.5 + 1 + 2	no effect on glucose formation, 16% less reducing sugars [160]
	phenolics	1.3	removal of phenolics increases sugar yield by 20 wt % (abs) [159]
		9	minor influence on cellulose conversion [158]
	vanillin	0.5	elongation of lag phase and 26.5% lower ethanol yield after SSF [160]
furan derivatives	HMF + furfural	4 (total)	no effect on cellulases [159]
		4 + 3.9	slight inhibition of cellulases [158]
	5-HMF + furfural	2 + 2	no effect on glucose formation, 15% less reducing sugars [160]
	5-HMF	0.5	elongation of lag phase and 16% lower ethanol yield after SSF [160]
organic acids	formic acid	11.5	strong reduction of cellulose conversion, inactivation of enzymes [160]
		1	48% lower ethanol yield after SSF [160]
	acetic acid	13	no effect on cellulases [159]
		15	up to 10 wt % (abs) lower cellulose conversion [158]
		2	no effect on cellulases, elongation of lag phase and 15% lower ethanol yield after SSF [160]
	levulinic acid	29	27% lower cellulose conversion [160]
		1	38% lower ethanol yield after SSF [160]
sugars	xylose	21	10 wt % (abs) lower glucose yield, 10% lower initial hydrolysis rate [159]
	xylo-oligomers	8	20 wt % (abs) lower glucose yield, 40% lower initial hydrolysis rate [159]
	soluble sugars	140	up to 20 wt % (abs) lower cellulose conversion [158]

2.2.3.1 Parameters for the Description of Pretreatment Liquids

Liquid-based pretreatment strategies rely on dilute or concentrated electrolyte solutions that can be aqueous or organic solvent-based. Several parameters have been suggested to correlate pretreatment effectiveness with characteristics of the pretreatment strategy including the pretreatment liquid (see Tab. 2.4).

Severity factors Taking pretreatment as a chemical reaction, a first attempt to characterize pretreatment is the severity factor $\mathrm{SF} = \log R_0$ with reaction ordinate R_0 (first termed H-factor [161] or prehydrolysis factor [162]). Originally, it was developed to characterize the kraft pulping process and it has since been used in many studies to describe pretreatment kinetics. R_0, and thus SF, accounts for the residence time of a pretreatment process τ at temperature T:

$$R_0 = \tau \exp\left(\frac{T - T_\mathrm{R}}{14.75}\right). \tag{2.1}$$

SF is based on the assumption that reaction kinetics follow first-order reactions and that rate constants have an Arrhenius-type dependence on temperature (i.e., an increase in relative reaction rates with an increase in temperature) [161, 162]. Usually, the reference temperature T_R is arbitrarily set to 100 °C with a relative reaction rate of unity. Furthermore, the value 14.75 in Eq. (2.1) is an empirical value accounting for an approximate doubling of reaction rates with an increase in temperature of 10 °C. Strictly speaking, a correlation between SF and pulp characteristics is only valid for a certain set of experimental conditions. A change of, for example, wood species, liquor composition or equipment requires the determination of a new SF–pulp characteristics correlation [161, 162]. Nevertheless, SF calculated from Eq. (2.1) is often used for different pretreatment strategies without further re-evaluation. Overend et al. [163] were the first to review correlations between SF and removal of cellulose, hemicellulose, and lignin after steam- and aqueous pretreatment of mainly northern hardwood. The authors concluded that the yield and composition of removed and recovered fraction after pretreatment can be correlated to SF.

Table 2.4: Parameters used for the description of biomass pretreatment.

Name	Formula	References	Application/Usefulness
Severity factors			
Severity factor	$\mathrm{SF} = \log R_0$ $R_0 = \tau \exp\left(\frac{T - T_\mathrm{R}}{14.75}\right)$	[161, 162]	• originally used for kraft pulping, often applied to aqueous pretreatment • accounts for changes in relative reaction rates • correlations between SF and pulp characteristics only valid for a certain set of experimental conditions • correlates mainly with removal of hemicellulose • does not consider pretreatment liquid
Combined severity factor	$\mathrm{CSF} = \log(R_0) - \mathrm{pH}$	[164, 165]	• considers proton concentration in pretreatment liquid • applied to aqueous and OS pretreatment • correlation with pretreatment results mostly confined to specific studies • does not consider type and concentration of solvent
Indicator-based solvent parameters			
Hammett acidity	$H_0 = \mathrm{p}K_{\mathrm{BH}^+} - \log\left(\frac{c_{\mathrm{BH}^+}}{c_\mathrm{B}}\right)$	[166]	• extension of pH scale towards strong acidic solutions • extent of protonation of a weak indicator base $c_{\mathrm{BH}^+}/c_\mathrm{B}$ measured spectroscopically • assumption of negligible activity corrections • correlations between pretreatment phenomena and H_0 mostly unsuccessful
Kamlet–Taft parameters	$XYZ = XYZ_0 + a \cdot \alpha + b \cdot \beta + s(\pi^* + d\delta) + h \cdot \delta_\mathrm{H} + e \cdot \xi$	[167, 168]	• linear solvation energy relationship between physicochemical property XYZ and acidity α, basicity β, and polarizability π^* of a solvent • measured spectroscopically • for a change in temperature and composition, parameters have to be determined newly • often used to characterize IL mixtures • correlations with ability of solvent (IL) to swell and dissolve cellulose/wood

Name	Formula	References	Application/Usefulness
Solubility parameters			
Hildebrand solubility parameter	$\delta = \sqrt{\frac{-E}{V_\mathrm{m}}} \cong \sqrt{\frac{\Delta H_\mathrm{v} - RT}{V_\mathrm{m}}}$	[169–171]	• square root of cohesive energy density • similar δ-values indicate solubility of a solute in a solvent • temperature and mixture corrections available • typically used to evaluate solubility of lignin in a solvent • often applied to OS and IL pretreatment
Hansen solubility parameters	$\delta^2 = \delta_\mathrm{D}^2 + \delta_\mathrm{P}^2 + \delta_\mathrm{H}^2$	[170, 172, 173]	• estimation of cohesive energy density with dispersive interactions δ_D, polar interactions δ_P and hydrogen bonds δ_H • temperature and mixture corrections available • solubility if solvent parameters are within the solvation sphere of a solute • often applied to OS and IL pretreatment

Another study shows that correlations between SF and residual xylan content after hydrothermal pretreatment can be generalized independent of the type of feedstock and specific experimental conditions (for 13 evaluated experimental series), whereas correlations between SF and residual acetyl content can only be combined for eucalyptus, corncob and poplar [174]. In spite of the observed correlations, the applicability of SF is limited because it only includes residence time and temperature as variables and no information about the composition of the pretreatment liquid.

The combined severity factor (CSF) was developed to account for the influence of catalyst in OS pretreatment of aspen wood by including the proton concentration $c_{\mathrm{H^+}}$ in the form of pH ($\mathrm{pH} = -\log c_{\mathrm{H^+}}$) [164]:

$$\mathrm{CSF} = \log(R_0) - \mathrm{pH}. \tag{2.2}$$

The kinetic analysis that SF and CSF are based on has been further detailed with fitting of parameters related to activation energy and structural accessibility. In this way, good agreement was achieved between model and experiment of acid-catalyzed hemicellulose solubilization for four types of biomass for low to moderate severities. More specifically, SF of the individual experiment series correlates with hemicellulose removal up to 70 wt %, whereas at higher severities (that are specific for each experiment series) the model overestimates hemicellulose removal [165]. The application of CSF is not restricted to hemicellulose removal. In several types of OS-pretreated biomass, lignin removal correlates with CSF [127, 175]. In contrast, sugar yields of multiple aqueous pretreatment strategies cannot be linked to SF or CSF, even when only one type of biomass is considered [176]. For OS pretreatment of empty palm fruit bunch with sulfuric acid catalyst, sugar yields correlate with CSF, whereas glucose yield after ethanol pretreatment with acetic acid catalyst of eucalyptus and bagasse flour does not correlate with CSF [127, 175]. Thus, the possibility of linking CSF to sugar yields remains unclear and likely limited to specific processes but fails even for simple aqueous pretreatments. Moreover, the extension of CSF to nonaqueous pretreatments is limited because the optimal CSF depends on the type of biomass and the influence of changing the type of solvent or solvent concentration is not covered by CSF [56].

In conclusion, SF and CSF can be helpful to improve process conditions for a specific pretreatment concept. A generalization seems doubtful, because the few existing correlations between SF/CSF and pretreatment results are mostly confined to a specific study and correlations are limited to biomass composition, whereas glucose yield is mainly determined by a mechanism not covered by CSF. Clearly, pH has a pre-

dominant influence, but pH is usually taken as measured at room temperature and not corrected for the influence of solvent, high ionic strengths and high temperatures of pretreatment (cf. Yawalata and Paszner [103], Teramoto et al. [127], Goh et al. [175]). Thus, CSF does not take into account the true proton concentration, which might blur correlations between CSF and pretreatment results.

Indicator-based solvent parameters As far as the influence of acidity is concerned, the simplified correlation between proton concentration and pH only holds for dilute aqueous solutions ($c_{H^+} \leq 0.1\,\mathrm{mol\,L^{-1}}$). To account for the influence of high ionic strengths due to high acid or salt concentrations, activity corrections are required. Furthermore, there is no common methodology to transfer the concept of pH to nonaqueous solvents. To describe acidity in concentrated and nonaqueous systems, which are often used for pretreatment, several solvent parameters have been developed.

The Hammett acidity H_0 extends the pH scale towards strong acidic solutions by measuring the extent of protonation of a weak, monoprotic indicator base (e.g., anilines):

$$H_0 = \mathrm{p}K_{\mathrm{BH^+}} - \log\left(\frac{c_{\mathrm{BH^+}}}{c_{\mathrm{B}}}\right). \tag{2.3}$$

The ratio of protonated to unprotonated base $c_{\mathrm{BH^+}}/c_{\mathrm{B}}$ can be measured by colorimetry, NMR or UV-vis spectroscopy. The latter is restricted to measurements of transparent solutions to not interfere with the color of the indicator [166, 177]. The Hammett acidity function relies on the assumption that the relative strength of two bases of the same charge type is independent of the solvent in which they are measured and that activity corrections are negligible [166]. Thus, when the base dissociation constant $\mathrm{p}K_{\mathrm{BH^+}}$ is known, H_0 is measurable also in nonaqueous solutions and acidities of two solutions with similar properties can be compared with the same or closely related indicators. Problems during determination of H_0 can arise due to interaction of the acid anion with the protonated indicator base [177].

H_0 has rarely been applied in the context of biomass pretreatment. In one study, the maximum sugar release of hydrolysis subsequent to pretreatment of macroalgae in IL mixtures relates to H_0 of the IL mixtures [178]. In contrast, correlations between H_0 of IL mixtures and cleavage of lignin model compounds in these mixtures are weak or not observable and reactivity is more associated to hydrogen bonding characteristics of the IL [179, 180].

Hydrogen bonds not only influence the properties of a solvent or solvent mixture that is applied as pretreatment liquid but also affect the interaction between biomass

and pretreatment liquid. Hence, some parameters refer to hydrogen bonding characteristics. Hydrogen-bond donating ability (acidity), hydrogen-bond accepting ability (basicity) and polarity/polarizability of a solvent can be described by the Kamlet–Taft (KT) parameters α, β and π^*, respectively [167]. In form of a linear solvation energy relationship, the KT parameters relate to a range of solvent-dependent physicochemical properties XYZ such as reaction rates, solubilities or spectral frequencies:

$$XYZ = XYZ_0 + a \cdot \alpha + b \cdot \beta + s(\pi^* + d\delta) + h \cdot \delta_{\mathrm{H}} + e \cdot \xi \tag{2.4}$$

with XYZ_0 measured in a reference system. The parameters a, b, s are solvent-independent correlation coefficients that are specific for the regarded property and the remaining terms account for example for influences of specific compounds on polarizability and basicity [168]. Like H_0, the solvatochromic KT parameters are determined spectroscopically. They can be derived from the wavelength of maximum absorption $\lambda_{\max}$ of a variety of dyes added to the respective solvent (i.e., $\lambda_{\max}$ is the physicochemical property XYZ in Eq. (2.4)). Using reference solvents (methanol for α, hexamethylphosphoric triamide for β and dimethyl sulfoxide for π^*), each parameter is normalized to a value of 1, although this does not represent an upper limit of the parameters [168, 181]. The usage of several dyes for the determination of KT parameters often results in inconsistent data reported in the literature, which make the values not directly comparable [181]. In binary solvent solutions, preferential solvation of the indicator dye can lead to nonideal relations between molar composition and KT parameters [182]. Moreover, KT parameters vary with temperature [183, 184]. For example, π^* of several ILs decreases up to 0.15 with an increase in temperature from 20 °C to 100 °C [184]. Due to the variations with temperature or upon addition of a second solvent (e.g., water to an IL) it is very laborious to determine all parameter sets that are of interest, when comparing the influence of changing process conditions on the dissolution of cellulose or the effectiveness of biomass pretreatment.

KT parameters are often used for the characterization of IL mixtures. For example, the ability of BMIM-based ILs to swell and dissolve wood or cellulose increases with increasing basicity β of the anion [98, 185]. Similarly, the hydrolysis rate of cellulose pretreated with pure BMIM-based ILs positively correlates with β, whereas after the addition of water to the tested ILs this correlation becomes invalid [186]. While it is plausible that the addition of even small amounts of water influences the KT parameters of ILs or other solvents such as DES [183, 184], the application of only β for the correlation of cellulose dissolution and biomass pretreatment is limited. For several ILs and some classical solvents with cellulose dissolution ability, the net basicity $\beta - \alpha$ seems to be more meaningful than β only [184]. Additionally, the

combination of β and density of ILs was shown to influence the ability to dissolve cellulose [187], while β divided by the mole fraction of water added to an IL relates to the extraction of low-molecular-mass hemicellulose polymers during IL pretreatment of birch wood [188].

The separate determination of polarizability and dipolarity, which are combined in the KT parameter π^*, is realized in the Catalán solvent scale [189]. Catalán solvent parameters have been determined for several ILs [190] but these values have not yet been linked to biomass pretreatment.

Altogether, these multiparameter approaches do not consider real mechanisms that are obviously based on particular interactions of local environments in the solvent. A further drawback of all solvent parameter concepts relying on dyes for spectroscopic determination is that the parameter values cannot be measured online, which would be useful for process monitoring in a biorefinery.

Solubility parameters The Hildebrand solubility parameter δ refers to the square root of cohesive energy density as an estimate of the energy that is required to separate molecules in a liquid from one another and can thus be used as an indicator for the solubility of a solute in a solvent (two substances with similar δ-values likely gain sufficient energy on mutual dispersion to allow for mixing) [169, 170]:

$$\delta = \sqrt{\frac{-E}{V_\mathrm{m}}} \cong \sqrt{\frac{\Delta H_\mathrm{v} - RT}{V_\mathrm{m}}}. \tag{2.5}$$

δ is often used for the characterization of polymers and there are several methods for its estimation [169]. Usually, the energy of vaporization to gas at zero pressure E is determined from the molar enthalpy of vaporization H_v. H_v, molar volume $V_\mathrm{m} = M/\rho$ or density ρ as well as δ-values for a range of typical solvents can be obtained from the literature. If necessary, the molar properties can be corrected for the influence of a changing temperature [169, 170]. Unknown V_m can for example be estimated with group contribution methods [170, 171] and ρ can be determined experimentally. Originally, the Hildebrand parameter was intended for nonpolar, non-hydrogen-bonding solvents [169], but its use has been extended to other types of solvents as well [170].

In the context of biomass pretreatment, mostly δ_lignin is estimated to approximately 23–26 $\mathrm{MPa}^{1/2}$ [137, 191, 192] as the parameter of a biomass component and it is typically used to evaluate the solubility of lignin in a certain pretreatment liquid (cf. Zhao et al. [56], Barton [170] for a list of δ for OS solvents). More specifically, the

lignin yield after OS extraction with different organic solvents varies with δ_{solvent} and a higher expected solubility of lignin in solvents is beneficial for the removal of up to 80 wt % lignin [137]. Similar observations have been made for lignin solubilization in EMIMAc: by adding solvents to EMIMAc, δ_{mixture} can be tuned to be close to δ_{lignin} for enhanced lignin solubility [192]. Furthermore, the swelling of OS pulp fibers in ethanol–water solutions positively correlates with the δ-value of these mixtures with highest swelling observed close to the estimated δ_{pulp} [193].

The determination of cohesive energy density (i.e., δ^2) has been refined by Hansen in form of the Hansen solubility parameters (HSP), which represent a point in three-dimensional space accounting for three different types of intermolecular interactions:

$$\delta^2 = \delta_{\text{D}}^2 + \delta_{\text{P}}^2 + \delta_{\text{H}}^2 \tag{2.6}$$

with contribution of dispersive/nonpolar interactions δ_{D}, polar interactions δ_{P} and hydrogen bonds δ_{H}, which are determined experimentally [170, 172]. Analogously to the Hildebrand parameter of a mixture, the HSP of a solvent mixture can be estimated with a volume-based mixing rule. Solutes (e.g., a polymer such as lignin) are described by a sphere with radius R_0 from the center of the respective solubility parameters. For solubility of a polymer in a solvent, the vector of the solvent's HSP must terminate within the solubility sphere of the polymer. With changing temperature, the solvent's HSP can move in or out of the solubility sphere and hence they require temperature correction [173].

According to Hansen's theory, the differing solubility parameters of cellulose and lignin result in these two components not being oriented towards each other, whereas hemicellulose can interact with both, stabilizing the wood structure. Therefore, wood as a composite material cannot be dissolved (in the classical definition) [194]. Nevertheless, some solvents alter the ultrastructure of lignocellulosic biomass in accordance with HSP. BMIMBr–ethanol–water mixtures have successfully been prepared based on HSP to selectively fractionate cellulose and lignin from pine wood with a purity of more than 90 wt % each [195]. Furthermore, for a range of organic solvents and lignin, the solvent–solute distance of HSP correlates with the degree of delignification after OS pretreatment of sugarcane bagasse and rice straw [196, 197]. However, the applicability of HSP is thus restricted to the removal of lignin and HSP can only indirectly be used for the prediction of sugar yields after enzymatic hydrolysis in case the relation between lignin removal and hydrolysis yields is known. With regard to cellulose, HSP are ambiguous and prediction of cellulose solubility with HSP is not reliable [198].

In conclusion, there are both studies that show limitations of the applicability of these parameters as well as studies that successfully correlate the above discussed parameters for the characterization of pretreatment liquids with pretreatment effects. Nevertheless, in most cases the evaluation of parameters with regard to pretreatment effects is qualitative and there is only a limited number of studies that provide quantitative relationships. Furthermore, the currently available data do not provide one range of general descriptors that is beneficial for pretreatment. Thus, more studies are needed that can be combined for a universally applicable regression between parameters for the description of pretreatment liquids and pretreatment effects.

In one review comparing a variety of solvent parameters (including the above mentioned), four independent solvent properties were identified: (1) hydrogen bond donation ability, (2) hydrogen bond acceptance/electron pair donation ability, (3) polarity and polarizability, and (4) solvent stiffness (i.e., cohesive energy density) [199]. However, none of the parameter concepts discussed above considers all four independent solvent properties and hence we suggest that more than one parameter concept should be looked at to comprehensively describe the solvation ability of a pretreatment liquid. This could, for example, be the Hildebrand or Hansen solubility parameters in combination with the KT parameters to evaluate the potential for solution of extracted biomass components in the pretreatment liquid. Furthermore, in our opinion more research should be carried out to investigate not only the solution potential but also quantitative relationships between the reviewed parameters and enzymatic hydrolysis after pretreatment. Nevertheless, catalytic reactions that lead to cleavage of biomass components which are then soluble in the pretreatment liquid are not covered by the reviewed parameters.

2.2.3.2 Biomass Interaction with Solvents and Ions in Pretreatment Liquids

As indicated above, wood itself is insoluble and at the current status, solubility parameters alone cannot explain the effects of swelling and pretreatment of wood [194]. Besides solubility of extracted components in the pretreatment liquid, (reactive) interactions between biomass and solvents and ions of pretreatment liquids play a role during pretreatment. So far, these interactions have not been described quantitatively but a quantitative description should include the components and conditions of the reactions (solvents, ions, concentrations etc.).

The type of solvent does not only influence the amount of lignin that is potentially soluble in the pretreatment liquid (see Section 2.2.2.2) but also the composition of

the extracted lignin. For OS pretreatment, this results in lignin extracted with organic solvents having a higher purity than that extracted with acidic solutions due to additional cleavage of hemicellulose and oxidation as well as acetylation reactions of the acidic lignin [200]. Nevertheless, organic solvents such as the linear alcohols methanol, ethanol and 1-propanol also react with lignin and are thus incorporated into the extracted lignin [137].

The role of ions has been well studied for biomass pretreatment and cellulose dissolution in ILs. In this context, cations [201, 202] and anions [185] both determine the ability of an IL to dissolve cellulose. Likewise, some anions are not suited for swelling and disintegrating biomass (e.g., dicyanamide) [98], whereas other anions lead to higher sugar yields after enzymatic hydrolysis (e.g., acetate) [104]. Sugars that are released during pretreatment can even react and covalently bind to the C(2)-carbon of the imidazolium cation in EMIMAc [203], while BMIM-based ILs react with the reducing end of cellulose [204]. Thus, depending on the combination of cation and anion, ILs may not only be solvents in the classical definition but also react with components of biomass and hence influence the outcome of a pretreatment.

The importance of ions is further reflected in depolymerization and dissolution of cellulose where charged species effectively disrupt the hydrogen-bond network of cellulose. Therefore, the addition of salts to ammonium-based solvents enhances cellulose dissolution [205, 206] or aids auto-catalytic [207] as well as acid-catalyzed [208, 209] depolymerization of cellulose in aqueous solutions.

Ions also play a role as catalysts determining the acidity of neutral OS pretreatment liquids, which in turn controls pretreatment selectivity and disintegration of biomass [105]. More specifically, during OS pretreatment of spruce, the extent of disintegration depends on the type of anion, whether the anion is in salt or acid form and the concentration of the catalyst. Additionally, divalent cations of chloride salts effectively disintegrate softwood, whereas mono- and trivalent cations are too weak and too aggressive, respectively. Aggressive disintegration with trivalent cations stands for a complete destruction of fibers by unselective cleavage of both lignin and carbohydrates. Furthermore, disintegration correlates with pH of the pretreatment liquid after pretreatment, which is influenced by acetic acid formed due to the release of acetyl groups from wood. In an optimal pH range between 3.5 and 4.2, biomass is disintegrated, whereas at higher and lower pH, biomass is not disintegrated and fibers are completely destructed, respectively [103, 210]. Analogously, acid-catalyzed depolymerization of hemicellulose from beech wood in a biphasic solvent system consisting of water and 2-methyltetrahydrofuran remains effective if the pH of the aqueous phase is below 2 [211]. Besides pH, the acid strength of the catalyst (i.e., pK_a)

is important when describing ions of a pretreatment liquid: For OS pretreatment of Japanese cedar, the sugar yield after enzymatic hydrolysis linearly correlates with the (aqueous) pK_a of most employed catalysts, with a $pK_a < 0$ being most effective to increase digestibility [212]. Similarly, for acid-catalyzed conversion of the biomass model compounds xylose and cellobiose in the organic solvent γ-valerolactone and the IL EMIMCl, respectively, reactivities and selectivities increase below a pK_a of the acid catalyst of 0 and -2 [213, 214].

Unlike in acidic pretreatment liquids, the extent of both deacetylation and delignification is independent of concentration and type of cation for pretreatment of aspen wood in alkali metal hydroxide solutions. In contrast, the stoichiometric ratio between base in the pretreatment liquid and the amount of acetyl groups in added wood linearly correlates with the amount of removed acetyl groups after pretreatment [124]. In studies on acetosolv OS pretreatment, however, the process variables cooking time, temperature, and liquid-to-wood ratio have less influence on pulp yield and pulp composition than the concentrations of acetic acid (i.e., the solvent) and catalyst [141, 215]. Furthermore, there is a threshold value for catalyst concentration, above which lignin condensation reactions occur [215].

Besides the concentration of the individual components in the pretreatment liquid, the water content impacts pretreatment effectiveness especially in concentrated pretreatment liquids. While water is tolerable in high concentrations for OS pretreatment (typically up to 50 wt % [56]), pretreatment with ILs is more sensitive to the water content. An increasing water content significantly impacts the solubility of spruce and pine wood in ILs [98, 117] and above 10.7 wt %, water limits disintegration of beech wood in EMIMAc [19].

In conclusion, pretreatment liquids act as more than classical solvents for extracted biomass components, because reactive interactions between biomass and active species in the pretreatment liquid can significantly influence the outcome of a pretreatment strategy. Hence, ions added to the pretreatment liquid as salts or acids mostly support disintegration of biomass or catalyze decrystallization of cellulose, while the type of solvent influences the extent of lignin removal as well as lignin composition. The overall composition, especially the water content of the pretreatment liquid, further determines the outcome of pretreatment, sometimes in very narrow ranges.

2.3 Summary and Conclusion

Economic and carbon-efficient production of biofuels and bioproducts in lignocellulosic biorefineries relies on effective pretreatment and hydrolysis strategies that achieve high sugar yields for further conversion. In this context, a variety of pretreatment phenomena on several scales are essential for high sugar yields. An effective pretreatment increases the surface area that is accessible to enzymes in the hydrolysis step. Typically, this is connected to a macroscopic disintegration of the biomass in combination with formation of pores on an ultrastructural level. Furthermore, lignin should be removed from the composite biomass so that the overall lignin content is reduced while redeposition of the solubilized lignin is avoided to make the cellulose fraction more accessible. On the molecular level, a reduced crystallinity of pure cellulose clearly correlates with an increased enzymatic digestibility while pretreatment of lignocellulosic biomass often leads to an increased biomass crystallinity together with an increased digestibility. However, this does not necessarily imply a correlation between biomass crystallinity and digestibility because changes in biomass crystallinity after pretreatment are often affected by other factors (e.g., accessible surface area or removal of lignin) that may have more influence on digestibility than the crystallinity itself. Deacetylation of the hemicellulose fraction during pretreatment can additionally enhance digestibility of the pretreated biomass albeit in a limited extent. Moreover, it is important that the carbohydrate fractions in lignocellulosic biomass are not degraded due to severe pretreatment conditions because degradation products as well as components that are solubilized during pretreatment can negatively influence hydrolysis and fermentation. To avoid severe pretreatment with undesired outcomes, the influence of process conditions as well as solvents and ions of the pretreatment liquid on the occurrence of pretreatment phenomena should be known.

Overall, the composition of the pretreatment liquid plays a decisive role in determining the outcome of pretreatment. The complete mechanism of effective biomass pretreatment is unknown due to the complex structure of lignocellulosic biomass, but clearly pretreatment phenomena are connected to the molecular composition of pretreatment liquids. Cations and anions of salt or acid catalysts significantly influence the extent of disintegration and facilitate cellulose depolymerization, thus allowing for high sugar yields. Moreover, the type and concentration of solvent on the one hand influence the maximum removal of lignin as a result of lignin solubility and on the other hand influence lignin composition due to reactive interactions between lignin and solvent molecules. Hence, a solvent can turn into a catalyst due to reactions with biomass components. By and large, the composition of the pretreatment liquid affects pretreatment results more than process variables, although a compre-

hensive analysis across studies is only meaningful if the ratio of biomass to liquid is also considered. In the past, several parameters have been evaluated with regard to the correlation between pretreatment phenomena and characteristics of the pretreatment strategy. These include the severity factor and further derived factors mostly for aqueous pretreatments, solvent parameters (Hammett, Kamlet–Taft) to describe acid–base characteristics of electrolyte solutions such as ILs and OS pretreatment liquids, and solubility parameters (Hildebrand, Hansen) to, for example, evaluate solubility of lignin in a pretreatment liquid. However, these lumped parameters are mostly not sufficient to cover all observed phenomena, while the large variety of hitherto tested pretreatment liquids makes it difficult to define one common parameter to characterize them. Additionally, reactive interactions of solvents and ions with biomass have been observed but have not yet been quantified and parameterized. With regard to the catalytic activity in acidic pretreatments, a low pH of the aqueous phase or an (aqueous) pK_a of the catalyst below approximately 0 to -2 appears beneficial for an effective pretreatment. However, this has neither been systematically compared for varying pretreatment liquids nor been extended towards alkaline pretreatment.

In general, phenomenological changes across scales that occur during pretreatment should be comprehensively correlated taking account of changes in biomass structure and composition as well as the role of components in a pretreatment liquid. One promising option would be to develop more advanced multivariate analyses that consider solubility of biomass components and determine how interactions between pretreatment liquid and lignocellulosic biomass lead to an effective pretreatment (e.g., as a combination of the reviewed parameters). Additionally, advanced analytical tools should be employed to allow for a standardized evaluation of pretreatment experiments and hence improved comparability of research results of different disciplines. For example, changed swelling characteristics of biomass resulting from changed particle size, porosity and/or chemical composition after pretreatment should be explored as an indicator of accessibility. At the process level, an increased sugar yield resulting from increased accessibility after pretreatment is connected to changed costs. Thus, an integrated perspective considering yields as well as costs for the solvent and equipment is required for the design of novel, cheap and effective pretreatment liquids.

This overview shows that liquid-based pretreatment of lignocellulosic biomass is a process step with mechanisms on multiple levels of scale that are not yet completely understood. Presumably, the pretreatment mechanisms are often connected to the composition of the pretreatment liquid. This thesis therefore includes a multi-scale analysis of pretreatment of lignocellulosic biomass paying special attention to the role of the pretreatment liquid.

Chapter 3

Materials and Methods

The outcome of biomass pretreatment is influenced by the composition of the pretreatment liquid as well as molecular interactions of species therein. In this thesis, EMIMAc, an IL well-known for effective biomass pretreatment, is investigated with low-field NMR spectroscopy to resolve molecular interactions with water and acetic acid. Furthermore, experiments are presented for pretreatment of beech wood with mixtures of EMIMAc and an OS process based on acetic acid (i.e., acetosolv). To evaluate the impact of pretreatment effectiveness on the process performance of biofuel production, a screening of several alternative pretreatment strategies at an early design stage is carried out. The experimental and methodical details of aspects related to pretreatment from molecular interaction in the pretreatment liquid (Section 3.2), via biomass pretreatment experiments on lab scale (Section 3.1) to the process perspective (Section 3.3) are illustrated in this chapter.

3.1 Pretreatment of Beech Wood

First, in Subsection 3.1.1, the experimental procedure for pretreatment of beech wood with ILs and acetosolv liquids is described. Then, Subsection 3.1.2 gives details on the compositional analysis of the recovered fraction and presents methods relying on low-field NMR spectroscopy that were developed for the analysis of acetyl content in the recovered fraction as well as the qualitative and quantitative analysis of dissolved components.

3.1.1 Pretreatment Experiments

For the pretreatment with ILs, EMIMAc (Iolitec, purity grade > 95%, impurities not further specified by manufacturer; our own NMR analyses show > 97.5 wt %

purity) was used without further processing or purification. Mixtures of EMIMAc and deionized water (AQUADEM DL) or acetic acid (Merck, 100%) were prepared by weight to cover the range from concentrated EMIMAc down to dilute solutions in steps of approximately 10 mol %. The water content in EMIMAc was determined with coulometric Karl Fischer titration (Metrohm 831 KF with Hydranal-Coulomat E, reproducibility $< 0.3\%$) and accounted for in the calculation of weight and mole fractions. The determination of water content was repeated regularly to check whether the water content remained constant during the measurement series.

The employed acetosolv pretreatment liquids consisted of acetic acid (VWR, 100%) with a variety of catalyst acids of different pK_a (the organic acids formic acid (Merck, 99%) and oxalic acid (Merck, dihydrate form) as well as the inorganic acids phosphoric acid (Acros organics, 95%; Applichem, 85%), sulfuric acid (Merck, 95%; Applichem, 72%; Carl Roth, 1 mol L^{-1}), hydrochloric acid (Kruse, 30%; Merck, 1 mol L^{-1}; Carl Roth, 37%) and hydroiodic acid (VWR, 57%)). All employed catalyst acids are stronger acids than acetic acid (i.e., lower pK_a). The pretreatment liquids were prepared by weight and the water content was not further adjusted but resulted from the purity of the employed catalyst acids (i.e., the water content increased with increasing catalyst molarity). All chemicals were used as received without further purification.

Two main sets of acetosolv pretreatment liquids were investigated. For the first set, pretreatment liquids of all above-mentioned catalysts were prepared at similar molalities to evaluate the influence of the acid strength of the catalyst. These acetosolv experiments were carried out at an approximate ratio of catalyst to acetic acid of 0.25 $mmol_{cat}\ g_{AA}^{-1}$. The second set consisted of acetic acid in combination with hydrochloric, sulfuric or phosphoric acid as three representative catalyst acids to evaluate the influence of varying catalyst molarities (i.e., one type of catalyst at different molar concentrations). The mineral acids sulfuric and hydrochloric acid were chosen because both have been employed for acetosolv pretreatment (cf. Kin [216], Shui et al. [217]). Regarding less strong catalyst acids, the applicability of oxalic acid as a catalyst acid is limited by solubility of oxalic acid in acetic acid–water mixtures [218]. Hence, oxalic acid was not selected for the experiments with varying catalyst molarities but we chose phosphoric acid as the third catalyst acid complementing the other two mineral acids.

Additionally, a few experiments with a higher water content of up to 50 mol % were carried out by adding deionized water (inhouse, conductivity approximately 0.8 µS cm^{-1}) to adjust the water content. Pure acetic acid was used as a reference pretreatment liquid without catalyst to distinguish between the influence of acetic acid as main solvent and catalyst acids. Furthermore, reference experiments containing

only water with catalyst acids were carried out to evaluate the interplay of acetic acid and catalyst acid.

By and large, the experimental procedure for IL and acetosolv pretreatment followed the same protocol. When indicated, slight modifications were made between IL and acetosolv experiments; otherwise, conditions were the same. Beech veneer chips (10 mm×2 mm, stored at ambient temperature, average moisture content of 4.5 wt %) at 5 wt % biomass loading were used for all pretreatment experiments. 100 mg and 500 mg beech were used for the IL and acetosolv experiments, respectively (acetosolv experiments carried out in duplicate). Experiments were conducted in 50 ml centrifuge tubes that were heated for 2 h in an aluminum heating block at 115 °C and atmospheric pressure (typical IL and acetosolv pretreatment conditions; cf. Brandt et al. [57], Viell et al. [107], Ligero et al. [141], Vila et al. [215], Parajó et al. [219]). The samples were stirred at 200 rpm (IL) or 250 rpm (acetosolv) with a magnetic stir bar (15 mm length, 9 mm diameter). Full submersion of the beech chips was checked periodically. After pretreatment, the samples were cooled down with tap water. 20 mL of deionized water was added to the IL experiments and stirred for 5 min at 300 rpm to remove IL attached to the biomass. The IL samples were centrifuged at 10,000 rpm for 10 min, the supernatant decanted (no further analysis) and the washing step repeated. After cooling, the acetosolv samples were directly centrifuged at 10,000 rpm for 10 min and the supernatant was separated for the analysis of the dissolved fraction with low-field NMR. The remaining pretreated, wet biomass (IL and acetosolv) was filtered by vacuum with filter crucible POR4 (pore size 10–16 µm) and washed at least 3 times with deionized water. The filter crucibles with the recovered biomass were dried for at least 16 h at 105°C in a drying oven. The procedure of experiments is sketched in Fig. 3.1.

In the following, recovered fraction w_r refers to the recovered, dry mass after pretreatment m_r as a fraction of the initial amount of beech wood m_wood taking into account the moisture content w_m of the wood:

$$w_\mathrm{r} = \frac{m_\mathrm{r}}{m_\mathrm{wood}(1 - w_\mathrm{m})}. \tag{3.1}$$

The term non-recovered fraction w_nr refers to the mass fraction that was not recovered (i.e., solubilized in the pretreatment liquid, not recovered in filter crucible due to small particle size etc.) and is calculated from the closure constraint of wood mass balance:

$$w_\mathrm{nr} = 1 - w_\mathrm{r}. \tag{3.2}$$

The recovered fraction was stored at ambient temperature until further analysis (composition, acetylation, enzymatic hydrolysis).

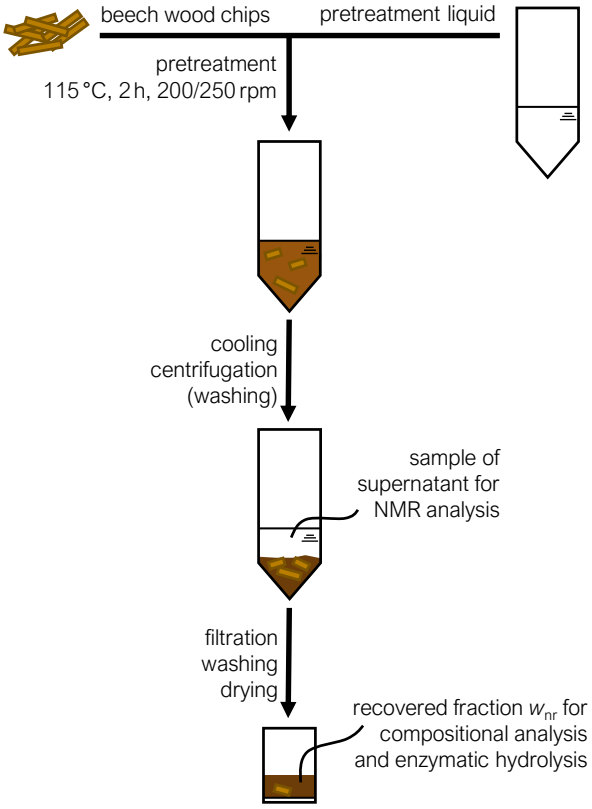

Figure 3.1: Scheme of the experimental procedure for pretreatment of beech wood. The focus is on the main steps where samples are taken. The color and size of the sketched wood chips do not reflect the actual changes during pretreatment.

3.1.2 Analysis of Recovered and Dissolved Fraction

Prior to component analysis and enzymatic hydrolysis, the dried biomass samples were milled in a centrifugal grinding mill (ZM 200 Fritsch, 0.5 mm mesh size).

Acid hydrolysis to determine the composition of native and pretreated beech wood was carried out according to the NREL protocol *Determination of Structural Carbohydrates and Lignin in Biomass* [130]. Native beech had an average composition of 41.8 wt % cellulose (measured as glucose), 26.2 wt % hemicellulose (measured as 19.8 wt % xylose and 6.4 wt % mannose) and 17.3 wt % acid-insoluble lignin.

Enzymatic hydrolysis of pretreated beech wood was carried out in an enzyme–buffer solution containing 0.1 mol L^{-1} sodium acetate at pH 4.8 for 72 h. It should be noted that hydrolysis conditions slightly differed between IL and acetosolv exper-

iments. Enzymatic hydrolysis of IL-pretreated beech was carried out with 84 mg g^{-1} protein (cellulase from Celluclast (Novozymes)) per biomass at a biomass loading of 20 mg mL^{-1} in 2 mL Eppendorf tubes. The IL samples were hydrolyzed in a thermomixer at 900 rpm and 45 °C. Enzymatic hydrolysis of acetosolv-pretreated beech was carried out in a solution containing 14.05 µL mL^{-1} Celluclast with a biomass loading of 1 wt % in 1.5 mL Eppendorf tubes. The acetosolv samples were hydrolyzed in a thermomixer at a stirring rate of 1000 rpm and a temperature of 50 °C. Assuming a protein concentration of 122 g L^{-1} in Celluclast [126], the hydrolysis conditions for the IL experiments result in 13.77 µL mL^{-1} Celluclast (i.e., similar to acetosolv hydrolysis) while for the acetosolv experiments approximately 171.4 mg g^{-1} protein per biomass was available (i.e., approximately twice as much as for the IL experiments due to the different biomass loadings). Whether the sugar yield after hydrolysis is influenced by the different ratios of protein to biomass is not further investigated in this thesis but sugar yields are taken as is. For the evaluation of hydrolysis effectiveness, the amounts of cellobiose and glucose released during hydrolysis were taken for the calculation of the sugar yield from the cellulose fraction.

For the determination of acetyl content, 200 mg of dry wood were added to 10 g of 1 mol L^{-1} sodium hydroxide solution and heated at 80 °C for 1 h. After heating, the samples were centrifuged at 10,000 rpm for 10 min. A sample of the supernatant was taken for NMR analysis to determine the concentration of acetic acid and further calculate the acetyl content. The solid fraction after deacetylation was filtered and dried in the same manner as the recovered fraction of the pretreated samples.

^{1}H NMR spectra for the analysis of supernatants of acetosolv pretreatment and deacetylation liquids were recorded on a Magritek Spinsolve Carbon benchtop NMR (42.5 MHz). For each spectrum, 64 scans were collected (6.4 s acquisition time, 15 s repetition time, 90° excitation pulse). Phase and baseline correction as well as referencing of peak positions was done with MestReNova software (version 9.1.0 Mestrelab Research S.L.). For the evaluation of spectra, the methyl peak of acetic acid was referenced to 2.04 ppm and 2.084 ppm in concentrated acetosolv solutions and in dilute deacetylation liquids, respectively. Peak areas for the quantitative evaluation of components were integrated with PEAXACT (version 4.5 S-PACT GmbH).

The low concentration of dissolved wood components and degradation products together with the reduced resolution of the low-field NMR spectrometer hamper a quantification of individual components. Nevertheless, the total area of a spectrum A_{tot} is proportional to the amount of hydrogen atoms in the sample $n_{\mathrm{H,tot}}$ which comprises signals of dissolved components. Therefore, in this thesis, a method is developed to estimate the amount of dissolved protons from the spectral area of the

supernatant after pretreatment (see Fig. 3.1) as a fraction of the protons in the wood sample. The amount of hydrogen atoms originating from solubilized components $n_{\mathrm{H,s}}$ can be estimated as the difference between the total amount of hydrogen atoms in a sample $n_{\mathrm{H,tot}}$ and the amount of hydrogen atoms originating from the pretreatment liquid $n_{\mathrm{H,p\text{-}liq}}$

$$n_{\mathrm{H,s}} = n_{\mathrm{H,tot}} - n_{\mathrm{H,p\text{-}liq}}. \tag{3.3}$$

Here, $n_{\mathrm{H,s}}$ does not differentiate where the protons originate from (i.e., sugars dissolved during pretreatment, acetic acid formed due to deacetylation etc.). $n_{\mathrm{H,p\text{-}liq}}$ can be calculated from the molar composition of pretreatment liquids considering the number of hydrogen atoms in one component $n_{\mathrm{H},i}$ for all components in the pretreatment liquid

$$n_{\mathrm{H,p\text{-}liq}} = \sum_{i=1}^{n_{\mathrm{p\text{-}liq}}} n_i n_{\mathrm{H},i} \quad i \in \{\mathrm{AA},\ \mathrm{cat},\ \mathrm{w}\}. \tag{3.4}$$

The total amount of protons $n_{\mathrm{H,tot}}$ in a sample equals the total area of a spectrum A_{tot} divided by a conversion factor $f_{A-n_{\mathrm{H}}}$ that relates area and amount of protons

$$n_{\mathrm{H,tot}} = A_{\mathrm{tot}}/f_{A-n_{\mathrm{H}}}. \tag{3.5}$$

This conversion factor can be calculated from the peak area of the methyl group $A_{\mathrm{CH_3}}$ and the known amount of acetic acid in the pretreatment liquid n_{AA}

$$f_{A-n_{\mathrm{H}}} = \frac{A_{\mathrm{CH_3}} c_{\mathrm{int}}}{3 n_{\mathrm{AA}}} \tag{3.6}$$

with the factor 3 accounting for 3 hydrogen atoms that contribute to the signal of the methyl group and a further constant c_{int} that accounts for the incomplete integration of the peak (it cannot be integrated completely due to partial superposition with signals of solubilized components). Details on integration ranges and determination of c_{int} are given in Appendix B.

The total amount of protons in the wood sample $n_{\mathrm{H,wood}}$ that is used for the experiments is estimated with

$$n_{\mathrm{H,wood}} = m_{\mathrm{wood}}(w_{\mathrm{H,wood}}(1 - w_{\mathrm{m}}) + w_{\mathrm{H,H_2O}} w_{\mathrm{m}})/M_{\mathrm{H}}. \tag{3.7}$$

The hydrogen weight fraction of wood $w_{\mathrm{H,wood}}$ is taken as 0.06 from the average elemental composition of wood [81] and the hydrogen weight fraction of water $w_{\mathrm{H,H_2O}} = 0.112$. Lastly, the fraction of wood protons dissolved in the pretreatment liquid $x_{\mathrm{H,s}}$ is estimated with

$$x_{\mathrm{H,s}} = n_{\mathrm{H,s}}/n_{\mathrm{H,wood}}. \tag{3.8}$$

3.2 Proton Exchange Experiments

The analysis of H/D exchange reactions can serve to elucidate the acid-base characteristics of an IL–solvent mixture and determine precise composition ranges of interaction patterns. This thesis describes the changes of the kinetics of H/D exchange at C(2)-position between EMIMAc and solvents. Two different protic solvents were chosen to determine the influence of varying acid strengths added to EMIMAc: water and acetic acid. For the composition range from pure IL to pure solvent, we monitored the H/D exchange with low-field NMR spectroscopy. From spectral information, the amount of C(2)-deuterated cation was estimated for the discussion of reaction order. Details on equipment and experimental procedure for the investigation of EMIMAc-based mixtures are given in Subsection 3.2.1 and Subsection 3.2.2, respectively. In Subsection 3.2.3 we explain the modeling of the proton exchange kinetics considering pseudo-first-order and second-order reaction mechanisms as well as the influence of solvent content and dissociation of the solvent in the case of water.

3.2.1 Chemicals, Devices and Data Analysis

EMIMAc, deionized water and acetic acid were used as described in Subsection 3.1.1. Mixtures of IL and deionized water or acetic acid and the respective deuterated solvents (D_2O, Sigma Aldrich 99.9% D and acetic acid-d_4, VWR 99.5% D) were prepared by weight.

^{1}H NMR spectra were recorded on a Magritek Spinsolve Carbon benchtop NMR (42.5 MHz). The measuring temperature was 28 °C inside the device and the samples were prepared at ambient temperature. The approximate total volume for each measurement was 0.5 mL in standard NMR tubes. Standard scan measurements were done for chemical shift and peak area analysis (4 scans, 90° excitation pulse, 7 µs pulse width, 200 µs dwell time, 6.554 s acquisition time, 15 s repetition time). Phase and baseline correction of all spectra as well as the analysis of chemical shifts were done

with MestReNova software (version 9.1.0 Mestrelab Research S.L.). The peak areas were calculated with PEAXACT (version 4.2 S-PACT GmbH).

For the presented experiments, temperature was not measured. However, the temperature control inside the NMR spectrometer results in fast equilibrium due to small sample size and a large surface to volume ratio of the NMR tubes. Reference experiments with an ethylene glycol sample heated to 80 °C and a methanol sample heated to 50 °C show a decrease to 28 °C inside the NMR device within less than ten minutes with the most significant decrease occurring in less than four minutes (see Fig. A.2 in appendix), which is faster by an order of magnitude compared to the fastest experiment in this work.

pH measurements of the mixtures were carried out with a standard pH meter (WTW multi 3420 Set C, 4-point calibration, ±0.004 pH) at ambient temperature.

3.2.2 Experimental Procedure

After thoroughly mixing of the two components (making sure that no air bubbles interfere and disturb the signal), the NMR tube was immediately placed into the NMR device and repeated measurements were started. The intervals for the repeated measurements ranged from 15 s to 1 h depending on the total experiment duration, which was between 0.5 and 48 hours. The intervals were selected so as to have a sufficient amount of data points over time during the decrease of the C(2)-H peak, allowing for accurate fitting of the exchange kinetics. The parameters for repeated measurements were the same as for standard scans with just one scan per spectrum.

In the experiments with deuterated solvents, an exchange only at the C(2)-H position with hydroxyl groups of the deuterated solvents was observed (i.e., a decrease in C(2)-H peak area with a simultaneous increase in water or acetic acid hydroxyl peak). All other peaks remained constant during the investigated time frame. To further check that exchange only occurs with the C(2)-position, the sum of the hydroxyl and C(2)-H peak was monitored and was found to be constant during the experiments. The total area of the spectra was also constant. Distorted C(2)-H peaks, especially at the beginning of repeated measurements, indicated inhomogeneities in solvent content due to incomplete mixing and therefore those mixtures were excluded for the calculation of the proton exchange rate constants. The evaluation of peak areas and the calculation of relative numbers of hydrogen atoms require a reference proton. Here, the C(4,5)-H signals were chosen as a reference. Because the peaks of the two ring protons are mostly overlapped in the low-field NMR spectrum, they were counted as the equal of two hydrogen atoms.

The progress of the exchange was characterized by analyzing the C(2)-H peak area which showed an exponential decrease during exchange and reached a constant value in equilibrium. For most experiments, the equilibrium was reached quickly and measured completely. The exceptions are samples with either very high or very low solvent content. At very high solvent contents, exchange took more than several days and was not measured completely. Therefore, these mixtures were excluded from the evaluation of proton exchange. On the other hand, at low solvent contents, an increased viscosity due to the high amount of EMIMAc caused problems with mixing and larger variances occurred. Thus, mixtures containing less than 30 mol % of water as well as those with less than 10 mol % acetic acid were not evaluated in terms of proton exchange.

The deuteration of the solvents has no significant effect on reaction rate constants as can be seen from a comparison with partially deuterated solvents (see Fig. A.3 (a) in appendix). Therefore, we assume that the results of the exchange experiments are directly comparable to the results with non-deuterated solvents.

3.2.3 Modeling of Proton Exchange

The hydrogen deuterium exchange was modeled on two different levels of detail to study the reaction characteristics in terms of reaction order and reaction partners, generally assuming a second-order mechanism. First, a pseudo-first-order analysis was carried out to determine the second-order reaction rate constants for the exchange reaction between IL and water. This is a common approach when determining rate constants of H/D exchange reactions [220–222]. In a second step, we used a more detailed modeling approach to estimate second-order reaction rate constants in the system of EMIMAc and dissociated water.

3.2.3.1 Pseudo-First-Order Analysis

To calculate the observed exchange rate constants, for each experiment the areas of the C(2)-H peak of the $EMIM^+$ cation were normalized as follows

$$A_{\mathrm{norm}}(t) = A_{\mathrm{rel}}(t=0) \cdot \frac{A(t) - \min_t(A(t))}{\max_t(A(t)) - \min_t(A(t))}. \tag{3.9}$$

The prefactor $A_{\mathrm{rel}}(t=0)$ refers to the relative amount of hydrogen at the C(2)-position in the first recorded spectrum of one experiment. It accounts for the fact that at the beginning of the measurements ($t = 0$), the exchange has already progressed

to a certain extent. The maximum and minimum values were determined for each experiment individually and were only used for the calculation of normalized areas of the respective experiment. In total, the area was normalized between 0 and 1 in accordance with Amyes and Richard [223]. A pseudo-first-order exchange rate constant was calculated from the natural logarithm of normalized area against time

$$\ln(A_{\mathrm{norm}}(t)) = -k_{\mathrm{obs}} \cdot t. \tag{3.10}$$

Second-order rate constants were obtained from the slope of plotting the observed rate constants k_{obs} over the mole fraction of solvent assuming that

$$k_{\mathrm{obs}} = k_2 \cdot [\mathrm{solvent}]. \tag{3.11}$$

3.2.3.2 Detailed Dissociation Mechanism

The detailed modeling study focuses on the system of EMIMAc and water, in which the water fraction is composed of normal water introduced into the system as the basic water content of the IL, and deuterated water that was added to visualize the H/D exchange. Here, dissociation equilibria of all water species as well as the kinetically-limited exchange reaction have to be considered simultaneously. Modeling chemical systems with reactions in different time scales, namely fast equilibrium reactions and slow kinetically-limited reaction steps, can be challenging especially if the species participate in reactions on both time scales. A model accounting for the different time scales was set up following the systematic procedure described by Walz et al. [21].

The overall kinetically-limited H/D exchange is modeled as a reaction between EMIMAc and the hydroxide ion of water as proposed by Allen et al. [224] and is assumed to be an elementary reaction

$$\mathrm{EMIMAc_H} + \mathrm{OD^-} \overset{\mathrm{r_1}}{\rightleftharpoons} \mathrm{EMIMAc_D} + \mathrm{OH^-}. \tag{3.12}$$

$\mathrm{EMIMAc_H}$ refers to the normal cation and $\mathrm{EMIMAc_D}$ to the cation which is deuterated at C(2)-position. In diluted solutions of D_2O, the assumption that an abstracted hydrogen atom would always be replaced by a deuterium atom is valid since D_2O is in large excess. However, when also analyzing solutions with a higher electrolyte concentration, this assumption is no longer valid as the ratio of H to D increases more and more, considering the water content of EMIMAc which introduces non-deuterated water into the system. Hence, for the dissociation of water, the two dissociation equilibria of H_2O and D_2O as well as two further dissociation equilibria for the formation

of HDO have to be included to fully model the dissociation

$$H_2O \overset{K_w}{\rightleftharpoons} H^+ + OH^- \tag{3.13}$$

$$D_2O \overset{K_{dw}}{\rightleftharpoons} D^+ + OD^- \tag{3.14}$$

$$HDO \overset{K_{w,4}}{\rightleftharpoons} H^+ + OD^- \tag{3.15}$$

$$HDO \overset{K_{w,5}}{\rightleftharpoons} D^+ + OH^-. \tag{3.16}$$

The rate of reaction (r_1 in Eq. (3.12)) can be explicitly described with

$$r_1 = k_{f,1} c_{EMIMAc_H} c_{OD^-} - k_{r,1} c_{EMIMAc_D} c_{OH^-} \tag{3.17}$$

with forward and reverse reaction rate constants $k_{f,1}$ and $k_{r,1}$, respectively. Here, the absolute amounts of IL species c_{EMIMAc_H} and c_{EMIMAc_D} can be calculated from spectral information and weighed-in components. Assuming ideal solutions, the dissociation equilibria can be described with the respective dissociation constants and concentrations of the individual species

$$K_w = \frac{c_{H^+} c_{OH^-}}{c_{H_2O}} \tag{3.18}$$

$$K_{dw} = \frac{c_{D^+} c_{OD^-}}{c_{D_2O}} \tag{3.19}$$

$$K_{w,4} = \frac{c_{H^+} c_{OD^-}}{c_{HDO}} \tag{3.20}$$

$$K_{w,5} = \frac{c_{D^+} c_{OH^-}}{c_{HDO}}. \tag{3.21}$$

Strictly speaking, the assumption of ideal conditions is valid only for diluted systems where the activity coefficients of the individual species are close to one (i.e., considering concentrations instead of activities). The investigated composition range, however, covers all mole fractions from diluted solutions to concentrated electrolytic mixtures. Thus, the model equations require an activity correction. The activity coefficient of water in several ILs has been determined [225]. In another approach the ILs were assumed to be either completely dissociated or paired and the respective activity coefficients were determined [226]. Furthermore, changing values of K_w have been observed in mixtures of water and imidazolium-based ILs [227]. However, neither the activity values for the system of EMIMAc and dissociated water considering both hydrogen and deuterium nor the composition-dependent water dissociation constants are available in the literature. Therefore, the simplification of assuming ideal solutions with constant K_w is inevitable. This simplification is also performed in other publications dealing with H/D exchange kinetics in concentrated ILs [228].

The common dissociation constant of water $K_w = c_{H^+} c_{OH^-}$ was modified taking into consideration the concentration of water c_{H_2O} to obtain the constant required for equilibrium (3.18). Dividing the self-dissociation constant of water $K_w = 10^{-14}\,\mathrm{mol^2\,L^{-2}}$ by $c_{H_2O} = 55.51\,\mathrm{mol\,L^{-1}}$ leads to a dissociation constant of $1.8 \times 10^{-16}\,\mathrm{mol\,L^{-1}}$ for the equilibrium (3.18). Analogously, the dissociation constant for the heavy water equilibrium (3.19) was calculated to be $2 \times 10^{-17}\,\mathrm{mol\,L^{-1}}$. The dissociation constant for HDO in the equilibria (3.20) and (3.21) is not available in the literature and thus has to be estimated. $K_{w,4}$ and $K_{w,5}$ were assumed to have the same value and to lie between the dissociation constants of normal and heavy water. Exact determination of the dissociation constants $K_{w,4}$ and $K_{w,5}$ would require separate experiments that go beyond the scope of this thesis.

Fitting of the model equations to the experimentally observed values allows an estimation of forward and reverse reaction rate constants. To estimate rate constants, which are valid over a certain composition range, the conducted experiments have to be fitted simultaneously. Detailed simulations and respective parameter estimations were done with gPROMS 4.2.0.

3.3 Screening of Processing Pathways for Biofuel Production

Alternative pathways in biofuel production can be evaluated with RNFA [229, 230]. In RNFA, a reaction network of various (intermediate) components with possible conversion steps serves as a basis for finding the optimal production pathway of biofuels under consideration of economic and environmental criteria. This optimization of biofuel production by minimizing carbon loss and specific fuel cost is described in Subsection 3.3.1. We choose two representative biofuel products, ethanol and ethyl levulinate, that feature biotechnological and chemocatalytic conversion and are qualified as fuel components for spark-ignition engines [231].

In this thesis, we focus on the impact of pretreatment and hydrolysis yields as well as biomass composition on different conversion pathways with regard to the pretreatment strategy, focusing on liquid-based pretreatment. Hence, we compile various pathways for pretreatment and enzymatic hydrolysis from the literature in an existing reaction network for the production of ethanol and ethyl levulinate from lignocellulosic biomass [230], as described in Subsection 3.3.2.

3.3.1 Biofuel Production in RNFA

RNFA is a screening tool based on a reaction network of various components and conversion steps. It enables to find the optimal process pathway at an early stage of process design. RNFA comprises a mass-based analysis and does not include an energetic evaluation. A process pathway screening with RNFA is beneficial if the choice of production pathways is not straightforward (as in the case of ethanol), but, rather there are several alternative, partially interlinked production pathways without an obvious optimal pathway (as in the case of ethyl levulinate). Figure 3.2 shows the reaction network for the production of ethanol and ethyl levulinate from biomass, where each arrow represents a reaction from one component, depicted as node, to another component. The network is a sub-network of the one published by Ulonska et al. [230] and comprises only those reactions that are relevant for the production of ethanol and ethyl levulinate via enzymatic hydrolysis. Furthermore, the yields for fermentation of sugars and subsequent downstream processing reactions are kept as in the original publication whereas the yields of reactions R1–R5 for biomass pretreatment and enzymatic hydrolysis as well as the biomass composition are varied.

In particular, reactions R1, R2 and R3 refer to biomass pretreatment for the fractionation of cellulose, hemicellulose and lignin, respectively. Reactions R1–R3 are not varied independently, since they belong to one specific pretreatment experiment and thus they are coupled via mass balances. Nevertheless, we consider the fractionation of the three main components as three separate reactions because each component has individual fractionation yields. Reaction R4 refers to the conversion of hemicellulose to xylose and reaction R5 describes the enzymatic hydrolysis of cellulose to glucose.

Stoichiometry and yield data of the individual reactions serve as input for the calculation of stationary mole balances. The output of the biofuel production network is fixed to an energy equivalent of $100,000\,\mathrm{t}$ ethanol per year to ensure comparability of the solutions in terms of capacity. Furthermore, RNFA gives cost estimates for the realization of individual pathway designs. For the comparison of biofuels, specific fuel production cost is chosen as economic criterion and carbon loss as environmental criterion. To find the optimal fuel production pathway, both criteria should be minimized:

$$\begin{aligned} \min & \left\{ \begin{array}{l} \text{Fuel cost} \\ \text{Carbon loss} \end{array} \right\} \\ \text{s.t.} \quad & \text{Stoichiometry \& yield constraints} \\ & \text{Fuel cost (feedstock, invest, waste).} \end{aligned} \tag{3.22}$$

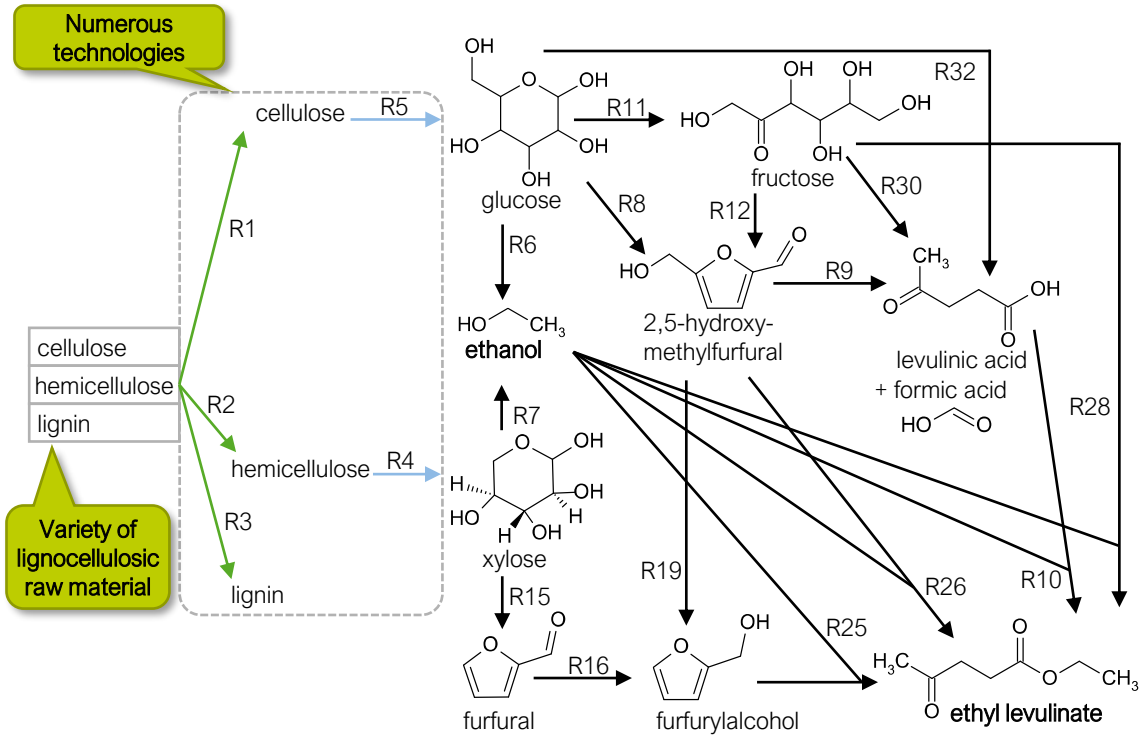

Figure 3.2: Reaction network for the production of the biofuels ethanol and ethyl levulinate including biomass fractionation (R1, R2 and R3), and hydrolysis of cellulose (R5) and hemicellulose (R4) adapted from Ulonska et al. [230].

Unless otherwise stated, reaction yields as well as the mathematical formulation of the optimization problem were chosen as in the publication by Voll and Marquardt [229] with the modifications by Ulonska et al. [230] and König et al. [32]. The optimization problem is formulated as a mixed-integer nonlinear program and solved in GAMS (version number 25.1.1 [232]) with the deterministic global solver BARON (version number 18.5.8 [233, 234]). The multi-objective optimization problem is converted into a single-objective problem using the ϵ-constraint method.

The specific fuel production costs C_{spec} are calculated from the total annualized cost in relation to the heating value $\Delta H_{\text{comb,fuel}}$ of the fuel stream b_{fuel}:

$$C_{\text{spec}} = \frac{\text{TIC} + C_{\text{raw}} + C_{\text{waste}}}{\Delta H_{\text{comb,fuel}} \cdot b_{\text{fuel}}}. \tag{3.23}$$

With a fixed energy equivalent to be produced, the denominator has the same constant value for the ethanol and ethyl levulinate screenings. Total investment costs (TIC) are

calculated from investment costs (IC) corrected for the influence of interest rate and assumed runtime of the biofuel production facility (see Tab. C.1 in appendix). RNFA provides an evaluation of production pathways at an early design stage and hence does not include a detailed estimation of IC considering for example solid loadings during biomass pretreatment. Instead, IC correlate with the annual throughput and the number of functional units (see Eq. C.1): For each active reaction (i.e., chosen by the algorithm for the optimal solution) one functional unit is considered in the calculation of IC. However, the number of functional units has been adapted for pretreatment reactions (R1–R3) which take place in one reactor (i.e., one functional unit) as well as hydrolysis reactions (R4, R5) which are also considered to be one functional unit.

Furthermore, costs for raw material C_{raw} and waste C_{waste} can be calculated considering the number of feed streams n_{raw} (biomass, hydrogen, water and oxygen) as well as the number of waste streams n_{waste}:

$$C_{\mathrm{raw}} = \sum_{j=1}^{n_{\mathrm{raw}}} f_{\mathrm{raw},j}\, M_{\mathrm{raw},j}\, P_{\mathrm{raw},j} \tag{3.24}$$

$$C_{\mathrm{waste}} = \sum_{i=1}^{n_{\mathrm{waste}}} (w_{\mathrm{waste},i} + b_{\mathrm{waste},i})\, M_{\mathrm{waste},i}\, P_{\mathrm{waste}} \tag{3.25}$$

with specific prices $P_{\mathrm{raw},j}$ and molar masses $M_{\mathrm{raw},j}$ for the molar input streams $f_{\mathrm{raw},j}$ and specific prices P_{waste} and molar masses $M_{\mathrm{waste},i}$ for the waste streams of side-product $w_{\mathrm{waste},i}$ and by-product $b_{\mathrm{waste},i}$. As our focus is on the impact of pretreatment and hydrolysis yields as well as biomass composition, we assume a constant price for lignocellulosic biomass independent of the specific type that is used for biofuel production (see Tab. C.2 in appendix).

Carbon loss (CL) is calculated from the carbon efficiency η^{C}

$$\mathrm{CL} = 1 - \eta^{\mathrm{C}} \tag{3.26}$$

where η^{C} refers to the carbon atoms in the fuel stream as a fraction of the carbon atoms in all input streams in the production process of a biofuel:

$$\eta^{C} = \frac{b_{\mathrm{fuel}}\, n_{\mathrm{C,fuel}}}{\sum_{j=1}^{n_{\mathrm{raw}}} f_{\mathrm{raw},j}\, n_{\mathrm{C},j}}. \tag{3.27}$$

To estimate carbon loss and fuel cost, RNFA requires yield parameters for all reactions as input (see Tab. C.3 in appendix for yields of reactions 6–32). The calculation of yields for the pretreatment and hydrolysis steps from literature data is explained in the following.

3.3.2 Biomass Pretreatment in RNFA

The evaluation of fractionation effectiveness during pretreatment is usually carried out with a mass-based analysis in the literature while RNFA is mole-based. Hence, the weight fractions $w_{i,\mathrm{raw}} = m_{i,\mathrm{raw}}/m_{\mathrm{raw}}$ of the three main components cellulose (c), hemicellulose (hc) and lignin (l) for the native biomass as well as the recovered pretreated biomass are converted to mole fractions $x_{i,\mathrm{raw}} = (m_{i,\mathrm{raw}}/M_i)/(\sum_i^{n_{\mathrm{bio}}} m_{i,\mathrm{raw}}/M_i)$. We assume that the input stream of biomass m_{raw} consists of the three main components as well as a fraction *other* that closes the mass balance: $m_{\mathrm{raw}} = \sum_{i=1}^{n_{\mathrm{bio}}} m_{i,\mathrm{raw}} + m_{\mathrm{other}} \quad i \in \{\mathrm{c}, \mathrm{hc}, \mathrm{l}\}$. The molar masses of the monomer units are taken as: $M_{\mathrm{c}} = 162.14\,\mathrm{g\,mol^{-1}}$, $M_{\mathrm{hc}} = 150.13\,\mathrm{g\,mol^{-1}}$, $M_{\mathrm{l}} = 180.2\,\mathrm{g\,mol^{-1}}$. As an assumption, we use the molar mass of lignin also for the fraction *other* and include x_{other} in the lignin mole fraction because in the context of RNFA, neither can be utilized in further processing steps.

Figure 3.3 gives a schematic overview of the streams that we consider for the analysis of pretreatment effectiveness. After the pretreatment step p, the biomass is split into a *recovered* (r), solid fraction and a non-recovered fraction which is assumed to be completely *solubilized* (s) in the pretreatment liquid (see Fig. 3.1), whereas both fractions consist of cellulose (c), hemicellulose (hc) and lignin (l):

$$m_{\mathrm{raw}} = m_{\mathrm{r}} + m_{\mathrm{s}} \tag{3.28}$$

$$m_p = m_{\mathrm{c},p} + m_{\mathrm{hc},p} + m_{\mathrm{l},p} \quad p \in \{\mathrm{s}, \mathrm{r}\} \tag{3.29}$$

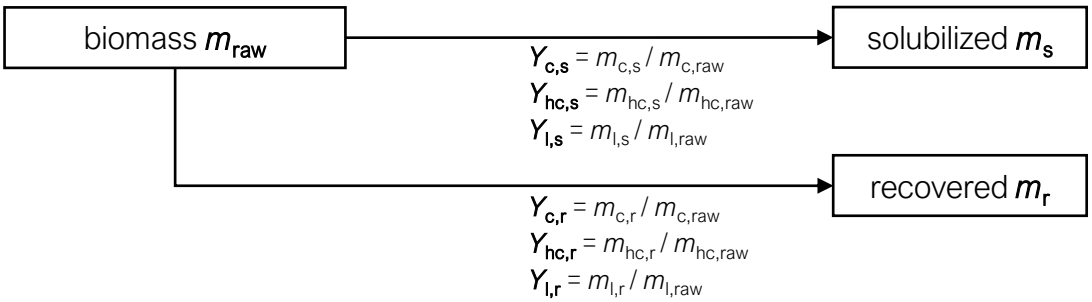

Figure 3.3: Scheme of the considered pretreatment process streams that serve as input data for the RNFA. The stream of raw material (raw) is split into a solubilized fraction (s) and a recovered fraction (r). Each biomass containing stream consists of cellulose (c), hemicellulose (hc) and lignin (l). After pretreatment, the molar fractionation yields ($Y_{i,p}$) of the individual compounds are calculated.

Amount and composition of the recovered and the solubilized fraction (Eqs. (3.28) and (3.29)) are used to calculate the molar fractionation yields $Y_{i,p}$ of the pretreatment step p for the three main components:

$$Y_{i,p} = \frac{m_{i,p}/M_i}{m_{i,\mathrm{raw}}/M_i} \quad \forall i,p \quad i \in \{\mathrm{c,\ hc,\ l}\}, p \in \{\mathrm{s,\ r}\}. \tag{3.30}$$

For pretreatment and hydrolysis reactions, the molar- and weight-based fractionation yields for each component are equivalent since the molar masses in Eq. (3.30) cancel out. The composition of both recovered fraction and solubilized fraction are not available in all evaluated references. Therefore, we consider only the highest given yield for each component (c, hc, l) for either the solubilized or the recovered stream and allocate this yield to reactions R1, R2 and R3: $Y_i = \max(Y_{i,\mathrm{r}}, Y_{i,\mathrm{s}})$. Mostly, we used the yield of the recovered fraction of cellulose and the yield of the solubilized fraction of hemicellulose.

Usually, the non-converted biomass components are burned for heat integration. Therefore, they are not considered as waste streams causing additional disposal costs in Eq.(3.25).

Hydrolysis yields Y_{xyl} and Y_{glu} are calculated for reaction R4 from the amount of xylose (xyl) after the hydrolysis step h as a fraction of the available hemicellulose after the pretreatment step and for reaction R5 from glucose (glu) as a fraction of the available cellulose, respectively:

$$Y_{\mathrm{xyl}} = \frac{m_{\mathrm{xyl,h}}/M_{\mathrm{xyl}}}{m_{\mathrm{hc},p}/M_{\mathrm{hc}}} \quad p \in \{\mathrm{s,\ r}\} \tag{3.31}$$

$$Y_{\mathrm{glu}} = \frac{m_{\mathrm{glu,h}}/M_{\mathrm{glu}}}{m_{\mathrm{c},p}/M_{\mathrm{c}}} \quad p \in \{\mathrm{s,\ r}\}. \tag{3.32}$$

We do not account for differences in enzymatic conversion rates for glucose and xylose.

The benchmark for the comparison of different pretreatment concepts is the ideal fractionation of biomass combined with an ideal enzymatic hydrolysis (i.e., the yields of reaction R1–R5 are equal to 1). This means that after pretreatment and enzymatic hydrolysis, all carbohydrates of the respective input stream of biomass are available in form of sugars for further conversion to the selected biofuels.

The first analysis considers six different pretreatment concepts using beech wood as feedstock: DA [235], IL [19], kraft [236], LHW [237], a one-phasic [238] as well as a two-phasic OS (organocat (OC)) [126, 239] concept (see Appendix C for selection of references). The composition of beech wood for the benchmark is set to the com-

position with the minimal reported lignin fraction. Table 3.1 gives an overview of the compositions and yields of the considered references.

Table 3.1: Molar compositions and yields considered for the screening of pretreatment of beech wood. The evaluated pretreatment concepts are kraft, ionic liquid (IL), dilute acid (DA), liquid hot water (LHW), organocat (OC) and organosolv (OS) in comparison to the benchmark of ideal pretreatment.

	Ideal	**Kraft**	**IL**	**DA**	**LHW**	**OC**	**OS**
Ref.		[236]	[19]	[235]	[237]	[126, 239]	[238]
$x_{\mathrm{c,raw}}$	0.44	0.44	0.43	0.4	0.43	0.37	0.37
$x_{\mathrm{hc,raw}}$	0.36	0.36	0.28	0.22	0.28	0.17	0.23
$x_{\mathrm{l,raw}}$	0.21	0.21	0.29	0.39	0.3	0.46	0.41
Y_{c}	1	1	0.9	0.97	0.88	0.96	0.94
Y_{hc}	1	0.93	0.78	0.79	0.9	0.76	0.87
Y_{l}	1	0.91	0.69	0.77	0.78	0.58	0.79
Y_{xyl}	1	1	1	1	0.39	1	1
Y_{glu}	1	0.89	1	1	0.76	0.37	0.81

The second analysis focuses on OS pretreatment as one specific pretreatment concept fractionating different types of biomass: sugarcane bagasse [240–242], softwoods spruce [238, 242, 243] and pine [244–246], and hardwoods tulip tree (TT) [247], elm [246] and beech [238]. Analogous to the first analysis, the composition for the benchmark is set to the composition with minimal reported lignin fraction. Table 3.2 gives an overview of the biomass composition and yields of the considered references for OS pretreatment.

The third analysis aims at characterizing the general influence of biomass composition and pretreatment on the production of biofuels. To this end, the input biomass composition and yields for pretreatment and hydrolysis do not rely on literature data but are systematically varied. The influence of a changing lignin content is investigated from 0 to 0.85. Cellulose and hemicellulose content are changed accordingly considering a fixed c/hc ratio of 1.7, corresponding to the ratio of average cellulose content (0.4257) to average hemicellulose content (0.2526) of the investigated literature data. Furthermore, the influence of a changing cellulose to hemicellulose ratio at a fixed lignin content of 0.3218 (average of literature data) is investigated. In both

cases, the yields for reactions R1–R5 correspond to the average values of the investigated literature: $Y_c = 0.8639$, $Y_{hc} = 0.862$, $Y_l = 0.724$, $Y_{xyl} = 0.9414$, $Y_{glu} = 0.7903$.

Table 3.2: Molar compositions and yields considered for the screening of organosolv pretreatment based on a variety of biomasses in comparison to the benchmark of ideal pretreatment: **(a)** benchmark and softwoods (spruce and pine), **(b)** sugarcane bagasse and hardwoods (tulip tree (TT), elm, and beech).

(a)	**Ideal**	**Spruce**			**Pine**		
Ref.	●	[238] △	[243] ▲	[242] △	[244] ▲	[245] ▲	[246] ▲
$x_{c,raw}$	0.48	0.42	0.49	0.4	0.46	0.48	0.45
$x_{hc,raw}$	0.28	0.19	0.23	0.25	0.24	0.27	0.30
$x_{l,raw}$	0.24	0.4	0.28	0.36	0.3	0.24	0.24
Y_c	1	0.69	0.9	1	0.61	0.59	0.83
Y_{hc}	1	0.9	0.99	0.84	1	1	0.76
Y_l	1	0.7	0.58	0.53	0.71	0.8	0.56
Y_{xyl}	1	1	1	1	1	1	1
Y_{glu}	1	0.29	1	1	0.7	1	0.21

(b)	**Sugarcane bagasse**			**TT**	**Elm**	**Beech**
Ref.	[240] ◆	[241] ◆	[242] ◆	[247] ■	[246] ■	[238] □
$x_{c,raw}$	0.42	0.43	0.45	0.42	0.48	0.37
$x_{hc,raw}$	0.25	0.3	0.30	0.23	0.28	0.23
$x_{l,raw}$	0.32	0.28	0.24	0.34	0.24	0.41
Y_c	0.86	0.85	0.83	1	0.8	0.94
Y_{hc}	0.97	0.9	0.76	0.75	0.62	0.87
Y_l	0.88	0.84	0.56	0.69	0.59	0.79
Y_{xyl}	1	1	1	1	0.56	1
Y_{glu}	1	0.96	0.21	0.88	0.56	0.81

Chapter 4

Results and Discussion

This chapter first presents the results of biomass pretreatment in mixtures of EMIMAc followed by the analysis of C(2)-hydrogen–deuterium exchange in these mixtures in Section 4.1. In Section 4.2, a detailed analysis of acetosolv pretreatment of beech wood is presented. Lastly, in Section 4.3, the impact of pretreatment on the process performance of biofuel production is evaluated.

4.1 Ionic Liquid-Based Biomass Pretreatment

EMIMAc is a well-known, effective IL for the pretreatment of wood [57, 107] and the dissolution of cellulose [118, 248]. However, in both cases, the water content in the IL is a limiting factor. Upon addition of water, disintegration of biomass is hindered [19, 117, 249] and the amount of cellulose dissolved is drastically reduced [250]. Furthermore, cellulose is completely insoluble above a certain threshold mole fraction for water [250, 251]. This poses a problem for the processing of biomass with ILs since water is ubiquitous in biomass and hence limits pretreatment effectiveness. In contrast, the addition of organic solvents to an IL-based pretreatment process proves beneficial for sugar yields [252] and acetic acid added to an IL acts both as catalyst to hydrolyze biomass components and as co-solvent for increased solubility of biomass components [253]. It is thus important to know how water and other solvents affect the properties of an IL-based pretreatment liquid for robust process designs.

In the following, we investigate how the addition of water and acetic acid to EMIMAc influences pretreatment results in Subsection 4.1.1. To evaluate whether pretreatment results can be connected to interactions between components in EMIMAc-based pretreatment liquids, mixtures of EMIMAc with water and acetic acid are analyzed with low-field NMR spectroscopy thus resolving molecular interactions in Subsection 4.1.2.

4.1.1 Biomass Pretreatment with EMIMAc

Figure 4.1 (a) depicts beech wood after pretreatment in EMIMAc–water mixtures from concentrated IL down to dilute electrolyte solutions. The visual appearance of pretreated wood samples changes with the water content of the pretreatment liquid. Macroscopically, beech wood completely disintegrates in concentrated EMIMAc mixtures down to a mole fraction of $x_{\mathrm{EMIMAc}} = 0.68$. Upon further addition of water, there is a transition range with reduced disintegration between $0.68 > x_{\mathrm{EMIMAc}} > 0.44$. For $x_{\mathrm{EMIMAc}} < 0.44$, the beech wood chips appear macroscopically unchanged after pretreatment. The disintegration limit of 8.5 wt % water in EMIMAc observed by Viell [249] corresponds to approximately 53 mol % EMIMAc. This is in line with the observation of reduced disintegration in the transition range. Likewise, a change in macroscopic pulp appearance has been observed after pretreatment of poplar wood with EMIMAc–water mixtures between 10 and 15 wt % water (corresponding to 49 and 37 mol % EMIMAc, also coinciding with the transition range) [254]. Thus, the limiting water content for biomass disintegration seems to be a characteristic of the pretreatment liquid that is valid for different types of biomass.

Compared to EMIMAc–water mixtures, macroscopic disintegration after pretreatment in EMIMAc–acetic acid mixtures shows similar effects as visible in Fig. 4.1 (b). Beech wood disintegrates completely down to a mole fraction of $x_{\mathrm{EMIMAc}} = 0.78$ and the transition from complete to no disintegration lies between $0.78 > x_{\mathrm{EMIMAc}} > 0.38$, although the samples with 58 and 47 mol % EMIMAc show only minimal signs of disintegration (i.e., slightly frayed edges of the wood chips). In comparison to water, acetic acid in EMIMAc hinders complete disintegration at lower solvent contents, while the transition to no disintegration seems to comprise a larger composition range.

The evaluation of mass balances proves difficult due to the small amount of wood that was used for the pretreatment experiments with IL. Even small amounts of IL that remain attached to the wood after pretreatment result in false and inconsistent values for the recovered fraction. Furthermore, not enough material was available for a comprehensive analysis of biomass composition after pretreatment. Nevertheless, to evaluate pretreatment effectiveness, the samples were enzymatically hydrolyzed.

The total sugar yield after enzymatic hydrolysis is shown in Fig. 4.2 (a). Here, total sugar yield refers to the amount of cellobiose, glucose and xylose available after enzymatic hydrolysis of the pretreated samples as a fraction of glucose and xylose present in native beech (as determined from acid hydrolysis according to Sluiter et al. [130]). The dashed line refers to the total sugar yield after enzymatic hydrolysis of untreated beech wood as a reference. After pretreatment with pure EMIMAc, glucose and xy-

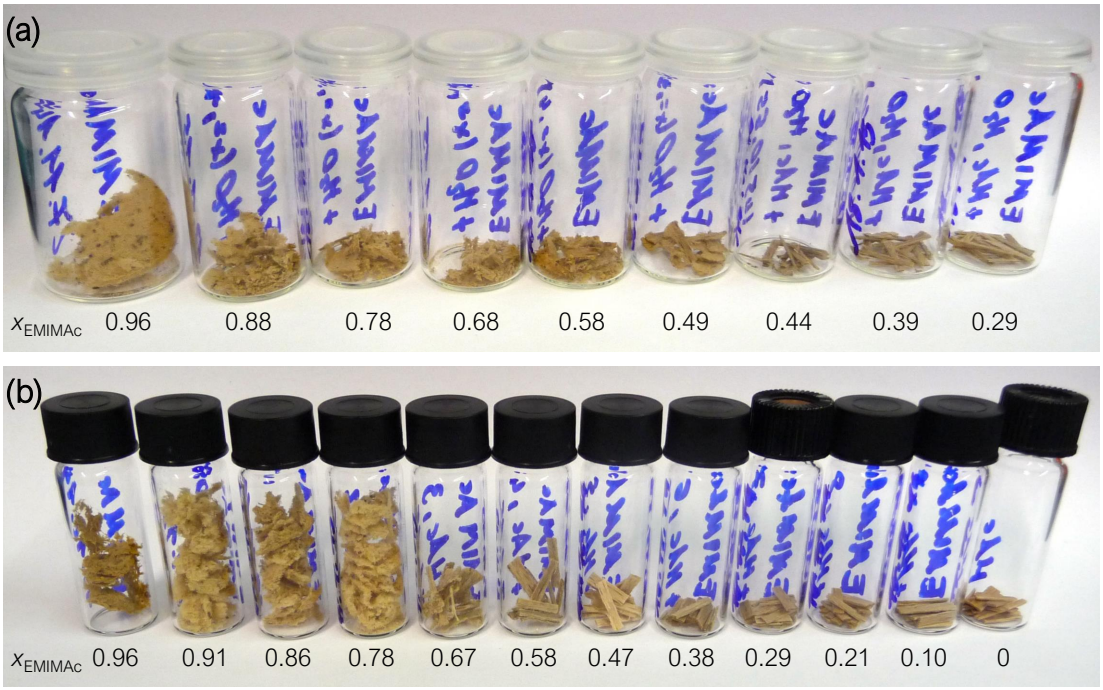

Figure 4.1: **(a)** Disintegration of beech wood after pretreatment with EMIMAc and water. **(b)** Disintegration of beech wood after pretreatment with EMIMAc and acetic acid. The numbers below the vials indicate the mole fraction of EMIMAc. The mole fraction of $x_{\mathrm{EMIMAc}} = 0.96$ for the experiments to the left results from the basic water content of EMIMAc (i.e., no additional solvent added). Hence, the mixtures of EMIMAc and acetic acid always contain a small amount of water ($x_{\mathrm{H_2O}} < 0.04$).

lose are completely released during enzymatic hydrolysis indicating a very effective pretreatment. With increasing water and acetic acid content, sugar yields decrease in both cases, while the effect is stronger for the addition of acetic acid. Furthermore, for both solvents, there seems to be a limiting mole fraction below which the total sugar yield drastically drops from around 70 wt % to below 30 wt %. This threshold lies between 44 and 49 mol % EMIMAc in mixtures with water and between 67 and 78 mol % EMIMAc in mixtures with acetic acid. These compositions correspond to the lower and upper limit of the visually-observed transition range for reduced disintegration in mixtures with water and acetic acid, respectively. Presumably, macroscopic disintegration is connected to structural changes in the biomass that facilitate enzymatic hydrolysis (cf. Viell et al. [19]). However, samples that are not disintegrated after pretreatment in EMIMAc–acetic acid mixtures show sugar yields similar to untreated

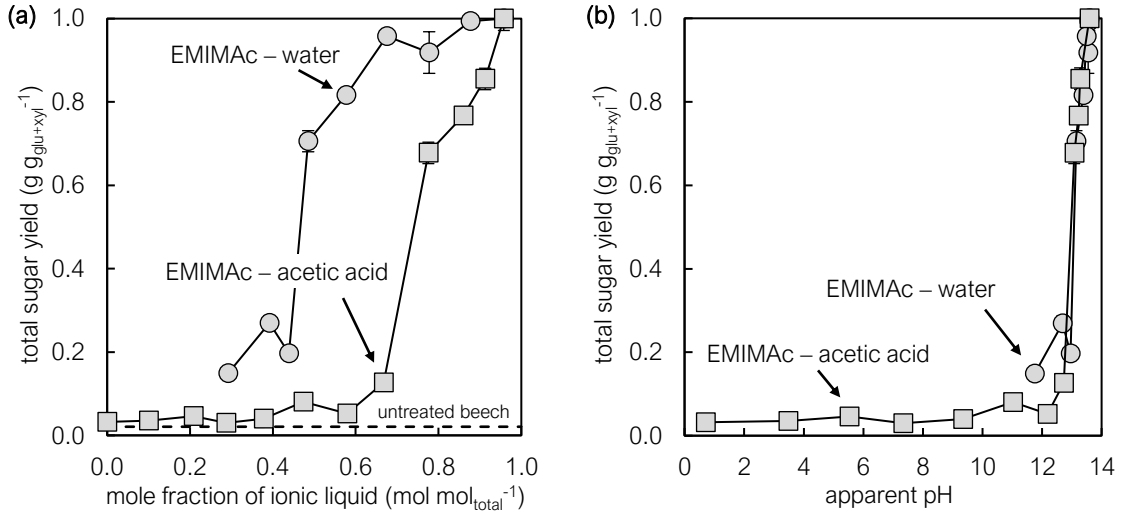

Figure 4.2: **(a)** Total sugar yield after pretreatment of beech wood with mixtures of EMIMAc with water and acetic acid. The dashed line refers to sugar yield after enzymatic hydrolysis of untreated beech wood. **(b)** Total sugar yield in relation to apparent pH of the pretreatment liquids.

beech wood, while pretreatment with EMIMAc–water mixtures results in slightly increased sugar yields despite the absence of disintegration. Hence, pretreatment in mixtures of EMIMAc and water induces structural changes that increase hydrolysis yields even before beech wood disintegrates. In comparison, the relation between total sugar yield and mole fraction of EMIMAc in mixtures with acetic acid shows a similar shape, but is shifted to higher EMIMAc mole fractions in the pretreatment liquid.

To further explore the relation between the drop in sugar yields and the decreasing extent of disintegration after pretreatment in mixtures of EMIMAc with water and acetic acid, a detailed compositional analysis should be carried out. A compositional analysis allows to further compare whether the macroscopic disintegration in combination with high sugar yields results from the same changes during pretreatment on a molecular scale upon the addition of water or acetic acid. Especially the role of lignin removal with regard to disintegration should be investigated considering the different lignin extraction abilities of pretreatment liquids ranging from concentrated IL mixtures to both aqueous and organic acid-based solutions. For the above-mentioned reasons, an evaluation of biomass composition was not possible for the experiments carried out for this thesis. Therefore, possible influences of characteristics of the pretreatment liquids on pretreatment effectiveness are investigated in more detail in the following.

Since EMIMAc is an alkaline IL, the alkalinity of the mixtures reduces upon the addition of water and acetic acid. As a simple measure for acid–base properties of an electrolyte solution, we measured the apparent pH in mixtures of EMIMAc with water and acetic acid (see Fig. A.1 in appendix). It should be noted that apparent pH refers to the value measured as is (i.e., no corrections for activity and increased ionic strength). Interestingly, pH as a function of mixture composition also appears shifted to lower EMIMAc contents when comparing acetic acid and water similar to the relation between sugar yields.

Figure 4.2 (b) shows the total sugar yield versus the apparent pH in mixtures of EMIMAc. Here, the curves for the addition of both solvents coincide. In strong alkaline mixtures with pH>13, pretreatment results in high sugar yields of 67 wt % and more. Below, the overall sugar drastically drops down to less than 30 wt %.

Similarly, the effectiveness of kraft pretreatment relates to pH. The high pH in kraft pulping liquors (11–14) allows for comparable diffusion rates of the pretreatment liquid in longitudinal and radial directions of the wood. This leads to swelling of wood [255]. However, pH decreases during kraft pulping because alkaline substances are consumed for the neutralization of acids that are cleaved during pretreatment (e.g., due to deacetylation of hemicelluloses). As a result, the concentration of active alkali decreases [72, 255]. Although swelling is related to disintegration of beech wood in EMIMAc–water mixtures [19], the influence of a specific pH seems to be different for kraft and EMIMAc pretreatment because the pH range for the transition from high to low sugar yields is very narrow. Hence, the basicity of mixtures of EMIMAc should be resolved in more detail to describe this change in pretreatment effectiveness. Since phenomena during pretreatment are often too complex to be directly tangible, characterization of pretreatment liquids in the absence of biomass serves as a starting point to resolve molecular interactions between EMIMAc and solvents added as a function of composition.

In the literature, properties of IL solutions have been described by several parameters. These include Kamlet–Taft basicity β [98], preferential solvation upon addition of solvents [256] and the role of the acidic C(2)-H in imidazolium cations [202]. However, Kamlet–Taft parameters do not correlate with disintegration effects after pretreatment of beech in three different ILs and are therefore not sufficient to explain the properties of EMIMAc–water mixtures that lead to disintegration [249].

In general, the liquid structure in a mixture of IL and solvent changes depending on the ionic content: a concentrated ionic medium with Coulombic forces turns into a dilute solution with co-existence of molecular and ionic domains [257]. More precisely, the cation [201, 202] and the anion [98, 185] both interact via molecular forces that

are changed upon addition of molecular solvents. Furthermore, the liquid structure of an IL mixed with the conjugate acid of its anion relates to acidity in these mixtures due to the formation of acid–anion clusters [258]. From a molecular point of view, the characterization of IL–solvent mixtures relates to dissociation equilibria and hydrogen bonding. On the one hand, the dissociation of water or acids is influenced by an increasing electrolyte concentration [259, 260]. Furthermore, in concentrated ILs, carbenes can be formed due to abstraction of the C(2)-proton, especially with highly basic anions such as acetate [261]. On the other hand, the length of hydrogen bonds in EMIMAc–water mixtures changes with water content [262]. In particular the C(2)-position is very much involved [203, 204] and also key in the formation of hydrogen bonds. Hence, we investigate the interaction at C(2)-position in mixtures of EMIMAc and water or acetic acid to describe molecular interactions in view of the observed changes in pretreatment effectiveness in the following.

4.1.2 C(2)-Hydrogen–Deuterium Exchange in Mixtures of EMIMAc

The analysis of hydrogen bonding between IL and water has been achieved by NMR spectroscopy. Some IL–water mixtures have been described by the C(2)-H chemical shift [185], others by deuterium exchange observed with NMR spectroscopy [263, 264]. In particular, the H/D exchange rate correlates with the hydrogen bond strength of the anion [265]. Moreover, the exchange can be inhibited in the case where the Cl^- anion is completely solvated by water molecules at low water contents [228], while acid impurities can significantly increase the exchange rate [266]. In some systems, the exchanged fraction in equilibrium does not linearly correlate with the water content but rather with the pD (i.e., pH in the case of deuterated water) of the solution [267]. In contrast, conformational changes of an imidazolium cation relate to the H/D exchange although the pD remains neutral in solutions containing a Cl^- anion [264]. Hydrogen exchange in EMIMAc–water mixtures even shows a discontinuity at 43 mol % water and is faster than in other 1,3-dialkylimidazolium ILs with less basic anions [224]. The effect of additional solvents other than water on such an H/D exchange with ILs has not yet been tested.

H/D exchange has also been used to describe the accessibility of hydroxyl groups in cellulose [268, 269]. With this technique, structural changes of biomass after pretreatment and drying can be described and mechanistic understanding of salt-assisted cellulose hydrolysis deepened [112, 207, 270]. The kinetics of H/D exchange of cellulose in deuterium oxide correlate with the crystallinity of cellulose [271]. Also, the

influence of an increasing amount of H_2O in the D_2O-based exchange medium has been discussed [272]. However, the latter case was not modeled in detail and H/D exchange studies with other solvents than water have not yet been carried out. For the description of H/D exchange kinetics between biomolecules and other media, the fundamental H/D interaction characteristics of the applied solvents need to be known.

These literature investigations show that the H/D exchange at the C(2)-position depends both on the molecular structures of the species involved as well as the mixture composition. Clearly, the acid–base properties of an IL solution play a major role when characterizing H/D exchange but it is not entirely clear whether the pH of a mixture determines the exchange kinetics or is rather a result of ionic interactions. The analysis of exchange reactions between EMIMAc and water as well as acetic acid in this subsection can thus serve to elucidate the acid–base characteristics of an EMIMAc–solvent mixture and determine precise composition ranges of interaction patterns.

4.1.2.1 Cation, Anion and Solvent Molecule Chemical Shifts

Figure 4.3 (a) shows representative ^{1}H NMR spectra of EMIMAc, acetic acid and water as well as mixtures thereof. Generally, the characteristics of both pure component and mixture spectra are in accordance with published spectra of EMIMAc [258, 273]. Also, the composition-dependent changes of chemical shift in mixtures of EMIMAc with water agree well with the literature [274, 275]. The hydroxyl groups of water and acetic acid as well as the C(2)-H peak of EMIMAc are clearly visible and separated from the other peaks due to the CH and NH moieties. As can be seen from Fig. 4.3 (a), the C(2)-proton is the most deshielded proton of EMIMAc showing the largest shift. Protons at position 4 and 5 of the cation are partly overlapping depending on solvent content (see Fig. 4.3 (c) for numbering of carbon atoms). Owing to the resolution of the low-field NMR spectrometer, the signals of hydrogens close to the nitrogen atoms in the cation (position 6 and 7) are overlapped in the region of 4 ppm. The CH_3-groups of the anion and ethyl side-chain (positions 8 and 10) are the most shielded protons in the range from 1 to 2 ppm.

The mixtures of EMIMAc with water or acetic acid show certain changes in the position as well as the shape of the peaks depending on the mole fraction of the added solvent. These effects are most pronounced for C(2)-H and hydroxyl protons. The protons at the C(4) and C(5) position of the $EMIM^+$ cation show less changes upon addition of a proton donor. The two peaks overlap for most composition ranges. Their shape changes from a peak with two visible tips to a peak with a single tip

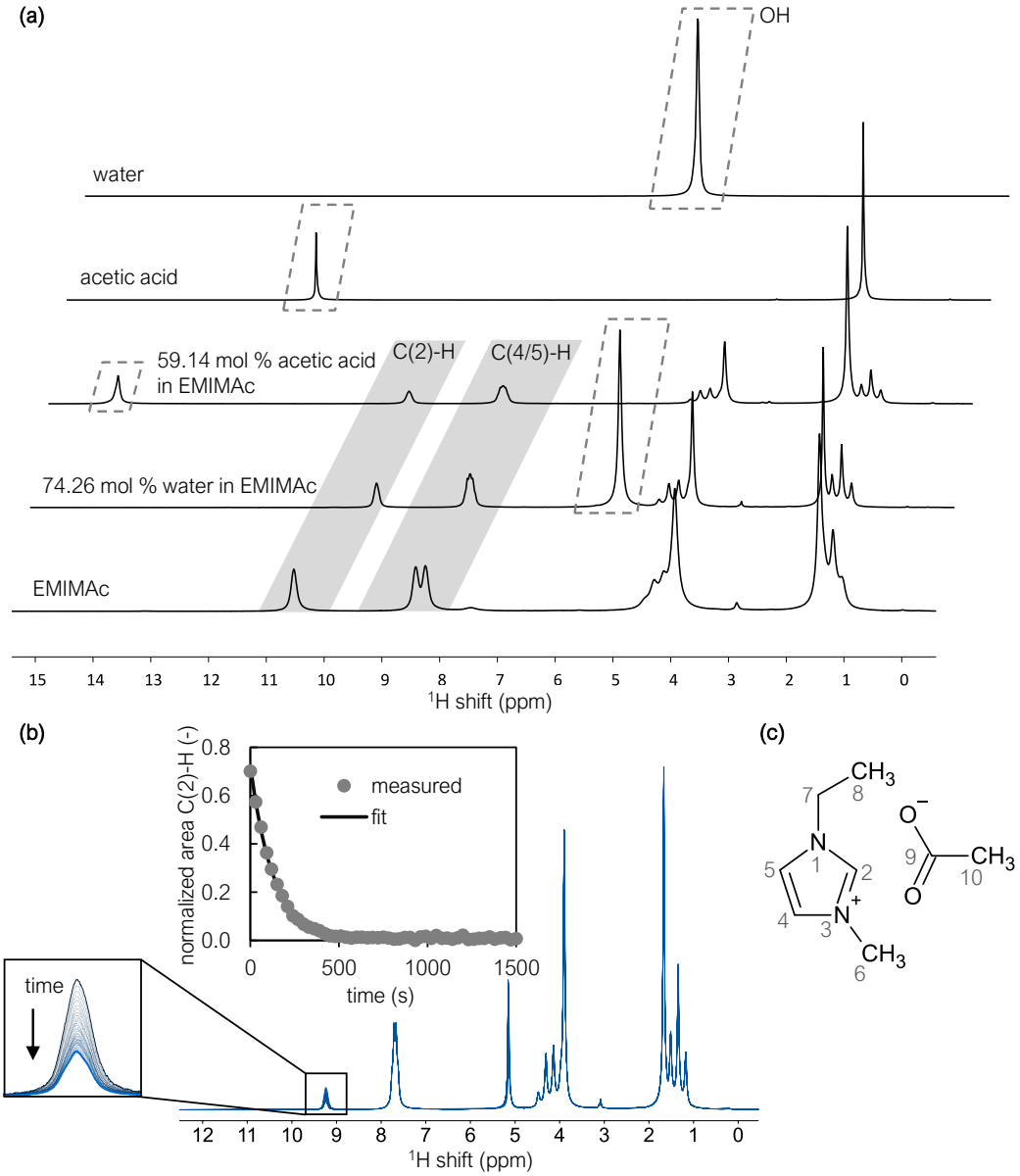

Figure 4.3: **(a)** ^{1}H NMR spectra of water, acetic acid, EMIMAc in mixtures with acetic acid or water, and pure EMIMAc (from top down). The peaks at 4.8 ppm, 11.09 ppm, 14.22 ppm and 5.19 ppm in the upper four spectra refer to the hydroxyl shift (marked by the dashed boxes). The peaks at 9.16 ppm, 9.41 ppm and 10.52 ppm in the lower three spectra refer to the C(2)-H in EMIMAc. The C(4,5)-H signal is right next to the C(2)-H peak (both highlighted with gray boxes). **(b)** Decrease of C(2)-H peak in spectra with time in experiments with deuterated water and normalized peak area over time with pseudo-first-order fit. **(c)** Numbering of carbon and respective hydrogen atoms of EMIMAc.

upon the addition of a solvent. The peaks of alkyl side chains of the cation and the alkyl group in the acetate anion are largely overlapped and show the smallest changes in peak position by variation of the mole fraction, compared to the other peaks in the spectra. The strongly exposed C(2)-H makes it susceptible to proton–deuteron exchange which will be studied in the following section.

4.1.2.2 Characteristics of Proton Exchange at C(2)-Position

H/D exchange at the C(2)-position of the $EMIM^+$ cation was evaluated quantitatively as a function of the mixture composition. This includes mixtures of EMIMAc with deuterated water or deuterated acetic acid covering the composition range from diluted mixtures to concentrated ionic solutions. Figure 4.3 (b) shows an example of a time series of proton exchange spectra. The zoom on the C(2)-H peak reveals that the peak decreases with time. Also shown is the course of normalized peak area over time and the respective fit according to Eq. (3.10) showing an exponential decrease of C(2)-H peak area.

Description of Equilibrium Proton exchange only at the C(2)-position is in accordance with Wong and Keck [276] who reported exchange rates in 1-methylimidazole at the C(2)-position more than 30,000 times faster than at the C(4)- or C(5)-position. However, while it took up to 40 days to reach equilibrium for other ILs such as $BMIMBF_4$ [277], the time to reach equilibrium after proton exchange in EMIMAc is much faster, that is, between two hours and two days for the reported experiments (aqueous mixtures between 5 mol % and 70 mol % EMIMAc and acidic mixtures above 25 mol % EMIMAc, see Subsection 3.2.2). Figure 4.4 shows the amount of IL which is deuterated at the C(2)-position, $EMIMAc_D$, after reaching equilibrium in the exchange experiments with deuterated water and deuterated acetic acid, respectively.

Even at high solvent contents with an excess of deuterons available, incomplete H/D exchange at the C(2)-position was reached for experiments with D_2O. The maximum exchange limit seems to be at approximately 85% $EMIMAc_D$. Likewise, at lower solvent contents no complete exchange is achieved. Maximum possible exchange is marked by the dashed line considering that water has two deuterons for exchange. The fact that there is only incomplete exchange suggests that the back reaction from the deuterated to the non-deuterated cation takes place to a certain extent. Moreover, the exchanged fraction in equilibrium does not seem to be a completely linear function of the water content but levels off for low IL contents below approximately 30 mol %. In addition, the profile of equilibrium exchange does not follow the dashed line. Thus,

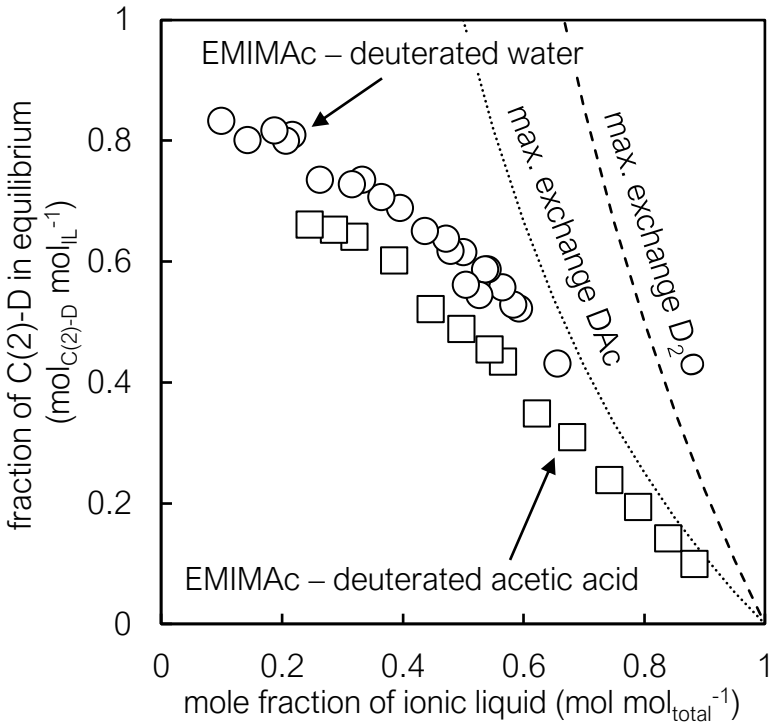

Figure 4.4: Fraction of IL deuterated at the C(2)-position in equilibrium after proton–deuteron exchange between deuterated solvent and EMIMAc. The lines refer to the maximum exchange possible with water (dashed line, two deuterons available for exchange) and acetic acid (dotted line, one deuteron available for exchange).

the exchange mechanism does not only depend on the number of available protons but is rather limited by the H/D exchange rates.

In mixtures with deuterated acetic acid, the exchanged fraction in equilibrium shows similar effects. Again, there is incomplete deuteration at the C(2)-position for any mole fraction because the equilibrium value of $EMIMAc_D$ lies below the maximum possible exchange (in this case marked by the dotted line considering that acetic acid offers one proton for exchange). Furthermore, the general equilibrium value is lower than in aqueous solutions and the maximum observed exchanged fraction for low IL contents lies around 65%.

Overall, the extent of deuteration in any of the investigated mixtures seems to be a function of the underlying H/D exchange equilibrium constant as determined by the ratio of forward and reverse exchange reaction rate constants.

Exchange Kinetics To resolve the composition ranges in view of the intrinsic interaction pattern, a closer look at the exchange kinetics is taken in the following section. For a first analysis, the experiments were evaluated according to the so-called pseudo-first-order principle in order to deduce second-order rate constants. For this purpose, the observed reaction rate constant k_{obs} was calculated for each experiment according to Eq. (3.10). Moreover, differences in reaction behavior of the two solvents can be analyzed by comparing the individual rate constants.

To improve the understanding of the correlation of exchange kinetics and acid–base properties of the investigated solutions, the observed exchange rate constant k_{obs} as a function of pH value of the mixtures is analyzed as described in the following. Figure 4.5 shows the observed proton exchange rate constants plotted over apparent pH of a solution of EMIMAc with normal water or acetic acid of the same composition as was investigated for the exchange experiments. As above (see Fig. 4.2 (b)), apparent pH refers to the value as was measured with the pH meter (i.e., the influence of increasing electrolyte concentration or activity correction was not accounted for). If the H/D exchange was a second-order reaction catalyzed by H^+ or OH^- and the respective deuterated ions, then a linear correlation between observed exchange rate constant and pH would be observed.

In aqueous solutions, the correlation is linear up to pH = 12. At higher pH values, a slight downward deviation from the linear correlation can be seen in the graph. This means that the observed exchange rate constant k_{obs} is lower than expected from a linear correlation with pH. Thus, at increasing pH, additional factors influence the exchange.

The three experiments with acetic acid below a pH of 8.5 agree well with the linear trend given by the exchange rate constants in aqueous mixtures. This implies that the exchange follows the same pH-dependent kinetics as observed with water in diluted solutions. In experiments with acetic acid and a pH above 8.5 (thus more concentrated solutions), a deviation from the linear correlation is visible. The observed rate constants are lower than expected from a linear relationship as indicated by the line, similar to the exchange experiments with water.

Towards high pH values, the observed exchange rate constants approximate an upper limit and the two curves approach and coincide in the strong alkaline regime with pH >13. This is the same pH regime of mixtures of EMIMAc with acetic acid and water that allow for high sugar yields (see Fig. 4.2). Although it remains unclear to what extent the proton exchange can directly be connected to pretreatment mechanisms, exchange kinetics as well as sugar yield are similar in the high pH regime for both types of EMIMAc-based mixtures.

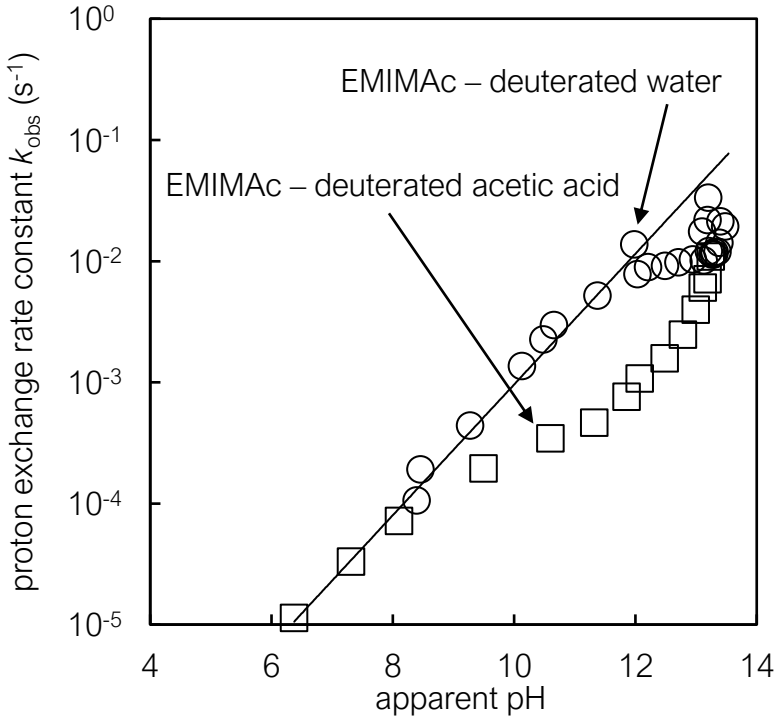

Figure 4.5: Observed proton exchange rate constants plotted versus the apparent pH (as measured) of EMIMAc mixed with deuterated water and deuterated acetic acid. The line serves as a guide to the eye.

In summary, the correlation of observed reaction rate constants and pH seems applicable for diluted solutions of EMIMAc for both investigated solvents. With an increasing EMIMAc content, and likewise increasing pH, the correlation does not hold. The pH value above which a deviation from the linear relationship occurs is specific for the added solvent. However, the mole fraction of EMIMAc above which a deviation from the linear relationship occurs is similar (approx. 35 mol % EMIMAc in aqueous mixtures and approx. 32 mol % EMIMAc in acidic solutions). Therefore, the correlation between mole fraction of IL and observed rate constants was evaluated. The calculation of second-order rate constants relies on the slope of pseudo-first-order constants over the mole fraction of solvent (see Eq. (3.11)), which is to be determined next.

Figure 4.6 shows the observed exchange rate constants, calculated for each experiment individually from Eq. (3.10), over mole fraction of EMIMAc. The observed proton exchange rate constants in EMIMAc with water decrease slightly from their highest value at high IL contents, having one outlier at approximately equimolar com-

position. The rate constants show a second, larger slope with decreasing EMIMAc content below 20–30 mol % EMIMAc. There is no overall linear dependence of the observed rate constants on the mole fraction of IL. In other words, the reaction between the IL and water does not follow a general second-order dependence that can be deduced from a pseudo-first-order evaluation.

With acetic acid, the observed exchange rate constants are generally lower than with water as a proton donor at the same molar composition. The slope in the concentrated EMIMAc samples is lower, too. The observed exchange rate constants with acetic acid show a small decrease in slope with increasing concentration of EMIMAc but the transition is not as distinguished as with water in EMIMAc.

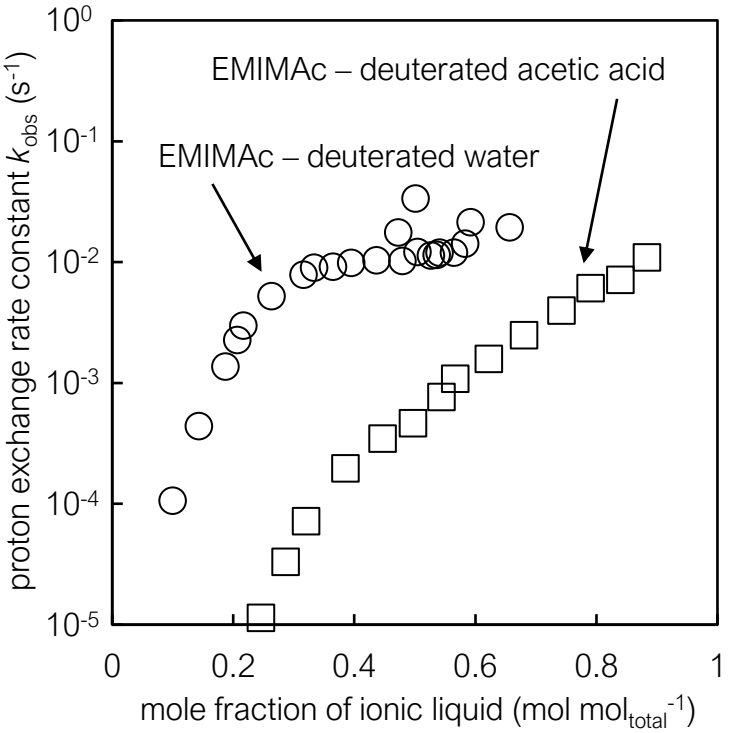

Figure 4.6: Observed proton exchange rate constants calculated from the pseudo-first-order exchange reaction at C(2)-H versus the mole fraction of EMIMAc.

In principle, several factors can influence an H/D exchange reaction and can thus lead to a deviation from an overall second-order reaction scheme (i.e., a linear correlation between observed rate constants and composition) and also determine whether the exchange increases or decreases with the mole fraction of the IL, which is discussed in the following.

Notably, the observed behavior seems to depend on the combination of ions. The H/D exchange in mixtures of BMIMCl and D_2O shows opposing characteristics to the experiments presented here. Yasaka et al. [228] detected a significant reduction of observed exchange rate constants in the concentrated regime with decreasing amount of deuterated water and a rather steady exchange rate constant in the aqueous regime. They connected this to a deactivation of water molecules bound to the chloride anion in concentrated ionic systems. In the systems of EMIMAc with water or acetic acid, however, the more concentrated IL solutions show a much stronger attraction of anion and cation that also facilitates proton exchange with the solvent, whereas the freely moving ion pairs in the dilute regime seem to have reduced interaction with the solvent, which results in slow and not measurable H/D exchange. It has to be examined whether the exchange kinetics of BMIMCl and EMIMAc can be connected via pH of the IL solutions. The pH was not measured in the cited study so that the reported data cannot be directly compared to our results.

Another factor that could limit the H/D exchange reaction is diffusion of the species participating in the reaction. Hall et al. [274] determined the self-diffusion coefficient of water to be higher than the one of the $EMIM^+$ cation throughout the whole concentration range of EMIMAc–water mixtures. Therefore, it can be assumed that the H and D species of water are equally distributed and do not limit the exchange.

Additionally, mass transfer as a result of viscosity could influence the exchange kinetics so that in highly viscous systems the exchange rate is reduced. However, for an increased viscosity at high EMIMAc contents (see Fig. A.3 (b) in appendix), fast exchange reactions are observed. This appears counter intuitive as for an increased viscosity a reduced reaction potential would be expected. Thus, it can be concluded that on the one hand the strong attraction between anion and cation in concentrated EMIMAc influences the exchange rate constant and not mass transfer or diffusion, but on the other hand the attractive forces between the charged species also increase the viscosity.

Besides aspects concerning convection, an increasing temperature can lead to higher exchange rate constants [224, 266]. Nevertheless, a reference sample heated to a temperature higher than the highest expected temperature increase due to mixing of EMIMAc and water cools down faster than the observed exchange (see Section 3.2.1 and Hall et al. [274]). Thus, an influence of temperature on the exchange is ruled out.

To sum up, neither temperature nor convection or diffusion of ions are the main causes for the deviation of a linear relation between observed rate constant and mole fraction of IL, thus yielding an overall second-order H/D-exchange.

From a comparison of chemical shifts of aqueous EMIMAc solutions, Chen et al. [278] classified three regions of interaction. The ions are associated in a network in concentrated mixtures. With the addition of water, the network is disrupted into a cluster structure and with further dilution, the cation–anion pairs change their association from C(2) hydrogen bonds to van der Waals attracting forces between the methyl groups in cation and anion (position 6 and 10) [273]. This changing association of ions could be one factor leading to the reduced H/D exchange in dilute solutions.

Therefore, two ranges with a different second-order mechanism are suggested: one that belongs to the cluster and network regime of high IL contents and one that belongs to the dilute ion-pair regime. The second-order rate constants thus have to be estimated with a more detailed model.

Modeling of Dissociation Equilibria and H/D Exchange Reaction in Mixtures of EMIMAc and Water The detailed model of the H/D exchange at the C(2)-position now takes into account both the stoichiometry and the dissociation equilibria of water. Figure 4.7 sketches the modeled exchange reaction between $EMIMAc_H$ and OD^- to form $EMIMAc_D$ and OH^- (see Eq. (3.12)). For reasons of clarity, only the dissociated D_2O molecule is shown and not the other species of water that were considered in the model Eqs. (3.18)–(3.21). $k_{f,1}$ and $k_{r,1}$ refer to the forward and reverse reaction rate constants for the exchange from H to D and back.

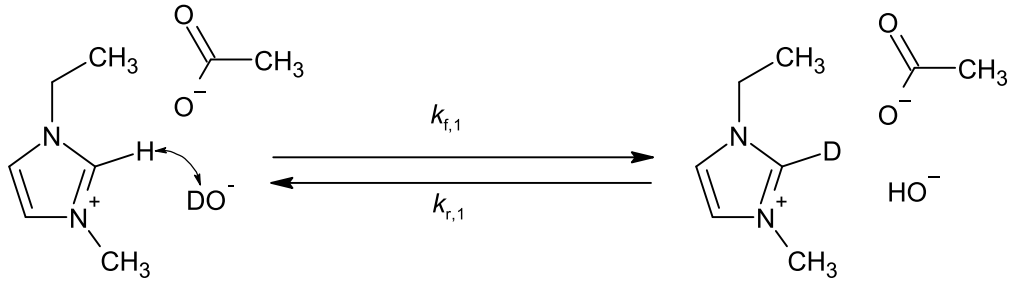

Figure 4.7: Modeled exchange mechanisms for H/D exchange in EMIMAc and water. For clarity, dissociated (normal) water as well as the undissociated water molecules H_2O, D_2O and HDO are not shown.

The model predictions were fitted to the experimentally observed values of $EMIMAc_D$ for the estimation of rate constants. The amount of free OH^-/OD^- cannot be reliably determined from pH and their respective pD measurements, since this study includes

highly ionic systems beyond the limit of established pH standards. Therefore, the amount of hydroxide ions is calculated from the water dissociation equilibria using the detailed modeling approach. At the same time, the dissociation constant for the water species HDO (Eqs. (3.20) and (3.21)) is estimated.

The applicability of the model and the assumptions were checked by simultaneous regression using systematically more and more data points to identify the composition range of identical kinetic interaction, hence fixed exchange rate constants.

Figure 4.8 shows the results of the parameter estimation of forward and reverse reaction rate constants, $k_{f,1}$ and $k_{r,1}$, as well as the estimated dissociation constants of HDO, $K_{w,4}$ and $K_{w,5}$, as a function of the mole fraction of IL. The 95% confidence intervals for all estimated reaction rate constants are between one and two orders of magnitude smaller than the estimated values, which indicates a good fit.

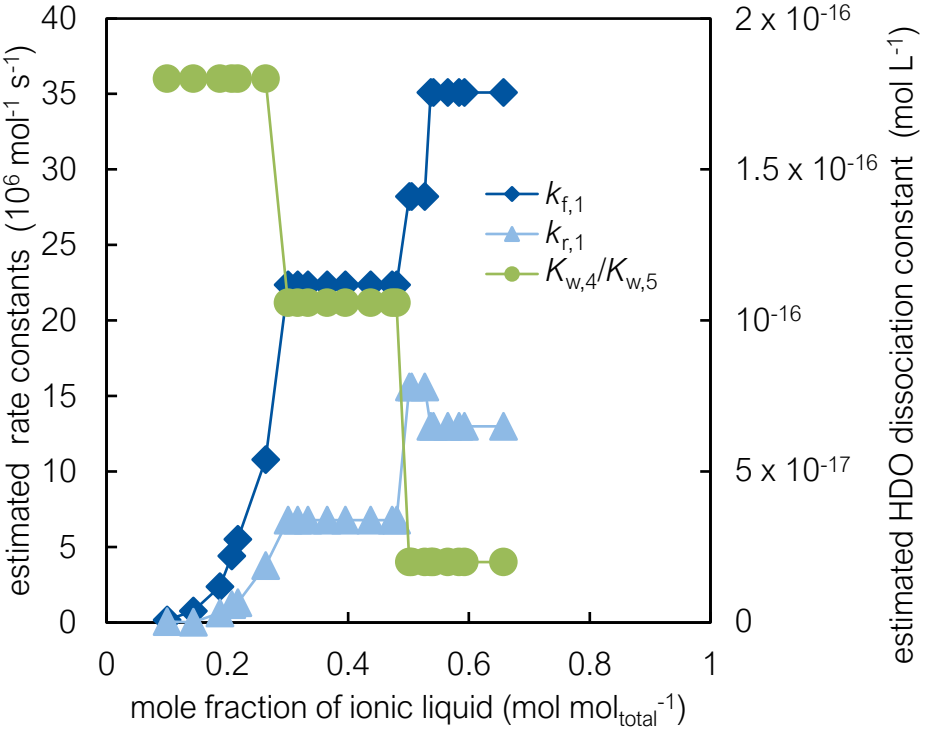

Figure 4.8: Estimated forward (blue diamonds, left axis) and reverse (blue triangles, left axis) reaction rate constants for proton exchange between EMIMAc and water versus the mole fraction of EMIMAc. Estimated dissociation constants for water species HDO (green circles, right axis).

Simultaneous fitting of experiments was possible for two composition ranges including a transition regime above a mole fraction of EMIMAc of 30 mol %. The transition

from IL-based solutions to concentrated aqueous solutions lies in a narrow span around the equimolar composition where only three experiments can be grouped together for simultaneous parameter estimation. Two of these experiments have almost the same composition and are therefore hard to differentiate in the graph. In contrast to the above presented results, this analysis with the detailed model shows that also in the concentrated regime a change in mechanism occurs when considering the dissociation of water.

In the dilute, ionic pair regime below 30 mol % EMIMAc, each data point had to be fitted individually. Similar to the rate constants for pseudo-first-order reactions (see Fig. 4.6), the rate constants decrease with decreasing IL content. The individual rate constants indicate that the depicted model can represent the concentrated regime with two different sets of parameters while the dilute regime has to be investigated in more detail.

The estimated dissociation constant for HDO is constant in the aqueous regime. Overall, the dissociation constants $K_{w,4}$ and $K_{w,5}$ decrease from the value of normal water dissociation K_w to the value of heavy water dissociation K_{dw} in two steps with increasing IL content. The second decrease of HDO dissociation constant also corresponds with a change in the estimated rate constants at approximately equimolar composition.

In principle, the parameter estimation can be carried out assuming other values of the dissociation constants of water. We tested three other possibilities next to the presented variant (see Fig. A.4 in appendix for results). In comparison, the estimated forward and reverse reaction rate constants have different absolute values in all four investigated possibilities. Nevertheless, in all four cases, the rate constants are in the same order of magnitude and increase towards higher IL content. In addition, the experiments in the aqueous regime (below 30 mol % EMIMAc) have to be fitted individually in all cases to obtain reasonable fitting results. Moreover, in none of the tested variants could all experiments in the concentrated regime be fitted simultaneously. At least two sets of experiments had to be grouped for the parameter estimation, but the transition between the simultaneously fitted experiments appears not as sharp as the limit of the aqueous regime. In the concentrated regime, the transition lies somewhere around the point of equimolar composition (more precisely between 47 and 54 mol % EMIMAc). Hence, the detailed model shows that there are two regimes of interaction in the IL-dominated concentration range which were not differentiated with the pseudo-first-order approach.

The detection of two major changes in the interaction pattern of H/D exchange in EMIMAc corresponds to the observations by Chen et al. [273, 278]. As mentioned

above, they suggest that the network-based association of EMIMAc ions in the concentrated IL regime changes to a cluster structure upon addition of water and further on leads to a different association of ions in the dilute ionic pair regime.

This parameter estimation indicates that a second-order exchange mechanism initiated by the hydroxide ion is not valid over the entire composition range with the given model assumptions. Higher reaction orders were not evaluated, because in the literature H/D exchange is commonly assumed to be of second order (cf. Amyes and Richard [223], Yasaka et al. [228], Ohta et al. [267]). For further verification of the hypotheses, more detailed thermodynamic models, considering for example activities, are required. The need for further research on thermodynamic data on equilibria in ILs and IL-solvent mixtures has already been mentioned in the literature [279]. Moreover, a change in reaction mechanism for the aqueous regime or additional dissociation equilibria require an adaptation of the reaction equations in the model.

Despite the variance in estimated reaction rate constants, the results of the detailed model show that the ion interaction pattern of EMIMAc does not change with the addition of water in the concentrated IL regime between 70 mol % EMIMAc and approximately equimolar composition. The results further suggest that the range of strong ion interaction reaches far into the aqueous region up to a ratio of water molecules to IL ions of approximately 2:1. In the aqueous regime below 30 mol % EMIMAc, the exchange rate constant is clearly reduced when more solvent is introduced.

In summary, the results of this study identify the composition range with associated IL ions interacting via the C(2)-position to be between 30 mol % and 70 mol % of EMIMAc. Further experiments need to be conducted to describe the effects observed in the aqueous regime. To study more complex reaction systems such as salt–solvent solutions containing different anions or a variety of molecular solvents, our experimental and modeling approach can simply be extended with other equilibria as well as H/D exchange reactions.

4.1.3 Conclusion

Concentrated EMIMAc effectively pretreats beech wood and allows for high sugar yields after enzymatic hydrolysis but the addition of water and acetic acid influences pretreatment results. Macroscopically, disintegration after pretreatment is reduced and above a threshold mole fraction that is specific for each solvent, beech chips appear unchanged after pretreatment. Together with the changed macroscopic disintegration after the addition of solvents, sugar yields drop. While the relation between

sugar yields and fraction of EMIMAc is specific for each solvent, the correlation between apparent pH of the mixture and sugar yield coincides for water and acetic acid, thus allowing for a direct comparison of pretreatment liquids. More specifically, in EMIMAc-based mixtures with pH exceeding 13, the total sugar yields exceed 67 wt %. Nevertheless, the strongly alkaline regime is not sufficiently resolved by pH, demanding for a more detailed analysis of molecular interactions in the pretreatment liquids.

Therefore, EMIMAc with the addition of water or acetic acid as proton donors was characterized with low-field NMR spectroscopy at ambient temperature to determine the composition ranges of ion–solvent interaction patterns in mixtures ranging from concentrated up to very dilute EMIMAc. Deuterated solvents were used to detect H/D exchange at the C(2)-position of the cation as the most prominent and most sensitive ion–solvent interaction.

We modeled the kinetics of proton exchange at the C(2)-position according to a pseudo-first-order reaction mechanism. The observed rate constants show a linear correlation with apparent pH of the aqueous mixtures only in the dilute regime below 30 mol % EMIMAc. In mixtures with acetic acid, a downward deviation from this correlation can be observed at similar EMIMAc mole fractions. Overall, the observed rate constants increase with increasing mole fraction of EMIMAc, both with water and acetic acid. Nevertheless, the H/D exchange cannot be explained by a simple second-order mechanism between solvent and EMIMAc as obvious from the nonlinear decrease of the exchange rate constant at high EMIMAc mole fractions.

More detailed modeling considering the dissociation of water precisely identifies the range of strong cation–anion interactions via the C(2)-position between 70 mol % and 30 mol %. While one general model of the whole composition range is yet impossible due to different and unknown molecular mechanisms, the results reveal fast H/D exchange even at mole fractions as low as 30 mol % EMIMAc in water.

EMIMAc-based processes can thus exploit the presence of strongly associated reactive ions down to this lower mole fraction limit. This contribution exemplifies a first step towards the thorough description of interactions between ILs and solvents considering both dissociation on a molecular level and the influence of ion association and thus liquid structure on a larger scale.

Overall, a direct correlation between the observed pretreatment effects and interaction of EMIMAc and solvent in terms of H/D exchange proves difficult. The correlation between pH and exchange kinetics is only valid for dilute solutions comprising less than 30 mol % EMIMAc and in the concentrated regime, the true molecular interaction mechanism remains unknown. To find the molecular causes within the pretreatment

liquid and in interaction with the biomass that lead to changed pretreatment results, more research is required that goes beyond the scope of this thesis.

As stated in Subsection 2.2.3, the species present in the pretreatment liquid have a strong impact on the outcome of pretreatment and it is therefore of interest to know the relation between composition of pretreatment liquid and pretreatment effectiveness. To investigate relations between phenomenological changes of the biomass during pretreatment and the composition of pretreatment liquids, we focus on a different pretreatment concept that shows disintegration effects and contains similar components. Hence, in the next section, acetosolv is examined as an exemplary pretreatment concept for beech wood aiming at the identification of simple criteria for the evaluation of pretreatment effectiveness.

4.2 Acetosolv Pretreatment of Wood for Biorefinery Applications

As a potential pretreatment concept for biorefineries, the OS process enables usage and recovery of both the lignin and the hemicellulose fraction besides the cellulose pulp [280, 281]. So far, several variants have been tested including OS pretreatment relying on acetic acid as main solvent with the addition of a further catalyst acid, the so-called acetosolv process [55, 56, 282, 283].

The advantage of acetic acid-based pretreatment liquids is an increased solubility for lignin in comparison to alcohols, allowing for pretreatment at mild conditions (i.e., temperatures below 100 °C and atmospheric pressure) [55, 56, 200]. Nevertheless, process conditions such as temperature, duration of the pretreatment and liquid-to-wood ratio appear less important for pulp yield and delignification than the composition of the pretreatment liquid [141, 215, 217]. In this context, a high concentration of acetic acid is beneficial for an effective removal of lignin [141, 215, 284], while the presence of a catalyst facilitates the removal of lignin in the first place [215, 217]. Nevertheless, the influence of water content on the removal of lignin remains unclear [285]. With regard to biorefinery applications, the influence of varying catalyst types and concentrations and their relation to pretreatment phenomena has not yet been systematically analyzed.

For the analysis of acetosolv pretreatment of beech wood, we divide this section according to the scales of the investigated pretreatment phenomena. Subsection 4.2.1 focuses on the macroscopic phenomenon of disintegration and overall mass balances. Subsection 4.2.2 deals with compositional changes after pretreatment, that is, the quantitative analysis of cellulose, hemicellulose and lignin content in the recovered fraction, the analysis of components that are solubilized during pretreatment and the evaluation of acetyl content of pretreated samples. In Subsection 4.2.3, pretreatment effectiveness is evaluated by sugar yields of enzymatic hydrolysis.

4.2.1 Disintegration and Mass Balances

For a systematic analysis of disintegration, we visually classify the separation of wood fibers after acetosolv pretreatment into five degrees of disintegration (DoD) as shown in Fig. 4.9. For the allocation of a DoD to a sample, we consider changes in shape of the pretreated wood chips only and do not focus on changes in color. DoD 0 shows no signs of disintegration. It is indistinguishable from untreated wood except

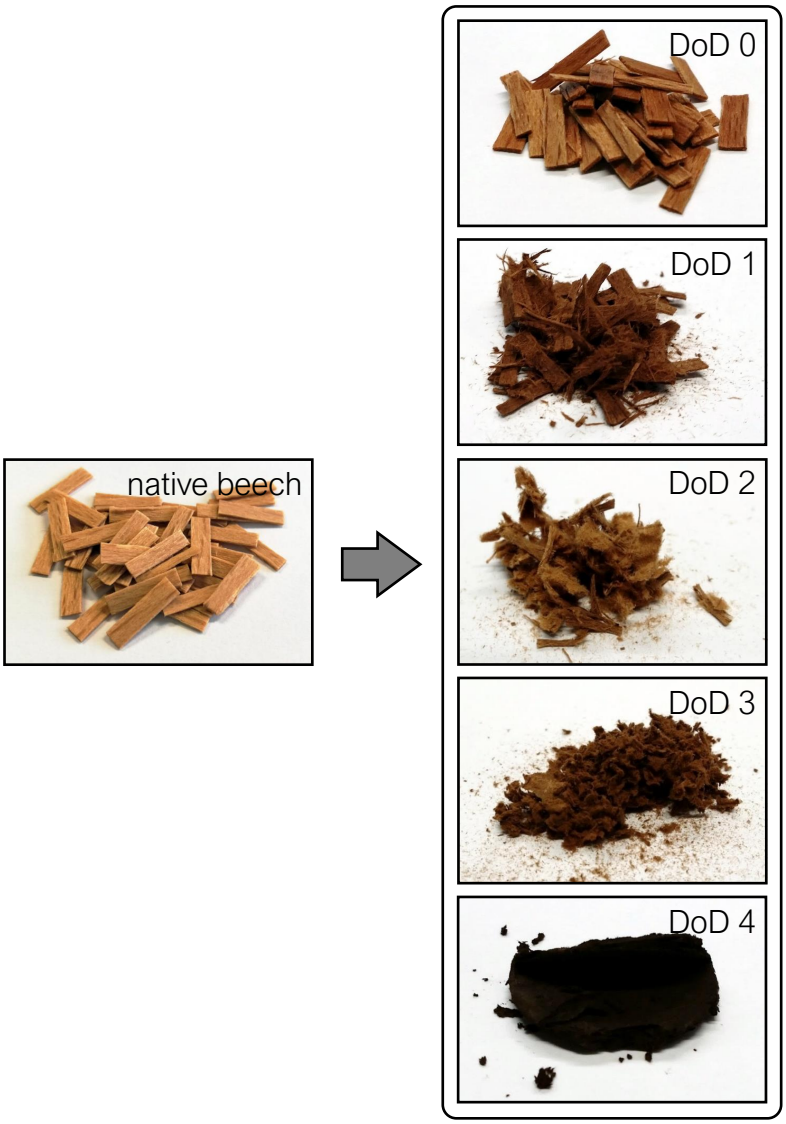

Figure 4.9: Classification of degrees of disintegration (DoD) after pretreatment by visual inspection in comparison to the native wood chips (10 mm×2 mm): DoD 0 (no disintegration), DoD 1 (moderate disintegration, slightly frayed wood chips), DoD 2 (strong disintegration, largely disintegrated wood), DoD 3 (complete disintegration) and DoD 4 (charred).

for a slight change in color towards a darker brown after pretreatment in some cases. DoD 1 refers to a moderate disintegration. The wood chips are slightly frayed after pretreatment but their original shape is still clearly visible. Furthermore, the amount of disintegrated wood is rather small in comparison to the amount of wood, which is

still in original shape. DoD 2 exhibits strong disintegration with largely disintegrated wood. Nevertheless, the form of the original chips is still visible. DoD 3 refers to complete disintegration of the wood. The original shape of the wood chips is no longer visible because fibers have been completely disintegrated from each other. DoD 4 is reached when the fibers are degraded after pretreatment and the wood is charred. In the following, we refer to disintegration or disintegrated wood when a sample reaches DoD 2 or 3 after pretreatment (i.e., DoD 1 is not sufficiently disintegrated, while DoD 4 refers to disintegrated but degraded wood samples).

For a first assessment of disintegration after acetosolv pretreatment, experiments with mineral acid catalysts are evaluated, because mineral acids are often employed as catalyst acids in organosolv pretreatment liquids [55]. Figure 4.10 depicts (a) samples of beech wood pretreated with hydrochloric, sulfuric and phosphoric acid in acetic acid as well as (b) samples of beech wood pretreated with the same mineral acid catalysts in water. With increasing catalyst concentration in acetic acid-based pretreatment liquids, all DoDs are reached with all three mineral acid catalysts. Furthermore, samples of a specific DoD have a similar visual appearance when pretreated with either one of the mineral acid catalysts. Hence, the type of catalyst does not influence the macroscopically visible disintegration. Nevertheless, it is noteworthy that the amounts of catalyst acid required to achieve a certain DoD differ by an order of magnitude from H_2SO_4 to HCl and from HCl to H_3PO_4 (see Tab. 4.1 for exact values of catalyst acid concentration in acetic acid and water, respectively). Furthermore, with increasing DoD and hence, with increasing catalyst concentration, the samples become darker (cf. Kin [216]).

While for the acetosolv experiments an increasing DoD up to charred wood is achieved with an increasing catalyst concentration, beech wood does not disintegrate in aqueous pretreatment liquids (i.e., DoD 0). Even at high catalyst concentrations that lead to charring of wood in acetic acid-based liquids (see Tab. 4.1), only the edges of the wood chips are charred in aqueous liquids, especially for sulfuric and phosphoric acid catalyst (right samples in Fig. 4.10 (b)). This absence of disintegration after pretreatment in aqueous liquids shows that acetic acid plays a major role in achieving disintegration of beech wood during acetosolv pretreatment. Supposedly, all DoDs can be reached irrespective of the type of catalyst acid added to the acetosolv liquids but DoD seems to depend on the acidity (i.e., proton concentration) of the respective pretreatment liquid. For the most part, acids added to glacial acetic acid as solvent remain undissociated, whereas the addition of even small amounts of water can lead to significant increases in the fraction of dissociated acid species [286]. Nevertheless, the relative order of acid dissociation constants in acetic acid appears proportional to

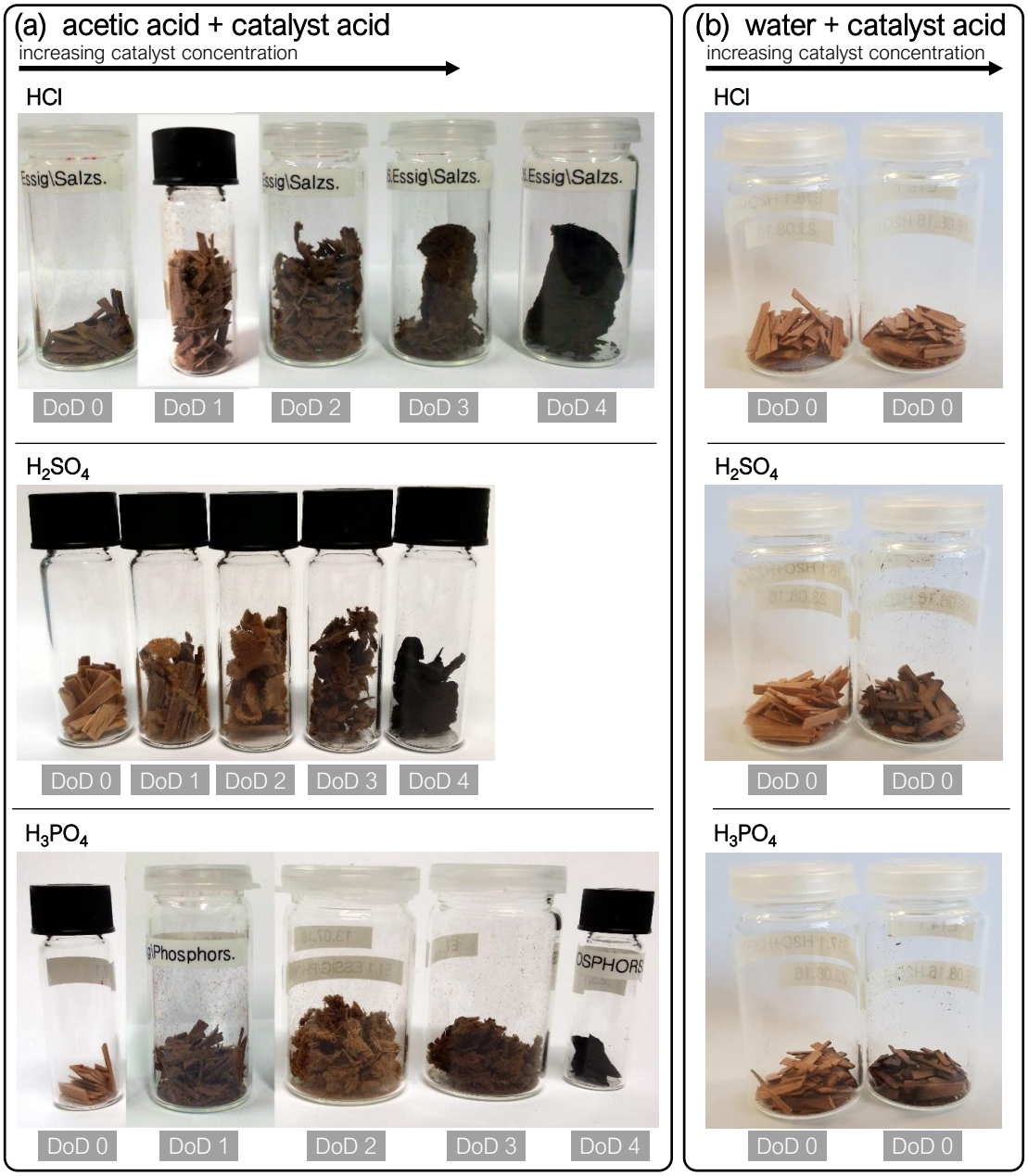

Figure 4.10: Beech wood pretreated with mineral acid catalysts **(a)** in acetic acid and **(b)** in water. From top down, catalyst acids are sorted according to increasing pK_a. Concentrations of catalyst acids increase from left to right (see Tab. 4.1 for values). The position of the vials does not indicate the relative ratios of increasing concentration but results from the size of the vials.

the order of these constants in water [287]. Hence, it is of interest to know how the acid strength of a catalyst acid influences the extent of disintegration.

Table 4.1: Concentration of catalyst acids ($\mathrm{mol\,L^{-1}}$) in acetic acid-based experiments (see Fig. 4.10 **(a)**, DoD 0 – DoD 4) as well as in water-based experiments (see Fig. 4.10 **(b)**, left and right sample).

Catalyst	**DoD 0**	**DoD 1**	**DoD 2**	**DoD 3**	**DoD 4**	**Left**	**right**
HCl	0.0156	0.0314	0.0591	0.1416	0.2826	0.1687	0.2937
H_2SO_4	0.0008	0.0056	0.006	0.0228	0.2354	0.0052	0.2348
H_3PO_4	0.0256	0.6425	1.752	3.168	8.151	1.893	4.792

To evaluate the influence of acid strength of catalyst acids in acetosolv liquids on the extent of disintegration, we carried out pretreatment experiments with a variety of catalyst acids. Usually, the acidity of an aqueous solution is indicated by pH. However, a measurement of pH in concentrated, nonaqueous solutions such as the acetosolv liquids requires activity corrections to estimate the amount of dissociated acid species. Because the development of models that account for these influences is not within the scope of this thesis, we take the pK_a difference between acetic acid and the catalyst acid as an indicator for the acid strength of the catalyst acid in acetosolv pretreatment liquids. This approach has successfully been applied in one study on organosolv pretreatment of Japanese cedar, where sugar yield after pretreatment and enzymatic hydrolysis could be correlated with the pK_a of a range of catalyst acids [212].

Figure 4.11 shows the water content of the pretreatment liquids versus the difference of pK_a between acetic acid and the tested catalyst acids for the experiments at constant ratio of catalyst acid to acetic acid. For concentrated acetosolv liquids (filled symbols) below a pK_a difference of 5, beech wood does not disintegrate (DoD 0). For an increased pK_a difference of 7.76 and 10.76 with sulfuric acid and hydrochloric acid, respectively, the samples are either charred after pretreatment in concentrated acetosolv liquids (filled symbols) or completely disintegrated with added water (striped symbols). Similarly, pretreatment with hydroiodic acid catalyst in acetic acid–water-based pretreatment liquids leads to complete disintegration of beech wood. As stated above, no disintegration is observed for the reference experiments with water and catalyst (checked symbols, see Fig. 4.10). Hence, the presence of acetic acid is essential to achieve disintegration, while with an increasing water content, the DoD decreases. In addition to acetic acid, a catalyst acid is required to disintegrate the wood because

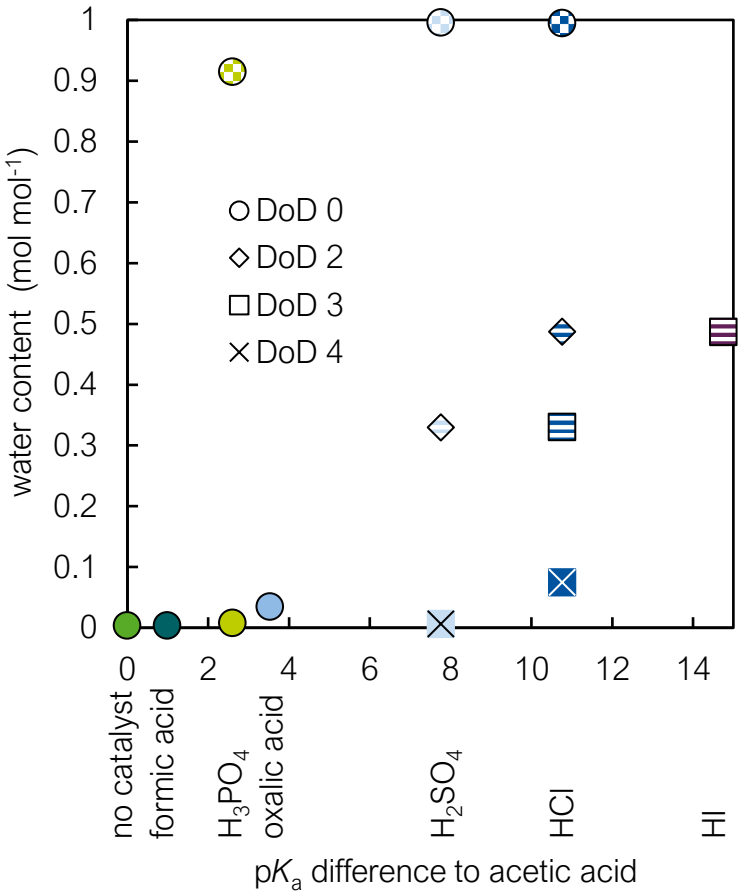

Figure 4.11: Water content of pretreatment liquids versus pK_a difference between acetic acid and catalyst acid. All catalyst acids are stronger acids than acetic acid. Acetosolv liquids contain approx. $0.25\,\mathrm{mmol_{catalyst}\,g_{AA}^{-1}}$. The filled symbols refer to concentrated acetosolv liquids (i.e., only acetic acid and catalyst acid), where the water content slightly varies due to the different purities of the employed catalyst acids. The striped symbols refer to acetosolv experiments where additional water was added to increase the water content and the checked symbols refer to reference experiments with only water and catalyst acid. The shape of the symbols indicates the DoD (see legend).

in the experiment with no catalyst (i.e., pure acetic acid as pretreatment liquid) no disintegration was observed.

Taking the influence of water content into consideration, an evaluation of pK_a only does not seem sufficient as a single evaluation criterion for the acid strength of the

catalyst acids with regard to disintegration effects. Furthermore, it is unclear how the concentration of the catalyst acids influences pretreatment results. Thus, in the following, three catalyst acids are examined in more detail by studying the influence of their concentration on mass balances and component analysis.

The relation between the non-recovered fraction after pretreatment and the concentration of catalyst acids (a) hydrochloric acid, (b) sulfuric acid and (c) phosphoric acid is sketched in Fig. 4.12. For all three catalyst acids, the non-recovered fraction of acetic acid-based experiments (filled symbols) increases with increasing concentration. Likewise, a positive correlation between non-recovered fraction and the concentration of hydrochloric acid catalyst has been observed in the literature for acetosolv pretreatment of eucalyptus and beech [215, 219]. Towards higher catalyst acid concentrations, the non-recovered fraction appears limited and remains rather constant.

With increasing concentration of catalyst acid and hence, increasing non-recovered fraction, the DoD increases successively. Thus, disintegration and non-recovered fraction seem to be interconnected independent of the type of catalyst acid. More specifically, DoD 0 to DoD 2 relate to a non-recovered fraction increasing from slightly more than 0 wt % to approximately 40 wt %, whereas DoD 3 is connected to the maximum recovered fraction in all observed cases. For DoD 4, on the other hand, the non-recovered fraction can decrease due to recondensation of solubilized components. This is visible for sulfuric acid and especially for phosphoric acid.

Furthermore, our experiments show that the range of increasing non-recovered fraction (i.e., the transition from DoD 0 to DoD 2) in relation to catalyst concentration is specific for each catalyst acid. In case of sulfuric acid, a minimum concentration of 1.5–2.9 mmol L^{-1} is required to initiate the removal of a significant fraction of wood (i.e., 10 wt % non-recovered fraction). In this concentration range, the pretreated samples show no signs of disintegration (DoD 0). This lower threshold for removal of biomass components is not visible for the other two acids, possibly not resolved due to few data points in the respective concentration ranges. For hydrochloric and phosphoric acid, the lowest tested concentrations with significant removal of biomass components are 0.008 and 0.47 mol L^{-1}, respectively. Similarly, the transition from increasing non-recovered fraction to the maximum non-recovered fraction is around 0.004–0.0045 mol L^{-1}, 0.06–0.142 mol L^{-1} and 0.9–1.75 mol L^{-1} for sulfuric, hydrochloric and phosphoric acid, respectively. However, this order of concentration values does not correlate with the order of pK_a, which is p$K_{a,HCl}$ < pK_{a,H_2SO_4} < pK_{a,H_3PO_4}.

In another study on acetosolv pretreatment of beech wood, sulfuric acid was less effective as catalyst acid than hydrochloric acid, which matches the order of pK_a [216]. In comparison, the pretreatment liquids applied by Kin [216] were not composed of

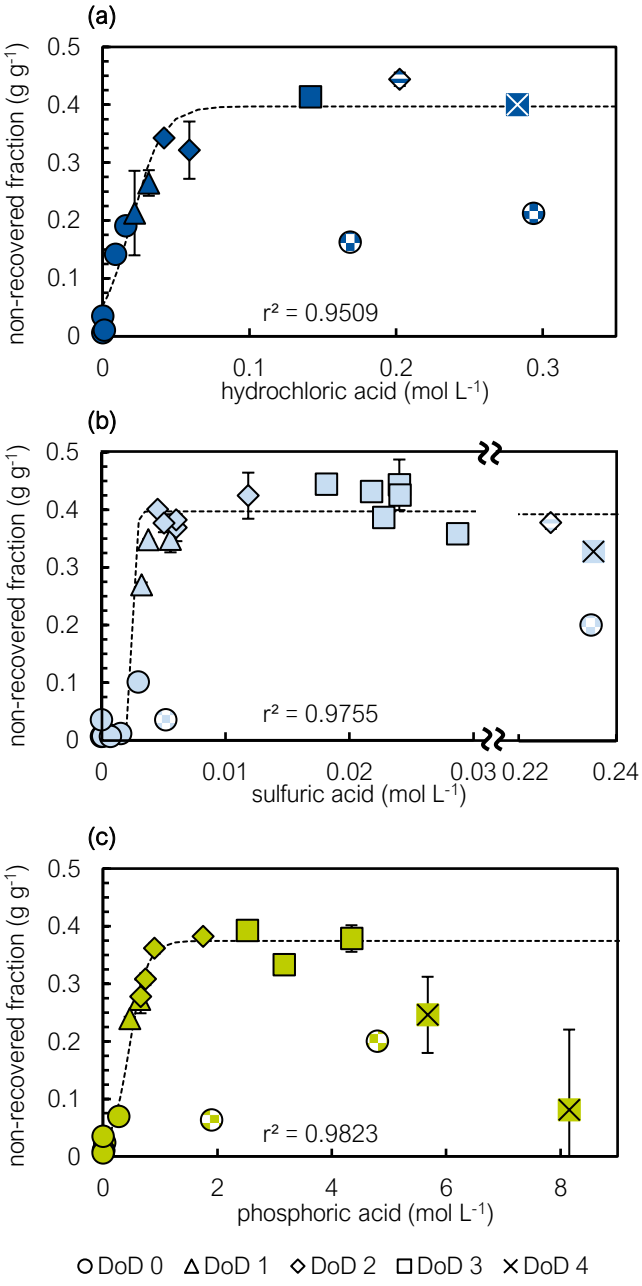

Figure 4.12: Non-recovered fraction of beech wood versus concentration of **(a)** hydrochloric acid, **(b)** sulfuric acid and **(c)** phosphoric acid as catalyst acid. Filled symbols refer to liquids with only acetic acid and catalyst acid, striped symbols refer to liquids with water added to acetic acid and catalyst acid, and checked symbols refer to reference experiments with only water and catalyst acids. The shape of the symbols indicates the DoD (see legend). Error bars are shown only for measurements with standard deviation above symbol size.

concentrated acetic acid, but contained an increased water content of 20 wt %. In contrast, the acetosolv liquids in this study contain only trace amounts of water due to the purity of the acid added as catalyst. For hydrochloric acid, the water content is slightly higher than for sulfuric acid due to the higher purity of the latter. However, the exact relation between disintegration and water content as well as catalyst concentration cannot be resolved by a simple comparison to literature.

As a first step towards the quantification of the influence of catalyst concentration, the non-recovered fraction is fitted as a function of the catalyst concentration (the dashed lines in Fig. 4.12 (a)–(c)). Often, the solubilization of biomass components during pretreatment is modeled as a first-order reaction [81, 219, 281, 288]. However, biomass is a heterogeneous raw material that shows untypical kinetic behavior in many cases (i.e., the assumption of a first-order reaction is not applicable due to changes in reaction parameters during pretreatment or changing reactivities for different fractions of the individual components). To model this untypical kinetic behavior, xylan and lignin solubilization during formic acid pretreatment of wheat straw could be related to an extended severity factor in combination with a logistic function [289]. Similarly, a logistic function reflects bulk and residual solubilization of biomass components during formic acid-based pretreatment of sugarcane bagasse [290]. Hence, we chose a logistic function to model the relation between catalyst concentration and non-recovered fraction. Further details on the function and fitted parameters are given in Appendix B. Mainly, the fit supports the observation that the maximum non-recovered fraction is independent of the type of catalyst acid but is specific for beech or for acetosolv-pretreated beech.

As observed above, the presence of water reduces the degree of disintegration. This is also revealed in the analysis of the non-recovered fraction for all three catalyst acids. In aqueous liquids (checked symbols), catalyst acid concentrations that lead to charring of wood in concentrated acetosolv liquids (i.e., DoD 4) only lead to DoD 0 with slightly charred edges (see also Fig. 4.10). Moreover, for these reference experiments, the non-recovered fraction amounts to approximately 20 wt %, which is lower than the maximum non-recovered fraction for disintegrated samples but higher than the non-recovered fraction for DoD 0 observed with acetic acid-based pretreatment liquids. Similarly, a limited non-recovered fraction of up to 20 wt % was observed for pretreatment of beech wood in aqueous oxalic acid [291].

In experiments with an acetic acid–water mixture as solvent (striped symbols), the non-recovered fraction reaches the upper limit of approximately 40 wt % but with DoD 3 at catalyst concentrations that lead to charring of wood (i.e., DoD 4) in concentrated acetosolv liquids. Hence, besides enabling disintegration, the presence of acetic acid

in the pretreatment liquid allows for increased solubilization of removed components. As a result, a rather high maximum non-recovered fraction of 40 wt % is achieved due to disintegration in combination with high solubility for biomass components.

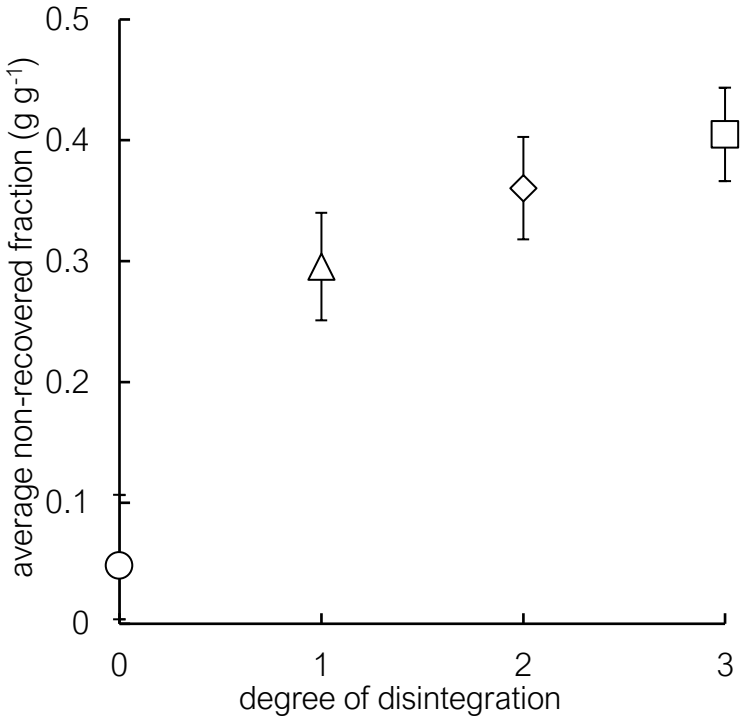

Figure 4.13: Non-recovered fraction versus degree of disintegration after acetosolv pretreatment. Points are average values for all above shown experiments with sulfuric, hydrochloric and phosphoric acid catalysts. The shape of the symbols corresponds to the DoD.

Figure 4.13 shows the average non-recovered fraction of all experiments with mineral acid catalysts for DoDs 0 to 3 of beech wood after pretreatment (i.e., the average of all experiments with filled symbols shown in Fig. 4.12). It is visible that also for the average points, the non-recovered fraction increases with increasing DoD (i.e., the recovered fraction is reduced with increasing disintegration). On average, a removed fraction of approximately 30 wt % seems to be the threshold to even slight disintegration (DoD 1). Analogously, Nitsos et al. [237] observed formation of degradation products after hydrothermal pretreatment of beech wood only above 30 wt % removed fraction. These observations indicate that the compounds of beech wood are removed consecutively so that only above this limit disintegration is initiated and at the same time degradation products are formed. Therefore, it is of interest to know which fac-

tors exactly lead to the disintegration of beech wood. A first step is the component analysis of the recovered fraction to determine whether the removal of certain components correlates with disintegration. Hence, in the next section, we analyze changes in the composition of the samples after pretreatment with the different catalyst acids.

4.2.2 Compositional Changes after Pretreatment

First, we quantitatively analyze the pretreated beech wood samples in terms of cellulose, hemicellulose and lignin removed during pretreatment in relation to the overall non-recovered fraction. Second, we qualitatively analyze the components that are dissolved during pretreatment and can thus be determined via NMR spectroscopy of the pretreatment liquids after pretreatment. Third, we estimate the fraction of dissolved components from NMR spectra. Fourth, changes in acetyl content of selected samples after pretreatment are discussed with regard to the influence of the pretreatment liquid composition.

4.2.2.1 Analysis of Recovered Material

The fraction of removed components is calculated from the composition and amount of the recovered fraction in comparison to the composition and initial amount of native beech wood.

For pretreatment concepts relying on enzymatic hydrolysis for the release of sugars, it is desirable that a large fraction of cellulose remains in the pretreated sample. This means that glucose is not removed or degraded during pretreatment. For many of our experiments, the standard deviation of removed glucose is high (see Fig. B.1 in appendix) and therefore, it is unclear how much cellulose actually remains in the pretreated samples. These fluctuations could be caused by an inhomogeneous distribution of sugars in disintegrated samples or by a wrong weight of the recovered fraction due to acetic acid or catalyst acid still being attached to the wood. Furthermore, an underestimation of the glucose content of native beech could lead to negative values of removed glucose. Some experiments show a rather high fraction of glucose removed during pretreatment in combination with a high DoD. Here, aggressive catalyst acids at high concentrations (see Tab. B.2 in appendix) probably hydrolyze and/or degrade sugars as has been observed for spruce, which was extensively disintegrated after organosolv pretreatment [105]. Nevertheless, it seems that for most experimental conditions, glucose (i.e., cellulose) stays in the recovered fraction.

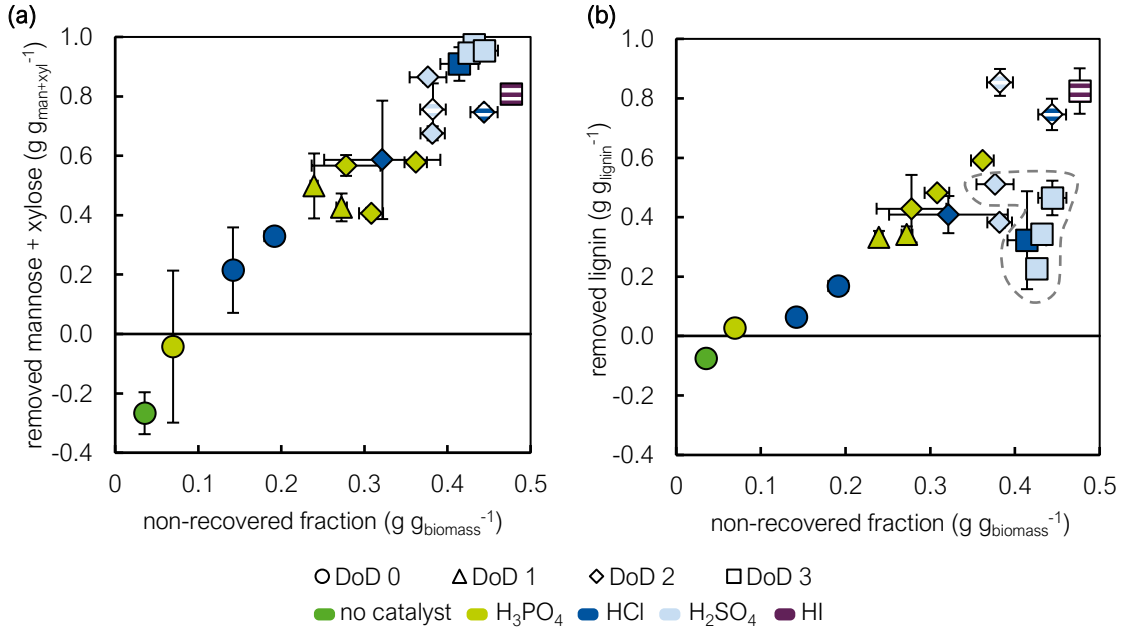

Figure 4.14: Fraction of **(a)** mannose and xylose, and **(b)** lignin removed during pretreatment with acetic acid-based liquids (filled symbols) and acetic acid–water-based liquids (striped symbols) versus non-recovered fraction. The content of hemicellulose as xylose + mannose and the content of lignin in native beech is 26.2 wt % and 17.3 wt %, respectively. The area delineated by the dashed curve includes experiments with an extraordinary high fraction of lignin remaining in the pretreated material and at the same time a high amount of glucose removed during pretreatment. Shape and color of the symbols indicate the DoD and the employed catalyst acid, respectively (see legend). Error bars are shown only for measurements with standard deviation above symbol size.

The sum of removed xylose and mannose as mostly detected sugars of the hemicellulose fraction versus the non-recovered fraction is depicted in Fig. 4.14 (a). In most cases, the standard deviation is low and the graph shows a clear linear correlation between the fraction of hemicellulose sugars removed and the non-recovered fraction. Furthermore, both the samples with concentrated acetic acid-based pretreatment liquids (filled symbols) and the samples with an increased water content in the pretreatment liquids (striped symbols) apparently follow the same correlation. For each catalyst acid, the fraction of removed hemicellulose sugars increases with increasing acid concentration (see Tab. B.2 in appendix). For the presented experi-

ments, hemicellulose sugars amount to the highest share of the removed components. Nevertheless, especially for the experiments with a high quantity of removed hemicellulose sugars (i.e., complete disintegration with a high non-recovered fraction), other components are removed as well. Moreover, for all (but one) of the disintegrated samples, at least half of the hemicellulose sugars are removed during pretreatment. Thus, the removal of a major fraction of hemicellulose is a prerequisite for disintegration, though this is rather a necessary condition and not sufficient to achieve disintegration.

Figure 4.14 (b) shows the fraction of (acid-insoluble) lignin removed during acetosolv pretreatment versus the non-recovered fraction. Generally, lignin has the lowest standard deviations among the quantified components. Similar to hemicellulose, lignin shows a mostly linear correlation between the fraction of lignin removed and the non-recovered fraction, which is in agreement with other studies on organosolv and acetosolv pretreatment [102, 141]. Unlike the removal of hemicellulose sugars, the removal of lignin shows an offset and is only initiated between a non-recovered fraction of 10 to 20 wt %. This means that first a part of hemicelluloses is removed before the lignin content is significantly reduced during pretreatment (i.e., hemicellulose and lignin are removed successively). Similarly, for acetosolv pretreatment of eucalyptus wood, high delignification is reached when at the same time the pentose concentration in pulping liquors is high (i.e., a large fraction of hemicellulose removed) [219].

For disintegrated samples (DoD 2 and 3), the extent of disintegration in relation to the lignin content is partly ambiguous. More specifically, the visual classification of strong and complete disintegration includes samples with both a high and low fraction of lignin removed. This refers to the samples with an increased water content in the pretreatment liquid (striped symbols) and those that show a rather high amount of glucose removed after pretreatment (highlighted by the dashed curve as in Fig. B.1). On the one hand, the strongly acidic conditions which lead to degradation of the cellulose fraction during pretreatment at the same time inhibit an effective removal of lignin. On the other hand, acetic acid–water-based pretreatment allows for an effective removal of lignin with the majority of lignin being removed irrespective of the type of catalyst acid. Thus, in this study, a rather high water content seems to be beneficial to achieve removal of lignin due to a higher solubility for lignin fragments and/or due to a more effective cleavage of lignin in comparison to pretreatment liquids composed of concentrated acetic acid and high catalyst acid concentrations. An increase or reduction in lignin solubility due to different water contents in (acetosolv) pretreatment liquids can have a significant impact on pretreatment effectiveness and hence process performance. However, more experiments are needed to determine the ratio of acetic acid and water with optimal lignin solubility.

As a first, simple evaluation of acetosolv pretreatment liquids with high and very low water content, lignin solubility can be estimated. Often, estimates for the solubility of (bio)polymers in a solvent rely on Hildebrand parameters. According to Hildebrand, solvents allow for solubility of a solute, if their parameters are similar. The Hildebrand parameter value for lignin ranges between 23 and 26 $MPa^{1/2}$ [137, 191, 192], while the values for acetic acid and water are determined to 20.7 and 47.9 $MPa^{1/2}$ (25 °C), respectively [292] (note the differently higher reported value for acetic acid in the compilation of Zhao et al. [56]). Hence, lignin solubility should be maximal in liquids containing a high volume fraction of acetic acid as a result of the volume-based mixing rule to estimate Hildebrand parameters of a mixture (cf. Barton [292]). Both in concentrated acetic acid and in aqueous solutions, lignin solubility remains below the maximum according to Hildebrand's theory. Correspondingly, solubility of sugarcane bagasse lignin is highest in mixtures containing around 80 vol % acetic acid [284]. Neglecting the rather small density change in acetic acid–water solutions, a volume fraction of around 80 vol % corresponds to a mole fraction of approximately 55 mol %. This is in line with our observation of facilitated lignin removal in pretreatment liquids containing 50 mol % acetic acid in comparison to nearly pure acetic acid. A quantitative relation between lignin solubility and the ratio of acetic acid to water still has to be determined especially with regard to pretreatment process performance.

To conclude, several aspects of the magnitude of recovered material and its composition are linked to disintegration of beech wood after acetosolv pretreatment. For disintegrated samples, the non-recovered fraction exceeds 25 wt %. This corresponds to the removal of approximately one half and one third of the hemicellulose and lignin fraction, respectively. To achieve disintegration in concentrated acetic acid pretreatment liquids, a minimum concentration for each catalyst acid is required: HCl $\gtrsim$ 0.04 mol L^{-1}, H_2SO_4 $\gtrsim$ 0.005 mol L^{-1}, H_3PO_4 $\gtrsim$ 0.65 mol L^{-1} (see Fig. 4.12). Nevertheless, disintegration also relates to the interplay of acid and water content and hence, this specific threshold of catalyst concentration is probably increased with the addition of water.

4.2.2.2 Qualitative Analysis of Dissolved Components

With the aid of NMR spectroscopy, components that are dissolved in the pretreatment liquid after the experiments can be detected. This analysis of removed components complements the above analysis of the recovered fraction. Nevertheless, it should be noted that this analysis of low-field NMR spectra is limited to the detection of dissolved components without a detailed analysis of degradation pathways. Sample

spectra of aqueous and acetic acid-based pretreatment liquids after pretreatment are given in Fig. B.2 in the appendix.

Spectra of the reference experiments with water and catalyst show only slight signals of sugars and acetic acid. The latter is probably formed due to deacetylation of beech wood during pretreatment. With the absence of disintegration and hence a high recovered fraction in the reference experiments, it seems plausible that only a few components are dissolved in these pretreatment liquids after pretreatment.

In the spectra of acetosolv pretreatment liquids relying on concentrated acetic acid, dissolved wood components (lignin, sugars) and degradation products (furfural, formic acid) show clear peaks. Both furfural and formic acid can be formed due to degradation reactions of C5- as well as C6-sugars [81, 293]. Signals of solubilized components and degradation products do not appear similarly for all experiments (see Tab. B.3 in appendix). Nevertheless, lignin is visible for all experiments with acetic acid-based pretreatment liquids indicating that a certain fraction of the lignin is always extracted independent of the type and concentration of catalyst acid. Besides a very weak lignin signal, the spectra of the reference experiment with only acetic acid and no catalyst acid show no other components. Sugar signals are mostly observed with sulfuric acid catalyst, corresponding to the hydrolysis of cellulose in experiments with sulfuric acid discussed above. In addition to sugar signals, the experiments with sulfuric acid show the strongest signals of degradation products followed by hydrochloric acid and phosphoric acid. This order is in line with the observation that with sulfuric acid, the lowest acid concentrations are required to achieve a certain DoD, whereas for phosphoric acid, the highest concentrations are required (i.e., not in line with the order of pK_a). Mostly, the furfural peaks are more pronounced the higher the employed acid concentration while the appearance of the formic acid peak cannot directly be linked to catalyst acid concentration. The spectra of experiments with acetic acid–water-based pretreatment liquids show peaks of formic acid as well as furfural. Nevertheless, the evaluation of exact relations between catalyst concentration and the appearance of degradation products requires a quantitative analysis of the latter.

4.2.2.3 Determination of Dissolved Fraction

As discussed above, with increasing non-recovered fraction, hemicellulose is continuously removed, followed by continuous removal of lignin (see Fig. 4.14). Since both components have a hydrogen weight fraction of $w_{H,hc} = w_{H,l} = 0.0671$, solubilized protons should linearly correlate with non-recovered fraction. Figure 4.15 shows the estimated fraction of wood protons dissolved in the pretreatment liquid versus the

non-recovered fraction for the experiments with concentrated acetosolv pretreatment liquids. The dashed line in Fig. 4.15 serves as a reference for the expected amount of removed wood protons assuming that wood moisture is solubilized completely independent of the non-recovered fraction and that the components hemicellulose and lignin are successively solubilized as indicated by the amount of removed components depending on non-recovered fraction (see Appendix B for detailed information).

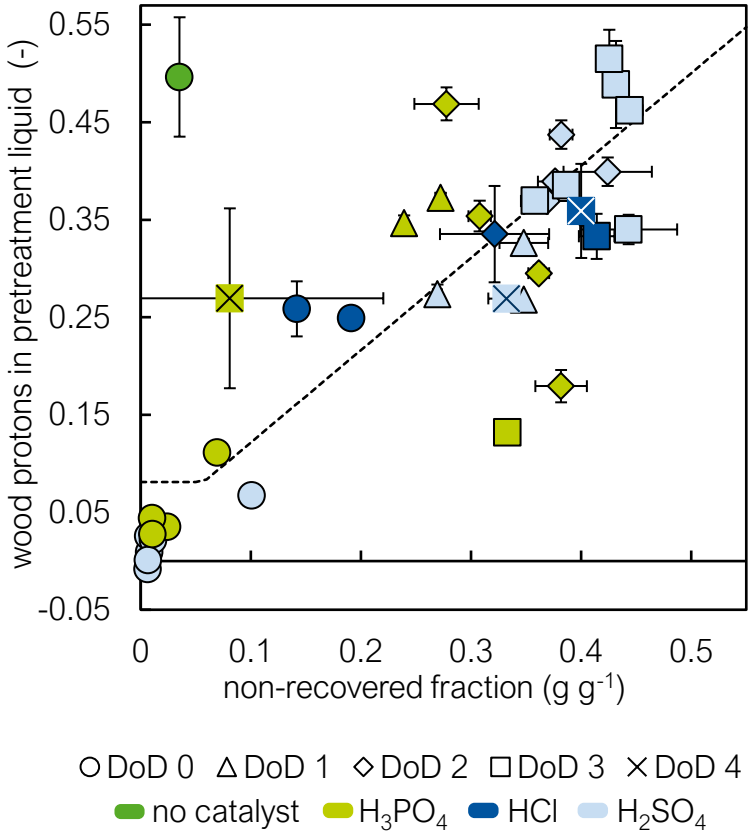

Figure 4.15: Estimated fraction of wood protons dissolved during pretreatment versus non-recovered fraction of wood after pretreatment for acetic acid-based pretreatment liquids. The dashed line represents an estimation of removed protons based on the composition of the recovered fraction.

In most cases, the fraction of dissolved protons corresponds to the non-recovered fraction. For sulfuric and hydrochloric acid, there is a rather linear correlation between dissolved protons and non-recovered fraction of wood while for phosphoric acid, the data are clearly more scattered. Moreover, the reference experiment without catalyst

shows the highest deviation between dissolved protons and the non-recovered fraction. Nevertheless, excluding the reference experiment, a high coefficient of determination of $R^2 = 0.7516$ signifies a relation between the non-recovered fraction and the fraction of dissolved protons. Thus, the fraction of dissolved protons can serve as a simple indicator of the magnitude of the non-recovered fraction.

Several factors can influence the amount of dissolved protons or their determination with the presented method and hence cause the observed scatter of data points. This includes factors influencing the elemental composition of pretreated samples. Changes in O/C ratio of the biomass' surface after a variety of pretreatments correlate to the presence or removal of components such as lignin or acetyl groups [50, 294, 295]. However, due to the very similar hydrogen weight fraction of the three main components of lignocellulosic biomass, a change in biomass composition after pretreatment probably has little impact on the amount of hydrogen in biomass. In contrast, thermal treatment of beech wood not only causes weight loss but also increases the carbon content [81] and with increasing severities of hydrothermal pretreatment (i.e., high temperature, long reaction times, high acid concentrations), C/O and C/H ratios increase, suggesting a beginning carbonization of the lignocellulosic biomass [165]. In this way, formation of C-C bonds in strongly hydrolyzed samples would lead to a reduction of protons due to the release of H_2O. This could be a reason for the high estimated fraction of dissolved wood protons for the phosphoric acid sample with DoD 4 although the other two samples with DoD 4 show a similar fraction of dissolved protons and non-recovered material. Overall, changes in the elemental composition of biomass during pretreatment mostly do not affect the hydrogen content and therefore this aspect rather has a minor influence on the determination of dissolved protons.

Furthermore, a discrepancy between non-recovered fraction and dissolved fraction could arise from small particles that are neither solubilized (i.e., not visible in the spectrum) nor hold back during filtration, probably affecting mostly the disintegrated samples. To further quantify this aspect, detailed mass balances of recovered, solubilized, and remaining (small particle) fraction should be determined for some samples.

The influencing factors arising from the developed method can be grouped into 3 main aspects. (1) A changed value of the integration constant c_{int} results in a constant offset of the estimated fraction of dissolved protons. More specifically, even small changes of c_{int} result in large variations of proton fraction and hence, this value has to be determined carefully. (2) The spectral area $A_{\mathrm{CH_3}}$ and its ratio to A_{tot} influence the determined fraction of dissolved protons. Even small changes in peak area have a large effect on accuracy due to the small amount of protons that can potentially be introduced from the wood sample in comparison to the amount of protons from

the pretreatment liquid (for the tested conditions they differ by a factor of approx. 20). Solubilized particles with peaks in the range of the methyl peak can slightly increase A_{CH_3} and thus lead to an underestimation of dissolved protons. Moreover, the method is highly sensitive for changes in the ratio of A_{CH_3}/A_{tot} (e.g., resulting from increased water content or high amount of phosphoric acid which contributes threefold to the OH-peak). For this reason, samples with higher water content are not shown due to infeasible values. Furthermore, it should be noted that a change of measurement parameters (number of scans, repetition time etc.) results in changes of intensity and hence changed peak area. This requires the repeated determination of c_{int} and a new correlation. (3) The amount of dissolved protons not only depends on the total amount of protons estimated from the spectra but also on the amount of hydrogen originating from the pretreatment liquid. Here, especially catalyst and water content influence the result due to their small concentration in most cases. For the concentrated acetosolv liquids, trace water in acetic acid can make up as much as the water content from catalyst.

In conclusion, the amount of water present in the pretreatment liquids apparently has a large impact on the accuracy of the determined fraction of dissolved protons due to changed spectral properties and influences in the calculated composition of the pretreatment liquid. This resembles the observation of the fit of the non-recovered fraction depending on catalyst concentration, which seems to be valid only for one specific water content. More experiments are required to systematically quantify the influence of water and incorporate the water content as a further parameter into this method (e.g., including the peak position of the OH-peak). In this way, the application range of this method could be extended.

4.2.2.4 Acetyl Content

Figure 4.16 shows the water content of pretreatment liquids versus the acetyl content of pretreated biomass samples. For most experiments, pretreatment liquids contain approximately $0.25\,\mathrm{mmol_{catalyst}\,g_{AA}^{-1}}$ (i.e., the same experiments that were analyzed for the influence of catalyst acid strength in Fig. 4.11). Since hydrochloric and sulfuric acid catalyst in pure acetic acid lead to undesired charring of wood at this ratio, a lower ratio of $0.06\,\mathrm{mmol_{catalyst}\,g_{AA}^{-1}}$ is chosen for the measurement of acetyl content for these two acids (light and dark blue filled symbols).

The acetyl content of native beech of 4.17 wt % is in accordance with values for beech wood mentioned in the literature, which vary between 3.8 and 4.7 wt % [215, 237, 296]. Except for the hydroiodic acid experiment with a slightly reduced acetyl content,

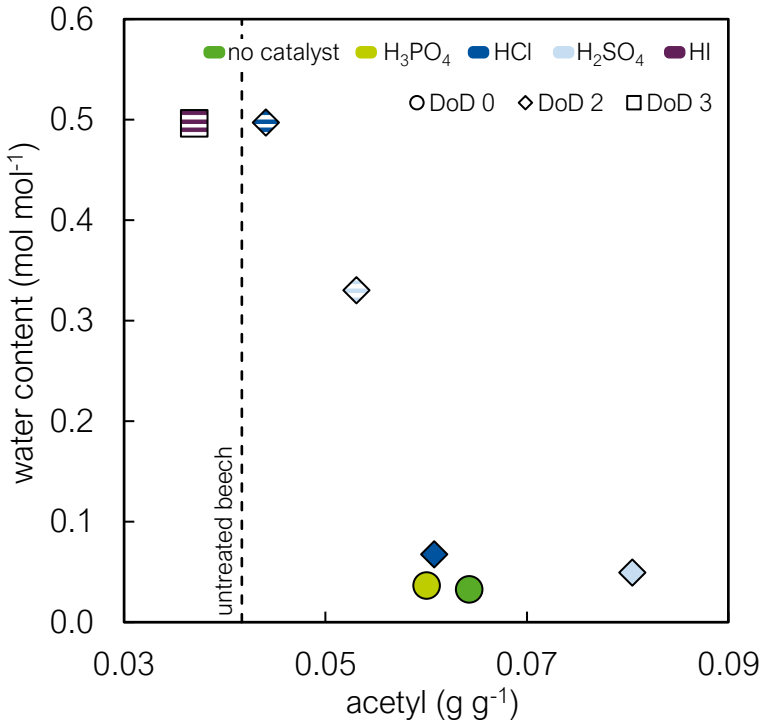

Figure 4.16: Water content of pretreatment liquids versus acetyl content of pretreated biomass samples. Filled symbols refer to liquids with only acetic acid and catalyst acid and striped symbols refer to liquids with water added to acetic acid and catalyst acid. The shape and color of the symbols indicate the DoD and the employed catalyst acid, respectively (see legend). The dashed line indicates the acetyl content measured for native beech wood.

all evaluated experiments exhibit an increase in acetyl content compared to native beech. This means that cellulose and/or lignin are acetylated during pretreatment with the employed acetosolv liquids. Similarly, in other studies, acetylation of either cellulose or lignin has been observed after acetosolv pretreatment of different types of biomass [157, 200, 284]. However, a low acetyl content has been identified as being beneficial for high sugar yields after enzymatic hydrolysis. Unlike low delignification or partial decrystallization of cellulose, the effect of a high acetyl group content cannot be compensated for with increased hydrolysis times [122]. Therefore, a reduction of acetyl content during pretreatment should be aimed at.

For the investigated experiments, visual disintegration does not correlate with acetyl content, because samples with DoD 2 are spread over the range of measured acetyl

contents. Nevertheless, the sample with the lowest acetyl content is the only one that is completely disintegrated after pretreatment.

Regarding the composition of the pretreatment liquid, the water content as well as the strength of the catalyst acid influence the acetyl content after pretreatment. It is notable that the acetyl content decreases with decreasing acetic acid content (i.e., increasing water content). Moreover, at similar water contents and comparable catalyst concentration, the application of a stronger catalyst acid (i.e., lower pK_a) results in a lower acetyl content of the pretreated sample. Correspondingly, the lignin content in the recovered fraction decreases with increasing water content and catalyst acid concentration. Conversely, pretreatment in concentrated acetosolv liquids with catalyst acids of low concentration or low strength is associated with high acetyl and lignin contents in the recovered fraction. Thus, acetylation of lignin could hinder its removal despite the above discussed high solubility that is expected in these liquids.

4.2.3 Enzymatic Hydrolysis

Generally, high sugar yields after enzymatic hydrolysis are desirable for economic feasibility of lignocellulosic biorefineries. For most experiments though, the sugar yield after hydrolysis is rather low with approximately 5 wt % yield referred to native beech (i.e., in the range of the reference experiment without catalyst, see Tab. B.2 in appendix, and only minimally exceeding the value for untreated beech, see Fig. 4.2). The current set of experiments hence does not suggest an optimal operating point for pretreatment but gives indications for the intrinsic differences of acetosolv pretreatment. Several effects could cause the observed low sugar yields after hydrolysis: the absence of disintegration (i.e., a low increase in surface area), hydrolysis and/or degradation of the cellulose fraction in case of sulfuric acid catalyst (i.e., lower amount of cellulose left for enzymatic hydrolysis), redeposition of solubilized lignin [215, 288, 297] or an increase in acetyl content in comparison to native beech [157, 200, 284].

The two highest sugar yields of 20 to 25 wt % (see Tab. S2) are observed after pretreatment with approximately equimolar acetic acid–water mixtures and hydroiodic or hydrochloric acid catalyst. Both samples are disintegrated after pretreatment. Furthermore, these are two of the three experiments with the highest amount of lignin removed (see Fig. 4.14) as well as an acetyl content in the range of untreated beech (see Fig. 4.16). Hence, our findings are in line with observations from the literature that both a low lignin and acetyl content are beneficial for enzymatic hydrolysis. As discussed above, the exact relation between the composition of acetosolv pretreatment liquids (i.e., water content as well as type and concentration of catalyst acid)

and the investigated pretreatment phenomena is yet unclear. This requires further research, especially to resolve the influence of a changing water content in the regime of concentrated acetic acid with regard to lignin removal and lignin solubility.

The sugar yields obtained with the above discussed experiments correspond to a cellulose-to-glucose conversion yield of approximately 50 wt %. This yield is clearly higher than yields of acetosolv-pretreated pine and eucalyptus, which are in the range of 10 and 30 to 40 wt %, respectively [157, 297]. However, in comparison to other pretreatment concepts such as alcohol-based OS pretreatment with cellulose conversion exceeding 50 wt % [56] or ILs with virtually complete cellulose conversion [19] (see Subsection 4.1.1), the researched acetosolv conditions lead to rather low sugar yields and need improvement (e.g., deacetylation, testing of improved pretreatment liquids).

4.2.4 Conclusion

Beech wood was pretreated with a variety of acetosolv liquids composed of acetic acid, different types of catalyst acid and varying water contents as an exemplary pretreatment concept to resolve correlations between pretreatment phenomena and composition of pretreatment liquids. Although, for the tested conditions, the highest sugar yields after enzymatic hydrolysis exceed other reported yields by 10 percentage points and more, the sugar yields are rather low with a maximum yield of 25 wt %. Hence, temperature and residence time need improvement for a further increase in sugar yields. More importantly, this study of varying acid and solvent composition enables the analysis of pretreatment phenomena on several scales directly related to the composition of pretreatment liquids. To classify the separation of wood fibers during acetosolv pretreatment, we define five degrees of disintegration from no disintegration to charring of wood. Our experiments show that the degree of disintegration depends on the concentration of catalyst acid and acetic acid. The comparison to aqueous pretreatment liquids reveals that the presence of acetic acid is required to achieve disintegration at all. This is due to an increased catalytic activity of acetic acid in acetosolv liquids containing at least equal amounts of acetic acid and water. In all cases, an increasing concentration of mineral acid catalysts increases the degree of disintegration. Likewise, the non-recovered fraction after pretreatment increases up to a threshold of approximately 40 wt %. This maximum of non-recovered fraction is independent of the type of catalyst acid. Further analysis of the composition reveals that the magnitude of the non-recovered fraction linearly correlates with the amount of both removed hemicellulose and removed lignin. The removal of half of the hemicelluloses followed by the removal of one third of lignin is a prerequisite for

the disintegration of acetosolv-pretreated beech wood. As disintegration relates to the amount and composition of the recovered fraction, the pretreatment liquids were analyzed with NMR spectroscopy thus enabling a qualitative description of solubilized components and degradation products as well as a quantitative estimation of the dissolved fraction. With regard to the composition of pretreatment liquids, an equimolar ratio of acetic acid and water in combination with a strong catalyst acid allows for a high delignification and prevents an increase in acetyl content, which proves beneficial for enzymatic hydrolysis. Consequently, disintegration in combination with a non-recovered fraction of around 40 wt % serves as a necessary condition for effective pretreatment. Such a quick and robust analysis of DoD and first estimation of dissolved fraction from NMR spectra complements a more laborious wet chemical analysis and thus allows for an easy screening of pretreatment conditions with regard to a competitive application in biorefineries.

As stated above, the sugar yields of the current set of experiments exceed reported yields for acetosolv pretreatment of other types of biomass but remain below reported yields for the pretreatment of beech wood (e.g., kraft, IL [19, 236]). Therefore, it is of interest to know how a changed effectiveness of pretreatment and hydrolysis impacts the process performance of biofuel production. Hence, in the next section, we examine economically and environmentally viable ranges for the amount of carbohydrates available after pretreatment.

4.3 Minimal Viable Sugar Yield of Biomass Pretreatment

As discussed in Subsection 2.1, the overall effectiveness of combined pretreatment and enzymatic hydrolysis is one of the key factors influencing environmental and economic performance of lignocellulosic biorefineries. Since the underlying mechanisms of effective pretreatment and subsequent hydrolysis as well as the role of solvents and ions for biomass pretreatment are not yet completely understood (see Subsections 2.2.2 and 2.2.3), it is very difficult to judge specific pretreatment conditions directly. Thus, the conventional approach explores the viability of one pretreatment concept considering specific biomass composition, pretreatment effectiveness, and enzymatic hydrolysis. However, a general analysis of the effectiveness of biomass pretreatment and subsequent hydrolysis strategies does not exist. The determination of economically and environmentally viable ranges for the amount of sugars available after pretreatment and hydrolysis represents a first step towards a general understanding of pretreatment.

Early-stage evaluation based on material balances allows to assess alternative production pathways of a biorefinery [229, 298]. Particularly, RNFA represents an established tool for the evaluation of alternative pathways in biofuel production considering economic and environmental criteria [229, 230]. In this section, we present the results of RNFA to determine the impact of pretreatment and hydrolysis yields as well as biomass composition on different conversion pathways focusing on liquid-based pretreatment strategies.

In Subsection 4.3.1, we first describe the influence of pretreatment and hydrolysis effectiveness on the process performance of biofuel production for beech wood as one specific species of biomass. Second, in Subsection 4.3.2, we evaluate published data on OS pretreatment as a well-known pretreatment concept [56, 299] to determine the range of carbon loss and fuel cost for one representative pretreatment concept with different species of lignocellulosic biomass. Naturally, numerous combinations of biomass species with different pretreatment technologies are conceivable. However, data from the literature is limited. Thus, in Subsection 4.3.3, we third conduct a generic analysis of pretreatment and hydrolysis yields in combination with changing compositions of biomass to describe the overall relation between carbon loss and fuel cost and to define the boundaries of economic fuel production. In Subsection 4.3.4, the results of the acetosolv pretreatment experiments (see Section 4.2) are evaluated with RNFA to assess the potential of acetosolv as a pretreatment strategy for biofuel production from beech wood.

4.3.1 Analysis of Pretreatment of Beech Wood

Figure 4.17 shows the results of the RNFA for beech wood. To distinguish between the influence of pretreatment effectiveness and the influence of hydrolysis effectiveness, we consider the reported fractionation yields in combination with (a) the reported hydrolysis yields (i.e., yields of reactions R1–R5 as calculated from literature) and (b) with ideal hydrolysis yields (i.e., yields of reactions R1–R3 as calculated from literature and $Y_{R4} = Y_{R5} = 1$). Carbon loss is plotted as a function of the specific fuel costs for the production of ethanol and ethyl levulinate.

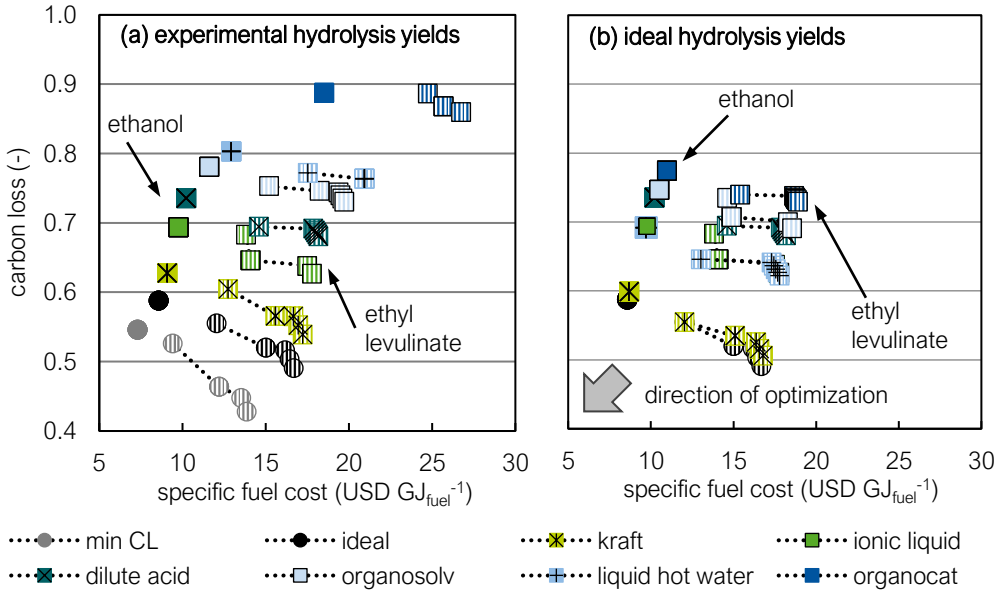

Figure 4.17: Results of the ethanol (filled symbols) and ethyl levulinate (striped symbols) production screening for beech wood as biomass feedstock **(a)** considering both reported fractionation and enzymatic hydrolysis yields and **(b)** considering only the reported fractionation yields combined with ideal hydrolysis yields.

Overall, the results show a singleton Pareto front for ethanol (i.e., the minima of carbon loss and fuel cost coincide for each analyzed pretreatment concept) due to only one direct production route from xylose and glucose each (R6 and R7 in Fig. 3.2), which are both active for all analyses. In contrast, there is a noticeable trade-off between minimal fuel cost and minimal carbon loss for ethyl levulinate. The production of ethyl levulinate offers several optional production pathways that differ in terms of overall yield and number of process steps. For the presented analyses, the only active pathways are the production pathways R11–R12–R26 starting from glucose

and R15–R16–R25 starting from xylose in different combinations with fermentation of sugars (R6 and R7, see Tab. C.4 and C.5 in appendix). The minimization of fuel costs leads to a lower number of active pathways (i.e., fewer functional units), which results in significantly reduced investment costs (cf. Ulonska et al. [230]). For all screened pretreatment concepts, the xylose pathway is inactive for the point of minimal ethyl levulinate fuel costs due to lower yields than the glucose pathway. At the same time, carbon loss is not minimal because less material is converted in comparison to the other points. Conversely, for the minimization of carbon loss, the xylose pathway is active leading to higher fuel costs.

From a production cost perspective, ethanol is cheaper than ethyl levulinate for all considered pretreatment technologies mainly due to the lower number of reactions in the production network and because, in most cases, a slightly higher amount of costly biomass is required for the production of ethyl levulinate.

From an environmental perspective, the results are substantially different. The production of ethanol shows higher carbon losses than the production of ethyl levulinate for all pretreatment variants. Besides losses due to yield constraints of the individual reactions, one molecule of CO_2 is released (i.e., one carbon atom lost) for each molecule of ethanol produced during fermentation. For the production of ethanol, all available sugar molecules are fermented, whereas for the production of ethyl levulinate only a fraction of the sugars is fermented to produce ethanol for reactions R25 and R26. This leads to the overall higher carbon loss for ethanol in comparison to ethyl levulinate.

Figure 4.17 (b) shows the screening results considering reported fractionation yields combined with ideal hydrolysis yields. In the context of RNFA, ideal hydrolysis means that during the hydrolysis step, all sugars that are present after pretreatment are made available for further processing (i.e., maximum yield) independent of the specific reaction conditions (e.g., substrate loadings, time of hydrolysis). In comparison to the benchmark, specific fuel costs increase only slightly when evaluating the influence of pretreatment on the production of one type of biofuel. In contrast, the carbon loss ranges approximately from 0.6 to 0.8 for ethanol and from slightly below 0.5 to almost 0.75 for ethyl levulinate. Kraft pretreatment has almost the same values of carbon loss and fuel costs as the benchmark for both biofuels. The remaining investigated pretreatment concepts exhibit increased carbon loss with a narrow ranking: LHW $>$ IL $>$ DA $>$ OS $>$ OC. With ideal hydrolysis, the different performances of the pretreatment concepts arise from variations in the fractionation yields for cellulose and hemicellulose in combination with a slightly varied composition of the raw material.

Considering reported yields for both fractionation and hydrolysis clearly influences the screening of pretreatment concepts as can be seen from a comparison of Fig. 4.17 (a) and (b). As a result, the ranking of pretreatment concepts in Fig. 4.17 (a) is as follows: kraft > IL > DA > OS > LHW > OC. Especially the results for LHW and OC pretreatment differ. Incomplete hydrolysis leads to an increase of carbon loss of approximately 0.1 in both cases and an estimated fuel cost difference of up to $10\,\mathrm{USD\,GJ^{-1}_{fuel}}$, which renders them unfavorable for realization in a biorefinery compared to the other pretreatment concepts. For the remaining investigated pretreatment technologies, inclusion of experimental hydrolysis yields leads to minor changes of carbon loss and fuel cost. Thus, enzymatic hydrolysis is close to or at the optimum for these references. Whether this ranking is generally true or depends on the combination of pretreatment and type of biomass (the specific chosen references) should be validated by a more extensive comparison including several references for each pretreatment concept. However, such an analysis is beyond the scope of this thesis. Furthermore, the overall costs for the pretreatment and hydrolysis step are similar in RNFA due to the same number of functional units and disregard of solvent costs, which might not be true for a more detailed process design. Generally, the pretreatment and hydrolysis step are capital intensive [78]. In addition, solvent-intensive pretreatment concepts such as the OS process often show a poor economic performance due to high costs for solvent recycling [66, 67]. Thus, the estimated price might be too low. Nevertheless, a comparison of different pretreatment concepts shows that the costs for reactors and associated costs such as catalyst recovery often level out. This results in little differences in projected economic performances [78]. Hence, the presented analysis allows a simple comparison of pretreatment concepts based on the individual fractionation effectiveness and hydrolysis performance.

Additionally to the benchmark, we include a pathway screening with minimum achievable carbon loss (min CL) in Fig. 4.17 (a). Here, all yields of the reaction network equal 1. Both carbon loss and fuel costs of the min CL screening are close to the benchmark, which shows that the established yields of the downstream processing reactions are near to the optimum. In conclusion, fractionation yields are the crucial yields in most cases, whereas the effectiveness of enzymatic hydrolysis presents a bottleneck only in two cases.

Overall, the estimated range of fuel cost for the analyzed process variants seems reasonable when comparing to published data. The 2018 average price for bioethanol is $27\,\mathrm{USD\,GJ^{-1}}$ [300], which shows that RNFA rather underestimates real fuel prices. Ethyl levulinate costs have been estimated to $12\,\mathrm{USD\,GJ^{-1}}$ [76], which is at the lower end of RNFA estimates. Nevertheless, not all of the screened pretreatment con-

cepts would be realized in a biorefinery context due to economically more attractive markets. For example, the prices for hardwood kraft pulp vary between 500 and 800 USD t^{-1} [301]. In comparison, a fuel price of 10 USD $GJ^{-1}_{ethanol}$ corresponds to a price of 277 USD $t^{-1}_{ethanol}$. Thus, it is more profitable to sell kraft pretreated pulp directly instead of converting it further to a lower-priced biofuel. Combusting the biomass would lead to a price of 0.05 USD kg^{-1}/19.51 MJ kg^{-1} [302] = 2.56 USD GJ^{-1}, which marks a lower limit for profitable biofuel production. All presented concepts surpass this lower limit.

The analysis of pretreatment concepts with beech wood verifies that pretreatment and hydrolysis have a significant influence on the process performance of biofuel production. Reduced sugar yields due to incomplete fractionation and hydrolysis increase both carbon loss and fuel cost. Furthermore, an evaluation of a pretreatment concept is only meaningful in combination with the respective hydrolysis yields but pretreatment yields dominate the performance of both steps (cf. Alvira et al. [38], Ding et al. [121]). Likewise, the composition of the biomass and the corresponding yield after pretreatment is of particular interest.

4.3.2 Analysis of Organosolv Pretreatment

To generalize the performance of pretreatment and to further determine the influence of varying biomass input streams, a second analysis is carried out with OS pretreatment for different feedstocks. The results of the RNFA are presented in Fig. 4.18.

For the same reasons as in the first analysis, there is only one point for each considered ethanol pretreatment but a Pareto front for ethyl levulinate. Again, ethyl levulinate shows higher specific fuel costs at a lower carbon loss when comparing the individual experiments. The benchmark in the analysis of beech wood differs from the benchmark in this analysis due to different compositions of biomass that were used for the calculation of the benchmarks (see Tab. 3.1 and 3.2). The pathways, which are active for the production of ethyl levulinate based on OS pretreatment, are similar to the pathways, which are active for ethyl levulinate produced from beech wood (i.e., glucose pathway R11–R12–R26 and xylose pathway R15–R16–R25 in combination with fermentation of sugars R6 and R7, see Tab. C.6 and C.7 in appendix). Again, the glucose pathway is favored for the point of minimal cost with two exceptions: one process based on spruce wood (△ in Fig. 4.18) and one process based on pine wood (▲ in Fig. 4.18). Due to the low cellulose hydrolysis yields in these two experiments, the xylose pathway is favorable for the production of ethyl levulinate at minimal costs.

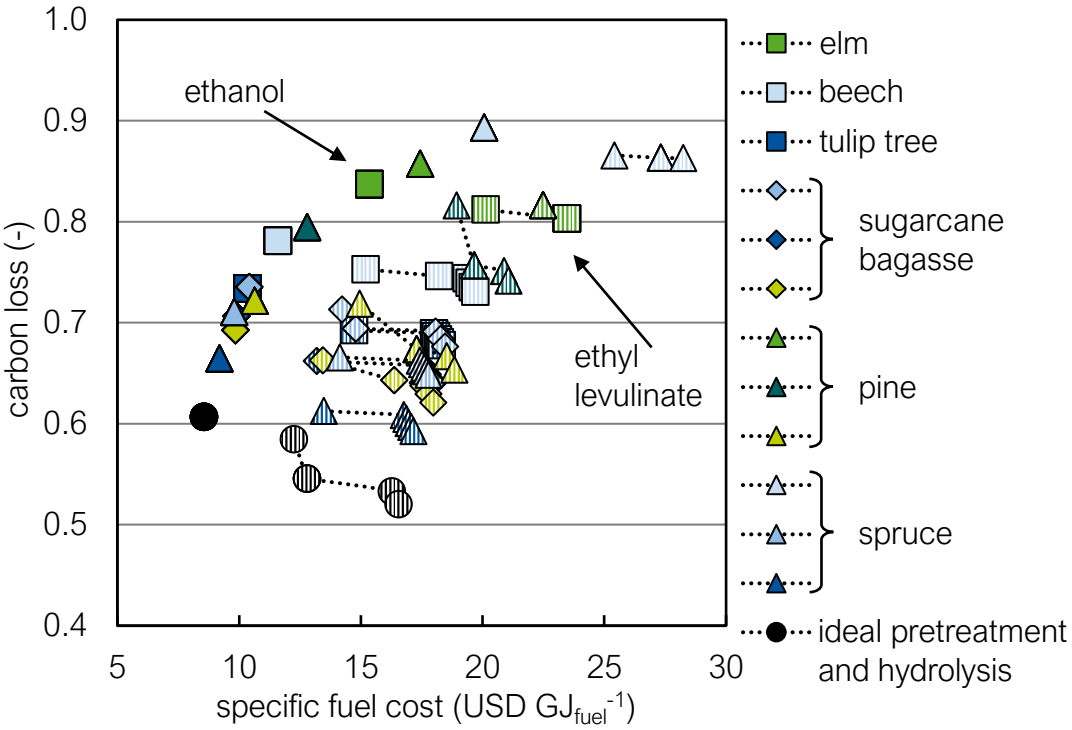

Figure 4.18: Screening results for the production of ethanol (filled symbols) and ethyl levulinate (striped symbols) based on organosolv pretreatment. Hardwood feed streams are marked with a square, softwood with a triangle and non-woody biomass is marked with a diamond. The symbols correspond to the symbols given in Tab. 3.2.

The low sugar yields after hydrolysis also result in these two experiments being ranked last in the OS screening.

Overall, the OS screening results cover a large range of fuel cost and carbon loss, similar to the results in Fig. 4.17 (a). A ranking of the screening results in terms of the biomass type is not straightforward. All experiments based on sugarcane bagasse are in the range of carbon loss around 0.7 at the same time achieving relatively low fuel costs. This leads to the conclusion that non-woody biomass is favorable for Organosolv pretreatment. The results for biofuel production from hardwood show a larger span of carbon loss from approximately 0.7 to 0.85 with a respective increase in fuel costs. The results for softwood cover an even larger span of carbon loss and fuel cost. Moreover, both the best and the worst results are calculated for spruce wood in this analysis. Since the composition of the investigated spruce samples is rather similar in both references, the main reasons for this deviation are the reported fractionation

and hydrolysis yields presumably due to different experimental conditions (composition of pretreatment liquid, liquid-to-wood ratio, temperature or pretreatment time). Verification of this hypothesis and consideration of these aspects would require the comparison of further variables such as the severity of a pretreatment concept or parameters for the description of pretreatment liquids (see Subsection 2.2.3).

The correlation between carbon loss and specific fuel costs shows two regimes. Below a carbon loss of approximately 0.8, fuel costs increase only marginally with an increase in carbon loss. Contrary to this, the increase in fuel cost is disproportionately high for a carbon loss above approximately 0.8. Even small increases in carbon loss lead to a high increase in fuel cost in this second regime. This turning point is more pronounced for ethanol than for ethyl levulinate. Thus, to avoid high fuel costs, pretreatment strategies resulting in a carbon loss below 0.8 should be aimed at.

Based on this analysis, it is unclear if and how a certain biomass composition in combination with individual fractionation and hydrolysis yields results in a low carbon loss. To examine the underlying correlation between specific fuel costs and carbon loss in more detail, an analysis based on representative biomass compositions and yields is presented in the next section.

4.3.3 Analysis of Minimal Viable Sugar Yield

The aim of this analysis is to detect boundaries of economically favorable production of biofuels based on the total carbohydrate yield after hydrolysis. To this end, values for biomass composition and the yields for pretreatment and hydrolysis were varied in plausible ranges between 0 and 1 based on the considered references. The hypothetical data should enable to analyze the behavior observed with real biomass of different composition.

Figure 4.19 (a) shows the results for the representative analysis of varying lignin content with a fixed cellulose/hemicellulose ratio and average pretreatment and hydrolysis yields. For comparison, screenings based on average lignin content are also included for ethanol and ethyl levulinate. The points increase from 0 mol % lignin to 85 mol % lignin in steps of 5 mol %. The results follow a clear curve from low carbon loss with low fuel costs at low lignin contents to a carbon loss above 0.9 and high fuel costs at high lignin contents. Moreover, the Pareto front for the ethyl levulinate results has a similar shape for most points. Only towards a higher lignin content, the Pareto front narrows (i.e., a lower range of carbon loss and fuel cost for the results of a specific lignin content). The same production pathways are active for the different

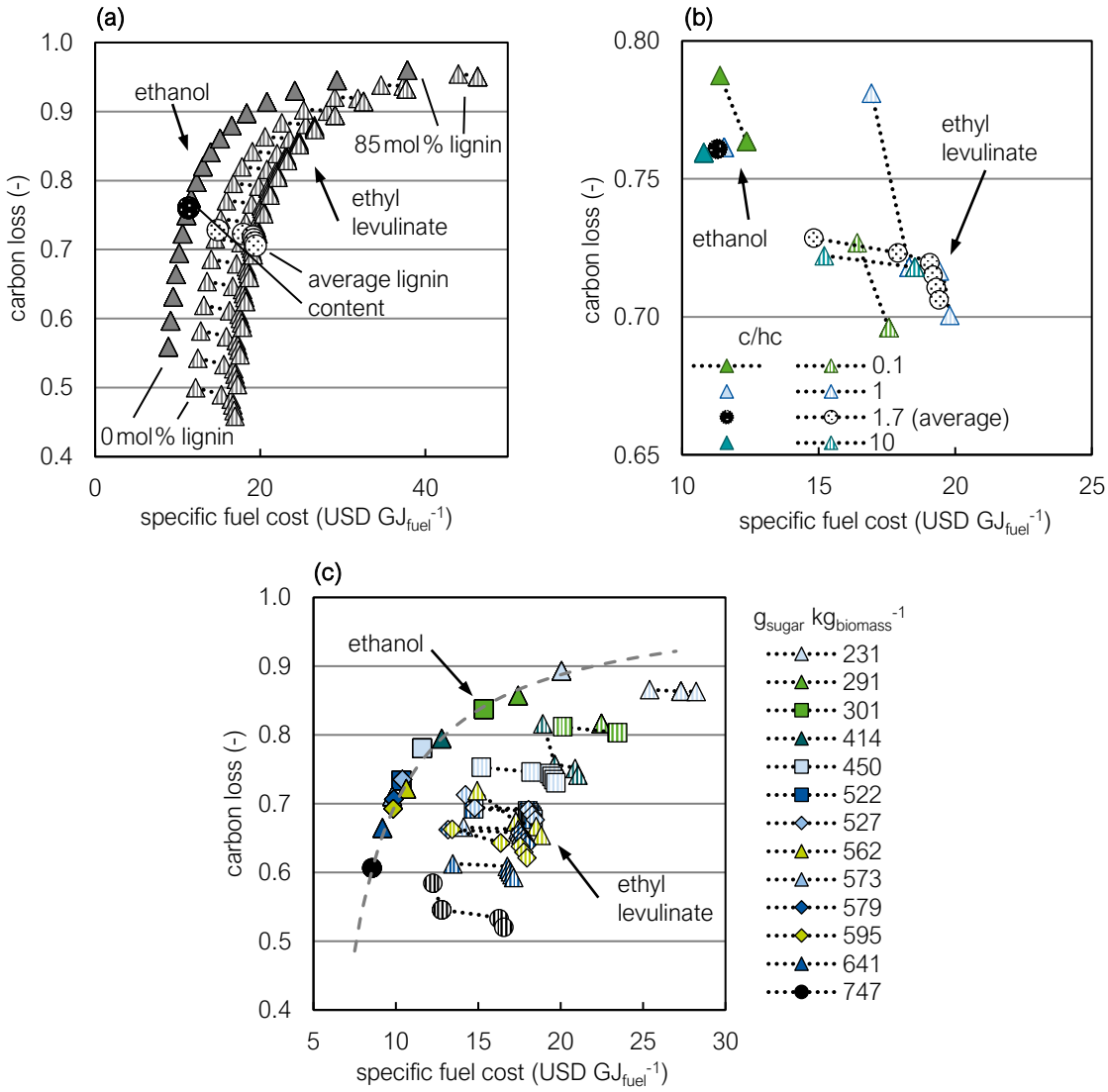

Figure 4.19: Results of the biofuel production screening with changing biomass composition as well as sugar yields for biofuels ethanol (filled symbols) and ethyl levulinate (striped symbols): **(a)** variation of lignin content at a fixed ratio of cellulose to hemicellulose (c/hc = 1.7), **(b)** variation of cellulose to hemicellulose ratio at fixed lignin content ($x_{\mathrm{l,raw}} = 0.3218$), **(c)** results of organosolv screening as shown above with sugar yield after hydrolysis indicated in the legend. The symbols refer to the same experiments as in the organosolv screening (see Subsection 4.3.2 and Tab. 3.2). The dashed line sketches the reciprocal correlation between carbon loss and fuel cost for ethanol.

points of the Pareto front, due to the constant ratio of cellulose to hemicellulose. In conclusion, a low lignin content of the feedstock biomass is clearly beneficial for a low carbon loss and low fuel costs. This is consistent with earlier studies showing that the production of biofuels derived from lignin is economically not feasible [63]. A low lignin content not only implies an increased fraction of carbohydrates that can effectively be converted to biofuels, but also diminishes the inhibition potential of enzymes during hydrolysis [121].

Figure 4.19 (b) shows the screening results for a variation of c/hc ratio at a fixed average lignin content with average pretreatment and hydrolysis yields. For ethanol production with a low cellulose content (c/hc = 0.1), there is a Pareto front because for the point with minimal costs, hydrolysis of cellulose and fermentation of glucose is inactive. With increasing c/hc ratio, carbon loss and fuel cost decrease slightly. Therefore, a high cellulose content is beneficial for the production of ethanol (cf. Alvira et al. [38], Tao et al. [75]). For ethyl levulinate, the shape of the Pareto front changes with changing c/hc ratio and the individual points of the different Pareto fronts partly overlap. Due to the possibility of choosing different pathways for the production of ethyl levulinate, a change in c/hc ratio can be balanced both in terms of carbon loss and fuel cost.

Figure 4.19 (c) shows the results of the OS screening (see Subsection 4.3.2). The points and symbols are the same as the ones used in Fig. 4.18 but the legend indicates the amount of sugar which is available for biofuel production after pretreatment and hydrolysis. The overall sugar yield can be calculated from the composition of the biomass multiplied with the pretreatment and hydrolysis yields: $w_{\mathrm{sugar}} = w_{\mathrm{c,raw}} \cdot Y_{\mathrm{c}} \cdot Y_{\mathrm{glu}} + w_{\mathrm{hc,raw}} \cdot Y_{\mathrm{hc}} \cdot Y_{\mathrm{xyl}}$. Clearly, the overall ranking of the screening results correlates with the amount of sugar that is available after hydrolysis.

To deduce the connection between carbon loss, fuel cost and the available sugars, the RNFA equations are analyzed in more detail in the following. For the present analysis, only the feed stream of biomass $f_{\mathrm{raw,bio}}$ is relevant for the calculation of carbon loss from Eqs. (3.26) and (3.27) since the other feed streams (hydrogen, water and oxygen) do not contain any carbon atoms. As RNFA considers a fixed fuel production, the nominator of Eq. (3.27) is constant for a specific type of biofuel whereas the denominator changes depending on the magnitude of the biomass input stream. In conclusion, the denominator can be reformulated to: $\sum_{j=1}^{n_{\mathrm{raw}}} f_{\mathrm{raw},j}\, n_{\mathrm{C},j} = f_{\mathrm{raw,bio}} n_{\mathrm{C,bio}}$. For the evaluated studies, $n_{\mathrm{C,bio}}$ varies marginally between 6.5 and 7.5 depending on the individual composition and therefore, the carbon loss is mainly proportional to the input stream of biomass according to the following relation:

$$\mathrm{CL} \propto (1 - \mathrm{const.}/f_{\mathrm{raw,bio}}). \tag{4.1}$$

When evaluating the influences on specific fuel costs, the biomass costs are at least one order of magnitude larger than costs for auxiliaries and waste. Investment costs are in the same order of magnitude as biomass costs but are similar for the different pretreatment concepts due to the same production pathways. In conclusion, changes in specific fuel costs C_{spec} are mainly caused by a changing quantity of biomass that is required for the production of the specified fuel equivalent depending on the effectiveness of the individual pretreatment concepts:

$$C_{\mathrm{spec}} \propto f_{\mathrm{raw,bio}}. \tag{4.2}$$

Combining Eqs. (4.1) and (4.2) results in the overall relation between carbon loss and fuel cost:

$$\mathrm{CL} \propto (1 - \mathrm{const.}/C_{\mathrm{spec}}). \tag{4.3}$$

This equation reflects the observed carbon loss and cost correlation (exemplarily sketched for ethanol in Fig. 4.19 (c)). For a carbon loss approaching its upper limit of 1, the fuel costs increase strongly. When the carbon loss approaches small values, there is a minimum value for the specific fuel costs which is determined by the constant. This constant in Eq. (4.3) is process specific and is not further determined for this analysis.

The analysis shows that to reach a fixed fuel equivalent as output, a certain amount of convertible carbohydrates is required depending on the yields of active production pathways. Thus, the biomass input stream $f_{\mathrm{raw,bio}}$ increases to reach the required amount of sugars when either the amount of cellulose or hemicellulose in the biomass is low or fractionation and hydrolysis yields are low. Conversely, high yields or a high carbohydrate content in the biomass lead to a reduction of the input biomass stream. The overall sugar yield that results from biomass composition, pretreatment and hydrolysis yields thus determines the quantity of the biomass input stream. Therefore, carbon loss and fuel cost are directly connected to the overall sugar yield after hydrolysis. The strongly increasing fuel costs above a carbon loss of 0.8 correspond to an overall sugar yield of approximately $400\,\mathrm{g_{sugar}\,kg_{biomass}^{-1}}$ (approximate turning point of sketched curve in Fig. 4.19 (c)) that can be regarded as a minimum overall sugar yield for an economically beneficial production of biofuels. This value can serve as an indicator to judge the yield of biomass pretreatment strategies in general.

This study emphasizes that pretreatment is an integral part of the biomass conversion process. Therefore, it should be considered with specific pretreatment and hydrolysis yields in combination with further conversion and downstream processing from the very early stages of process development for the production of biofuels. Furthermore, only a complete analysis of raw material, solid recovery and hydrolysis yields from one experiment allows to correctly evaluate mass balances (cf. Dale and Ong [77]) and determine whether a combination of pretreatment and subsequent enzymatic hydrolysis exceeds the above suggested minimum overall sugar yield of $400\,\mathrm{g_{sugar}\,kg^{-1}_{biomass}}$ for a specific feedstock biomass.

Lignocellulosic biomasses with a low lignin content (i.e., high carbohydrate content) can be pretreated with conditions that might not extract all available carbohydrates (i.e., low yields for reactions R1–R5) but still exceed the minimum sugar yield. Contrarily, a high lignin content (i.e., low carbohydrate content) makes pretreatment difficult because in this case pretreatment conditions are required that make available most of the cellulose and hemicellulose fraction and also enable high hydrolysis yields. This logic has to be anticipated when choosing a hypothetical site that offers only a specific feedstock [303] as well as during process development for a specific feedstock.

Strictly speaking, the suggested minimum sugar yield for an economically beneficial production of biofuels has to be validated for each individual process concept during detailed process design. Nevertheless, this lower limit helps to quickly evaluate research results and to decide whether a pretreatment concept can be feasible or not. To evaluate the potential of the acetosolv pretreatment experiments presented in Section 4.2, the experimental results are integrated into the RNFA in the next subsection.

4.3.4 Analysis of Acetosolv Pretreatment of Beech Wood

For the evaluation of acetosolv in RNFA, only the two points with the highest sugar yields after enzymatic hydrolysis are considered. These correspond to pretreatment of beech wood with approximately equimolar acetic acid–water mixtures and hydroiodic or hydrochloric acid catalyst (see Subsection 4.2.3). For the calculation of yields, we assume that all xylose which is solubilized in the pretreatment liquid after pretreatment can be recovered (i.e., $Y_{\mathrm{xyl}} = 1$). The yields for lignin, cellulose and glucose are calculated from experimentally measured data (i.e., amount and composition of the recovered fraction as well as yields of enzymatic hydrolysis). The molar composition of the employed beech chips and the yields that serve as input for RNFA are given in Tab. 4.2. Interestingly, Y_{c} is at the optimum for the HCl experiment with Y_{hc} and

Y_l fluctuating around 0.75, whereas Y_c is reduced for the HI experiment, but Y_hc and Y_l have higher values of around 0.82. This hints towards a different fractionation mechanism of each catalyst.

Table 4.2: Molar composition and yields considered for the screening of acetosolv pretreatment of beech wood. The evaluated experiments are the two with the highest sugar yield after enzymatic hydrolysis corresponding to pretreatment of beech wood with approximately equimolar acetic acid–water mixtures and hydrochloric (HCl) or hydroiodic acid (HI) catalyst.

	HCl	**HI**
$x_\mathrm{c,raw}$	0.4223	0.4223
$x_\mathrm{hc,raw}$	0.2903	0.2903
$x_\mathrm{l,raw}$	0.2874	0.2874
Y_c	1	0.9171
Y_hc	0.7506	0.8107
Y_l	0.7461	0.8251
Y_xyl	1	1
Y_glu	0.5115	0.4837

Fig. 4.20 shows the results of the RNFA of acetosolv pretreatment in the context of the analysis of pretreatment of beech wood (see Fig. 4.17). The active pathways are similar to those of the above discussed screenings with the same characteristics for the points of minimal cost and minimal carbon loss in the ethyl levulinate results (see Tab. C.8 in appendix). Carbon loss and fuel cost based on acetosolv pretreatment almost coincide with the points for OS-pretreated beech in RNFA. Nevertheless, the acetosolv experiments are rather at the lower end in the fuel cost–carbon loss correlation, when comparing with other pretreatment concepts. In comparison with the evaluated literature data for the pretreatment of beech wood (see Tab. 3.1), the recovery of cellulose in the acetosolv experiments is good (i.e., the cellulose fraction almost completely remains in the recovered fraction). The removal of lignin is above the average value of the investigated literature for both acetosolv experiments. In comparison to the specific values for pretreatment of beech wood, delignification with HCl catalyst is rather at the lower end of the evaluated data and hence Y_l should be improved to render acetosolv pretreatment of beech wood with HCl catalyst more effective. The fractionation of hemicellulose needs improvement in both cases as the experimentally determined values are lower than the average yield for hemicellulose.

Clearly, the glucose yields of enzymatic hydrolysis after acetosolv pretreatment are lower than the majority of reported glucose yields for beech wood and hence, Y_{glu} remains as a major bottleneck of the tested acetosolv pretreatment conditions. As expected due to the rather low sugar yields, acetosolv pretreatment needs improvement to be competitive with effective pretreatment concepts. Nevertheless, the criterion of $400\,g_{sugar}\,kg_{biomass}^{-1}$ is (just) met with $w_{sugar} = 0.401$ for the experiment with hydroiodic acid and $w_{sugar} = 0.4134$ for the experiment with hydrochloric acid.

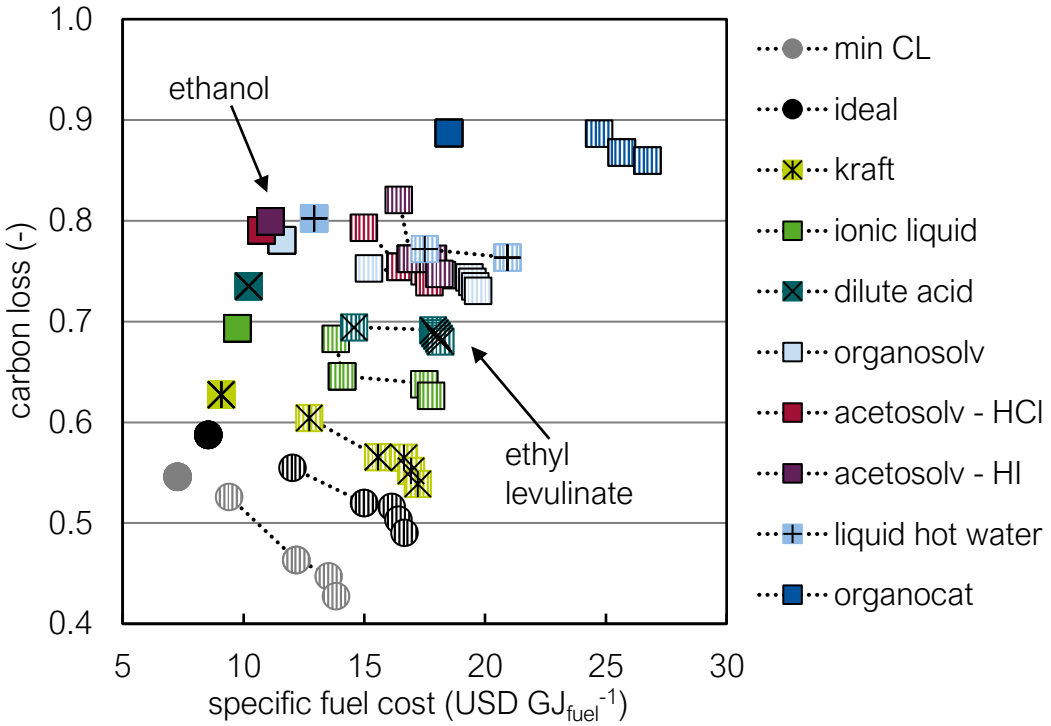

Figure 4.20: Results of the RNFA for acetosolv pretreatment of beech wood in comparison to the results of the screening of biofuel production with beech as feedstock (see Fig. 4.17).

4.3.5 Conclusion

Section 4.3 evaluates the influence of various biomass pretreatment concepts and enzymatic hydrolysis on the production process performance of the biofuels ethanol and ethyl levulinate. Reaction Network Flux Analysis is used for the screening of processes at early stage to minimize fuel cost and carbon loss. Fuel cost and carbon loss strongly depend on pretreatment and hydrolysis yields as the inclusion of literature

data for the pretreatment of beech wood and organosolv-based pretreatments of a variety of feedstock biomass species reveals. The comparison of ethanol and ethyl levulinate shows that there can be a trade-off between carbon loss and specific fuel costs. In case of ethanol, the trade-off is insignificant due to the direct, short production pathways from both xylose and glucose. In case of ethyl levulinate, different combinations of production pathways are selected for minimal costs versus minimal carbon loss.

Furthermore, a detailed analysis shows that carbon loss correlates with the reciprocal value of specific fuel costs or total sugar yield. In particular, a carbon loss below approximately 80% corresponds to the pretreatment strategies with a high economic potential. This threshold in carbon loss coincides with an overall sugar yield of approximately 400 g total carbohydrates per kg of lignocellulosic biomass. To classify a pretreatment as economically beneficial, this critical sugar output should be exceeded either by a large (accessible) carbohydrate content of the feedstock biomass or by effective fractionation and hydrolysis.

Chapter 5

Conclusions and Outlook

The conversion of lignocellulosic biomass to biofuels and biochemicals requires a pretreatment to cleave the composite-like structure of biomass and thus facilitate further conversion. In the case of liquid-based pretreatment, the composition of the pretreatment liquid plays a crucial role for the effectiveness of pretreatment with regard to improved sugar yields after enzymatic hydrolysis as a process step subsequent to pretreatment. This work investigates liquid-based pretreatment of lignocellulosic biomass and addresses challenges of correlating properties of pretreatment liquids with changes of biomass characteristics after pretreatment as well as the development of tools for the evaluation of pretreatment strategies.

The efficacy of EMIMAc as pretreatment liquid is limited by the addition of solvents. This relates to a reduction of both macroscopic disintegration and sugar yield after enzymatic hydrolysis of beech wood pretreated in mixtures of EMIMAc with acetic acid and water. To increase the understanding of molecular mechanisms that determine the effectiveness of a pretreatment liquid, interactions between species in mixtures of EMIMAc and deuterated solvents are visualized by simple low-field NMR measurements. The analysis of interaction kinetics of H/D exchange at the C(2)-position of the EMIM cation reveals that the observed pseudo-first-order rate constants linearly correlate with pH only in the dilute regime below 30 mol % EMIMAc, which corresponds to ineffective pretreatment liquids. More detailed modeling of the exchange reaction considering a second-order mechanism and dissociation of water reveals that even this detailed model does not suffice to describe one reaction mechanism which is valid for the complete composition range because rate constants vary with the content of EMIMAc in the investigated mixtures. High exchange rate constants in concentrated mixtures indicate that cations and anions strongly interact via the C(2)-position down to a mole fraction of 30 mol % EMIMAc. Overall, the changes in pretreatment effectiveness cannot be directly correlated to the analyzed interactions and hence, H/D exchange alone does not allow for an explanation of pretreatment

results. Nevertheless, this kinetic analysis presents a first step towards a thorough description of molecular interactions between ILs and solvents considering dissociation on a molecular level and the influence of liquid structure on a larger scale.

To resolve correlations between pretreatment phenomena and the composition of pretreatment liquids, acetosolv pretreatment of beech wood is chosen as an exemplary pretreatment concept. Although sugar yields after enzymatic hydrolysis are lower than those after pretreatment with EMIMAc, the obtained sugar yields partially exceed hitherto determined sugar yields for acetosolv pretreatment. Moreover, this study of varying composition of acetosolv liquids shows that macroscopic changes after pretreatment are connected to mass balances as well as compositional changes and enables their relation to the composition of pretreatment liquids. We classify the macroscopic disintegration after pretreatment into five degrees of disintegration. The degree of disintegration increases with increasing concentration of catalyst acid while acetic acid is required to achieve disintegration at all. Furthermore, with increasing disintegration, the non-recovered fraction of beech wood after acetosolv pretreatment increases up to a maximum of 40 wt %, which is independent of the type of catalyst acid. With regard to biomass composition, beech wood disintegrates if approximately half of the hemicelluloses and one third of lignin are removed during pretreatment. To further describe the removal of components, pretreatment liquids were analyzed with NMR spectroscopy after pretreatment to qualitatively and quantitatively measure solubilized components. Concerning the composition of pretreatment liquids, an equimolar ratio of acetic acid and water in combination with a strong catalyst acid proves beneficial for enzymatic hydrolysis due to high delignification and no increase in acetyl content. Consequently, disintegration with a non-recovered faction of 40 wt % serves as a necessary condition for effective pretreatment. Thus, the macroscopic criterion of disintegration in combination with a quick and simple estimation of dissolved fraction with low-field NMR spectroscopy allows for a fast evaluation of possibly effective pretreatment conditions to only chose promising experiments for a detailed but laborious wet chemical analysis of recovered fraction and enzymatic hydrolysis.

At the process level, the influence of various biomass pretreatment concepts in combination with enzymatic hydrolysis on the production process performance of the biofuels ethanol and ethyl levulinate is evaluated. RNFA is used for the screening of processes at early stage to minimize fuel cost and carbon loss. Both criteria depend on pretreatment and hydrolysis yields as revealed by the inclusion of literature data for the pretreatment of beech wood and OS-based pretreatment of a variety of feedstock biomass species. In some cases, carbon loss and specific fuel costs show a trade-off

that increases with the number and length of production pathways as is the case for ethyl levulinate in comparison to ethanol. In more detail, carbon loss correlates with the reciprocal value of specific fuel costs or total sugar yield. In particular, a carbon loss below approximately 80% denotes the pretreatment strategies with a high economic potential. This threshold in carbon loss corresponds to an overall sugar yield of approximately 400 g total carbohydrates per kg of lignocellulosic biomass. To classify a pretreatment as economically beneficial, this critical sugar output should be exceeded either by a large (accessible) carbohydrate content of the feedstock biomass or by effective fractionation and hydrolysis.

Altogether, the analysis of pretreatment on multiple scales up to the process perspective conducted in this thesis presents a step towards mechanistic understanding of pretreatment of biomass. Nevertheless, many aspects still remain unclear and require more research. With regard to the topics investigated in this thesis, this includes an extension of the kinetic analysis of molecular interactions in pretreatment liquids, the improvement of analytical evaluation of pretreatment phenomena as well as the assessment of pretreatment effectiveness from a process perspective.

Since the measurements of H/D exchange kinetics were carried out at slightly above ambient temperature only, it remains unknown to what extent temperature influences the kinetics. Therefore, spectral information from Raman and IR measurements at pretreatment temperatures could be used to further resolve the kinetics of molecular interactions and determine the relation of these interactions to pretreatment effects. However, molecular interactions are specific for a certain composition of a pretreatment liquid and hence the kinetic analysis cannot be used to compare different types of pretreatment liquids, especially in terms of acid–base properties. As stated above, the description of acid–base properties with pH is limited to dilute aqueous solutions, which represent only a small fraction of pretreatment liquids. Therefore, sophisticated models should be developed that account for a changed activity of species in different types of concentrated electrolyte solutions at increased temperatures.

A further step for the development of correlations between characteristics of pretreatment liquids and pretreatment phenomena concerns the analysis of non-recovered fraction after acetosolv pretreatment of beech wood as a function of catalyst concentration. More specifically, this refers to the extension of the steepness k of the logistic fit to account for the water content in the pretreatment liquid as well as the acid strength of the individual catalyst acid, for example based on a kinetic analysis considering the extended severity factor or other solvent/solubility parameters in combination with a measure of acidity of the catalyst such as pK_a or Hammett acidity (see Subsection 2.2.3). The inclusion of water content in the correlation requires an additional

set of pretreatment experiments with consistently varied water content in acetosolv liquids for different types of catalysts. These additional pretreatment experiments with complete analysis of the recovered fraction will allow for a more comprehensive evaluation of (acetosolv) pretreatment liquids instead of empirically fitted functions that are valid for a limited set of experiments only. Besides compositional analysis, a further characterization of the fraction of lignin removed during pretreatment as well as the lignin in the recovered fraction (e.g., analysis of lignin molecular weights) helps to further quantify the influence of lignin depolymerization and lignin solubility in different acetosolv pretreatment liquids. Eventually, this could facilitate the improvement of acetosolv pretreatment liquids that contain an increased water content to keep acetic acid as disintegration agent but at the same time a reduced concentration of catalyst acid to prevent degradation reactions.

As stated above, macroscopic disintegration in combination with estimation of overall mass balances from NMR spectra are simple indicators that describe necessary conditions for effective pretreatment. To increase the robustness of the presented method, advanced chemometric methods such as indirect hard modeling can be used for the determination of peak areas irrespective of superposition [24, 304]. However, minimal changes in peak areas due to the low amount of protons from biomass on the one hand as well as large peak shifts due to changing water contents in the pretreatment liquid on the other hand, require precise model calibration to obtain reliable results. Moreover, disintegration and overall mass balances do not suffice to determine effectively pretreated samples because the interaction between lignin and the pretreatment liquid is another important aspect for effective pretreatment. This refers to the differentiation of samples, where the pretreatment liquid allows for high lignin solubility in combination with high delignification thus facilitating enzymatic hydrolysis. To complement the two indicators developed in this thesis, an analytical procedure for a quick estimation of lignin content in the recovered fraction after pretreatment would be beneficial. In this way, samples with a high non-recovered fraction and high amount of removed lignin could be differentiated from undesired samples with a high non-recovered fraction but degraded cellulose (as was observed for the acetosolv experiments).

In many cases, disintegration and pretreatment effectiveness appear to be related to swelling of wood in a pretreatment liquid. However, previous investigations in the literature focused on swelling characteristics in a limited range of pretreatment liquids only. This demands for further investigations to determine whether the extent of swelling in general acts as a prerequisite for effective pretreatment. Lastly, correlations between swelling and parameters for the description of pretreatment liquids should

be comprehensively evaluated for a variety of different pretreatment liquids.

From a process perspective, the screening for the production pathway performance of biofuels based on RNFA can be detailed to account for further pretreatment-specific influences. On the one hand, this refers to a more precise estimation of costs considering for example specific costs for the pretreatment liquids as well as costs for enzymes. On the other hand, integration of process streams could discover solvents that can preferentially be used as components of a pretreatment liquid depending on the specific downstream processing.

Although many aspects of pretreatment of lignocellulosic biomass remain unknown, the analyses and methods presented in this thesis improve the understanding of mechanisms of biomass pretreatment on several scales and thus contribute to the development of improved pretreatment strategies for the production of fuels and chemicals in lignocellulosic biorefineries.

Appendix A

Ionic Liquids

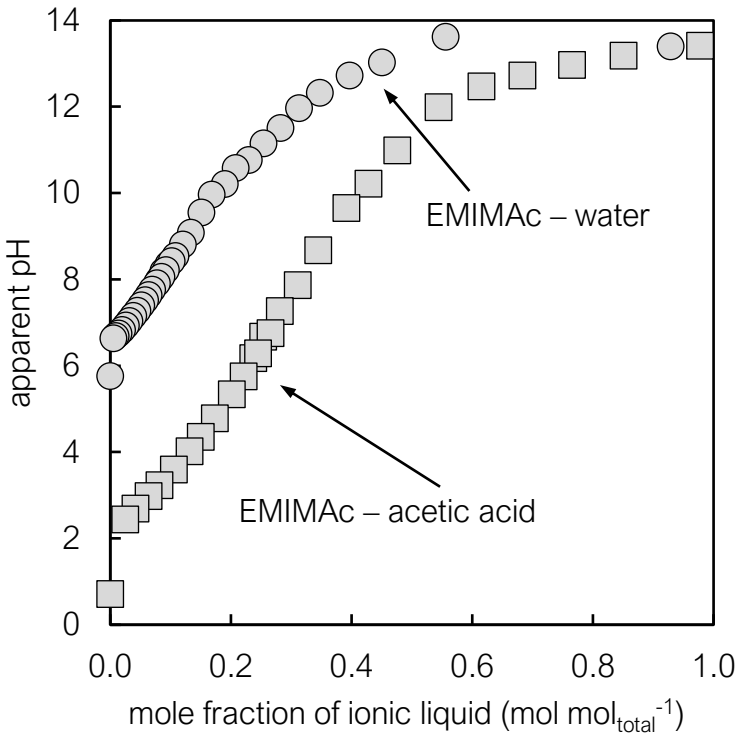

Figure A.1: Apparent pH in mixtures of EMIMAc with water and acetic acid. Apparent pH refers to the value as was measured with the pH meter (i.e., the influence of increasing electrolyte concentration or activity correction was not accounted for).

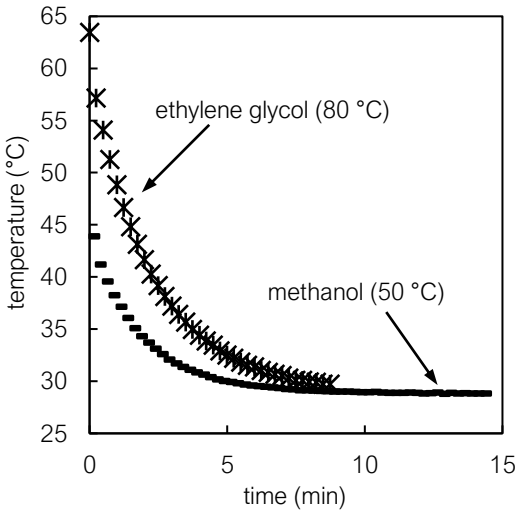

Figure A.2: Temperature decrease of methanol and ethylene glycol heated in NMR tubes. The temperature inside the NMR tube is estimated according to Ammann et al. [305]. Note that the temperature of the first recorded spectrum is below the set temperature due to rapid cooling when shifting the tube from the external heating block inside the NMR device.

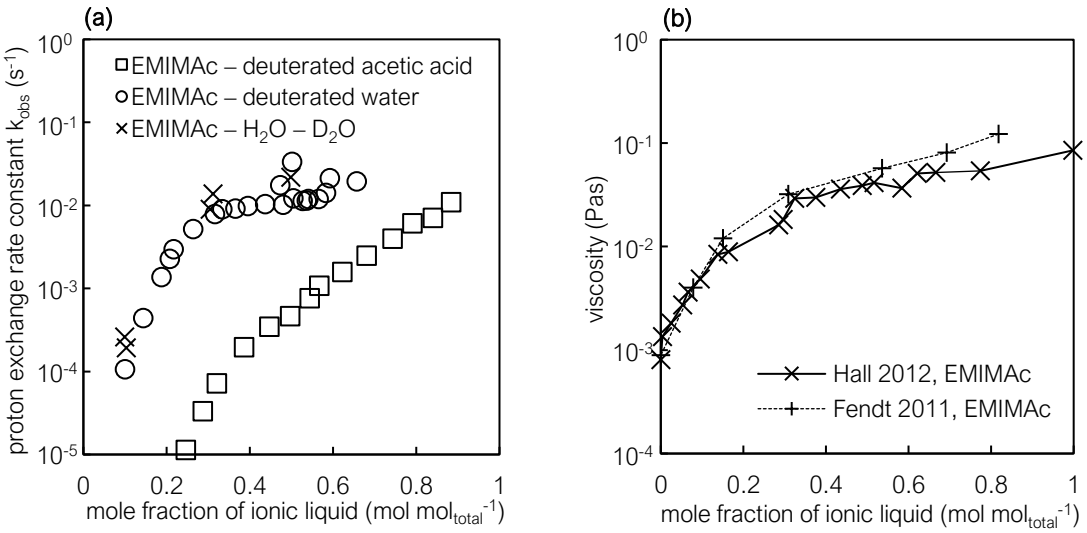

Figure A.3: **(a)** Pseudo-first-order exchange rate constants with mixtures of H_2O and D_2O (50/50 and 75/25 w/w) in comparison to exchange rate constants with fully deuterated solvents. **(b)** Viscosity of mixtures of EMIMAc with water, data from Hall et al. [274], Fendt et al. [306].

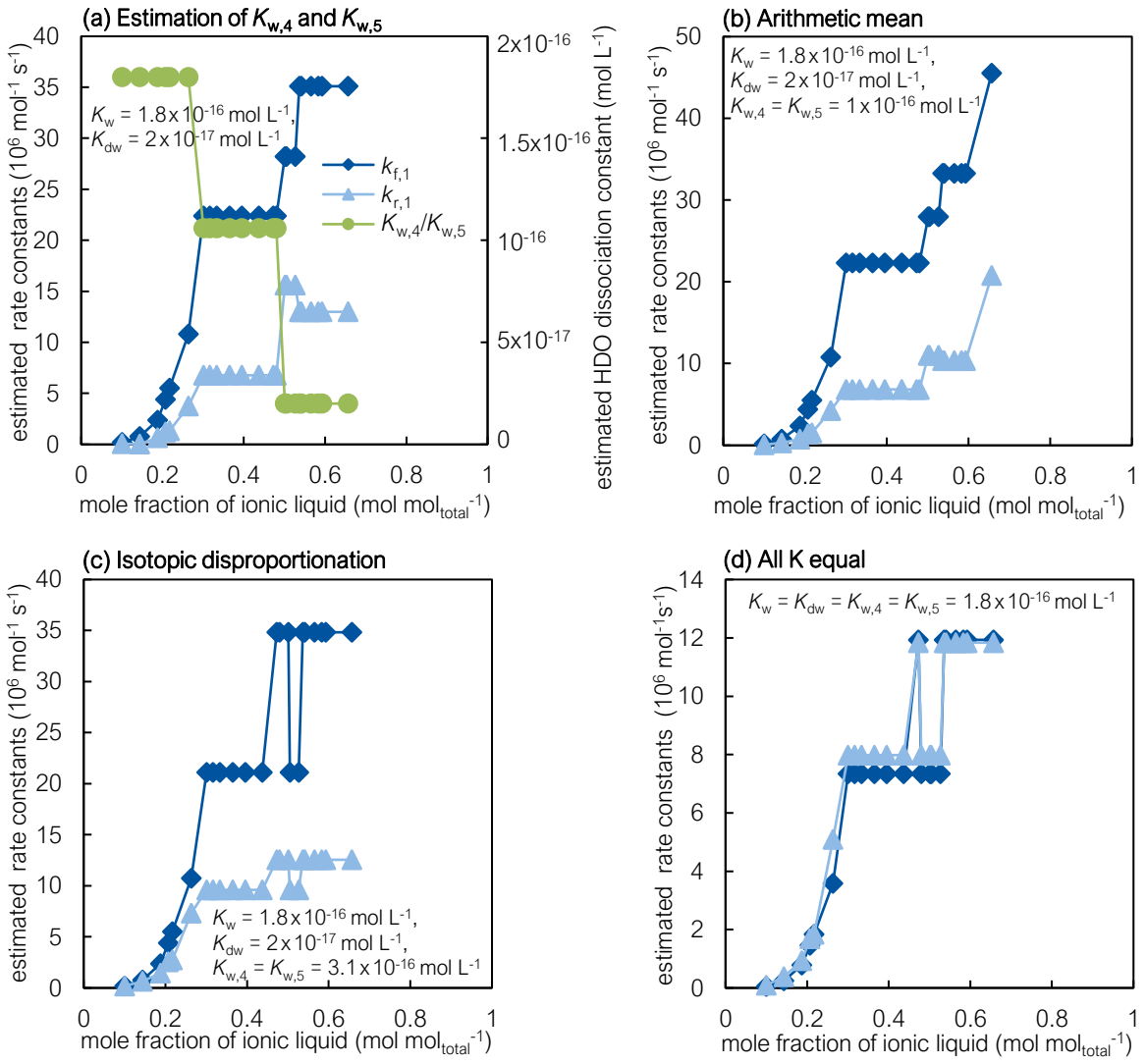

Figure A.4: Different variants of estimated exchange rate constants and dissociation constants:

(a) Estimation of HDO dissociation constants $K_{\mathrm{w},4}$ and $K_{\mathrm{w},5}$ as shown in the main text. Dissociation constant of water $K_{\mathrm{w}} = 1.8 \times 10^{-16}\mathrm{mol\,L^{-1}}$ and heavy water $K_{\mathrm{dw}} = 2 \times 10^{-17}\mathrm{mol\,L^{-1}}$.

(b) The dissociation constants of HDO, $K_{\mathrm{w},4}$ and $K_{\mathrm{w},5}$, are assumed to be the arithmetic mean of the normal and heavy water dissociation constants.

(c) $K_{\mathrm{w},4}$ and $K_{\mathrm{w},5}$ are calculated so that the isotopic disproportionation between water, heavy water and HDO is considered: $\mathrm{HDO}^2/(\mathrm{H_2O} \cdot \mathrm{D_2O}) = 3.7$ [307].

(d) All four dissociation constants are assumed to have the same value of normal water dissociation $K_{\mathrm{w}} = 1.8 \times 10^{-16}\mathrm{mol\,L^{-1}}$.

Appendix B

Acetosolv Pretreatment

Fitting of Non-Recovered Fraction

Evaluation of the non-recovered fraction as a function of the catalyst concentration represents a first step towards the quantification of the influence of catalyst concentration. Our approach resembles the logistic function chosen by Dong et al. [289] and Chang et al. [290] for the modeling of pretreatment phenomena during formic acid pretreatment of wheat straw and sugarcane bagasse, respectively. Since time and temperature were not varied for the acetosolv experiments, they are not included in the function. Furthermore, we assume that the biomass cannot be solubilized completely during pretreatment but instead we consider a maximum limit of non-recovered fraction after pretreatment $w_{\mathrm{nr,max}}$. A similar assumption has already been made to model incomplete lignin solubilization during acetosolv pretreatment [284, 288]. Each fit includes all samples (i.e., DoD 0 to DoD 4) in concentrated acetosolv liquids (filled symbols) except for the two samples with DoD 4 for phosphoric acid, which are excluded due to the high standard deviations. To correlate the non-recovered fraction w_{nr} with the concentration of each catalyst acid c_{cat}, we use the following logistic function:

$$w_{\mathrm{nr}} = \frac{w_{\mathrm{nr,max}}}{(1 + e^{-w_{\mathrm{nr,max}} \cdot k \cdot c_{\mathrm{cat}}} \cdot (\frac{w_{\mathrm{nr,max}}}{w_{\mathrm{nr,0}}} - 1))}. \tag{B.1}$$

The parameters $w_{\mathrm{nr,max}}$ and $w_{\mathrm{nr,0}}$ refer to the maximum value of the non-recovered fraction and the non-recovered fraction at a catalyst concentration of 0 (i.e., pretreatment without catalyst acid), respectively. k denotes the steepness of the increase of the non-recovered fraction with catalyst acid concentration. All parameter values are determined individually for each catalyst acid. Overall, the logistic function of Eq. (B.1) represents the experimental data well as indicated by the high coefficients of determination (see Fig. 4.12). The fitted values for the three parameters depending on the type of catalyst acid are given in Tab. B.1.

Table B.1: Fitting parameters for Eq. (B.1).

	HCl	**H_2SO_4**	**H_3PO_4**
$w_{\mathrm{nr,max}}$ ($\mathrm{g\,g^{-1}}$)	0.397	0.397	0.374
k ($\mathrm{L\,mol^{-1}}$)	238	1.58×10^4	16.9
$w_{\mathrm{nr},0}$ ($\mathrm{g\,g^{-1}}$)	0.0532	6.45×10^{-8}	0.01997

The estimated maximum non-recovered fraction is similar for all three catalyst acids: For complete disintegration, a maximum of approximately 40 wt % of beech wood is removed. Thus, this parameter is independent of the catalyst acid but is specific for beech or for acetosolv-pretreated beech. A comparable overall limit has been observed by Parajó et al. [219] with 50 wt % recovered fraction after acetosolv pretreatment of eucalyptus wood. The fluctuation of points around the upper limit of the non-recovered fraction might be due to the fact that especially at higher DoDs very small particles are formed, which are not hold back uniformly during filtration. Analogously, the estimated values for $w_{\mathrm{nr},0}$ in case of hydrochloric and sulfuric acid are in the range of the non-recovered fraction determined in the experiment without catalyst (see Tab. B.2), while the value for sulfuric acid appears rather low. Nevertheless, this parameter should have a fixed value independent of the type of catalyst acid for a general analysis. In contrast, an increasing value of k correlates with a decreasing amount of catalyst acid required to achieve disintegration. Hence, this parameter indicates the strength of the employed acetosolv liquids resulting from the acidity of the catalyst acid and/or the influence of the water content. A generalization of this analysis could aid to further describe acid properties of the investigated electrolyte solutions.

Compositional Changes after Pretreatment

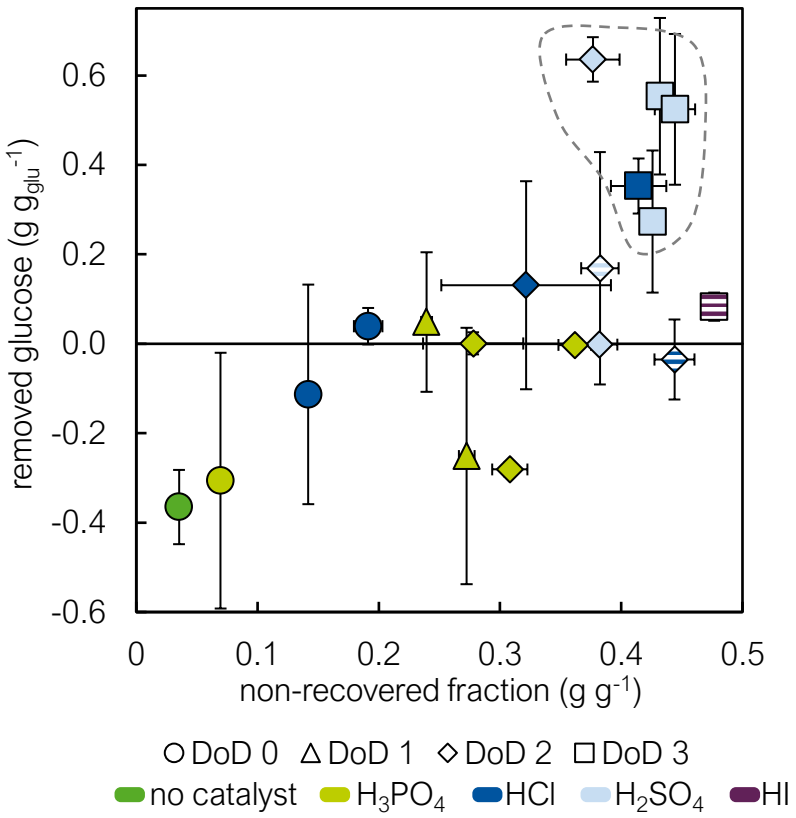

Figure B.1: Glucose removed during pretreatment with acetic acid-based liquids (filled symbols) and acetic acid–water-based liquids (striped symbols) versus non-recovered fraction. The content of cellulose as glucose in native beech is 41.8 wt %. The area delineated by the dashed curve highlights experiments with an extraordinary high fraction of lignin remaining in the pretreated material and at the same time a high amount of glucose removed during pretreatment. The shape and color of the symbols indicate the DoD and the employed catalyst acid, respectively (see legend). Error bars are shown only for measurements with standard deviation above symbol size.

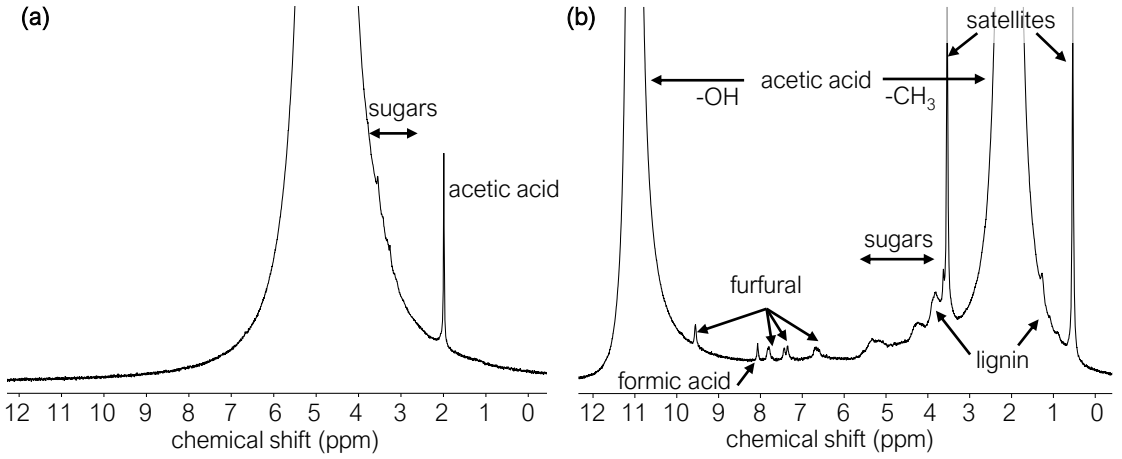

Figure B.2: NMR spectra of pretreatment liquids after pretreatment with signals of dissolved components: **(a)** Pretreatment liquid consisting of water and sulfuric acid (234.48 mmol L^{-1}) and **(b)** acetosolv pretreatment liquid consisting of acetic acid and sulfuric acid (21.78 mmol L^{-1}).

Figure B.2 (a) shows a sample spectrum of a reference experiment with only water and sulfuric acid catalyst. Here, only slight signals of sugars between 3 ppm and 4 ppm (mostly covered by the dominant water peak around 4.75 ppm) and acetic acid around 2 ppm are visible. The acetic acid peak is visible for all experiments, whereas the sugar signals are more pronounced at higher concentrations of catalyst acid in water.

Figure B.2 (b) shows a sample spectrum of an acetosolv pretreatment liquid after pretreatment including signals of the dissolved biomass components. Dominant peaks arise from the acetic acid methyl and hydroxyl group. The peak of the latter is superimposed with the hydroxyl peak of other components, mainly water and catalyst acid. Due to the low concentration of dissolved components, their signal intensities are much smaller than the solvent peaks. The poor signal to noise ratio at these low concentrations would lead to high errors in a quantitative analysis (e.g., via peak integration). Nevertheless, peaks of some dissolved wood components (sugars, lignin) and degradation products (furfural, formic acid) are clearly visible, which allows for a qualitative analysis of dissolved components complementing the component analysis of the recovered fraction. Owing to the low resolution of the spectrometer, all sugar signals are superimposed between 3.8 ppm and 5.6 ppm and visual differentiation between the different types of sugars (glucose, xylose, mannose) is not possible. The signals of the solubilized lignin are clearly visible and only partially superimposed with the main peak of lignin arising at 3.8 ppm and further lignin peaks around 1.3 ppm.

Similar signals have been observed for measurements of lignin with low-field NMR spectroscopy [308]. Between 9.5 ppm and 6.5 ppm, four peaks of furfural arise and around 8.1 ppm is the signal of formic acid.

Integration of Spectra

Figure B.3 shows the spectrum of pure acetic acid that was used for the calculation of the integration constant c_{int} (see Eq. (3.6)). The dashed lines in the zoom on the methyl peak represent the integration limits for the determination of A_{CH_3}. The upper integration limit was set to 3.22 ppm to avoid superposition with signals of solubilized biomass components and degradation products in spectra of pretreatment liquids (see Fig. B.2 (b) in appendix). The lower integration limit was set to -0.5 ppm. The total peak area A_{tot} was integrated between -0.5 ppm and 13 ppm. No offsets or baseline corrections were used for the integration.

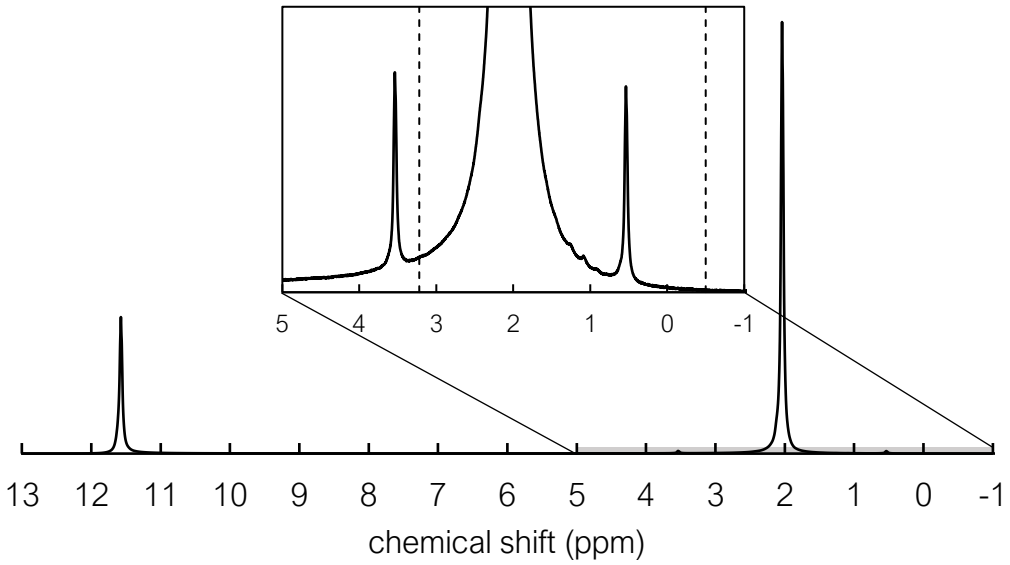

Figure B.3: Spectrum of acetic acid that was used for the determination of c_{int}. The zoom shows the area highlighted in gray with integration limits for the methyl peak (-0.5 – 3.22 ppm).

For an ideal spectrum of acetic acid, 3 and 4 protons contribute to the methyl peak area and total spectral area, respectively. This results in a ratio of 0.75. c_{int} is calculated from the quotient of the ideal value and the ratio of $A_{\mathrm{CH_3}}/A_{\mathrm{tot}}$ in the measured acetic acid spectrum:

$$c_{\mathrm{int}} = \frac{0.75}{A_{\mathrm{CH_3}}/A_{\mathrm{tot}}} = 1.043. \tag{B.2}$$

c_{int} is valid for all spectra, while the factor $f_{A-n_{\mathrm{H}}}$ (see Eq. (3.6)) is calculated for each spectrum individually.

To estimate the fraction of removed protons $x_{\mathrm{H,rem}}$, linear regression of removed hemicellulose $m_{\mathrm{hc,rem}}$ and lignin $m_{\mathrm{l,rem}}$ with non-recovered fraction (see Fig. 4.14) gives the following equations

$$m_{\mathrm{hc,rem}} = 0.2842 w_{\mathrm{nr}} - 0.0166 \tag{B.3}$$

$$m_{\mathrm{l,rem}} = 0.1556 w_{\mathrm{nr}} - 0.009. \tag{B.4}$$

For values of $w_{\mathrm{nr}} < 0.05$, infeasible values of negative removal result from the regression equations. In these cases, the amount of removed hemicellulose and lignin is set to 0. Wood moisture is assumed to be completely solubilized independent of the non-recovered fraction. Lastly, the amount and fraction of removed protons is estimated from the removed components considering the individual weight fractions of hydrogen:

$$n_{\mathrm{H,rem}} = (m_{\mathrm{hc,rem}} w_{\mathrm{H,hc}} + m_{\mathrm{l,rem}} w_{\mathrm{H,l}} + m_{\mathrm{wood}} w_{\mathrm{m}} w_{\mathrm{H,H_2O}})/M_{\mathrm{H}} \tag{B.5}$$

$$x_{\mathrm{H,rem}} = n_{\mathrm{H,rem}}/n_{\mathrm{H,wood}}. \tag{B.6}$$

Table B.2: Experimental conditions for acetosolv experiments. Note that the non-recovered fraction w_{nr} as well as the glucose (glu) and xylose (xyl) yields refer to the initial amount of dry biomass, while the acetyl content refers to the recovered fraction. The fraction of removed components refers to the respective fraction of glucose, xylose + mannose and lignin in native beech.

Pretreatment liquid					**Pretreatment samples**							
Catalyst	c_{cat}	**Mole fractions** ($\mathrm{mol\,mol^{-1}}$)			**DoD**	w_{nr}	**Removed components** ($\mathrm{g\,g^{-1}}$)			**Acetyl**	**Yield** ($\mathrm{g\,g^{-1}}$)	
	($\mathrm{mol\,L^{-1}}$)	**cat**	**H_2O**	**AA**		($\mathrm{g\,g^{-1}}$)	**glu**	**xyl + man**	**lignin**	($\mathrm{g\,g^{-1}}$)	**glu**	**xyl**
–	0	0	0.0326	0.9674	0	0.0354	-0.3648	-0.2664	-0.0749	0.0643	0.0448	0.0203
HCl	0.14161	0.0077	0.0674	0.9250	3	0.4143	0.3529	0.9092	0.3223	nd	nd	nd
	0.05906	0.0033	0.0474	0.9494	2	0.3215	0.1309	0.5864	0.4088	0.0608	0.1148	0.0364
	0.01561	0.0009	0.0365	0.9626	0	0.1913	0.0392	0.3294	0.1686	nd	0.0364	0.0282
	0.00863	0.0005	0.0572	0.9424	0	0.1419	-0.1130	0.2151	0.0637	nd	0.0359	0.0299
	0.20253	0.0076	0.4969	0.4956	2	0.4439	-0.0352	0.747	0.7458	0.0441	0.2206	0.0272
H_2SO_4	0.02178	0.0012	0.0329	0.9659	3	0.4318	0.5537	0.9737	0.3432	nd	0.0367	0.0144
	0.02408	0.0014	0.0227	0.9760	3	0.4258	0.2733	0.9465	0.227	nd	0.0334	0.0132
	0.01814	0.0010	0.0223	0.9767	3	0.4442	0.5243	0.9542	0.4654	nd	0.0430	0.0158
	0.00602	0.0003	0.0493	0.9504	2	0.3820	-0.0018	0.6756	0.3826	0.0805	0.0736	0.0296
	0.00505	0.0003	0.0466	0.9531	2	0.3765	0.6357	0.8644	0.5109	nd	nd	nd
	0.22659	0.0099	0.3297	0.6604	2	0.3824	0.1688	0.7588	0.8538	0.0531	0.0752	0.0093
H_3PO_4	0.27338	0.0150	0.0362	0.9487	0	0.0696	-0.3060	-0.0425	0.0266	0.0601	0.0323	0.0304
	0.74114	0.0395	0.0422	0.9182	2	0.3080	-0.2808	0.4063	0.4821	nd	0.0411	0.0269
	0.64248	0.0345	0.0410	0.9245	1	0.2724	-0.2508	0.4264	0.3412	nd	nd	nd
	0.90216	0.0476	0.0442	0.9082	2	0.3616	-0.0027	0.5782	0.5908	nd	0.0435	0.0267
	0.65722	0.0347	0.0636	0.9017	2	0.2779	0.0098	0.567	0.4288	nd	nd	nd
	0.46882	0.0252	0.0551	0.9197	1	0.2394	0.0487	0.4988	0.3317	nd	0.0521	0.0356
HI	0.20114	0.0075	0.4962	0.4963	3	0.4765	0.0829	0.8078	0.8248	0.037	0.1851	0.0192

Table B.3: Visibility of components solubilized in pretreatment liquid after acetosolv pretreatment of beech wood: + strong signal, o signal visible, - signal hardly visible, x component not visible in spectrum.

Catalyst acid	c_{cat} **(mol L^{-1})**	**Lignin**	**Sugars**	**Furfural**	**Formic acid**
no catalyst	-	-	x	x	x
HCl	0.14161	+	o	+	-
	0.05906	+	o	+	-
	0.01561	+	x	x	x
	0.00863	+	x	x	-
	0.20253	+	o	+	x
H_2SO_4	0.02178	+	+	+	+
	0.02408	+	+	+	o
	0.01814	+	+	+	-
	0.00602	+	+	-	x
	0.00505	+	+	-	-
	0.22659	+	o	o	x
H_3PO_4	0.27338	+	x	x	o
	0.74114	+	-	-	-
	0.64248	+	-	-	-
	0.90216	+	-	-	-
	0.65722	+	-	x	-
	0.46882	+	-	x	-
HI	0.20114	+	o	o	x

Appendix C

Pretreatment in RNFA

Model and Reaction Parameters

Total investment costs TIC are calculated from investment costs IC corrected for the influence of interest rate ir and assumed runtime t_{run} of the biofuel production facility: $\mathrm{TIC} = (\mathrm{IC} \cdot ir)/(1-(1+ir)^{t_{\mathrm{run}}})$ [230, 309]. IC are estimated according to the following equation

$$\mathrm{IC} = \frac{\mathrm{CEPCI}_{2014}}{\mathrm{CEPCI}_{2010}} \cdot \mathrm{Inv1} \cdot (b_{\mathrm{product}} M_{\mathrm{product}})^{\mathrm{Inv2}} \cdot \mathrm{NFU} \tag{C.1}$$

with NFU the number of functional units. The economic parameters relevant to RNFA investment cost calculations are given in Tab. C.1.

Table C.1: Economic Parameters for RNFA.

Parameter	**Unit**	**Value**	**Ref.**
interest rate ir	year^{-1}	0.08	-
plant run time t_{run}	year	10	-
CEPCI_{2010}	-	550.8	[310]
CEPCI_{2014}	-	576.1	[310]
Inv1	-	7000	[309]
Inv2	-	0.68	[309]

Additionally, Tab. C.2 gives an overview of specific prices for raw materials and waste.

Table C.2: Specific prices for raw material and waste. †Average value.

Parameter	Unit	Value	Ref.	Assumption
$P_{\text{lignocell. biomass}}$	$\text{USD}\,\text{kg}^{-1}_{\text{biomass}}$	0.05	[311]	-
P_{H_2}	$\text{USD}\,\text{kg}^{-1}_{\text{H}_2}$	2.8†	[311]	biomass gasification
P_{water}	$\text{USD}\,\text{kg}^{-1}_{\text{water}}$	0.0005	[312]	-
P_{waste}	$\text{USD}\,\text{kg}^{-1}_{\text{waste}}$	0.23044	[313]	-

Table C.3 shows the conditions of the reactions considered in RNFA screenings.

Due to the assumption of ideal recycles, yield Y_j is effectively set equal to selectivity S_j without any purges. Thus, only yield information $Y_j = S_j$ is needed.

Table C.3: Input for the reaction network of RNFA.

Reaction	$\boldsymbol{Y_j = S_j}$ $(\text{mol}\,\text{mol}^{-1})$	Ref.
R6	0.95	[68]
R7	0.85	[68]
R8	0.70	[314]
R9	1.00	[314]
R10	0.97	[315]
R11	0.96	[316]
R12	0.99	[317]
R15	0.90	[318]
R16	0.99	[319]
R19	0.96	[320]
R25	0.95	[321]
R26	0.99	[322]
R28	0.84	[323]
R30	0.95	[324]
R32	0.60	[325]

Criteria for Selection of References

For the calculation of yields from published studies, we selected references according to the following constraints. First, we only considered references that include an analysis of raw material, solid recovery and hydrolysis from one experiment. This means for example that studies were not included in the analysis if they rely on estimates for the composition of the raw material. Second, we did not explicitly take into account the specific recalcitrant structure of different types of biomass as well as the influence of degradation products formed during pretreatment and hydrolysis which can both influence subsequent yields. However, since each data set of composition and yields was taken from a single reference, influences of biomass structure and degradation products on the specific pretreatment and hydrolysis yields are indirectly taken into consideration for the pretreatment and hydrolysis step. Third, the yields of further fermentation and downstream processing reactions have the same value for all analyses [230], which means that they are not influenced by the outcome of a specific pretreatment concept (see also Tab. C.3).

Active Fluxes

For ethanol screenings, fluxes R1–R7 are active in all cases.

Tables C.4 and C.5 present all active fluxes of RNFA screenings for the production of ethyl levulinate from beech wood considering ideal and experimental hydrolysis yields, respectively. Tables C.6 and C.7 present all active fluxes of RNFA screenings for the production of ethyl levulinate from a variety of OS-pretreated biomasses. Table C.8 presents active fluxes of RNFA screenings for the production of ethyl levulinate from acetosolv-pretreated beech wood considering the experimental results presented in Section 4.2. Fluxes R1–R5 are active in all ethyl levulinate screenings and are therefore not listed in the tables.

Table C.4: Active reaction fluxes in RNFA for all six points of the Pareto curve of ethyl levulinate production based on beech wood with ideal hydrolysis yields. Cost and carbon loss are taken as objectives. The intermediate points are numbered consecutively.

Pretreatment	**min Cost (1)**	**2**	**3**	**4**	**5**	**min CL (6)**
ideal	R7, R11, R12, R26	R7, R11, R12, R15, R16, R25, R26	R7, R11, R12, R15, R16, R25, R26	R6, R7, R11, R12, R15, R16, R25, R26	R6, R7, R11, R12, R15, R16, R25, R26	R6, R11, R12, R15, R16, R25, R26
kraft	R7, R11, R12, R26	R7, R11, R12, R15, R16, R25, R26	R7, R11, R12, R15, R16, R25, R26	R6, R7, R11, R12, R15, R16, R25, R26	R6, R7, R11, R12, R15, R16, R25, R26	R6, R11, R12, R15, R16, R25, R26
ionic liquid	R7, R11, R12, R26	R6, R7, R11, R12, R26	R6, R7, R11, R12, R26	R6, R7, R11, R12, R26	R6, R7, R11, R12, R15, R16, R25, R26	R6, R11, R12, R15, R16, R25, R26
dilute acid	R6, R7, R11, R12, R26	R6, R7, R11, R12, R15, R16, R25, R26	R6, R7, R11, R12, R15, R16, R25, R26	R6, R7, R11, R12, R15, R16, R25, R26	R6, R7, R11, R12, R15, R16, R25, R26	R6, R11, R12, R15, R16, R25, R26
organosolv	R7, R11, R12, R26	R6, R7, R11, R12, R26	R6, R7, R11, R12, R26	R6, R7, R11, R12, R26	R6, R7, R11, R12, R15, R16, R25, R26	R6, R11, R12, R15, R16, R25, R26
liquid hot water	R7, R11, R12, R26	R6, R7, R11, R12, R15, R16, R25, R26	R6, R7, R11, R12, R15, R16, R25, R26	R6, R7, R11, R12, R15, R16, R25, R26	R6, R7, R11, R12, R15, R16, R25, R26	R6, R11, R12, R15, R16, R25, R26
organocat	R6, R7, R11, R12, R26	R6, R7, R11, R12, R15, R16, R25, R26	R6, R7, R11, R12, R15, R16, R25, R26	R6, R7, R11, R12, R15, R16, R25, R26	R6, R7, R11, R12, R15, R16, R25, R26	R6, R11, R12, R15, R16, R25, R26

Table C.5: Active reaction fluxes in RNFA for all six points of the Pareto curve of ethyl levulinate production based on beech wood with experimental hydrolysis yields. Cost and carbon loss are taken as objectives. The intermediate points are numbered consecutively.

Pretreatment	**min Cost (1)**	**2**	**3**	**4**	**5**	**min CL (6)**
min CL	R7, R8, R26	R7, R8, R15, R16, R25, R26	R7, R8, R15, R16, R25, R26	R7, R8, R15, R16, R25, R26	R6, R7, R8, R15, R16, R25, R26	R6, R8, R15, R16, R19, R25
ideal	R7, R11, R12, R26	R7, R11, R12, R15, R16, R25, R26	R7, R11, R12, R15, R16, R25, R26	R6, R7, R11, R12, R15, R16, R25, R26	R6, R7, R11, R12, R15, R16, R25, R26	R6, R11, R12, R15, R16, R25, R26
kraft	R7, R11, R12, R26	R7, R11, R12, R15, R16, R25, R26	R7, R11, R12, R15, R16, R25, R26	R6, R7, R11, R12, R15, R16, R25, R26	R6, R7, R11, R12, R15, R16, R25, R26	R6, R11, R12, R15, R16, R25, R26
ionic liquid	R7, R11, R12, R26	R6, R7, R11, R12, R26	R6, R7, R11, R12, R26	R6, R7, R11, R12, R26	R6, R7, R11, R12, R15, R16, R25, R26	R6, R11, R12, R15, R16, R25, R26
dilute acid	R6, R7, R11, R12, R26	R6, R7, R11, R12, R15, R16, R25, R26	R6, R7, R11, R12, R15, R16, R25, R26	R6, R7, R11, R12, R15, R16, R25, R26	R6, R7, R11, R12, R15, R16, R25, R26	R6, R11, R12, R15, R16, R25, R26
organosolv	R7, R11, R12, R26	R7, R11, R12, R15, R16, R25, R26	R6, R7, R11, R12, R15, R16, R25, R26	R6, R7, R11, R12, R15, R16, R25, R26	R6, R7, R11, R12, R15, R16, R25, R26	R6, R11, R12, R15, R16, R25, R26
liquid hot water	R6, R7, R11, R12, R26	R6, R11, R12, R15, R16, R25, R26	R6, R11, R12, R15, R16, R25, R26	R6, R11, R12, R15, R16, R25, R26	R6, R11, R12, R15, R16, R25, R26	R6, R11, R12, R15, R16, R25, R26
organocat	R7, R11, R12, R26	R7, R11, R12, R15, R16, R25, R26	R7, R11, R12, R15, R16, R25, R26	R7, R11, R12, R15, R16, R25, R26	R6, R11, R12, R15, R16, R25, R26	R6, R11, R12, R15, R16, R25, R26

Table C.6: Active reaction fluxes in RNFA for all six points of the Pareto curve of ethyl levulinate production based on a variety of softwoods with organosolv pretreatment. Cost and carbon loss are taken as objectives. The intermediate points are numbered consecutively.

Pretreatment	**min Cost (1)**	**2**	**3**	**4**	**5**	**min CL (6)**
ideal ●	R7, R11, R12, R26	R6, R7, R11, R12, R26	R6, R7, R11, R12, R26	R6, R7, R11, R12, R26	R6, R7, R11, R12, R15, R16, R25, R26	R6, R11, R12, R15, R16, R25, R26
softwood						
spruce [238] △	R6, R15, R16, R25	R6, R11, R15, R16, R25, R28	R6, R11, R15, R16, R25, R28	R6, R11, R15, R16, R25, R28	R6, R11, R15, R16, R25, R28	R6, R11, R12, R15, R16, R25, R26
spruce [243] ▲	R6, R7, R11, R12, R26	R6, R7, R11, R12, R15, R16, R25, R26	R6, R7, R11, R12, R15, R16, R25, R26	R6, R7, R11, R12, R15, R16, R25, R26	R6, R7, R11, R12, R15, R16, R25, R26	R6, R11, R12, R15, R16, R25, R26
spruce [242] △	R6, R7, R11, R12, R26	R6, R7, R11, R12, R15, R16, R25, R26	R6, R7, R11, R12, R15, R16, R25, R26	R6, R7, R11, R12, R15, R16, R25, R26	R6, R7, R11, R12, R15, R16, R25, R26	R6, R11, R12, R15, R16, R25, R26
pine [244] ▲	R7, R11, R12, R26	R7, R11, R12, R15, R16, R25, R26	R7, R11, R12, R15, R16, R25, R26	R7, R11, R12, R15, R16, R25, R26	R6, R8, R15, R16, R25, R26	R6, R11, R12, R15, R16, R25, R26
pine [245] △	R7, R11, R12, R26	R7, R11, R12, R15, R16, R25, R26	R7, R11, R12, R15, R16, R25, R26	R7, R11, R12, R15, R16, R25, R26	R6, R7, R11, R12, R15, R16, R25, R26	R6, R11, R12, R15, R16, R25, R26
pine [246] ▲	R6, R7, R15, R16, R25	R6, R7, R15, R16, R25	R6, R7, R15, R16, R25	R6, R7, R15, R16, R25	R6, R7, R15, R16, R25	R6, R7, R15, R16, R25

Table C.7: Active reaction fluxes in RNFA for all six points of the Pareto curve of ethyl levulinate production based on non-woody biomass (sugarcane bagasse) and a variety of hardwoods with organosolv pretreatment. Cost and carbon loss are taken as objectives. The intermediate points are numbered consecutively.

Pretreatment	**min Cost (1)**	**2**	**3**	**4**	**5**	**min CL (6)**
sugarcane bagasse						
[240] ◆	R7, R11, R12, R26	R6, R7, R11, R12, R15, R16, R25, R26	R6, R7, R11, R12, R15, R16, R25, R26	R6, R7, R11, R12, R15, R16, R25, R26	R6, R7, R11, R12, R15, R16, R25, R26	R6, R11, R12, R15, R16, R25, R26
[241] ◆	R7, R11, R12, R26	R7, R11, R12, R15, R16, R25, R26	R7, R11, R12, R15, R16, R25, R26	R6, R7, R11, R12, R15, R16, R25, R26	R6, R7, R11, R12, R15, R16, R25, R26	R6, R11, R12, R15, R16, R25, R26
[242] ◆	R7, R11, R12, R26	R6, R7, R11, R12, R26	R6, R7, R11, R12, R26	R6, R7, R11, R12, R15, R16, R25, R26	R6, R7, R11, R12, R15, R16, R25, R26	R6, R11, R12, R15, R16, R25, R26
hardwood						
tulip tree [247] ■	R6, R7, R11, R12, R26	R6, R7, R11, R12, R15, R16, R25, R26	R6, R7, R11, R12, R15, R16, R25, R26	R6, R7, R11, R12, R15, R16, R25, R26	R6, R7, R11, R12, R15, R16, R25, R26	R6, R11, R12, R15, R16, R25, R26
elm [246] ■	R6, R7, R11, R12, R26	R6, R11, R12, R15, R16, R25, R26	R6, R11, R12, R15, R16, R25, R26	R6, R11, R12, R15, R16, R25, R26	R6, R11, R12, R15, R16, R25, R26	R6, R11, R12, R15, R16, R25, R26
beech [238] ■	R7, R11, R12, R26	R7, R11, R12, R15, R16, R25, R26	R6, R7, R11, R12, R15, R16, R25, R26	R6, R7, R11, R12, R15, R16, R25, R26	R6, R7, R11, R12, R15, R16, R25, R26	R6, R11, R12, R15, R16, R25, R26

Table C.8: Active reaction fluxes in RNFA for all six points of the Pareto curve of ethyl levulinate production based on acetosolv pretreatment of beech wood with different catalyst acids considering experimental hydrolysis yields. Cost and carbon loss are taken as objectives. The intermediate points are numbered consecutively.

Catalyst acid	**min Cost (1)**	**2**	**3**	**4**	**5**	**min CL (6)**
HCl	R7, R11, R12, R26	R7, R11, R12, R15, R16, R25, R26	R7, R11, R12, R15, R16, R25, R26	R7, R11, R12, R15, R16, R25, R26	R6, R7, R11, R12, R15, R16, R25, R26	R6, R11, R12, R15, R16, R25, R26
HI	R7, R11, R12, R26	R7, R11, R12, R15, R16, R25, R26	R7, R11, R12, R15, R16, R25, R26	R7, R11, R12, R15, R16, R25, R26	R6, R7, R11, R12, R15, R16, R25, R26	R6, R11, R12, R15, R16, R25, R26

Bibliography

[1] C. Marks and J. Viell. Solvents and ions for pretreatment in lignocellulosic biorefineries. *Process Biochemistry*, 113:241–257, 2022. doi: 10.1016/j.procbio.2022.01.001.

[2] C. Marks, A. Mitsos, and J. Viell. Change of C(2)-hydrogen–deuterium exchange in mixtures of EMIMAc. *Journal of Solution Chemistry*, 48(8-9):1188–1205, 2019. doi: 10.1007/s10953-019-00899-7.

[3] C. Marks and J. Viell. Acetosolv pretreatment of wood for biorefinery applications. *Biomass Conversion and Biorefinery*, 2021. doi: 10.1007/s13399-021-02023-6.

[4] C. Marks, A. König, A. Mitsos, and J. Viell. Minimal viable sugar yield of biomass pretreatment. *Biofuels, Bioproducts and Biorefining*, 14(2):301–314, 2020. doi: 10.1002/bbb.2074.

[5] A. Kochs. Screening ionischer Flüssigkeiten als Lösungsmittel für lignocelluläre Biomasse. *Internship report*, Process Systems Engineering, RWTH Aachen University, Germany, 2014.

[6] A. Schwabauer. Comparison of chemical biomass pretreatment processes. *Project thesis*, Process Systems Engineering, RWTH Aachen University, Germany, 2015.

[7] M. Offermann. Messung der Säure-/Basenstärke mit NMR-Spektroskopie. *Project thesis*, Process Systems Engineering, RWTH Aachen University, Germany, 2015.

[8] F. Bergs. Biomasseaufschluss mithilfe "deep eutectic solvents". *Project thesis*, Process Systems Engineering, RWTH Aachen University, Germany, 2015.

[9] D. Hambsch. Vorbehandlung von Holz in essigsäurebasierten Medien. *Bachelor's thesis*, Process Systems Engineering, RWTH Aachen University, Germany, 2015.

[10] C. Tomala. Analyse von Biomasse und Biomasseaufschlusslösungen mittels NMR. *Master's thesis*, Process Systems Engineering, RWTH Aachen University, Germany, 2015.

[11] M. Galowy. Modellierung von NMR-Spektren von Säure- und Salzgemischen. *Bachelor's thesis*, Process Systems Engineering, RWTH Aachen University, Germany, 2015.

[12] B. Hensel. Vorbehandlung von Holz in alkalischen Lösungen. *Project thesis*, Process Systems Engineering, RWTH Aachen University, Germany, 2016.

[13] F. Temme and D. Böning. Measurement of pH and pK_a with low-field NMR spectroscopy in diluted and concentrated electrolyte solutions. *Project thesis*, Process Systems Engineering, RWTH Aachen University, Germany, 2017.

[14] J. Mathias. Characterisation of multiphase electrolytic systems employing in-line spectroscopy. *Bachelor's thesis*, Process Systems Engineering, RWTH Aachen University, Germany, 2017.

[15] H. Ingendae. Reaktionsnetzwerke zur Vorbehandlung von Biomasse. *Project thesis*, Process Systems Engineering, RWTH Aachen University, Germany, 2017.

[16] M. Huang and D. Pflug. Experimentelle Validierung der pH-Modellierung in Medien einer Bioraffinerie. *Project thesis*, Process Systems Engineering, RWTH Aachen University, Germany, 2017.

[17] A. Jachertz and J. Kappes. Einfluss von Temperatur auf IR- und Raman-Spektren von Essigsäure in wässriger Lösung. *Project thesis*, Process Systems Engineering, RWTH Aachen University, Germany, 2019.

[18] T. Kitzing. Modellierung von Dissoziationsgleichgewichten in Elektrolytlösungen bei hohen Temperaturen und Drücken. *Bachelor's thesis*, Process Systems Engineering, RWTH Aachen University, Germany, 2019.

[19] J. Viell, H. Inouye, N. K. Szekely, H. Frielinghaus, C. Marks, Y. Wang, N. Anders, A. C. Spiess, and L. Makowski. Multi-scale processes of beech wood disintegration and pretreatment with 1-ethyl-3-methylimidazolium acetate/water mixtures. *Biotechnology for Biofuels*, 9:7, 2016. doi: 10.1186/s13068-015-0422-9.

[20] S. Stiefel, C. Marks, T. Schmidt, S. Hanisch, G. Spalding, and M. Wessling. Overcoming lignin heterogeneity: reliably characterizing the cleavage of technical lignin. *Green Chemistry*, 18(2):531–540, 2016. doi: 10.1039/c5gc01506e.

[21] O. Walz, C. Marks, J. Viell, and A. Mitsos. Systematic approach for modeling reaction networks involving equilibrium and kinetically-limited reaction steps. *Computers & Chemical Engineering*, 98:143–153, 2017. doi: 10.1016/j.compchemeng.2016.12.014.

[22] D. Di Marino, T. Jestel, C. Marks, J. Viell, M. Blindert, S. M. A. Kriescher, A. C. Spiess, and M. Wessling. Carboxylic acids production via electrochemical depolymerization of lignin. *ChemElectroChem*, 6(5):1434–1442, 2019. doi: 10.1002/celc.201801676.

[23] J. Viell, N. K. Szekely, G. Mangiapia, C. Hövelmann, C. Marks, and H. Frielinghaus. In operando monitoring of wood transformation during pretreatment with ionic liquids. *Cellulose*, 27(9):4889–4907, 2020. doi: 10.1007/s10570-020-03119-4.

[24] A. Echtermeyer, C. Marks, A. Mitsos, and J. Viell. Inline Raman spectroscopy and indirect hard modeling for concentration monitoring of dissociated acid species. *Applied Spectroscopy*, 75(5):506–519, 2021. doi: 10.1177/0003702820973275.

[25] S. J. Davis, N. S. Lewis, M. Shaner, S. Aggarwal, D. Arent, I. L. Azevedo, S. M. Benson, T. Bradley, J. Brouwer, Y.-M. Chiang, C. T. M. Clack, A. Cohen, S. Doig, J. Edmonds, P. Fennell, C. B. Field, B. Hannegan, B.-M. Hodge, M. I. Hoffert, E. Ingersoll, P. Jaramillo, K. S. Lackner, K. J. Mach, M. Mastrandrea, J. Ogden, P. F. Peterson, D. L. Sanchez, D. Sperling, J. Stagner, J. E. Trancik, C.-J. Yang, and K. Caldeira. Net-zero emissions energy systems. *Science (Washington, DC, United States)*, 360(6396):eaas9793, 2018. doi: 10.1126/science.aas9793.

[26] J. B. Zimmerman, P. T. Anastas, H. C. Erythropel, and W. Leitner. Designing for a green chemistry future. *Science (Washington, DC, United States)*, 367(6476):397–400, 2020. doi: 10.1126/science.aay3060.

[27] W. Marquardt, A. Harwardt, M. Hechinger, K. Kraemer, J. Viell, and A. Voll. The biorenewables opportunity – toward next generation process and product systems. *AIChE Journal*, 56(9):2228–2235, 2010. doi: 10.1002/aic.12380.

[28] G.-J. Gruter. The bio-based transition: bio-mass feedstock (2). 2nd generation (2G) (lignocellulose). *Chimica Oggi*, 36(2):60–61, 2018.

[29] P. Harrison, C. Malins, S. Searle, A. Baral, D. Turley, and L. Hopwood. *Wasted - Europe's untapped resource.* The International Council on Clean Transportation, 2014. URL `https://theicct.org/publications/wasted-europes-untapped-resource`. Accessed April 13, 2019.

[30] Fachagentur Nachwachsende Rohstoffe e.V. *Roadmap Bioraffinerien im Rahmen der Aktionspläne der Bundesregierung zur stofflichen und energetischen Nutzung nachwachsender Rohstoffe.* BMELV, BMBF, BMU, BMWi, May 2012.

[31] W. Leitner, J. Klankermayer, S. Pischinger, H. Pitsch, and K. Kohse-Höinghaus. Advanced biofuels and beyond: chemistry solutions for propulsion and production. *Angewandte Chemie, International Edition*, 56(20):5412–5452, 2017. doi: 10.1002/anie.201607257.

[32] A. König, K. Ulonska, A. Mitsos, and J. Viell. Optimal applications and combinations of renewable fuel production from biomass and electricity. *Energy & Fuels*, 33(2):1659–1672, 2019. doi: 10.1021/acs.energyfuels.8b03790.

[33] D. M. Alonso, J. Q. Bond, and J. A. Dumesic. Catalytic conversion of biomass to biofuels. *Green Chemistry*, 12(9):1493–1513, 2010. doi: 10.1039/c004654j.

[34] J. S. Luterbacher, D. Martin Alonso, and J. A. Dumesic. Targeted chemical upgrading of lignocellulosic biomass to platform molecules. *Green Chemistry*, 16(12):4816–4838, 2014. doi: 10.1039/C4GC01160K.

[35] N. Mosier, C. Wyman, B. Dale, R. Elander, Y. Lee, M. Holtzapple, and M. Ladisch. Features of promising technologies for pretreatment of lignocellulosic biomass. *Bioresource Technology*, 96(6):673–686, 2005. doi: 10.1016/j.biortech.2004.06.025.

[36] C. E. Wyman and B. E. Dale. Producing biofuels via the sugar platform. *CEP magazine*, pages 45–57, March 2015.

[37] D. Klein-Marcuschamer, P. Oleskowicz-Popiel, B. A. Simmons, and H. W. Blanch. The challenge of enzyme cost in the production of lignocellulosic biofuels. *Biotechnology and Bioengineering*, 109(4):1083–1087, 2012. doi: 10.1002/bit.24370.

[38] P. Alvira, E. Tomás-Pejó, M. Ballesteros, and M. Negro. Pretreatment technologies for an efficient bioethanol production process based on enzymatic hydrolysis: a review. *Bioresource Technology*, 101(13):4851–4861, 2010. doi: 10.1016/j.biortech.2009.11.093.

[39] Y. Shastri. Renewable energy, bioenergy. *Current Opinion in Chemical Engineering*, 17:42–47, 2017. doi: 10.1016/j.coche.2017.06.003.

[40] M. E. Himmel, S.-Y. Ding, D. K. Johnson, W. S. Adney, M. R. Nimlos, J. W. Brady, and T. D. Foust. Biomass recalcitrance: engineering plants and enzymes for biofuels production. *Science (Washington, DC, United States)*, 315(5813): 804–807, 2007. doi: 10.1126/science.1137016.

[41] J. van den Brink and R. P. de Vries. Fungal enzyme sets for plant polysaccharide degradation. *Applied Microbiology and Biotechnology*, 91(6):1477–1492, 2011. doi: 10.1007/s00253-011-3473-2.

[42] A. K. Chandel, G. Chandrasekhar, M. B. Silva, and S. Silvério da Silva. The realm of cellulases in biorefinery development. *Critical Reviews in Biotechnology*, 32(3):187–202, 2012. doi: 10.3109/07388551.2011.595385.

[43] M. Adsul, S. K. Sandhu, R. R. Singhania, R. Gupta, S. K. Puri, and A. Mathur. Designing a cellulolytic enzyme cocktail for the efficient and economical conversion of lignocellulosic biomass to biofuels. *Enzyme and Microbial Technology*, 133:109442, 2020. doi: 10.1016/j.enzmictec.2019.109442.

[44] J. S. van Dyk and B. I. Pletschke. A review of lignocellulose bioconversion using enzymatic hydrolysis and synergistic cooperation between enzymes–factors affecting enzymes, conversion and synergy. *Biotechnology Advances*, 30(6):1458–1480, 2012. doi: 10.1016/j.biotechadv.2012.03.002.

[45] S. Roth and A. C. Spiess. Laccases for biorefinery applications: a critical review on challenges and perspectives. *Bioprocess and Biosystems Engineering*, 38(12): 2285–2313, 2015. doi: 10.1007/s00449-015-1475-7.

[46] C. E. Wyman, B. E. Dale, R. T. Elander, M. Holtzapple, M. R. Ladisch, and Y. Y. Lee. Comparative sugar recovery data from laboratory scale application of leading pretreatment technologies to corn stover. *Bioresource Technology*, 96 (18):2026–2032, 2005. doi: 10.1016/j.biortech.2005.01.018.

[47] C. E. Wyman, B. E. Dale, R. T. Elander, M. Holtzapple, M. R. Ladisch, Y. Y. Lee, C. Mitchinson, and J. N. Saddler. Comparative sugar recovery and fermentation data following pretreatment of poplar wood by leading technologies. *Biotechnology Progress*, 25(2):333–339, 2009. doi: 10.1002/btpr.142.

[48] S. Sun, S. Sun, X. Cao, and R. Sun. The role of pretreatment in improving the enzymatic hydrolysis of lignocellulosic materials. *Bioresource Technology*, 199: 49–58, 2016. doi: 10.1016/j.biortech.2015.08.061.

[49] M. H. L. Silveira, A. R. C. Morais, A. M. da Costa Lopes, D. N. Olekszyszen, R. Bogel-Łukasik, J. Andreaus, and L. Pereira Ramos. Current pretreatment technologies for the development of cellulosic ethanol and biorefineries. *ChemSusChem*, 8(20):3366–3390, 2015. doi: 10.1002/cssc.201500282.

[50] P. Kumar, D. M. Barrett, M. J. Delwiche, and P. Stroeve. Methods for pretreatment of lignocellulosic biomass for efficient hydrolysis and biofuel production. *Industrial & Engineering Chemistry Research*, 48(8):3713–3729, 2009. doi: 10.1021/ie801542g.

[51] V. B. Agbor, N. Cicek, R. Sparling, A. Berlin, and D. B. Levin. Biomass pretreatment: fundamentals toward application. *Biotechnology Advances*, 29 (6):675–685, 2011. doi: 10.1016/j.biotechadv.2011.05.005.

[52] M. Galbe and O. Wallberg. Pretreatment for biorefineries: a review of common methods for efficient utilisation of lignocellulosic materials. *Biotechnology for Biofuels*, 12:294, 2019. doi: 10.1186/s13068-019-1634-1.

[53] H. W. Blanch, B. A. Simmons, and D. Klein-Marcuschamer. Biomass deconstruction to sugars. *Biotechnology Journal*, 6(9):1086–1102, 2011. doi: 10.1002/biot.201000180.

[54] A. T. W. M. Hendriks and G. Zeeman. Pretreatments to enhance the digestibility of lignocellulosic biomass. *Bioresource Technology*, 100(1):10–18, 2009. doi: 10.1016/j.biortech.2008.05.027.

[55] X. Zhao, K. Cheng, and D. Liu. Organosolv pretreatment of lignocellulosic biomass for enzymatic hydrolysis. *Applied Microbiology and Biotechnology*, 82 (5):815–827, 2009. doi: 10.1007/s00253-009-1883-1.

[56] X. Zhao, S. Li, R. Wu, D. Liu, and R. Wu. Organosolv fractionating pretreatment of lignocellulosic biomass for efficient enzymatic saccharification: chemistry, kinetics, and substrate structures. *Biofuels, Bioproducts and Biorefining*, 11(3):567–590, 2017. doi: 10.1002/bbb.1768.

[57] A. Brandt, J. Gräsvik, J. P. Hallett, and T. Welton. Deconstruction of lignocellulosic biomass with ionic liquids. *Green Chemistry*, 15(3):550–583, 2013. doi: 10.1039/c2gc36364j.

[58] J. S. Kim, Y. Y. Lee, and T. H. Kim. A review on alkaline pretreatment technology for bioconversion of lignocellulosic biomass. *Bioresource Technology*, 199:42–48, 2016. doi: 10.1016/j.biortech.2015.08.085.

[59] E. B. Heggset, K. Syverud, and K. Øyaas. Novel pretreatment pathways for dissolution of lignocellulosic biomass based on ionic liquid and low temperature alkaline treatment. *Biomass and Bioenergy*, 93:194–200, 2016. doi: 10.1016/j.biombioe.2016.07.023.

[60] Y. Zhao, Y. Wang, J. Y. Zhu, A. Ragauskas, and Y. Deng. Enhanced enzymatic hydrolysis of spruce by alkaline pretreatment at low temperature. *Biotechnology and Bioengineering*, 99(6):1320–1328, 2008. doi: 10.1002/bit.21712.

[61] T. Budtova and P. Navard. Cellulose in NaOH–water based solvents: a review. *Cellulose*, 23(1):5–55, 2016. doi: 10.1007/s10570-015-0779-8.

[62] L. J. Jönsson, B. Alriksson, and N.-O. Nilvebrant. Bioconversion of lignocellulose: inhibitors and detoxification. *Biotechnology for Biofuels*, 6:16, 2013. doi: 10.1186/1754-6834-6-16.

[63] K. Ulonska, A. Voll, and W. Marquardt. Screening pathways for the production of next generation biofuels. *Energy & Fuels*, 30(1):445–456, 2016. doi: 10.1021/acs.energyfuels.5b02460.

[64] J. Zakzeski, P. C. A. Bruijnincx, A. L. Jongerius, and B. M. Weckhuysen. The catalytic valorization of lignin for the production of renewable chemicals. *Chemical Reviews*, 110(6):3552–3599, 2010. doi: 10.1021/cr900354u.

[65] D. Klein-Marcuschamer, B. A. Simmons, and H. W. Blanch. Techno-economic analysis of a lignocellulosic ethanol biorefinery with ionic liquid pre-treatment. *Biofuels, Bioproducts and Biorefining*, 5(5):562–569, 2011. doi: 10.1002/bbb.303.

[66] J. Viell, A. Harwardt, J. Seiler, and W. Marquardt. Is biomass fractionation by organosolv-like processes economically viable? A conceptual design study. *Bioresource Technology*, 150:89–97, 2013. doi: 10.1016/j.biortech.2013.09.078.

[67] M. Nieder-Heitmann, K. Haigh, J. Louw, and J. F. Görgens. Economic evaluation and comparison of succinic acid and electricity co–production from sugarcane bagasse and trash lignocelluloses in a biorefinery, using different pretreatment methods: dilute acid (H_2SO_4), alkaline (NaOH), organosolv, ammonia

fibre expansion (AFEX™), steam explosion (STEX), and wet oxidation. *Biofuels, Bioproducts and Biorefining*, 14(1):55–77, 2020. doi: 10.1002/bbb.2020.

[68] D. Humbird, R. Davis, L. Tao, C. Kinchin, D. Hsu, A. Aden, P. Schoen, J. Lukas, B. Olthof, M. Worley, D. Sexton, and D. Dudgeon. Process design and economics for biochemical conversion of lignocellulosic biomass to ethanol: dilute-acid pretreatment and enzymatic hydrolysis of corn stover. Technical Report NREL/TP-5100-47764, National Renewable Energy Laboratory, Golden, Colorado, May 2011. URL `https://www.nrel.gov/docs/fy11osti/47764.pdf`. Accessed May 28, 2019.

[69] E. Johnson. Integrated enzyme production lowers the cost of cellulosic ethanol. *Biofuels, Bioproducts and Biorefining*, 10(2):164–174, 2016. doi: 10.1002/bbb.1634.

[70] L. Tao, E. C. D. Tan, A. Aden, and R. T. Elander. Techno-economic analysis and life-cycle assessment of lignocellulosic biomass to sugars using various pretreatment technologies. In S.-Y. Ding, J. D. Peterson, and J. Sun, editors, *Biological conversion of biomass for fuels and chemicals*, RSC energy and environment series, pages 358–380. RSC Publishing, London, 2014. ISBN 978-1-84973-424-0.

[71] D. M. Alonso, S. H. Hakim, S. Zhou, W. Won, O. Hosseinaei, J. Tao, V. Garcia-Negron, A. H. Motagamwala, M. A. Mellmer, K. Huang, C. J. Houtman, N. Labbe, D. P. Harper, C. Maravelias, T. Runge, and J. A. Dumesic. Increasing the revenue from lignocellulosic biomass: maximizing feedstock utilization. *Science Advances*, 3(5):e1603301, 2017. doi: 10.1126/sciadv.1603301.

[72] H. Sixta, editor. *Handbook of pulp*. Wiley-VCH, Weinheim, 2. repr edition, 2006. ISBN 3-527-30999-3.

[73] A. Wingren, M. Galbe, and G. Zacchi. Techno-economic evaluation of producing ethanol from softwood: comparison of SSF and SHF and identification of bottlenecks. *Biotechnology Progress*, 19(4):1109–1117, 2003. doi: 10.1021/bp0340180.

[74] A. R. G. da Silva, A. Giuliano, M. Errico, B.-G. Rong, and D. Barletta. Economic value and environmental impact analysis of lignocellulosic ethanol production: assessment of different pretreatment processes. *Clean Technologies and Environmental Policy*, 16(4):637–654, 2019. doi: 10.1007/s10098-018-01663-z.

[75] L. Tao, X. Chen, A. Aden, E. Kuhn, M. E. Himmel, M. Tucker, M. A. A. Franden, M. Zhang, D. K. Johnson, N. Dowe, and R. T. Elander. Improved

ethanol yield and reduced minimum ethanol selling price (MESP) by modifying low severity dilute acid pretreatment with deacetylation and mechanical refining: 2) techno-economic analysis. *Biotechnology for Biofuels*, 5:69, 2012. doi: 10.1186/1754-6834-5-69.

[76] D. J. Hayes, S. Fitzpatrick, M. H. B. Hayes, and J. R. H. Ross. The Biofine process - production of levulinic acid, furfural, and formic acid from llignocellulosic feedstocks. In B. Kamm, P. Gruber, and M. Kamm, editors, *Biorefineries - industrial processes and products*, pages 139–164. Wiley-VCH, Weinheim, 2005. ISBN 3-527-31027-4.

[77] B. E. Dale and R. G. Ong. Energy, wealth, and human development: why and how biomass pretreatment research must improve. *Biotechnology Progress*, 28 (4):893–898, 2012. doi: 10.1002/btpr.1575.

[78] T. Eggeman and R. T. Elander. Process and economic analysis of pretreatment technologies. *Bioresource Technology*, 96(18):2019–2025, 2005. doi: 10.1016/j.biortech.2005.01.017.

[79] M. Fahmy, M. I. Sohel, A. A. Vaidya, M. W. Jack, and I. D. Suckling. Does sugar yield drive lignocellulosic sugar cost? Case study for enzymatic hydrolysis of softwood with added polyethylene glycol. *Process Biochemistry*, 80:103–111, 2019. doi: 10.1016/j.procbio.2019.02.004.

[80] R. Wagenführ. *Holzatlas*. Hanser Fachbuchverlag, Leipzig, 6th edition, 2007. ISBN 978-3-446-40649-0.

[81] D. Fengel and G. Wegener. *Wood: chemistry, ultrastructure, reactions*. Walter de Gruyter & Co., Berlin and New York, paperback edition, 1989. ISBN 3-11-012059-3.

[82] G. Koch and G. Kleist. Application of scanning UV microspectrophotometry to localise lignins and phenolic extractives in plant cell walls. *Holzforschung*, 55 (6):563–567, 2001. doi: 10.1515/HF.2001.091.

[83] J. Fahlén and L. Salmén. Pore and matrix distribution in the fiber wall revealed by atomic force microscopy and image analysis. *Biomacromolecules*, 6(1):433–438, 2005. doi: 10.1021/bm040068x.

[84] L. A. Donaldson, M. Cairns, and S. J. Hill. Comparison of micropore distribution in cell walls of softwood and hardwood xylem. *Plant Physiology*, 178(3):1142–1153, 2018. doi: 10.1104/pp.18.00883.

[85] M. Xie, J. Zhang, T. J. Tschaplinski, G. A. Tuskan, J.-G. Chen, and W. Muchero. Regulation of lignin biosynthesis and its role in growth-defense tradeoffs. *Frontiers in Plant Science*, 9:1427, 2018. doi: 10.3389/fpls.2018.01427.

[86] T. Timell, S. Y. Lin, and C. W. Dence, editors. *Methods in lignin chemistry*. Springer series in wood science. Springer, Berlin and New York, 1992. ISBN 3-540-50295-5.

[87] A. Björkman. Lignin and lignin-carbohydrate complexes. *Industrial & Engineering Chemistry*, 49(9):1395–1398, 1957. doi: 10.1021/ie50573a040.

[88] N. Giummarella, Y. Pu, A. J. Ragauskas, and M. Lawoko. A critical review on the analysis of lignin carbohydrate bonds. *Green Chemistry*, 21(7):1573–1595, 2019. doi: 10.1039/C8GC03606C.

[89] M. Zeng, N. S. Mosier, C.-P. Huang, D. M. Sherman, and M. R. Ladisch. Microscopic examination of changes of plant cell structure in corn stover due to hot water pretreatment and enzymatic hydrolysis. *Biotechnology and Bioengineering*, 97(2):265–278, 2007. doi: 10.1002/bit.21298.

[90] Q. Zhang, P. Zhang, Z. J. Pei, and D. Wang. Relationships between cellulosic biomass particle size and enzymatic hydrolysis sugar yield: analysis of inconsistent reports in the literature. *Renewable Energy*, 60:127–136, 2013. doi: 10.1016/j.renene.2013.04.012.

[91] M. Yang, M. Xu, Y. Nan, S. Kuittinen, K. Hassan, J. Vepsäläinen, D. Xin, J. Zhang, and A. Pappinen. Influence of size reduction treatments on sugar recovery from Norway spruce for butanol production. *Bioresource Technology*, 257:113–120, 2018. doi: 10.1016/j.biortech.2018.02.072.

[92] J. Y. Zhu and X. J. Pan. Woody biomass pretreatment for cellulosic ethanol production: technology and energy consumption evaluation. *Bioresource Technology*, 101(13):4992–5002, 2010. doi: 10.1016/j.biortech.2009.11.007.

[93] M. T. Holtzapple, A. E. Humphrey, and J. D. Taylor. Energy requirements for the size reduction of poplar and aspen wood. *Biotechnology and Bioengineering*, 33(2):207–210, 1989. doi: 10.1002/bit.260330210.

[94] G. I. Mantanis, R. A. Young, and R. M. Rowell. Swelling of wood. Part II. Swelling in organic liquids. *Holzforschung*, 48(6):480–490, 1994. doi: 10.1515/hfsg.1994.48.6.480.

[95] T. N. Kleinert. Short note. Ethanol-water deglinification of sizeable pieces of wood. Disintegration into stringlike fiber bundles. *Holzforschung*, 29(3):107–109, 1975. doi: 10.1515/hfsg.1975.29.3.107.

[96] X. Zhang, J. Ma, Z. Ji, G.-H. Yang, X. Zhou, and F. Xu. Using confocal Raman microscopy to real-time monitor poplar cell wall swelling and dissolution during ionic liquid pretreatment. *Microscopy Research and Technique*, 77(8):609–618, 2014. doi: 10.1002/jemt.22379.

[97] P. Meier, T. Kaps, and U. Kallavus. Swelling of pinewood (*Pinus Sylvestris*) in binary aqueous solutions of organic substances. *Materials Science (Medžiagotyra)*, 11(2):140–145, 2005.

[98] A. Brandt, J. P. Hallett, D. J. Leak, R. J. Murphy, and T. Welton. The effect of the ionic liquid anion in the pretreatment of pine wood chips. *Green Chemistry*, 12(4):672–679, 2010. doi: 10.1039/b918787a.

[99] H. Miyafuji and N. Suzuki. Morphological changes in sugi (*Cryptomeria japonica*) wood after treatment with the ionic liquid, 1-ethyl-3-methylimidazolium chloride. *Journal of Wood Science*, 58(3):222–230, 2012. doi: 10.1007/s10086-011-1245-3.

[100] Z. Zhang, D. W. Rackemann, W. O. S. Doherty, and I. M. O'Hara. Glycerol carbonate as green solvent for pretreatment of sugarcane bagasse. *Biotechnology for Biofuels*, 6:153, 2013. doi: 10.1186/1754-6834-6-153.

[101] J. Xu, M.-H. Zong, S.-Y. Fu, and N. Li. Correlation between physicochemical properties and enzymatic digestibility of rice straw pretreated with cholinium ionic liquids. *ACS Sustainable Chemistry & Engineering*, 4(8):4340–4345, 2016. doi: 10.1021/acssuschemeng.6b00860.

[102] L. Paszner and N. C. Behera. Topochemistry of softwood delignification by alkali earth metal salt catalysed organosolv pulping. *Holzforschung*, 43(3):159–168, 1989. doi: 10.1515/hfsg.1989.43.3.159.

[103] D. Yawalata and L. Paszner. Cationic effect in high concentration alcohol organosolv pulping: the next generation biorefinery. *Holzforschung*, 58(1):7–13, 2004. doi: 10.1515/HF.2004.002.

[104] K. M. Torr, K. T. Love, B. A. Simmons, and S. J. Hill. Structural features affecting the enzymatic digestibility of pine wood pretreated with ionic liq-

uids. *Biotechnology and Bioengineering*, 113(3):540–549, 2016. doi: 10.1002/bit.25831.

[105] D. Yawalata and L. Paszner. Characteristics of NAEM salt-catalyzed alcohol organosolv pulping as a biorefinery. *Holzforschung*, 60(3):239–244, 2006. doi: 10.1515/HF.2006.039.

[106] J. Viell and W. Marquardt. Disintegration and dissolution kinetics of wood chips in ionic liquids. *Holzforschung*, 65(4):519–525, 2011. doi: 10.1515/HF.2011.072.

[107] J. Viell, H. Wulfhorst, T. Schmidt, U. Commandeur, R. Fischer, A. Spiess, and W. Marquardt. An efficient process for the saccharification of wood chips by combined ionic liquid pretreatment and enzymatic hydrolysis. *Bioresource Technology*, 146:144–151, 2013. doi: 10.1016/j.biortech.2013.07.059.

[108] H. E. Grethlein. The effect of pore size distribution on the rate of enzymatic hydrolysis of cellulosic substrates. *Bio/Technology*, 3(2):155–160, 1985. doi: 10.1038/nbt0285-155.

[109] N. D. Weiss, L. G. Thygesen, C. Felby, C. Roslander, and K. Gourlay. Biomass-water interactions correlate to recalcitrance and are intensified by pretreatment: an investigation of water constraint and retention in pretreated spruce using low field NMR and water retention value techniques. *Biotechnology Progress*, 33(1): 146–153, 2017. doi: 10.1002/btpr.2398.

[110] M. J. Selig, L. G. Thygesen, and C. Felby. Correlating the ability of lignocellulosic polymers to constrain water with the potential to inhibit cellulose saccharification. *Biotechnology for Biofuels*, 7(1):159, 2014. doi: 10.1186/s13068-014-0159-x.

[111] D. L. Williams and D. B. Hodge. Impacts of delignification and hot water pretreatment on the water induced cell wall swelling behavior of grasses and its relation to cellulolytic enzyme hydrolysis and binding. *Cellulose*, 21(1):221–235, 2014. doi: 10.1007/s10570-013-0149-3.

[112] M. Suchy, E. Kontturi, and T. Vuorinen. Impact of drying on wood ultrastructure: similarities in cell wall alteration between native wood and isolated wood-based fibers. *Biomacromolecules*, 11(8):2161–2168, 2010. doi: 10.1021/bm100547n.

[113] J. M. B. Fernandes Diniz, M. H. Gil, and J. A. A. M. Castro. Hornification–its origin and interpretation in wood pulps. *Wood Science and Technology*, 37(6): 489–494, 2004. doi: 10.1007/s00226-003-0216-2.

[114] M. Suchy, J. Virtanen, E. Kontturi, and T. Vuorinen. Impact of drying on wood ultrastructure observed by deuterium exchange and photoacoustic FT-IR spectroscopy. *Biomacromolecules*, 11(2):515–520, 2010. doi: 10.1021/bm901268j.

[115] M. J. Selig, N. D. Weiss, and Y. Ji. Enzymatic saccharification of lignocellulosic biomass: laboratory analytical procedure (LAP). Technical Report NREL/TP-510-42629, National Renewable Energy Laboratory, Golden, Colorado, March 2008.

[116] M. Abe, T. Yamada, and H. Ohno. Dissolution of wet wood biomass without heating. *RSC Advances*, 4(33):17136–17140, 2014. doi: 10.1039/c4ra01038h.

[117] I. Kilpeläinen, H. Xie, A. King, M. Granstrom, S. Heikkinen, and D. S. Argyropoulos. Dissolution of wood in ionic liquids. *Journal of Agricultural and Food Chemistry*, 55(22):9142–9148, 2007. doi: 10.1021/jf071692e.

[118] N. Sun, M. Rahman, Y. Qin, M. L. Maxim, H. Rodríguez, and R. D. Rogers. Complete dissolution and partial delignification of wood in the ionic liquid 1-ethyl-3-methylimidazolium acetate. *Green Chemistry*, 11(5):646–655, 2009. doi: 10.1039/b822702k.

[119] D. A. Fort, R. C. Remsing, R. P. Swatloski, P. Moyna, G. Moyna, and R. D. Rogers. Can ionic liquids dissolve wood? Processing and analysis of lignocellulosic materials with 1-n-butyl-3-methylimidazolium chloride. *Green Chemistry*, 9(1):63–69, 2007. doi: 10.1039/b607614a.

[120] L. Kyllönen, A. Parviainen, S. Deb, M. Lawoko, M. Gorlov, I. Kilpeläinen, and A. W. T. King. On the solubility of wood in non-derivatising ionic liquids. *Green Chemistry*, 15(9):2374–2378, 2013. doi: 10.1039/c3gc41273c.

[121] S.-Y. Ding, Y.-S. Liu, Y. Zeng, M. E. Himmel, J. O. Baker, and E. A. Bayer. How does plant cell wall nanoscale architecture correlate with enzymatic digestiblity? *Science (Washington, DC, United States)*, 338(6110):1055–1060, 2012. doi: 10.1126/science.1227491.

[122] L. Zhu, J. P. O'Dwyer, V. S. Chang, C. B. Granda, and M. T. Holtzapple. Structural features affecting biomass enzymatic digestibility. *Bioresource Technology*, 99(9):3817–3828, 2008. doi: 10.1016/j.biortech.2007.07.033.

[123] V. S. Chang and M. T. Holtzapple. Fundamental factors affecting biomass enzymatic reactivity. *Applied Biochemistry and Biotechnology*, 84(1–9):5–37, 2000. doi: 10.1385/ABAB:84-86:1-9:5.

[124] F. Kong, C. R. Engler, and E. J. Soltes. Effects of cell-wall acetate, xylan backbone, and lignin on enzymatic hydrolysis of aspen wood. *Applied Biochemistry and Biotechnology*, 34(1):23–35, 1992.

[125] J. K. Saini, A. K. Patel, M. Adsul, and R. R. Singhania. Cellulase adsorption on lignin: a roadblock for economic hydrolysis of biomass. *Renewable Energy*, 98:29–42, 2016. doi: 10.1016/j.renene.2016.03.089.

[126] Y. Wang, N. Anders, and A. C. Spieß. Cellulase adsorption during the hydrolysis of organosolv- and organocat-pretreated beech wood. *Energy & Fuels*, 31(9): 9507–9516, 2017. doi: 10.1021/acs.energyfuels.7b01454.

[127] Y. Teramoto, S.-H. Lee, and T. Endo. Pretreatment of woody and herbaceous biomass for enzymatic saccharification using sulfuric acid-free ethanol cooking. *Bioresource Technology*, 99(18):8856–8863, 2008. doi: 10.1016/j.biortech.2008.04.049.

[128] M. Herbaut, A. Zoghlami, A. Habrant, X. Falourd, L. Foucat, B. Chabbert, and G. Paës. Multimodal analysis of pretreated biomass species highlights generic markers of lignocellulose recalcitrance. *Biotechnology for Biofuels*, 11:52, 2018. doi: 10.1186/s13068-018-1053-8.

[129] B. Yang and C. E. Wyman. Effect of xylan and lignin removal by batch and flowthrough pretreatment on the enzymatic digestibility of corn stover cellulose. *Biotechnology and Bioengineering*, 86(1):88–95, 2004. doi: 10.1002/bit.20043.

[130] A. Sluiter, B. Hames, R. Ruiz, C. Scarlata, J. Sluiter, D. Templeton, and D. Crocker. Determination of structural carbohydrates and lignin in biomass: laboratory analytical procedure (LAP). Technical Report NREL/TP-510-42618, National Renewable Energy Laboratory, Golden, Colorado, July 2011.

[131] TAPPI. T 222 om-02: acid-insoluble lignin in wood and pulp, June 2006.

[132] G. Koch, B. Rose, R. Patt, and O. Kordsachia. Topochemical investigations on delignification of *Picea abies* [L.] Karst. during alkaline sulfite (ASA) and bisulfite pulping by scanning UV microspectrophotometry. *Holzforschung*, 57 (6):611–618, 2003. doi: 10.1515/HF.2003.092.

[133] B. S. Donohoe, S. R. Decker, M. P. Tucker, M. E. Himmel, and T. B. Vinzant. Visualizing lignin coalescence and migration through maize cell walls following thermochemical pretreatment. *Biotechnology and Bioengineering*, 101(5):913–925, 2008. doi: 10.1002/bit.21959.

[134] W. Liu, W. Chen, Q. Hou, S. Wang, and F. Liu. Effects of combined pretreatment of dilute acid pre-extraction and chemical-assisted mechanical refining on enzymatic hydrolysis of lignocellulosic biomass. *RSC Advances*, 8(19):10207–10214, 2018. doi: 10.1039/C7RA12732D.

[135] F. Schütt, N. P. Haas, L. Dehne, G. Koch, R. Janzon, and B. Saake. Steam pretreatment for enzymatic hydrolysis of poplar wood: comparison of optimal conditions with and without SO_2 impregnation. *Holzforschung*, 67(1):9–17, 2013. doi: 10.1515/hf-2012-0076.

[136] M. J. Selig, S. Viamajala, S. R. Decker, M. P. Tucker, M. E. Himmel, and T. B. Vinzant. Deposition of lignin droplets produced during dilute acid pretreatment of maize stems retards enzymatic hydrolysis of cellulose. *Biotechnology Progress*, 23(6):1333–1339, 2007. doi: 10.1021/bp0702018.

[137] D. T. Balogh, A. Curvelo, and R. de Groote. Solvent effects on organosolv lignin from *Pinus caribaea hondurensis*. *Holzforschung*, 46(4):343–348, 1992. doi: 10.1515/hfsg.1992.46.4.343.

[138] G. Wan, Q. Zhang, M. Li, Z. Jia, C. Guo, B. Luo, S. Wang, and D. Min. How pseudo-lignin is generated during dilute sulfuric acid pretreatment. *Journal of Agricultural and Food Chemistry*, 67(36):10116–10125, 2019. doi: 10.1021/acs.jafc.9b02851.

[139] S. D. Shinde, X. Meng, R. Kumar, and A. J. Ragauskas. Recent advances in understanding the pseudo-lignin formation in a lignocellulosic biorefinery. *Green Chemistry*, 20(10):2192–2205, 2018. doi: 10.1039/c8gc00353j.

[140] A. A. Schmatz, A. M. Salazar-Bryam, J. Contiero, C. Sant'Anna, and M. Brienzo. Pseudo-lignin content decreased with hemicellulose and lignin removal, improving cellulose accessibility, and enzymatic digestibility. *BioEnergy Research*, 14(1):106–121, 2021. doi: 10.1007/s12155-020-10187-8.

[141] P. Ligero, A. Vega, and M. Bao. Acetosolv delignification of *Miscanthus sinensis* bark: influence of process variables. *Industrial Crops and Products*, 21(2):235–240, 2005. doi: 10.1016/j.indcrop.2004.04.006.

[142] R. Kumar, G. Mago, V. Balan, and C. E. Wyman. Physical and chemical characterizations of corn stover and poplar solids resulting from leading pretreatment technologies. *Bioresource Technology*, 100(17):3948–3962, 2009. doi: 10.1016/j.biortech.2009.01.075.

[143] J. Kruyeniski, P. J. Ferreira, M. d. G. Videira Sousa Carvalho, M. E. Vallejos, F. E. Felissia, and M. C. Area. Physical and chemical characteristics of pretreated slash pine sawdust influence its enzymatic hydrolysis. *Industrial Crops and Products*, 130:528–536, 2019. doi: 10.1016/j.indcrop.2018.12.075.

[144] G. Bali, X. Meng, J. I. Deneff, Q. Sun, and A. J. Ragauskas. The effect of alkaline pretreatment methods on cellulose structure and accessibility. *ChemSusChem*, 8(2):275–279, 2015. doi: 10.1002/cssc.201402752.

[145] X. Zhao, L. Zhang, and D. Liu. Biomass recalcitrance. Part I: the chemical compositions and physical structures affecting the enzymatic hydrolysis of lignocellulose. *Biofuels, Bioproducts and Biorefining*, 6(4):465–482, 2012. doi: 10.1002/bbb.1331.

[146] M. Francisco, A. van den Bruinhorst, and M. C. Kroon. New natural and renewable low transition temperature mixtures (LTTMs): screening as solvents for lignocellulosic biomass processing. *Green Chemistry*, 14(8):2153–2157, 2012. doi: 10.1039/c2gc35660k.

[147] R. Wahlström, J. Hiltunen, M. P. de Souza Nascente Sirkka, S. Vuoti, and K. Kruus. Comparison of three deep eutectic solvents and 1-ethyl-3-methylimidazolium acetate in the pretreatment of lignocellulose: effect on enzyme stability, lignocellulose digestibility and one-pot hydrolysis. *RSC Advances*, 6(72):68100–68110, 2016. doi: 10.1039/c6ra11719h.

[148] M. Hall, P. Bansal, J. H. Lee, M. J. Realff, and A. S. Bommarius. Cellulose crystallinity – a key predictor of the enzymatic hydrolysis rate. *FEBS Journal*, 277(6):1571–1582, 2010. doi: 10.1111/j.1742-4658.2010.07585.x.

[149] S. Park, J. O. Baker, M. E. Himmel, P. A. Parilla, and D. K. Johnson. Cellulose crystallinity index: measurement techniques and their impact on interpreting cellulase performance. *Biotechnology for Biofuels*, 3:10, 2010. doi: 10.1186/1754-6834-3-10.

[150] N. Karuna and T. Jeoh. The productive cellulase binding capacity of cellulosic substrates. *Biotechnology and Bioengineering*, 114(3):533–542, 2017. doi: 10.1002/bit.26193.

[151] J. Bragatto, F. Segato, J. Cota, D. B. Mello, M. M. Oliveira, M. S. Buckeridge, F. M. Squina, and C. Driemeier. Insights on how the activity of an endoglucanase is affected by physical properties of insoluble celluloses. *The Journal of Physical Chemistry B*, 116(21):6128–6136, 2012. doi: 10.1021/jp3021744.

[152] J. P. Olsen, B. S. Donohoe, K. Borch, P. Westh, and M. G. Resch. Interrelationships between cellulase activity and cellulose particle morphology. *Cellulose*, 23 (4):2349–2361, 2016. doi: 10.1007/s10570-016-0979-x.

[153] P. Bansal, B. J. Vowell, M. Hall, M. J. Realff, J. H. Lee, and A. S. Bommarius. Elucidation of cellulose accessibility, hydrolysability and reactivity as the major limitations in the enzymatic hydrolysis of cellulose. *Bioresource Technology*, 107:243–250, 2012. doi: 10.1016/j.biortech.2011.12.063.

[154] W. Jiang, H. Peng, H. Li, and J. Xu. Effect of acetylation/deacetylation on enzymatic hydrolysis of corn stalk. *Biomass and Bioenergy*, 71:294–298, 2014. doi: 10.1016/j.biombioe.2014.09.028.

[155] K. Grohmann, D. J. Mitchell, M. E. Himmel, B. E. Dale, and H. A. Schroeder. The role of ester groups in resistance of plant cell wall polysaccharides to enzymatic hydrolysis. *Applied Biochemistry and Biotechnology*, 20-21(1):45–61, 1989. doi: 10.1007/BF02936472.

[156] X. Chen, J. Shekiro, M. A. Franden, W. Wang, M. Zhang, E. Kuhn, D. K. Johnson, and M. P. Tucker. The impacts of deacetylation prior to dilute acid pretreatment on the bioethanol process. *Biotechnology for Biofuels*, 5:8, 2012. doi: 10.1186/1754-6834-5-8.

[157] X. Pan, N. Gilkes, and J. N. Saddler. Effect of acetyl groups on enzymatic hydrolysis of cellulosic substrates. *Holzforschung*, 60(4):398–401, 2006. doi: 10.1515/HF.2006.062.

[158] D. B. Hodge, M. N. Karim, D. J. Schell, and J. D. McMillan. Soluble and insoluble solids contributions to high-solids enzymatic hydrolysis of lignocellulose. *Bioresource Technology*, 99(18):8940–8948, 2008. doi: 10.1016/j.biortech.2008.05.015.

[159] Y. Kim, E. Ximenes, N. S. Mosier, and M. R. Ladisch. Soluble inhibitors/deactivators of cellulase enzymes from lignocellulosic biomass. *Enzyme and Microbial Technology*, 48(4-5):408–415, 2011. doi: 10.1016/j.enzmictec.2011.01.007.

[160] M. Cantarella, L. Cantarella, A. Gallifuoco, A. Spera, and F. Alfani. Effect of inhibitors released during steam-explosion treatment of poplar wood on subsequent enzymatic hydrolysis and SSF. *Biotechnology Progress*, 20(1):200–206, 2004. doi: 10.1021/bp0257978.

[161] K. E. Vroom. The "H" factor: a means of expressing cooking times and temperatures as a single variable. *Pulp & Paper Magazine of Canada*, 58(3):228–231, 1957.

[162] D. J. Brasch and K. W. Free. Prehydrolysis-kraft pulping of *Pinus radiata* grown in New Zealand. *Tappi*, 48(4):245–248, 1965.

[163] R. P. Overend, E. Chornet, and J. A. Gascoigne. Fractionation of lignocellulosics by steam-aqueous pretreatments. *Philosophical Transactions of the Royal Society, A: Mathematical, Physical & Engineering Sciences*, 321(1561):523–536, 1987. doi: 10.1098/rsta.1987.0029.

[164] H. L. Chum, D. K. Johnson, S. K. Black, and R. P. Overend. Pretreatment-catalyst effects and the combined severity parameter. *Applied Biochemistry and Biotechnology*, 24(1):1–14, 1990. doi: 10.1007/BF02920229.

[165] N. Abatzoglou, E. Chornet, K. Belkacemi, and R. P. Overend. Phenomenological kinetics of complex systems: the development of a generalized severity parameter and its application to lignocellulosics fractionation. *Chemical Engineering Science*, 47(5):1109–1122, 1992. doi: 10.1016/0009-2509(92)80235-5.

[166] L. P. Hammett and A. J. Deyrup. A series of simple basic indicators. I. The acidity function of mixtures of sulfuric and perchloric acids with water. *Journal of the American Chemical Society*, 54(7):2721–2739, 1932. doi: 10.1021/ja01346a015.

[167] M. J. Kamlet, J.-L. M. Abboud, and R. W. Taft. An examination of linear solvation energy relationships. In R. W. Taft, editor, *Progress in physical organic chemistry*, pages 485–630. Wiley, New York, 1981. ISBN 0-471-06253-7.

[168] M. J. Kamlet, J.-L. M. Abboud, M. H. Abraham, and R. W. Taft. Linear solvation energy relationships. 23. A comprehensive collection of the solvatochromic parameters, π^*, α, and β, and some methods for simplifying the generalized solvatochromic equation. *The Journal of Organic Chemistry*, 48(17):2877–2887, 1983. doi: 10.1021/jo00165a018.

[169] J. H. Hildebrand and R. L. Scott. *The solubility of nonelectrolytes*. Reinhold Publishing Corporation, New York, 3rd edition, 1950.

[170] A. F. Barton. *CRC Handbook of solubility parameters and other cohesion parameters*. CRC Press LLC, Boca Raton, 2nd edition, 1991. ISBN 0-8493-0176-9.

[171] R. F. Fedors. A method for estimating both the solubility parameters and molar volumes of liquids. *Polymer Engineering and Science*, 14(2):147–154, 1974. doi: 10.1002/pen.760140211.

[172] C. M. Hansen. The universality of the solubility parameter. *Industrial & Engineering Chemistry Product Research and Development*, 8(1):2–11, 1969. doi: 10.1021/i360029a002.

[173] S. Abbott. HSP and temperature, 2020. URL `https://www.hansen-solubility.com/HSP-science/HSP-T.php`. Accessed May 1, 2020.

[174] G. Garrote, H. Domínguez, and J. C. Parajó. Interpretation of deacetylation and hemicellulose hydrolysis during hydrothermal treatments on the basis of the severity factor. *Process Biochemistry*, 37(10):1067–1073, 2002. doi: 10.1016/S0032-9592(01)00315-6.

[175] C. S. Goh, H. T. Tan, K. T. Lee, and N. Brosse. Evaluation and optimization of organosolv pretreatment using combined severity factors and response surface methodology. *Biomass and Bioenergy*, 35(9):4025–4033, 2011. doi: 10.1016/j.biombioe.2011.06.034.

[176] M. Pedersen and A. S. Meyer. Lignocellulose pretreatment severity – relating pH to biomatrix opening. *New Biotechnology*, 27(6):739–750, 2010. doi: 10.1016/j.nbt.2010.05.003.

[177] D. Fărcaşiu and A. Ghenciu. Determination of acidity functions and acid strengths by ^{13}C NMR. *Progress in Nuclear Magnetic Resonance Spectroscopy*, 29(3-4):129–168, 1996. doi: 10.1016/S0079-6565(96)01032-1.

[178] L. B. Malihan, G. M. Nisola, N. Mittal, J. G. Seo, and W.-J. Chung. Blended ionic liquid systems for macroalgae pretreatment. *Renewable Energy*, 66:596–604, 2014. doi: 10.1016/j.renene.2014.01.003.

[179] G. F. de Gregorio, C. C. Weber, J. Gräsvik, T. Welton, A. Brandt, and J. P. Hallett. Mechanistic insights into lignin depolymerisation in acidic ionic liquids. *Green Chemistry*, 18(20):5456–5465, 2016. doi: 10.1039/C6GC01295G.

[180] B. J. Cox, S. Jia, Z. C. Zhang, and J. G. Ekerdt. Catalytic degradation of lignin model compounds in acidic imidazolium based ionic liquids: Hammett acidity and anion effects. *Polymer Degradation and Stability*, 96(4):426–431, 2011. doi: 10.1016/j.polymdegradstab.2011.01.011.

[181] P. G. Jessop, D. A. Jessop, D. Fu, and L. Phan. Solvatochromic parameters for solvents of interest in green chemistry. *Green Chemistry*, 14(5):1245–1259, 2012. doi: 10.1039/c2gc16670d.

[182] S. Ding, L.-g. Wei, K.-l. Li, and Y.-c. Ma. Solvatochromic parameters and preferential solvation behavior for binary mixtures of 1,3-dialkylimidazolium ionic liquids with water. *Chinese Journal of Chemical Physics*, 29(4):497–507, 2016. doi: 10.1063/1674-0068/29/cjcp1601003.

[183] A. Pandey and S. Pandey. Solvatochromic probe behavior within choline chloride-based deep eutectic solvents: effect of temperature and water. *The Journal of Physical Chemistry B*, 118(50):14652–14661, 2014. doi: 10.1021/jp510420h.

[184] L. K. J. Hauru, M. Hummel, A. W. T. King, I. Kilpeläinen, and H. Sixta. Role of solvent parameters in the regeneration of cellulose from ionic liquid solutions. *Biomacromolecules*, 13(9):2896–2905, 2012. doi: 10.1021/bm300912y.

[185] A. Xu, J. Wang, and H. Wang. Effects of anionic structure and lithium salts addition on the dissolution of cellulose in 1-butyl-3-methylimidazolium-based ionic liquid solvent systems. *Green Chemistry*, 12(2):268–275, 2010. doi: 10.1039/b916882f.

[186] S. Xia, G. A. Baker, H. Li, S. Ravula, and H. Zhao. Aqueous ionic liquids and deep eutectic solvents for cellulosic biomass pretreatment and saccharification. *RSC Advances*, 4(21):10586–10596, 2014. doi: 10.1039/c3ra46149a.

[187] M. Abe, K. Kuroda, D. Sato, H. Kunimura, and H. Ohno. Effects of polarity, hydrophobicity, and density of ionic liquids on cellulose solubility. *Physical Chemistry Chemical Physics*, 17(48):32276–32282, 2015. doi: 10.1039/c5cp05808b.

[188] A. Roselli, M. Hummel, J. Vartiainen, K. Nieminen, and H. Sixta. Understanding the role of water in the interaction of ionic liquids with wood polymers. *Carbohydrate Polymers*, 168:121–128, 2017. doi: 10.1016/j.carbpol.2017.03.013.

[189] J. Catalán. Toward a generalized treatment of the solvent effect based on four empirical scales: dipolarity (SdP, a new scale), polarizability (SP), acidity (SA),

and basicity (SB) of the medium. *The Journal of Physical Chemistry B*, 113 (17):5951–5960, 2009. doi: 10.1021/jp8095727.

[190] A. Schade, N. Behme, and S. Spange. Dipolarity versus polarizability and acidity versus basicity of ionic liquids as a function of their molecular structures. *Chemistry – A European Journal*, 20(8):2232–2243, 2014. doi: 10.1002/chem.201304069.

[191] C. Schuerch. The solvent properties of liquids and their relation to the solubility, swelling, isolation and fractionation of lignin. *Journal of the American Chemical Society*, 74(20):5061–5067, 1952. doi: 10.1021/ja01140a020.

[192] P. Weerachanchai, S. K. Kwak, and J.-M. Lee. Effects of solubility properties of solvents and biomass on biomass pretreatment. *Bioresource Technology*, 170: 160–166, 2014. doi: 10.1016/j.biortech.2014.07.057.

[193] Y. Ni and A. R. P. van Heiningen. The swelling of pulp fibers derived from the ethanol-based organosolv process. *Tappi Journal*, 80(1):211–213, 1997.

[194] C. M. Hansen and A. Björkman. The ultrastructure of wood from a solubility parameter point of view. *Holzforschung*, 52(4):335–344, 1998. doi: 10.1515/hfsg.1998.52.4.335.

[195] H. Yu, J. Hu, and J. Chang. Selective separation of wood components based on Hansen's theory of solubility. *Industrial & Engineering Chemistry Research*, 50 (12):7513–7519, 2011. doi: 10.1021/ie102443p.

[196] Q. Zhang, X. Tan, W. Wang, Q. Yu, Q. Wang, C. Miao, Y. Guo, X. Zhuang, and Z. Yuan. Screening solvents based on Hansen solubility parameter theory to depolymerize lignocellulosic biomass efficiently under low temperature. *ACS Sustainable Chemistry & Engineering*, 7(9):8678–8686, 2019. doi: 10.1021/acssuschemeng.9b00494.

[197] L. P. Novo and A. A. S. Curvelo. Hansen solubility parameters: a tool for solvent selection for organosolv delignification. *Industrial & Engineering Chemistry Research*, 58(31):14520–14527, 2019. doi: 10.1021/acs.iecr.9b00875.

[198] R. Rinaldi and J. Reece. Solution-based deconstruction of (ligno)-cellulose. In M. Behrens and A. K. Datye, editors, *Catalysis for the conversion of biomass and its derivatives*, Max Planck research library for the history and development of knowledge, pages 435–462. Edition Open Access, Berlin, 2017. ISBN 978-3-945561-19-5.

[199] Y. Marcus. The properties of organic liquids that are relevant to their use as solvating solvents. *Chemical Society Reviews*, 22(6):409–416, 1993. doi: 10.1039/CS9932200409.

[200] F. Xu, J.-X. Sun, R. Sun, P. Fowler, and M. S. Baird. Comparative study of organosolv lignins from wheat straw. *Industrial Crops and Products*, 23(2): 180–193, 2006. doi: 10.1016/j.indcrop.2005.05.008.

[201] B. D. Rabideau, A. Agarwal, and A. E. Ismail. The role of the cation in the solvation of cellulose by imidazolium-based ionic liquids. *The Journal of Physical Chemistry B*, 118(6):1621–1629, 2014. doi: 10.1021/jp4115755.

[202] B. Lu, A. Xu, and J. Wang. Cation does matter: how cationic structure affects the dissolution of cellulose in ionic liquids. *Green Chemistry*, 16(3):1326–1335, 2014. doi: 10.1039/c3gc41733f.

[203] M. T. Clough, K. Geyer, P. A. Hunt, S. Son, U. Vagt, and T. Welton. Ionic liquids: not always innocent solvents for cellulose. *Green Chemistry*, 17(1): 231–243, 2015. doi: 10.1039/c4gc01955e.

[204] G. Ebner, S. Schiehser, A. Potthast, and T. Rosenau. Side reaction of cellulose with common 1-alkyl-3-methylimidazolium-based ionic liquids. *Tetrahedron Letters*, 49(51):7322–7324, 2008. doi: 10.1016/j.tetlet.2008.10.052.

[205] S. P. S. Chundawat, L. da Costa Sousa, S. Roy, Z. Yang, S. Gupta, R. Pal, C. Zhao, S.-H. Liu, L. Petridis, H. O'Neill, and S. V. Pingali. Ammonia-salt solvent promotes cellulosic biomass deconstruction under ambient pretreatment conditions to enable rapid soluble sugar production at ultra-low enzyme loadings. *Green Chemistry*, 22(1):204–218, 2020. doi: 10.1039/C9GC03524A.

[206] M. Kostag, T. Liebert, and T. Heinze. Acetone-based cellulose solvent. *Macromolecular Rapid Communications*, 35(16):1419–1422, 2014. doi: 10.1002/marc.201400211.

[207] Z. Jiang, J. Fan, V. L. Budarin, D. J. Macquarrie, Y. Gao, T. Li, C. Hu, and J. H. Clark. Mechanistic understanding of salt-assisted autocatalytic hydrolysis of cellulose. *Sustainable Energy & Fuels*, 2(5):936–940, 2018. doi: 10.1039/C8SE00045J.

[208] T. vom Stein, P. Grande, F. Sibilla, U. Commandeur, R. Fischer, W. Leitner, and P. Domínguez de María. Salt-assisted organic-acid-catalyzed de-

polymerization of cellulose. *Green Chemistry*, 12(10):1844–1849, 2010. doi: 10.1039/c0gc00262c.

[209] R. Rinaldi and F. Schüth. Acid hydrolysis of cellulose as the entry point into biorefinery schemes. *ChemSusChem*, 2(12):1096–1107, 2009. doi: 10.1002/cssc.200900188.

[210] D. Yawalata and L. Paszner. Anionic effect in high concentration alcohol organosolv pulping. *Holzforschung*, 58(1):1–6, 2004. doi: 10.1515/HF.2004.001.

[211] P. Grande. *Novel bio-based catalytic strategies for the fractionation and valorization of lignocellulose*. Dissertation, RWTH Aachen University, Aachen, 2014. URL `https://publications.rwth-aachen.de/record/444720`.

[212] J. Liu, R. Takada, S. Karita, T. Watanabe, Y. Honda, and T. Watanabe. Microwave-assisted pretreatment of recalcitrant softwood in aqueous glycerol. *Bioresource Technology*, 101(23):9355–9360, 2010. doi: 10.1016/j.biortech.2010.07.023.

[213] M. A. Mellmer, C. Sener, J. M. R. Gallo, J. S. Luterbacher, D. M. Alonso, and J. A. Dumesic. Solvent effects in acid-catalyzed biomass conversion reactions. *Angewandte Chemie, International Edition*, 53(44):11872–11875, 2014. doi: 10.1002/anie.201408359.

[214] L. Vanoye, M. Fanselow, J. D. Holbrey, M. P. Atkins, and K. R. Seddon. Kinetic model for the hydrolysis of lignocellulosic biomass in the ionic liquid, 1-ethyl-3-methyl-imidazolium chloride. *Green Chemistry*, 11(3):390–396, 2009. doi: 10.1039/b817882h.

[215] C. Vila, V. Santos, and J. C. Parajó. Optimization of beech wood pulping in catalyzed acetic acid media. *The Canadian Journal of Chemical Engineering*, 78(5):964–973, 2000. doi: 10.1002/cjce.5450780514.

[216] Z. Kin. The acetolysis of beech wood. *Tappi Journal*, 73(11):237–238, 1990.

[217] T. Shui, S. Feng, Z. Yuan, T. Kuboki, and C. C. Xu. Highly efficient organosolv fractionation of cornstalk into cellulose and lignin in organic acids. *Bioresource Technology*, 218:953–961, 2016. doi: 10.1016/j.biortech.2016.07.054.

[218] J. Strassburger and J. L. Torgesen. A phase study of the system: oxalic acid/acetic acid/water; its significance in oxalic acid crystal growth. *Journal of Research of the National Bureau of Standards, Section A: physics and Chemistry*, 67A(4):347–350, 1963. doi: 10.6028/jres.067A.037.

[219] J. C. Parajó, J. L. Alonso, and D. Vázquez. On the behaviour of lignin and hemicelluloses during the acetosolv processing of wood. *Bioresource Technology*, 46(3):233–240, 1993. doi: 10.1016/0960-8524(93)90126-V.

[220] V. Mullangi, X. Zhou, D. W. Ball, D. J. Anderson, and M. Miyagi. Quantitative measurement of the solvent accessibility of histidine imidazole groups in proteins. *Biochemistry*, 51(36):7202–7208, 2012. doi: 10.1021/bi300911d.

[221] T. L. Amyes, S. T. Diver, J. P. Richard, F. M. Rivas, and K. Toth. Formation and stability of n-heterocyclic carbenes in water: the carbon acid pK_{a} of imidazolium cations in aqueous solution. *Journal of the American Chemical Society*, 126(13):4366–4374, 2004. doi: 10.1021/ja039890j.

[222] Y. Bai, Milne, John S., Mayne, Leland, and S. W. Englander. Primary structure effects on peptide group hydrogen exchange. *Proteins: Structure, Function, and Genetics*, 17:75–88, 1993. doi: 10.1002/prot.340170110.

[223] T. L. Amyes and J. P. Richard. Determination of the pK_{a} of ethyl acetate: Brønsted correlation for deprotonation of a simple oxygen ester in aqueous solution. *Journal of the American Chemical Society*, 118:3129–3141, 1996. doi: 10.1021/ja953664v.

[224] J. J. Allen, S. R. Bowser, and K. Damodaran. Molecular interactions in the ionic liquid emim acetate and water binary mixtures probed via NMR spin relaxation and exchange spectroscopy. *Physical Chemistry Chemical Physics*, 16(17):8078–8085, 2014. doi: 10.1039/c3cp55384a.

[225] I. Khan, K. A. Kurnia, F. Mutelet, S. P. Pinho, and J. A. P. Coutinho. Probing the interactions between ionic liquids and water: experimental and quantum chemical approach. *The Journal of Physical Chemistry B*, 118(7):1848–1860, 2014. doi: 10.1021/jp4113552.

[226] L. D. Simoni, J. F. Brennecke, and M. A. Stadtherr. Asymmetric framework for predicting liquid−liquid equilibrium of ionic liquid−mixed-solvent systems. 1. Theory, phase stability analysis, and parameter estimation. *Industrial & Engineering Chemistry Research*, 48(15):7246–7256, 2009. doi: 10.1021/ie900461j.

[227] Y. Zhang, H. Du, X. Qian, and E. Y.-X. Chen. Ionic liquid–water mixtures: enhanced K_{w} for efficient cellulosic biomass conversion. *Energy & Fuels*, 24(4): 2410–2417, 2010. doi: 10.1021/ef1000198.

[228] Y. Yasaka, C. Wakai, N. Matubayasi, and M. Nakahara. Slowdown of H/D exchange reaction rate and water dynamics in ionic liquids: deactivation of solitary water solvated by small anions in 1-butyl-3-methyl-imidazolium chloride. *The Journal of Physical Chemistry A*, 111(4):541–543, 2007. doi: 10.1021/jp0673720.

[229] A. Voll and W. Marquardt. Reaction network flux analysis: optimization-based evaluation of reaction pathways for biorenewables processing. *AIChE Journal*, 58(6):1788–1801, 2012. doi: 10.1002/aic.12704.

[230] K. Ulonska, M. Skiborowski, A. Mitsos, and J. Viell. Early-stage evaluation of biorefinery processing pathways using process network flux analysis. *AIChE Journal*, 62(9):3096–3108, 2016. doi: 10.1002/aic.15305.

[231] E. Christensen, A. Williams, S. Paul, S. Burton, and R. L. McCormick. Properties and performance of levulinate esters as diesel blend components. *Energy & Fuels*, 25(11):5422–5428, 2011. doi: 10.1021/ef201229j.

[232] GAMS Development Corporation. Gams - general algebraic modeling system v25.1.1, 2018. URL `www.gams.com`. Accessed May 28, 2019.

[233] M. R. Kılınç and N. V. Sahinidis. Exploiting integrality in the global optimization of mixed-integer nonlinear programming problems with baron. *Optimization, Methods and Software*, 33(3):540–562, 2017. doi: 10.1080/10556788.2017.1350178.

[234] M. Tawarmalani and N. V. Sahinidis. A polyhedral branch-and-cut approach to global optimization. *Mathematical Programming*, 103(2):225–249, 2005. doi: 10.1007/s10107-005-0581-8.

[235] L. Shuai, Y. M. Questell-Santiago, and J. S. Luterbacher. A mild biomass pretreatment using γ-valerolactone for concentrated sugar production. *Green Chemistry*, 18(4):937–943, 2016. doi: 10.1039/C5GC02489G.

[236] K. Przybysz Buzała, H. Kalinowska, P. Przybysz, and E. Małachowska. Conversion of various types of lignocellulosic biomass to fermentable sugars using kraft pulping and enzymatic hydrolysis. *Wood Science and Technology*, 51(4):873–885, 2017. doi: 10.1007/s00226-017-0916-7.

[237] C. K. Nitsos, K. A. Matis, and K. S. Triantafyllidis. Optimization of hydrothermal pretreatment of lignocellulosic biomass in the bioethanol production process. *ChemSusChem*, 6(1):110–122, 2013. doi: 10.1002/cssc.201200546.

[238] A. Smit and W. Huijgen. Effective fractionation of lignocellulose in herbaceous biomass and hardwood using a mild acetone organosolv process. *Green Chemistry*, 19(22):5505–5514, 2017. doi: 10.1039/C7GC02379K.

[239] T. Vom Stein, P. M. Grande, H. Kayser, F. Sibilla, W. Leitner, and P. Domínguez de María. From biomass to feedstock: one-step fractionation of lignocellulose components by the selective organic acid-catalyzed depolymerization of hemicellulose in a biphasic system. *Green Chemistry*, 13(7):1772–1777, 2011. doi: 10.1039/c1gc00002k.

[240] Z. Zhang, W. O. S. Doherty, and I. M. O'Hara. Integration of salt-induced phase separation with organosolv pretreatment for clean fractionation of lignocellulosic biomass. *ACS Sustainable Chemistry & Engineering*, 5(6):5284–5292, 2017. doi: 10.1021/acssuschemeng.7b00617.

[241] X. Zhao and D. Liu. Fractionating pretreatment of sugarcane bagasse by aqueous formic acid with direct recycle of spent liquor to increase cellulose digestibility–the Formiline process. *Bioresource Technology*, 117:25–32, 2012. doi: 10.1016/j.biortech.2012.04.062.

[242] S. Agnihotri, I. A. Johnsen, M. S. Bøe, K. Øyaas, and S. Moe. Ethanol organosolv pretreatment of softwood (*Picea abies*) and sugarcane bagasse for biofuel and biorefinery applications. *Wood Science and Technology*, 49(5):881–896, 2015. doi: 10.1007/s00226-015-0738-4.

[243] A. Berlin, C. Muñoz, N. Gilkes, S. M. Alamouti, P. Chung, K.-Y. Kang, V. Maximenko, J. Baeza, J. Freer, R. Mendonça, and J. Saddler. An evaluation of British Columbian beetle-killed hybrid spruce for bioethanol production. *Applied Biochemistry and Biotechnology*, 137-140(1-12):267–280, 2007. doi: 10.1007/s12010-007-9057-z.

[244] E. Araque, C. Parra, J. Freer, D. Contreras, J. Rodríguez, R. Mendonça, and J. Baeza. Evaluation of organosolv pretreatment for the conversion of *Pinus radiata* D. Don to ethanol. *Enzyme and Microbial Technology*, 43(2):214–219, 2008. doi: 10.1016/j.enzmictec.2007.08.006.

[245] X. Pan, D. Xie, R. W. Yu, and J. N. Saddler. The bioconversion of mountain pine beetle-killed lodgepole pine to fuel ethanol using the organosolv process. *Biotechnology and Bioengineering*, 101(1):39–48, 2008. doi: 10.1002/bit.21883.

[246] H. Amiri and K. Karimi. Improvement of acetone, butanol, and ethanol production from woody biomass using organosolv pretreatment. *Bioprocess and Biosystems Engineering*, 38(10):1959–1972, 2015. doi: 10.1007/s00449-015-1437-0.

[247] B.-W. Koo, H.-Y. Kim, N. Park, S.-M. Lee, H. Yeo, and I.-G. Choi. Organosolv pretreatment of *Liriodendron tulipifera* and simultaneous saccharification and fermentation for bioethanol production. *Biomass and Bioenergy*, 35(5):1833–1840, 2011. doi: 10.1016/j.biombioe.2011.01.014.

[248] R. P. Swatloski, S. K. Spear, J. D. Holbrey, and R. D. Rogers. Dissolution of cellose with ionic liquids. *Journal of the American Chemical Society*, 124(18): 4974–4975, 2002. doi: 10.1021/ja025790m.

[249] J. Viell. *A pretreatment process for wood based on ionic liquids*. Dissertation, Rheinisch Westfälische Technische Hochschule Aachen, Aachen, 2014.

[250] K. A. Le, C. Rudaz, and T. Budtova. Phase diagram, solubility limit and hydrodynamic properties of cellulose in binary solvents with ionic liquid. *Carbohydrate Polymers*, 105:237–243, 2014. doi: 10.1016/j.carbpol.2014.01.085.

[251] C. S. Lovell, A. Walker, R. A. Damion, A. Radhi, S. F. Tanner, T. Budtova, and M. E. Ries. Influence of cellulose on ion diffusivity in 1-ethyl-3-methylimidazolium acetate cellulose solutions. *Biomacromolecules*, 11(11):2927–2935, 2010. doi: 10.1021/bm1006807.

[252] M. Chen, F. Malaret, A. E. J. Firth, P. Verdía, A. R. Abouelela, Y. Chen, and J. P. Hallett. Design of a combined ionosolv-organosolv biomass fractionation process for biofuel production and high value-added lignin valorisation. *Green Chemistry*, 22(15):5161–5178, 2020. doi: 10.1039/D0GC01143F.

[253] J. van Spronsen, M. A. T. Cardoso, G.-J. Witkamp, W. de Jong, and M. C. Kroon. Separation and recovery of the constituents from lignocellulosic biomass by using ionic liquids and acetic acid as co-solvents for mild hydrolysis. *Chemical Engineering and Processing: Process Intensification*, 50(2):196–199, 2011. doi: 10.1016/j.cep.2010.12.010.

[254] F. J. V. Gschwend, J. P. Hallett, and A. Brandt-Talbot. Exploring the effect of water content and anion on the pretreatment of poplar with three 1-ethyl-3-methylimidazolium ionic liquids. *Molecules*, 25(10):2318, 2020. doi: 10.3390/molecules25102318.

[255] E. Brännvall. The limits of delignification in kraft cooking. *BioResources*, 12 (1):2081–2107, 2016. doi: 10.15376/biores.12.1.Brannvall.

[256] A. Xu, Y. Zhang, Y. Zhao, and J. Wang. Cellulose dissolution at ambient temperature: role of preferential solvation of cations of ionic liquids by a cosolvent. *Carbohydrate Polymers*, 92(1):540–544, 2013. doi: 10.1016/j.carbpol.2012.09.028.

[257] D. R. MacFarlane, A. L. Chong, M. Forsyth, M. Kar, R. Vijayaraghavan, A. Somers, and J. M. Pringle. New dimensions in salt–solvent mixtures: a 4th evolution of ionic liquids. *Faraday Discussions*, 206:9–28, 2018. doi: 10.1039/c7fd00189d.

[258] J. A. McCune, P. He, M. Petkovic, F. Coleman, J. Estager, J. D. Holbrey, K. R. Seddon, and M. Swadźba-Kwaśny. Brønsted acids in ionic liquids: how acidity depends on the liquid structure. *Physical Chemistry Chemical Physics*, 16(42): 23233–23243, 2014. doi: 10.1039/c4cp03217a.

[259] D. R. MacFarlane, J. M. Pringle, K. M. Johansson, S. A. Forsyth, and M. Forsyth. Lewis base ionic liquids. *Chemical Communications (Cambridge, United Kingdom)*, 18:1905–1917, 2006. doi: 10.1039/b516961p.

[260] T. Vilarino and M. E. S. de Vicente. Theoretical calculations of the ionic strength dependence of the ionic product of water based on a mean spherical approximation. *Journal of Solution Chemistry*, 26(9):833–846, 1997. doi: 10.1007/BF02768261.

[261] O. Hollóczki, D. Gerhard, K. Massone, L. Szarvas, B. Németh, T. Veszprémi, and L. Nyulászi. Carbenes in ionic liquids. *New Journal of Chemistry*, 34(12): 3004–3009, 2010. doi: 10.1039/c0nj00380h.

[262] M. Brehm, H. Weber, A. S. Pensado, A. Stark, and B. Kirchner. Proton transfer and polarity changes in ionic liquid–water mixtures: a perspective on hydrogen bonds from ab initio molecular dynamics at the example of 1-ethyl-3-methylimidazolium acetate–water mixtures—part 1. *Physical Chemistry Chemical Physics*, 14(15):5030–5044, 2012. doi: 10.1039/c2cp23983c.

[263] C. S. Baek, Y. J. Lee, S. J. Lee, H.-C. Kim, and S. W. Jeong. C2-functionalized 1,3-dialkylimidazolium ionic liquids for efficient cellulose dissolution. *Journal of Molecular Liquids*, 234:111–116, 2017. doi: 10.1016/j.molliq.2017.03.086.

[264] Y. Yoshimura, N. Hatano, T. Takekiyo, and H. Abe. Direct correlation between the H/D exchange reaction and conformational changes of the cation in imidazolium-based ionic liquid–D_2O mixtures. *Journal of Solution Chemistry*, 43(9–10):1509–1518, 2014. doi: 10.1007/s10953-014-0181-4.

[265] S. Cha, M. Ao, W. Sung, B. Moon, B. Ahlström, P. Johansson, Y. Ouchi, and D. Kim. Structures of ionic liquid–water mixtures investigated by IR and NMR spectroscopy. *Physical Chemistry Chemical Physics*, 16(20):9591–9601, 2014. doi: 10.1039/c4cp00589a.

[266] D. Rico Del Cerro, R. Mera-Adasme, A. W. T. King, J. E. Perea-Buceta, S. Heikkinen, T. Hase, D. Sundholm, and K. Wähälä. On the mechanism of the reactivity of 1,3-dialkylimidazolium salts under basic to acidic conditions: a combined kinetic and computational study. *Angewandte Chemie, International Edition*, 57(36):11613–11617, 2018. doi: 10.1002/anie.201805016.

[267] S. Ohta, A. Shimizu, Y. Imai, H. Abe, N. Hatano, and Y. Yoshimura. Peculiar concentration dependence of H/D exchange reaction in 1-butyl-3-methylimidazolium tetrafluoroborate-D_2O mixtures. *Open Journal of Physical Chemistry*, 1(3):70–76, 2011. doi: 10.4236/ojpc.2011.13010.

[268] Y. Horikawa and J. Sugiyama. Accessibility and size of *Valonia* cellulose microfibril studied by combined deuteration/rehydrogenation and FTIR technique. *Cellulose*, 15(3):419–424, 2008. doi: 10.1007/s10570-007-9187-z.

[269] D. Reishofer and S. Spirk. Deuterium and cellulose: a comprehensive review. In O. J. Rojas and S. Asaadi, editors, *Cellulose chemistry and properties*, volume 271 of *Advances in polymer science*, pages 93–114. Springer International Publishing, Cham, 2016. ISBN 978-3-319-26013-6. doi: 10.1007/12_2015_321.

[270] R. Pönni, L. Rautkari, C. A. S. Hill, and T. Vuorinen. Accessibility of hydroxyl groups in birch kraft pulps quantified by deuterium exchange in D_2O vapor. *Cellulose*, 21(3):1217–1226, 2014. doi: 10.1007/s10570-014-0166-x.

[271] Y. Hishikawa, E. Togawa, Y. Kataoka, and T. Kondo. Characterization of amorphous domains in cellulosic materials using a FTIR deuteration monitoring analysis. *Polymer*, 40(25):7117–7124, 1999. doi: 10.1016/S0032-3861(99)00120-2.

[272] M. Wahba. Kinetics of the deuteration of cellulose: an infrafred study with D_2O–H_2O vapours. *Chemica Scripta*, 11(4-5):158–163, 1977.

[273] Y. Chen, S. Li, Z. Xue, M. Hao, and T. Mu. Quantifying the hydrogen-bonding interaction between cation and anion of pure [EMIM][Ac] and evidencing the ion pairs existence in its extremely diluted water solution: via ^{13}C, ^{1}H, ^{15}N and 2D NMR. *Journal of Molecular Structure*, 1079:120–129, 2015. doi: 10.1016/j.molstruc.2014.09.023.

[274] C. A. Hall, K. A. Le, C. Rudaz, A. Radhi, C. S. Lovell, R. A. Damion, T. Budtova, and M. E. Ries. Macroscopic and microscopic study of 1-ethyl-3-methylimidazolium acetate–water mixtures. *The Journal of Physical Chemistry B*, 116 (42):12810–12818, 2012. doi: 10.1021/jp306829c.

[275] Y. Chen, Y. Cao, X. Sun, and T. Mu. Hydrogen bonding interaction between acetate-based ionic liquid 1-ethyl-3-methylimidazolium acetate and common solvents. *Journal of Molecular Liquids*, 190:151–158, 2014. doi: 10.1016/j.molliq.2013.11.010.

[276] J. L. Wong and J. H. Keck. Positional reactivities and mechanisms of deuteration of 1-methylimidazole in pD and -D_0 regions. Reinvestigation of the kinetics of 2-hydrogen exchange in imidazole. *The Journal of Organic Chemistry*, 39(16): 2398–2403, 1974. doi: 10.1021/jo00930a015.

[277] N. Hatano, M. Watanabe, T. Takekiyo, H. Abe, and Y. Yoshimura. Anomalous conformational change in 1-butyl-3-methylimidazolium tetrafluoroborate–D_2O mixtures. *The Journal of Physical Chemistry A*, 116(4):1208–1212, 2012. doi: 10.1021/jp2097873.

[278] Y. Chen, Y. Cao, Y. Zhang, and T. Mu. Hydrogen bonding between acetate-based ionic liquids and water: three types of IR absorption peaks and NMR chemical shifts change upon dilution. *Journal of Molecular Structure*, 1058: 244–251, 2014. doi: 10.1016/j.molstruc.2013.11.010.

[279] M. Kar, N. V. Plechkova, K. R. Seddon, J. M. Pringle, and D. R. MacFarlane. Ionic liquids – further progress on the fundamental issues. *Australian Journal of Chemistry*, 72(2):3, 2019. doi: 10.1071/CH18541.

[280] R. C. Myerly, M. D. Nicholson, R. Katzen, and J. M. Taylor. The forest refinery. *CHEMTECH*, 11(3):186–192, 1981.

[281] C. Nitsos, U. S. L. Rova, and P. Christakopoulos. Organosolv fractionation of softwood biomass for biofuel and biorefinery applications. *Energies (Basel, Switzerland)*, 11(1):50, 2018. doi: 10.3390/en11010050.

[282] H. H. Nimz and R. Casten. Chemical processing of lignocellulosics. *Holz als Roh- und Werkstoff*, 44(6):207–212, 1986. doi: 10.1007/BF02611993.

[283] D. Schliephake. Umweltschonende Aufschlußverfahren von pflanzlichem Material zur Gewinnung von Faserzellstoffen. *Lenzinger Berichte*, 69:21–28, 1990.

[284] X. Zhao and D. Liu. Kinetic modeling and mechanisms of acid-catalyzed delignification of sugarcane bagasse by aqueous acetic acid. *BioEnergy Research*, 6 (2):436–447, 2013. doi: 10.1007/s12155-012-9265-4.

[285] R. A. Young. Acetic Acid-Based Pulping. In R. A. Young and M. Akhtar, editors, *Environmentally friendly technologies for the pulp and paper industry*, pages 133–156. Wiley, New York, 1998. ISBN 0-471-15770-8.

[286] T. L. Smith and J. H. Elliott. Acid–base equilibria in glacial acetic acid. *Journal of the American Chemical Society*, 75(14):3566–3571, 1953. doi: 10.1021/ja01110a075.

[287] N. F. Hall. Acid-base equilibria in non-aqueous solvents with particular reference to glacial acetic acid. *Chemical Reviews*, 8(2):191–212, 1931. doi: 10.1021/cr60030a003.

[288] G. Vázquez, G. Antorrena, and J. González. Kinetics of acid-catalysed delignification of Eucalyptus globulus wood by acetic acid. *Wood Science and Technology*, 29(4):267–275, 1995. doi: 10.1007/BF00202086.

[289] L. Dong, R. Wu, X. Zhao, and D. Liu. Phenomenological modeling and evaluation of formic acid pretreatment of wheat straw with an extended combined severity factor for biomass fractionation and enzymatic saccharification to produce bioethanol. *Journal of the Taiwan Institute of Chemical Engineers*, 81: 140–149, 2017. doi: 10.1016/j.jtice.2017.09.038.

[290] X. Chang, J. Zhang, R. Wu, and X. Zhao. Phenomenological modeling of formic acid fractionation of sugarcane bagasse by integration of operation parameters as an extended combined severity factor. *Molecules*, 26(9):2753, 2021. doi: 10.3390/molecules26092753.

[291] M. Fišerová, E. Opálená, and A. Illa. Comparative study of hemicelluloses extraction from beech and oak wood. *Wood Research*, 58(4):543–554, 2013.

[292] A. F. M. Barton. Solubility parameters. *Chemical Reviews*, 75(6):731–753, 1975. doi: 10.1021/cr60298a003.

[293] A. P. Dunlop. Furfural formation and behavior. *Industrial & Engineering Chemistry*, 40(2):204–209, 1948. doi: 10.1021/ie50458a006.

[294] P. Wen, T. Zhang, J. Wang, Z. Lian, and J. Zhang. Production of xylooligosaccharides and monosaccharides from poplar by a two-step acetic acid and peroxide/acetic acid pretreatment. *Biotechnology for Biofuels*, 12:87, 2019. doi: 10.1186/s13068-019-1423-x.

[295] S. P. S. Chundawat, B. Venkatesh, and B. E. Dale. Effect of particle size based separation of milled corn stover on AFEX pretreatment and enzymatic digestibility. *Biotechnology and Bioengineering*, 96(2):219–231, 2007. doi: 10.1002/bit.21132.

[296] N. Yilgor, O. Unsal, and S. N. Kartal. Physical, mechanical, and chemical properties of steamed beech wood. *Forest Products Journal*, 51(11-12):89–93, 2001.

[297] G. Vázquez, G. Antorrena, J. González, S. Freire, and I. Crespo. The influence of acetosolv pulping conditions on the enzymatic hydrolysis of Eucalyptus pulps. *Wood Science and Technology*, 34(4):345–354, 2000. doi: 10.1007/s002260000053.

[298] B. Bao, D. K. Ng, D. H. Tay, A. Jiménez-Gutiérrez, and M. M. El-Halwagi. A shortcut method for the preliminary synthesis of process-technology pathways: an optimization approach and application for the conceptual design of integrated biorefineries. *Computers & Chemical Engineering*, 35(8):1374–1383, 2011. doi: 10.1016/j.compchemeng.2011.04.013.

[299] M. N. Borand and F. Karaosmanoğlu. Effects of organosolv pretreatment conditions for lignocellulosic biomass in biorefinery applications: a review. *Journal of Renewable and Sustainable Energy*, 10(3):033104, 2018. doi: 10.1063/1.5025876.

[300] K. Naumann, J. Schröder, K. Oehmichen, H. Etzold, F. Müller-Langer, E. Remmele, K. Thuneke, T. Raksha, and P. Schmidt. *Monitoring Biokraftstoffsektor. 4. Auflage: DBFZ-Report Nr. 11.* Deutsches Biomasseforschungszentrum gemeinnützige GmbH, Leipzig, 2019. ISBN 978-3-946629-36-8.

[301] P. Petäjä. Pulp: signs that prices are finally levelling, 2018-12-13. URL `https://www.tissueworldmagazine.com/technical-theme/pulp-signs-that-prices-are-finally-levelling/`. Accessed June 18, 2019.

[302] University of Technology Vienna – Institute of Chemical Engineering, Fuel and Environmental Technology. Beech, 2019. URL `http://cdmaster2.vt.tuwien.ac.at/biobib/fuel24.html`. Accessed August 6, 2019.

[303] C. Reeb, R. Phillips, R. Venditti, T. Treasure, J. Daystar, R. Gonzalez, H. Jameel, and S. Kelley. Techno-economic analysis of various biochemical conversion platforms for biosugar production: trade-offs of co-producing biopower versus pellets for either a greenfield, repurpose, or co-location siting context. *Biofuels, Bioproducts and Biorefining*, 16(3):390–411, 2018. doi: 10.1002/bbb.1847.

[304] F. Alsmeyer, H.-J. Koß, and W. Marquardt. Indirect spectral hard modeling for the analysis of reactive and interacting mixtures. *Applied Spectroscopy*, 58 (8):975–985, 2004. doi: 10.1366/0003702041655368.

[305] C. Ammann, P. Meier, and A. E. Merbach. A simple multinuclear NMR thermometer. *Journal of Magnetic Resonance (1969-1992)*, 46(2):319–321, 1982. doi: 10.1016/0022-2364(82)90147-0.

[306] S. Fendt, S. Padmanabhan, H. W. Blanch, and J. M. Prausnitz. Viscosities of acetate or chloride-based ionic liquids and some of their mixtures with water or other common solvents. *Journal of Chemical & Engineering Data*, 56(1):31–34, 2011. doi: 10.1021/je1007235.

[307] Y. Kim, N. Hankyu, and H. Chung. Determination of the equilibrium constant of the isotropic disproportionation between water and heavy water using near-infrared spectroscopy. *Applied Spectroscopy*, 63(2):256–259, 2009. doi: 10.1366/000370209787391996.

[308] J. Rönnols, E. Danieli, H. Freichels, and F. Aldaeus. Lignin analysis with benchtop NMR spectroscopy. *Holzforschung*, 74(2):226–231, 2019. doi: 10.1515/hf-2018-0282.

[309] M. M. El-Halwagi. *Sustainable design through process integration: fundamentals and applications to industrial pollution prevention, resource conservation, and profitability enhancement*. Butterworth-Heinemann, Boston, MA, 2012. ISBN 978-1-85617-744-3.

[310] D. Lozowski. Economic indicators: chemical engineering plant cost index. *Chemical Engineering (Rockville, MD, U. S.)*, 6:80, 2017. URL `https://de.scribd.com/document/352561651/CEPCI-June-2017-Issue`.

[311] M. Ruth. Hydrogen production cost estimate using biomass gasification: independent review, 2011. URL `https://www.hydrogen.energy.gov/pdfs/51726.pdf`. Accessed January 8, 2016.

[312] R. K. Sinnott, J. M. Coulson, and J. F. Richardson. *Chemical engineering design (4th edition)*, volume 6 of *Coulson & Richardson's chemical engineering*. Elsevier Butterworth-Heinemann, Oxford, 2005.

[313] G. D. Ulrich and P. T. Vasudevan. Predesign for pollution prevention and control. *CEP magazine*, 127:53–60, 2007. URL `http://www.aiche.org/resources/publications/cep/2007/june/predesign-pollution-prevention-and-control`.

[314] B. Kamm, P. R. Gruber, and M. Kamm. *Biorefineries - industrial processes and products: status quo and future directions*. Wiley-VCH, Weinheim, 2006.

[315] G. Bartoli, M. Bosco, A. Carlone, R. Dalpozzo, E. Marcantoni, P. Melchiorre, and L. Sambri. Reaction of dicarbonates with carboxylic acids catalyzed by weak lewis acids: general method for the synthesis of anhydrides and esters. *Synthesis*, 22:3489–3496, 2007.

[316] S. L. Neidleman, W. F. Amon, and J. Geigert. Process for the production of fructose. U.S. Patent 4246347A, 1981.

[317] H. H. Szmant and D. D. Chundury. The preparation of 5-hydroxymethylfurfuraldehyde from high fructose corn syrup and other carbohydrates. *Journal of Chemical Technology & Biotechnology*, 31(1): 131–145, 1981.

[318] G. Marcotullio and W. de Jong. Chloride ions enhance furfural formation from d-xylose in dilute aqueous acidic solutions. *Green Chemistry*, 12(10):1739–1746, 2010.

[319] M. Tamura, K. Tokonami, Y. Nakagawa, and K. Tomishige. Rapid synthesis of unsaturated alcohols under mild conditions by highly selective hydrogenation. *Chemical Communications (Cambridge, United Kingdom)*, 49(63):7034–7036, 2013.

[320] F. M. A. Geilen, T. Vom Stein, B. Engendahl, S. Winterle, M. A. Liauw, J. Klankermayer, and W. Leitner. Highly selective decarbonylation of 5-(hydroxymethyl)furfural in the presence of compressed carbon dioxide. *Angewandte Chemie, International Edition*, 50(30):6831–6834, 2011.

[321] Z. Yang, Y.-B. Huang, Q.-X. Guo, and Y. Fu. RANEY® Ni catalyzed transfer hydrogenation of levulinate esters to γ-valerolactone at room temperature. *Chemical Communications (Cambridge, United Kingdom)*, 49(46):5328–5330, 2013. doi: 10.1039/c3cc40980e.

[322] P. Lanzafame, D. M. Temi, S. Perathoner, G. Centi, A. Macario, A. Aloise, and G. Giordano. Etherification of 5-hydroxymethyl-2-furfural (HMF) with ethanol to biodiesel components using mesoporous solid acidic catalysts. *Catalysis Today*, 175(1):435–441, 2011. doi: 10.1016/j.cattod.2011.05.008.

[323] R. Liu, J. Chen, X. Huang, L. Chen, L. Ma, and X. Li. Conversion of fructose into 5-hydroxymethylfurfural and alkyl levulinates catalyzed by sulfonic acid-functionalized carbon materials. *Green Chemistry*, 15(10):2895, 2013. doi: 10.1039/c3gc41139g.

[324] V. Badarinarayana, M. D. Rodwogin, B. D. Mullen, I. Purtle, and E. J. Molitor. Process to prepare levulinic acid. Patent WO2014189991A1, 2014.

[325] J. Ren, Di Xu, H. Cao, S. Wei, L. Dong, and M. E. Goodsite. Sustainability decision support framework for industrial system prioritization. *AIChE Journal*, 62(1):108–130, 2016. doi: 10.1002/aic.15039.